Diagnostic and Prognostic Markers for Thyroid Cancer

By

Kumar Alok Pathak

A Thesis submitted to the Faculty of Graduate Studies of

The University of Manitoba

In partial fulfillment of the requirements of the degree of

DOCTOR OF PHILOSOPHY

Department of Human Anatomy and Cell Science

University of Manitoba

Winnipeg

i

Table of Contents

Declaration of Publications

Parts of this dissertation have been peer reviewed and published as original research articles. These publications are appended at the end of this dissertation (Appendix)

1. **Pathak KA**, Klonisch T, Nason RW, Leslie WD. A prospective cohort study to assess the role of FDG-PET in differentiating benign and malignant follicular neoplasms. Ann Med Surg. 2016;12:27-31. (Role: Corresponding author)

2. **Pathak KA**, Lambert P, Nason RW, Klonisch T. Comparing a thyroid prognostic nomogram to the existing staging systems for prediction risk of death from thyroid cancers. Eur J Surg Oncol. 2016 Oct; 42(10):1491-6. (Role: Corresponding author)

3. **Pathak KA**, Klonisch T, Nason RW, Leslie WD. FDG-PET characteristics of Hürthle cell and follicular adenomas. Ann Nucl Med. 2016 Aug; 30(7):506-9. (Role: Corresponding author)

4. **Pathak KA**, Klonisch T, Nason RW. Stage II differentiated thyroid cancer: A mixed bag. J Surg Oncol. 2016 Jan; 113(1):94-7. (Role: Corresponding author)

5. **Pathak KA,** Mazurat A, Lambert P, Klonisch T, Nason RW. Prognostic nomograms to predict treatment outcomes of thyroid cancer Clin Endocrinol Metab. 2013 Dec;98 (12):4768-75. (Role :Corresponding author)

6. **Pathak KA,** Leslie WD, Klonisch TC, Nason RW. The changing face of thyroid cancer in a population-based cohort. Cancer Medicine 2013; 2:537–544. (Role: Corresponding author)

7. Hendrickson-Rebizant J, Sigvaldason H, Nason RW, **Pathak KA**. Identifying the most appropriate age threshold for TNM stage grouping of well-differentiated thyroid cancer. Eur J Surg Oncol. 2015 Aug; 41(8):1028-32. (Role: Corresponding author)

8. Mazurat A, Torroni A, Hendrickson-Rebizant J, Benning H, Nason RW, **Pathak KA.** The age factor in survival of a population cohort of well-differentiated thyroid cancer. Endocr Connect. 2013 Sep 23; 2(3):154-60. (Role: Corresponding author)

9. Nixon IJ, Wang LY, Migliacci JC, Eskander A, Campbell MJ, Aniss A, Morris L, Vaisman F, Corbo R, Momesso D, Vaisman M, Carvalho A, Learoyd D, Leslie WD, Nason RW, Kuk D, Wreesmann V, Morris L, Palmer FL, Ganly I, Patel SG, Singh B, Tuttle RM, Shaha AR, Gönen M, **Pathak KA**, Shen WT, Sywak M, Kowalski L, Freeman J, Perrier N, Shah JP. An International Multi-Institutional Validation of Age 55 Years as a Cutoff for Risk Stratification in the AJCC/UICC Staging System for Well-Differentiated Thyroid Cancer. Thyroid. 2016 Mar; 26(3):373-80. (Role: Contributed 20% cases to an international multi-centre study, edited manuscript)

10. Medapati M, Dahlmann M, Ghavami S, **Pathak KA**, Lucman L, Klonisch T, Hoang-Vu C, Stein U, Hombach-Klonisch S. RAGE mediates the pro-migratory response of extracellular S100A4 in human thyroid cancer cells. Thyroid 2015 May;25(5):514-27 (Contributed to study design, specimen collection, manuscript writing and editing)

11. Hombach-Klonisch S, Natarajan S, Thanasupawat T, Medapati M, **Pathak KA**, Ghavami S, Klonisch T. Mechanisms of therapeutic resistance in cancer (stem) cells with emphasis on thyroid cancer cells. Front Endocrinol (Lausanne). 2014 Mar 25;5:37 (Role: Contributed to the manuscript writing and editing)

Abstract

Statement of the problem: The objectives of our study were to evaluate the debatable diagnostic role of FDG-PET/CT in predicting the risk of malignancy in follicular neoplasm and to build prognostic models to predict the risks of relapse and death from thyroid cancer, as there is no universally acceptable model valid for different histological types of thyroid cancers.

Methods: The efficacy of FDG-PET/CT scan for predicting the risk of malignancy was assessed in a prospective cohort of 50 follicular neoplasms. Disease specific and relapse free survivals of a 2306-patient Manitoba thyroid cancer cohort were estimated by the Kaplan-Meier method and the independent influence of various prognostic factors was assessed by Cox Proportional Hazard models. Cumulative incidence of deaths and relapses from thyroid cancer was calculated by competing risk analysis, and was used to develop and validate prognostic nomograms, using R version 2.13.2 (www.r-project.org). A web-based prognostic model was developed to predict the disease specific survival, and validated internally and externally on an independent patient cohort from London, Ontario.

Results: FDG PET/CT had an overall accuracy of 81% in predicting risk of malignancy in non-Hürthle follicular cell neoplasms and 87% accuracy in distinguishing follicular and Hürthle cell adenomas. The age standardized incidence of thyroid cancer in Manitoba increased by 373% from 1970 to 2010, with the proportion of papillary cancers increasing from 58% to 85.9%, and that of anaplastic cancer falling from 5.7% to 2.1% (p<0.001).

The disease specific survival was adversely influenced by anaplastic histology, male gender, stage IV disease, incomplete surgical resection and age at diagnosis, during a median follow-up of 11.5 years. Prognostic nomograms were designed to predict the individualized 10-year risks of death and relapse from thyroid cancer, with their respective concordance indices of 0.92 and 0.76. A web-based model was successfully developed and externally validated with excellent discrimination. It compared favorably with the existing staging/risk stratification systems.

Conclusions: FDGPET/CT has a very good accuracy of predicting risk of malignancy in non-Hürthle follicular cell neoplasms. We have successfully developed and validated prognostic nomograms and a web model for predicting oncological outcome of thyroid cancer.

Acknowledgements

I wish to express a deep sense of gratitude to Dr. Thomas Klonisch, my advisor, and Dr. Kevin Coombs, Dr. Bill Leslie and Dr. Richard Nason, my advisory committee members, for guiding me for the last six years. I appreciate the countless hours that Dr. Klonisch and my advisory committee members have spent out of their extremely busy schedule. I thank Dr. Klonisch for all his constructive suggestions over these years and for reviewing the entire thesis. The extra efforts of Dr. Leslie for managing PET scans of follicular neoplasm and facilitating external validation of the Manitoba prognostic model deserve a special word of gratitude. The analysis of FDG-PET data, especially the partial volume correction and total lesion glycolysis, would not have been possible without the help of Dr. Andrew Goertzen. The external validation would not have been possible without data sharing with London Health Sciences Centre (LHSC), London, Ontario which was facilitated by Dr. Stan Van Umm and Ms. Sarah Nixey. I thank the leadership of Surgery program at the University of Manitoba especially Dr. Richard Nason and Dr. Jack McPherson for having faith in my abilities to accomplish this mammoth task. I want to thank them for their kind and empathic support. Any fruitful research project needs financial support, which was provided by the Department of Surgery research grants and CancerCare Manitoba Foundation.

I do not have enough words to acknowledge the assistance provided by the staff of Departments of Epidemiology and Cancer Registry, CancerCare Manitoba and Medical Records, CancerCare Manitoba and Health Sciences Centre in helping me with the data

Dedication

Dedicated to the thyroid cancer patients in the Province

of Manitoba, Canada, without whose unsung

contribution, this work would not have been possible.

-Kumar Alok Pathak

List of Tables

List of Figures

List of abbreviations

AIC	Akaike information criterion
AJCC	American Joint Cancer Committee
ANOVA	Analysis of variance
APC	Adenomatous polyposis coli
ASIR	Age standardized incidence rate
ATA	American Thyroid Association
ATC	Anaplastic thyroid cancer
AUROC	Area under receiver operating characteristic curve
BMI	Body mass index
BRAF	Serine/threonine-kinase B-type Raf kinase
CamKII	Calcium-calmodulin kinase II
CaN	Calcineurin
CCND	Central compartment lymph node dissection
CFR	Case fatality rate
CHEK2	Checkpoint kinase 2
CIF	Cumulative incidence function
CI	Confidence Interval
C-index	Concordance index
CDKN1B	Cyclin-dependent kinase inhibitor 1B
CTNNB1	β-catenin

DSS	Disease specific survival
EIF1AX	Eukaryotic translation initiation factor 1A, X-linked
ERK	Extracellular-signal-regulated kinase
ETE	Extra-thyroidal extension
FA	Follicular adenoma
FAP	Familial adenomatous polyposis
FDG PET/CT	18F-2-fluoro-2-deoxy-d-glucose positron emission tomography/computerized tomography
FN	Follicular neoplasm
FNAB	Fine needle aspiration biopsy
FTC	Follicular thyroid cancer
FVPTC	Follicular variant of papillary thyroid cancer
GTP	Guanosine triphosphate
HCN	Hürthle cell neoplasm
HCA	Hürthle cell adenomas
HR	Hazard ratio
ICDO	International Classification of Diseases for Oncology
MAPK	Mitogen-activated protein kinase
MEK	Mitogen-activated protein kinase
mice	Multivariate imputation by chained equations
MiR	MicroRNA
MTC	Medullary thyroid carcinoma

MTV	Metabolic tumor volume
NIS	Sodium-iodide symporter
NPV	Negative Predictive Value
NS	Not significant
NTRK1	Neurotrophic tyrosine kinase receptor type
PAX8	Paired box gene 8
PDTC	Poorly differentiated thyroid cancer
PI3K	Phosphatidylinositol 3'-kinase
PKC	protein kinase C
PPARγ	Peroxisome proliferator-activated receptor gamma
PPM1D	Protein phosphatase magnesium-dependent 1 delta
PPV	Positive predictive value
PTC	Papillary thyroid carcinoma
PTEN	Phosphatase and tensin homologue
RAI	Radioactive iodine
RAS	Rat sarcoma viral oncogene
RC	Recovery coefficient
RET	Rearranged during transfection
RFS	Relapse free survival
rhTSH	Recombinant human TSH
ROC	Receiver operating characteristic

RRA	Radioactive remnant ablation
SEER	Surveillance, epidemiology, and end results
SUV	Standardized uptake value
T3	L-tri-iodothyronine
T4	L-thyroxine
TERT	Telomerase reverse transcriptase
Tg	Thyroglobulin
THRB	Thyroid hormone receptor-β
TLG	Total lesion glycolysis
TNM	Tumor, Nodes, Metastasis
TP53	Tumor protein p53 gene
TRH	Thyrotropin-releasing hormone
TSH	Thyroid-stimulating hormone
UICC	Union Internationale Contre le Cancer
WDTC	Well differentiated thyroid cancer

Chapter 1

Introduction

Thyroid cancers represent a conglomerate of different histological types that have diverse clinical behavior. According to the global cancer statistics, thyroid cancer is the most common malignant endocrine tumor (1). It is the fastest growing cancer in Canadian Cancer Statistics 2015 with an estimated age standardized incidence rate (ASIR) of 14.9/10000 in 2015. ASIR has been increasing at the rate of 6.3% per year in males since 2001 and by 4.4% per year in females (2005-2010) (2). Although the incidence of thyroid cancer has been rising, it had an excellent 5-year relative survival ratio of 98% in 2011 (3). Patients with well differentiated thyroid cancers (WDTC), papillary (PTC) and follicular (FTC), typically have an excellent survival, whereas those with poorly differentiated (PDTC) and anaplastic thyroid cancers (ATC) have a very poor outcome.

Fine-Needle Aspiration Biopsy (FNAB) is the mainstay in diagnosis of thyroid cancer. The Bethesda system currently used to report thyroid cytopathology assessments has six diagnostic categories: (a) inadequate or non-diagnostic, (b) benign or hyperplastic, (c) atypia of undetermined significance/follicular lesion of undetermined significance, (d) follicular (FN) or Hürthle cell variant (HCN), (e) suspicious for malignancy, and (f) malignant (4, 5). FN and HCN are considered as an "indeterminate cytology" group in the Bethesda Classification (4, 6). FN represent a cluster of follicular adenoma (FA), follicular variant of papillary carcinoma (FVPTC), and FTC as outlined in Figure 1. Similarly, HCN could be benign Hürthle cell adenomas (HCA) or malignant Hürthle cell carcinoma. Both

1

HCN and FN are diagnostic challenges in the pathology assessment on frozen sections and FNAB, as a comprehensive assessment of capsular invasion is required. This often results in a second surgery (completion thyroidectomy) for the patients after the diagnosis of malignancy on paraffin sections.
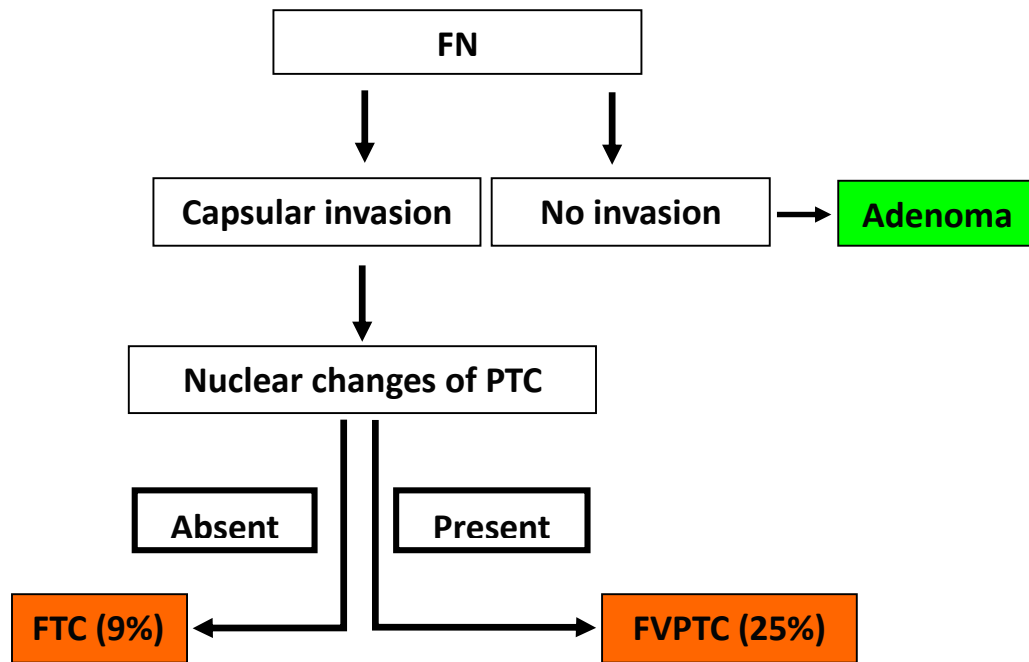
Figure 1: Classification of follicular neoplasms.
This classification is based on capsular invasion and nuclear changes. Capsular invasion distinguishes malignant follicular neoplasms shown in red (carcinoma) from benign ones shown in green (adenoma). Nuclear changes in malignant neoplasm helps in characterizing them as FVPTC or FTC.

The differentiation between the FN and HCN is made by identification of predominantly Hürthle cell populations on histopathological examination. The risk of malignancy in FN and HCN ranges from 15-30% with a higher risk associated with Hürthle cell variants (7). HCA are thought to be more aggressive than FA and may require an expert

thyroid pathologist for differentiating it from Hürthle cell carcinoma (8-10). If the malignant FN (minority) could be differentiated from benign FA (majority) by FNAB, these patients could directly be taken up for one-time total thyroidectomy, thereby avoiding a second surgery, and additional healthcare costs. [18F]-2-fluoro-2-deoxy-d-glucose (FDG) positron emission tomography/ computed tomography (PET/CT) scan has been used to discriminate benign and malignant follicular/ HCN with variable results and is not recommended for routine evaluation of thyroid nodules with indeterminate cytology (11, 12) as only about 40% of FDG-PET positive FN are thought to be malignant. Pooled sensitivity and accuracy of FDG-PET scan are reported to be 95% (95% confidence interval [95% CI]: 86%-99%) and 60% (95% CI: 53%-67%), respectively (11). Oncocytic adenomas (HCA) can masquerade as metastatic cancers due to their increased FDG uptake on PET/CT (13).

Survival in thyroid cancer is significantly influenced by a variety of factors, such as age, gender, histological type, stage of presentation and treatment. These factors have been incorporated into various staging/ prognostic scoring systems (14-28) to predict the oncological outcome of thyroid cancer. Most of these staging/ prognostic scoring are applicable only to the differentiated thyroid cancers (16-28) and provide stratified group risks rather than individualized risks. We have earlier reported that these prognostic factors can be incorporated in nomograms to provide visual explanation for predicted probabilities of an outcome as obtained by statistical predictive models that calculate the cumulative effect of weighted variables on the probability of that outcome (29). A nomogram can be

applied across different histological types to generate a numerical probability of an individual's clinical outcome, based on his/ her risk assessment. Nomograms have been used in prostate, lung, pancreas, breast, stomach, renal cancers and for sarcomas to predict treatment outcomes (30-37). Recently, a nomogram based on the Surveillance, Epidemiology, and End Results (SEER) database was developed to predict survival in thyroid cancer with inherent limitations like the lack of treatment and relapse details (38). In a busy clinical practice, the use of a paper nomogram to calculate the likely oncological outcome is both challenging and time consuming. Its reach to the global population is also very limited. A web-based computerized prognostic model to predict the probability of disease specific survival (DSS) is one such tool to overcome this limitation. This model can generate the numerical probability of oncological outcomes based on the cumulative effect of various prognostic factors (weighted by hazard ratio [HR]). It can be used for health care professionals anywhere in the world.

Most thyroid cancers have an indolent course and many failures take place years after diagnosis and initial treatment. Prolonged follow-up and low attrition of cohort are critical for testing the validity of a prognostic model (29). For a computerized prognostic model to be widely applicable it should be derived ideally from population-based data or from multi-institutional data. The population-based thyroid cancer cohort in Manitoba provides us with this unique opportunity, as CancerCare Manitoba is the sole tertiary cancer care center in the province of Manitoba with a population of about 1.2 million. Such

a model will not only be applicable to the population of Manitoba but will also be available for external validation at different institution and different population groups (29).

1.1 Goals

The goal of this study was to evaluate the efficacy of FDG PET/CT scan for predicting the risk of malignancy in indeterminate thyroid nodules, and to develop and validate models to predict the individualized oncological outcome of thyroid cancer.

1.2 Hypotheses

Hypothesis 1: FDG-PET /CT characteristics can be used to distinguish between benign and malignant indeterminate thyroid nodule.

Hypothesis 2: Prognostic markers can be used to develop models for predicting oncological outcome of thyroid cancers.

1.3 Specific Aims

Aim I: To assess the diagnostic role of FDG-PET /CT in differentiating between benign and malignant FN/HCN.

Aim II: To perform epidemiological analysis of prognostic markers in thyroid cancers.

Chapter 2

Literature Review

2.1 Anatomy and physiology of the thyroid gland

The thyroid gland is a butterfly-shaped organ that surrounds the anterior surface of the trachea and overlies the trachea-esophageal groove in the central compartment of the neck. It is made up of aggregates of colloid filled, flat -to-cuboidal follicular epithelial cells that line spherical follicles 50–500μm in diameter (39). Para-follicular calcitonin producing C cells are present at the junction of the upper and middle third of both thyroid lobes. They are located in a para-follicular location. The main functions of the thyroid gland are synthesis, storage and secretion of thyroid hormones, L-tri-iodothyronine (T3) and L-thyroxine (T4), under the control of the hypothalamic–pituitary axis. Thyrotropin-releasing hormone (TRH) is secreted from the hypothalamus. It stimulates the release of thyroid-stimulating hormone (TSH) from the anterior pituitary gland (39). Thyroglobulin (Tg) is synthesized and stored in the thyroid follicles as colloid providing a tyrosine-rich backbone for tyrosine iodination and iodotyrosyl coupling during T4 synthesis. T4 and T3 are released into the bloodstream after endocytosis and digestion of Tg. Serum thyroglobulin is used as a biochemical marker to identify relapse of WDTC. There is no role of preoperative Tg estimation in the diagnosis of thyroid cancer as it can be elevated in many benign thyroid diseases (12, 40) The sodium-iodide symporter (NIS) is an intrinsic plasma membrane protein that mediates active transport of iodide into the follicular thyroid cells (41). Subsequent iodide accumulation allows for effective therapeutic application of

6

radioactive iodine (RAI) and diagnostic thyroid scintigraphy. In ATC, this diagnostic option is lost due to decreased expression of NIS resulting in a loss of iodide accumulation (41).

2.2 Epidemiology of thyroid cancer

Thyroid cancers are the most common endocrine cancer tumor (1) and accounted for almost 6,000 newly diagnosed cancers in Canada in 2014, thereby representing 4.9% of all cancers in females and 1.4% of all cancers in males (42). Palpable thyroid nodules are seen in about 1% of men and 5% of women living in iodine-sufficient parts of the world (43, 44). Thyroid cancer is seen in 7–15% of thyroid nodules depending on the age, sex, radiation exposure, and family history (45, 46). Thyroid cancer has the most rapidly increasing incidence rate amongst all major cancers, showing a rise of 6.3% per year in males since 2001 and 4.4% per year in females (2005-2010) (2). The estimated ASIR of thyroid cancer was 14.9/10000 in 2015. Overall, the ASIR of thyroid cancer has increased from 1.8 and 6.5 per 100,000 in 1985 in Canadian males and in females to an estimated ASIR of 5.3 and 22.4, respectively in 2014. One in 60 Canadian women and 1 in 193 Canadian men will develop thyroid cancer and eventually 1 in 1351 females and 1 in 1538 males will die because of thyroid cancer (42). Thyroid cancer is three times more common in females than in males (42). Although the incidence of thyroid cancer has been rising, this cancer had an excellent 5-year relative survival ratio of 98% in 2011 (3). However, the mortality rates are significantly higher in men as compared to women, largely due to late diagnosis and more advanced disease in men at the time of initial diagnosis (47).

Primary thyroid cancers represent a conglomerate of different histological types of cancers arising from follicular cells (papillary, follicular and Hürthle cell cancers), calcitonin secreting para-follicular C cells (medullary thyroid carcinoma) and stromal elements (lymphoma and sarcoma) (48). Cancers arising from follicular cells can become de-differentiated to PDTC and ATC. Over 90% of all thyroid cancers are well-differentiated (WDTC) with an excellent overall 10-year survival rate that exceeds 95% (49). MTC and ATC account for 3% and 2% of all thyroid cancers respectively, while primary lymphoma and sarcoma of the thyroid are very rare (50, 51). ATC is among the most aggressive and deadly cancers, with a median survival of less than 6 months (52).

2.3   *Risk factors for thyroid carcinoma*

In epidemiology, a risk factor (determinant) is a variable that is associated with an increased risk of disease. Any characteristic, condition, or behavior that affects a person's chance of getting thyroid cancer can be considered a risk factor. It is important to distinguish risk factors causing thyroid cancer from those factors that are merely associated with this disease. According to the Bradford-Hill criteria for causal association, the following criteria need to be considered for cause and association (53).

1. *Strength of the association***:** For a relationship to be considered causal, a strong association between a risk factor and the outcome is required.

2. *Consistency of findings:* The same findings must be observed consistently across different population groups, in different study designs and should be reproducible at different times.

3. *Specificity of the association:* There should be a one-to-one relationship between the cause and the outcome.

4. *Temporal sequence of association:* The exposure to the risk factor must occur before the outcome under consideration.

5. *Biological gradient:* There should be a dose-response relationship. The change in disease rates should follow from corresponding changes in the exposure.

6. *Biological plausibility:* There should be a potential biological mechanism to explain the causation of disease by the risk factor.

7. *Coherence:* The relationship should agree with the current knowledge of the natural history of the disease.

8. *Experiment:* Introduction of exposure as well as its removal in experimental setting should alter the frequency of the outcome.

9. *Analogy:* In some circumstances it would be fair to judge whether the association is causal by looking at the effect of similar factors on causality.

The risk factors for thyroid cancer could be classified as environmental risk factors (exposure to ionizing radiation, age at the time of irradiation, iodine content in the food), demographic risk factors (gender and age; geographic and ethnic variability), biomedical risk factors (previous history of benign thyroid disease, body mass index, and hormonal

factors) and genetic risk factors (familial history and associated diseases, i.e. familial polyposis of colon, Cowden's disease, and Carney's complex). These factors result in genetic alterations like the activation of oncogenes, such as serine/threonine-kinase B-type Raf kinase (BRAF), rat sarcoma viral oncogene (RAS), rearranged during transfection (RET), and neurotrophic tyrosine kinase receptor type I (NTRK1), or the silencing of tumor suppressor genes, i.e. phosphatase and tensin homologue (PTEN), and the tumor protein p53 gene (TP53).

2.3.1   Environmental risk factors

Radiation: Cancers can develop in the thyroid 3-5 years after exposure to radiation therapy, but most cases occur 20-40 years after exposure. The risk of developing cancer depends on the amount of radiation and the age of the individual. About 10% of patients developed thyroid cancer after childhood radiation (54) and there is a 30-50% risk of malignancy in thyroid nodules in patients who had radiation to the thyroid in their childhood (55) for diagnostic or therapeutic purposes. Usually 40-50 Gray is given for childhood cancers, i.e. Wilms' tumor, neuroblastoma and lymphoma. In the past (1920-1960), radiation treatment was used even for benign conditions, such as acne, fungal infections of the scalp (tinea capitis), whooping cough, an enlarged thymus gland, or enlarged tonsils and adenoids. The risk of radiation from diagnostic imaging in children is uncertain, but radiation should be avoided in children unless absolutely necessary. When required, the lowest possible dose of radiation should be used (56-62).

Accidents, like the disaster at the nuclear power plant in Chernobyl in 1986, have led to an increase in thyroid cancer in the population around the disaster area. Young age (0-5 years old) at exposure was found to be a major risk factor and iodine deficiency increased the risk by about 3 fold. No significant increase in the risk for thyroid cancer was identified for radiation doses <100 mSv. The thyroid cancers identified in the Chernobyl region were usually PTC. They had a short latency (4-5 years) and a higher proportion of RET/PTC (50-86% vs. 13-43% for sporadic PTC) and AKAP9/BRAF (11% vs. 1% for sporadic PTC) rearrangements (63-65).

Diet: FTC is more common in areas of the world where people's diets are deficient in iodine. A low iodine diet with exposure to radioactivity may also increase the risk of PTC (63). Cruciferous vegetables (vegetables belonging to the cabbage family, like broccoli, cauliflower and Brussels sprouts) may prevent dietary iodine absorption, thereby increasing the risk of thyroid cancer (66, 67). Diets that are high in raw vegetables other than cruciferous vegetables show a slightly reduced risk of thyroid cancer (68). In developed countries, iodine is added to table salt to make sure it is part of the diet and this reduces the risk of endemic goiter and thyroid cancer. Conversely, the risk of thyroid cancer is high in developing countries/ areas with low levels of dietary iodine or where foods are not fortified with iodine (68). A high consumption of cheese and butter may increase the risk of thyroid cancer (67). However, a review of dietary risk factors did not find any consistent association of thyroid cancer risk with iodine intake through fortification, fish consumption, or with diets high in cruciferous vegetables (69).

Chemical: Exposure to certain chemical elements like nitrates, bicarbonates, sulfates, calcium, selenium, fluoride, chloride, magnesium, boron, manganese, iron, vanadium and their salts as well as radon-222, that are present in high concentrations in drinking water from volcanic areas, have been associated with the increased risk of thyroid cancer (70). However, the unequivocal causal association between chemical carcinogens and thyroid cancer still needs to be established.

2.3.2   Demographic risk factors

Thyroid cancer is a cancer of young adults. According to the Canadian Cancer Statistics (2014), thyroid cancer is the most common cancer in the 15-29 years age group and the second most common cancer in the 30-49 years age group (42). It is seen more often in women than in men (71). Higher incidence of thyroid cancer in young females prompted the thought that estrogen increases the levels of thyroid-stimulating hormone (TSH) in the body that may result in increased thyroid growth (72-74). However, most of the studies show no link between thyroid cancer and the use of medications to suppress lactation, fertility drugs or hormonal replacement therapy. The association between reproductive factors, such as the number of pregnancies, age of the woman at her first child, abortions, use of oral contraceptives, menopause, age at menarche, menstrual cycle irregularity and the risk of thyroid cancer has been inconsistent (69). Similarly, higher body mass index (BMI) and taller height may slightly increase the risk of thyroid cancer, but the biological plausibility of this weak association is unexplained (69, 75, 76).

2.3.3 Biomedical risk factors

Patients with benign thyroid disease like Hashimoto thyroiditis, appear to be at greatest risk of thyroid cancer within 4 years of onset of disease and the risk remains high for up to 10 years (77). Increased TSH secretion is thought to be a promoting factor rather than an initiating factor, which explains why thyroid cancers are not more common in the hyperthyroid state, but an elevated TSH level increases the risk of thyroid cancer recurrence. Benign breast conditions are associated with a 50% increased risk of thyroid cancer (78). Acromegaly results from an over-production of growth hormone and insulin-like growth factors, which may stimulate thyroid cells to grow and thereby increase the risk of thyroid cancer (79-82). Patient with a history of other cancers, like lymphoma, cancers of breast, oesophagus, and testes are also reported to be at a higher risk of thyroid cancer (83).

2.3.4 Genetic risk factors

Patients with a history of thyroid cancer in their first degree relatives are at a higher risk of developing thyroid cancer. It is estimated that 3.2% to 6.2% of thyroid cancers can be explained by familial factors. Most of the familial thyroid carcinoma are PTC, and a 4 to 10 fold increase in the incidence of PTC is reported in relatives of PTC patients (84). Familial PTC results from suspected genes on chromosomes 19 and 1. Familial PTC cases are known to have an early onset of disease and a more aggressive phenotype (85). Thyroid cancer is also known to be associated with a number of genetic conditions. Familial adenomatous polyposis (FAP) and Gardner syndrome is caused by a mutation of the

adenomatous polyposis coli (APC) gene that causes numerous polyps to develop in the large intestine and rectum as early as adolescence, along with tumors in the bone and soft tissues (in Gardner's syndrome). These patients are at an increased risk for developing other types of cancer, including thyroid cancer. Similarly, Cowden syndrome (multiple hamartoma syndrome/ PTEN hamartoma tumor syndrome) results from a mutation in the tumor suppressor gene PTEN that causes hamartomas with increased risk of cancers of the thyroid (PTC or FTC), uterus and breast. Carney complex is a very rare genetic disorder that increases the risk of developing certain cancers, including WDTC resulting from defects in the gene PRKAR1A (on chromosome 17q23-q24) (48). In the same way, Werner syndrome, a very rare condition caused by a mutation in the WRN gene that causes rapid premature aging after puberty, is associated with high risk of thyroid cancer (86).

An inherited abnormal RET gene is detected in 10-20% of all medullary thyroid cancer (MTC) cases. When MTC occurs alone, with no evidence of tumors elsewhere in the endocrine system, it is called familial MTC. When MTC occurs along with other cancers in the endocrine system, it is called multiple endocrine neoplasia syndrome type 2 (MEN2). There are 2 subtypes of MEN2: MEN2A – MTC occurs along with tumors in the adrenal glands (pheochromocytomas) and parathyroid gland tumors; MEN2B – MTC occurs along with pheochromocytomas and benign neuromas (tumors of nerve tissue). Neuromas in MEN2B commonly occur on the tongue, but they can also be found elsewhere on the body. In MEN2, MTC tends to develop at a young age, often during childhood or young adulthood, and is known to spread early. Somatic mutation of RET codon 918 in

exon 16 is seen in 40% to 50% of sporadic MTC and has been associated with lymph node metastases and decreased survival (87).

2.4 *Theories of thyroid carcinogenesis*

The mechanisms that prompt a thyroid cell to undergo malignant transformation are not well understood. Two theories have been proposed to explain this:

2.4.1 Fetal thyroid cell carcinogenesis theory

Fetal cell carcinogenesis regards carcinogenesis as an abnormal development of fetal thyroid cells. According to this theory, thyroid tumor cells are generated from the three types of fetal thyroid cells (88, 89): thyroid stem cells, thyroblasts, and prothyrocytes as outlined in Figure 2. Undifferentiated thyroid cancers or ATC are believed to be derived directly from the thyroid stem cells, whereas WDTC, such as PTC and FTC, are mainly derived from the thyroblasts (undifferentiated progenitor). Even though, both PTC and FTC are derived from thyroblasts, the latter are regarded as the more differentiated variants. FA do not possess cancerous characteristics and are thought to arise from the prothyrocytes (differentiated progenitor). Any event like the RET/PTC and PAX8-PPARγ rearrangements and mutations in BRAF that prevent the differentiation of fetal thyroid cells can cause cancer. According to this theory, these oncogenes act as an initiator but not as a promoter of thyroid carcinogenesis. Cancer cells are generated directly from fetal cells which already possess cancerous characteristics, without undergoing further differentiation and de-differentiation processes.
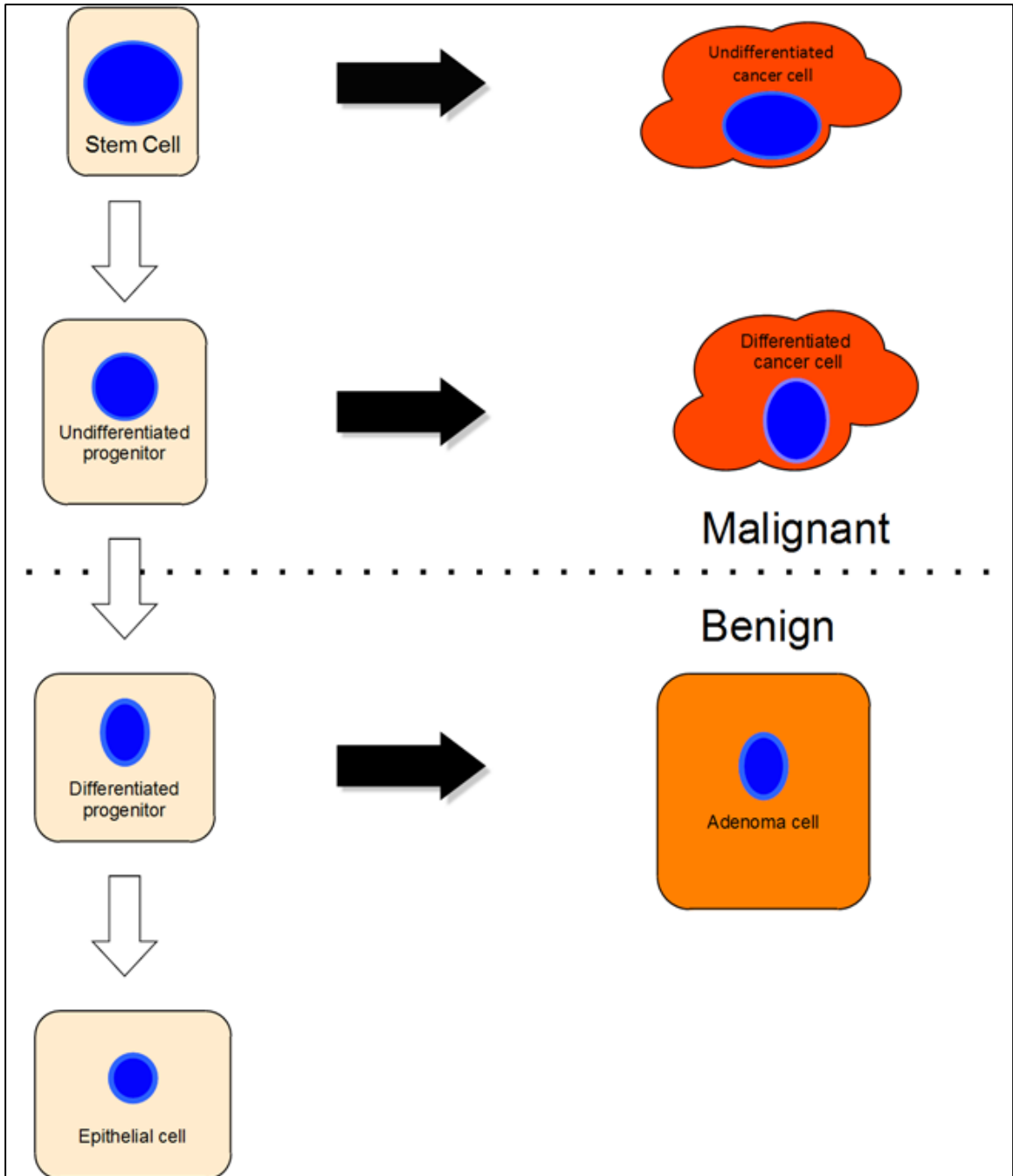
Figure 2: Fetal thyroid cell carcinogenesis model of thyroid carcinoma.
Black arrows indicate direct transformation of thyroid stem cells, undifferentiated progenitors (thyroblasts) and differentiated progenitors (prothyrocytes) to undifferentiated carcinoma, WDTC and FA. White arrows indicate normal maturation (pink colored cells) of stem cells to epithelial cells (thyrocyte). Light orange color of cell denotes benign neoplasm and the dark orange color represent malignant phenotypes.

2.4.2 Multistep carcinogenesis theory

The multistep carcinogenesis theory is based upon the premise of sequential events recorded during colon cancer pathogenesis (90) and proposes that most cancers are clonal in origin and arise from a single abnormal cell. Based on the multistep carcinogenesis theory, FTC are generated from FA and PTC are derived from precursor thyroid cells (91). PDTC and ATC may develop from PTC or FTC by de-differentiation or they may develop *de novo* without a pre-existing thyroid cancer (92-96). These clones progress as a result of number of inheritable alterations as summarized in Figure 3.
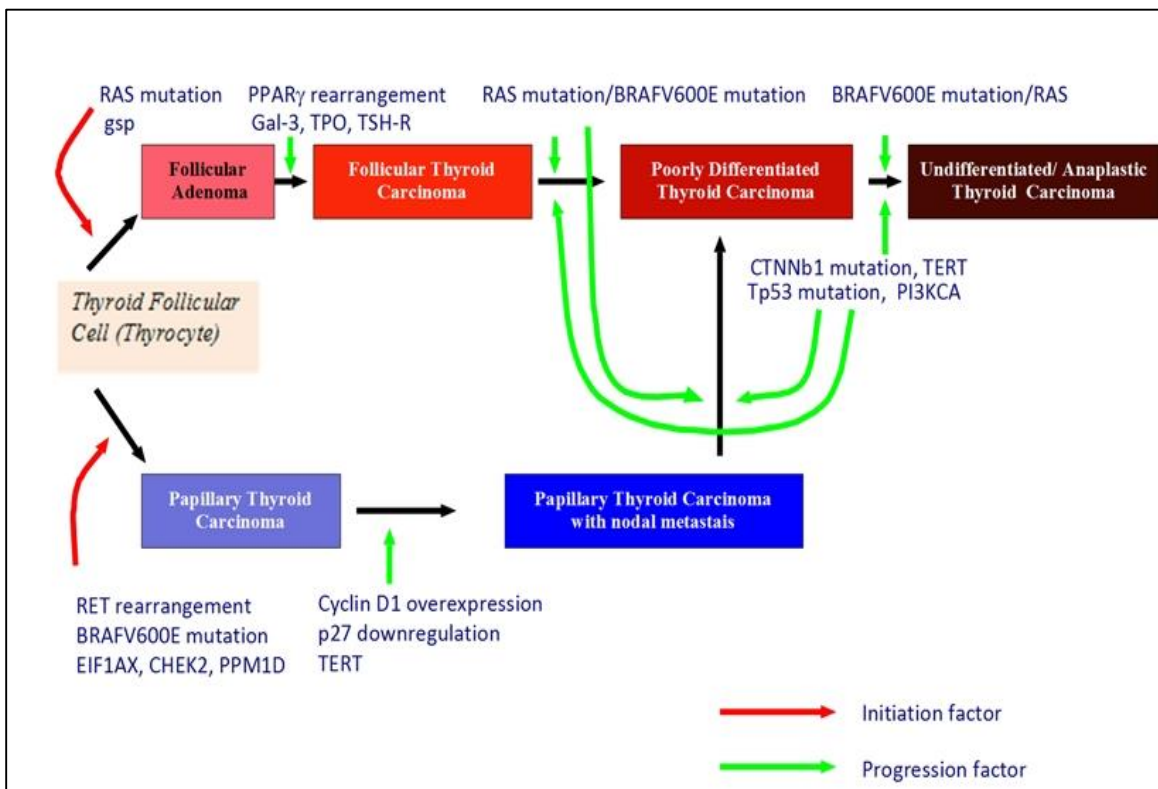
Figure 3: Multistep carcinogenesis model of thyroid carcinoma.
This model proposes a chain of sequential molecular events leading to thyroid carcinogenesis as indicated by the black arrows. Mutations initiating thyroid carcinogenesis are indicated by red arrows and the molecular changes leading to sequential progression are indicated by green arrows.

17

In addition to the known driver mutations, such as BRAF and RAS, the Cancer Genome Atlas study identified three novel significantly mutated genes in PTC, namely, Eukaryotic translation initiation factor 1A- X-linked (EIF1AX), Protein phosphatase magnesium-dependent 1 delta (PPM1D) and Checkpoint kinase 2 (CHEK2). EIF1AX mutation could be mutually exclusive with these known driver mutations or cluster with RAS mutation whereas, mutation of PPM1D and CHEK2 (DNA repair related genes) could co-occur with them (93, 96).

2.5   *Signaling pathways in thyroid cancer*

The main signaling pathways involved in thyroid carcinogenesis are the mitogen-activated protein kinase (MAPK) and phosphatidylinositol 3'-kinase (PI3K)/AKT pathways. Both signaling pathways are involved in the regulation of cellular proliferation, differentiation, and apoptosis. The activation of MAPK signaling pathway in thyroid cancer is initiated by binding of growth factors to receptor tyrosine kinases that dimerize to generate cell signals through transduction systems involving RAS, BRAF, mitogen-activated protein kinase (MEK) and extracellular-signal-regulated kinase (ERK). Activated ERK translocates to the nucleus and activates/phosphorylates various transcription factors associated with cell division and differentiation, such as MYC and ELK1 (97). The MAPK pathway plays a major role in PTC development (98, 99).

The PI3K family of related intracellular signal transducer enzymes phosphorylates the inositol ring of phosphatidylinositol. AKT is a serine/threonine kinase also known as

protein kinase B. Activation of PI3K/AKT plays a key role in cellular functions like cell proliferation and survival, by serial phosphorylation of a variety of substrates such as AKT and mTOR (100). A major consequence of activating PI3K/AKT signaling is the inhibition of cell cycle inhibitors. Genetic changes involving PI3K/AKT signaling pathways take place in various types of thyroid tumors, especially in FTC, radioactive iodine refractory metastatic PTC, ATC and less differentiated thyroid carcinomas at later stages of cancer progression (101), but they are rare in well-differentiated thyroid cancer (WDTC) (102).

The Wnt signaling pathway also contributes to thyroid carcinogenesis via a canonical or Wnt/β catenin dependent pathway and a non-canonical/ β-catenin-independent pathway. In the canonical pathway, Wnt signaling is activated by the binding of Wnt factors to the Frizzled (Fzd) receptor and LRP5/6 co-receptors. This reduces the proteasomal degradation of β-catenin (CTNNB1) and results in the nuclear binding of CTNNB1 to TCF/LEF transcription factors which causes the transcriptional activation of genes involved in proliferation. The CTNNB1 gene is located on chromosome 3p22-p21.3 and has two main cellular functions as a regulator of cadherin-mediated adhesion and as a mediator of WNT/CTNNB1 signaling pathway. Binding of the non-canonical Wnt factors (Wnt4, Wnt11, or Wnt5A) to different Fzd receptors and the Ror2 co-receptor causes signal transduction by two different pathways. The Ca^{2+} pathway promotes the activation of protein kinase C (PKC) and modulates cell adhesion and motility by activating calcium-calmodulin kinase (CamKII), and the phosphatase calcineurin (CaN). On the other hand, the planar cell polarity (PCP) pathway causes cytoskeleton rearrangements through

activation of the small GTPases RhoA and Rac and their downstream effectors Rock and JNK. This pathway is involved in the undifferentiated and anaplastic carcinoma (51). CTNNB1 exon 3 mutations and CTNNB1 accumulation in the nucleus can be identified in up to 25 % of PDTC and 66 % of undifferentiated/ ATC (103). Once the process of thyroid carcinogenesis is initiated, tumor progression is promoted by other factors, including PPARγ, cyclin D1 over-expression, p27 down-regulation, TP53 mutations and CTNNB1. RAS mutations can also lead to thyroid tumor progression (Figure 3).

2.6   Molecular markers of thyroid cancer

2.6.1   Genes involved in thyroid cancer

2.6.1.1 Papillary thyroid carcinoma

RET-PTC: The RET (rearranged during transfection) proto-oncogene on chromosome 10q11.2 encodes a membrane-anchored tyrosine kinase receptor (104). Chromosomal rearrangements occur between the 3' portion of the RET gene and the 5' portion of an unrelated gene at early stages of tumor development to produce an aberrant RET-PTC protein which causes ligand-independent activation of its intracellular tyrosine kinase domain. There are at least 15 different RET-PTC rearrangements. RET-PTC1 and RET-PTC3 are two most commonly identified rearrangements in PTC. RET-PTC1 and RET-PTC3 are formed by the fusion with the H4 (histone 4) gene and the ELE1 (a transcriptional co-activator of the androgen receptor) gene, respectively (105-107). The aggressive variant PTC subtype is closely associated with the RET-PTC3 oncogene, whereas the classic PTC variant is associated with RET-PTC1 (77, 105). The reported prevalence of RET-PTC in

PTC varies significantly. RET-PTC1is the most common type reported, and accounts for 60-70% of the rearrangements, whereas RET-PTC3 is responsible for 20-30% (108). RET-PTC rearrangements were described in thyroid tumors associated with radiation exposure. A higher prevalence of RET-PTC1 has been observed in contaminated areas after the Chernobyl disaster (109). Point mutations in RET are associated with MTC and multiple endocrine neoplasia (MEN2A and 2B). This mutation is present in 20% of classic PTC (110). RET/PTC rearrangements and mutations in the BRAF gene are mutually exclusive and do not occur in the same tumor (110).

BRAF: The serine/threonine protein kinase BRAF is located on chromosome 7q24, and has a critical role in cell signaling as a part of the MAPK signaling pathway. BRAF mutations have been implicated in approximately 40-45% of PTC, 10-15% of PDTC, and 20-30% of ATC (105). Activated versions of BRAF are generated by intra-chromosomal inversions that fuse the kinase domain of BRAF to the NH2-terminal portion of AKAP9. This results in BRAF/AKAP9 fusion proteins, which are found in about 11% of Chernobyl patients (111). BRAF mutations are associated with impaired iodine trapping through the sodium iodine symporter (NIS), decreased thyroid hormone synthesis and increased serum TSH levels (98). A BRAF point mutation at codon 600 results in a valine to glutamate (V600E) exchange and causes continuous phosphorylation of MAPK pathway effectors. The BRAF^{V600E} mutation is the most common genetic alteration found in thyroid cancer and is an independent predictor of treatment failure (112). It results in higher tumor recurrence, even in the patients with low-stage disease (113).

The most extensively studied mutation in thyroid cancer, in different ethnic groups, is the BRAF^{V600E} mutation. It has been reported to be associated with 29% to 83% of PTC and its variants, 10% of poorly-differentiated, and 15% of undifferentiated thyroid tumors (114-124). The BRAF^{V600E} mutation is the most potent isoform in stimulating the MAPK pathway (125). The BRAF^{V600E} mutation results in a 500-fold increase in activation of the MAPK pathway and is associated with the silencing of many thyroid-specific iodine metabolizing genes (126). Although the MAPK pathway is affected by many genetic alterations in PTC, the histological phenotype and expression profile is not necessarily the same among all, thereby suggesting that other pathways may be involved (110). The exact clinical implications of this mutation are debated. Some studies reported this mutation to be associated with persistent disease and death, extra-thyroidal extension, multifocality, presence of nodal metastases, advanced-stage disease, poor iodine uptake, and older age at initial presentation (110, 113, 127, 128). In contrast, other studies have failed to detect a significant relationship between clinical outcome and BRAF^{V600E} mutation (127-129). Since the BRAF mutation is exclusive to PTC, or ATC originating from PTC, it can be used to aid in the diagnoses of PTC (130). This BRAF mutation was helpful in establishing the diagnosis of PTC in 72% of malignant samples and in 16% of indeterminate FNAB (131). In another study, a diagnosis was established for 5 of 15 indeterminate FNAB samples using the BRAF^{V600E} mutation analysis (47). Since poorly-differentiated and ATC harbor the BRAF mutation rather than RET/PTC, it is believed that the BRAF^{V600E} mutation may predispose PTC to de-differentiation (118). Targeted expression of BRAF in transgenic mice has been reported to result in de-differentiation of PTC (132).

NTRK1: The proto-oncogene Neurotrophic Tyrosine Kinase Receptor type 1 (NTRK1) is located on the q arm of chromosome 1 and encodes the high affinity transmembrane receptor for nerve growth factor. Constitutive activation of NTRK1 has been detected in several tumor types. The fusion of the 3'-NTRK1 tyrosine kinase domain to 5´ sequences of at least three different genes (TPM3, TPR and TFG) leads to oncogenic activation of NTRK1. Interestingly, PTC arising in patients with a history of exposure to elevated levels of ionizing irradiation do not carry these known abnormalities. Similarly, NTRK1 rearrangements are rare in cases of sporadic PTC (133). The frequency of NTRK1 rearrangements in post-Chernobyl papillary thyroid tumors was equivalent to that of sporadic tumors (134).

PTEN: The protein tyrosine phosphatase family member phosphatase and tensin homolog (PTEN) was identified in 1997 as a tumor-suppressor gene located on 10q23.3 (135). PTEN inhibits PI3K signaling and, thus, suppresses AKT activity. The importance of the PTEN catalytic activity for its tumor suppressor function is highlighted by the fact that the majority of PTEN missense mutations detectable in tumor specimens target the phosphatase domain, and cause a loss in PTEN phosphatase activity (136). Genetic loss of PTEN is sufficient to induce thyroid cancer *in vivo* (137). Three to 10% of individuals with differentiated thyroid cancer are thought to carry a germ line PTEN mutation, whereas mutations or deletions in PTEN are rare events in sporadic thyroid cancer (138). Perhaps the strongest evidence in support of a role for PI3K signaling in the development of thyroid cancer is Cowden syndrome, where the thyroid cancer can be identified in approximately

two-thirds of affected individuals for this syndrome (139). PTEN also plays a critical role in DNA damage repair and response (137). Thus, the oncogenic potential of PTEN loss of function mutations may result in constitutive activation of the PI3K/AKT pathway and impaired DNA repair, which may contribute to the development of thyroid cancer.

TP53: The TP53 gene is located on chromosome 17p13.1 and consists of 11 exons encoding for the nuclear phosphoprotein and tumor suppressor protein TP53 which can bind to specific DNA sequences and acts as a transcription factor. TP53 participates in cell cycle arrest in the G1 phase of the cell cycle in the context of DNA repair. TP53 is also involved in apoptosis (140). TP53 plays a central role in the response to DNA damage through its ability to activate DNA repair, arrest cell cycle progression and induce apoptosis. Thus, TP53 acts as an important guardian of genomic stability by preventing malignant transformation of thyroid cells. Mutations resulting in the loss of TP53 function can induce genomic instability and this leads to cancer progression. TP53 was reported to be mutated or absent in majority of ATC (141). Mutations in this gene result in angiogenesis, growth, and de-differentiation (41). Mutations in TP53 are recognized as late genetic events associated with the de-differentiation of a PTC to highly aggressive undifferentiated carcinomas. The TP53 mutation, mostly involving alterations in exons five to eight of the gene, occurs in approximately 17-38% poorly differentiated thyroid cancer and 67-88% of undifferentiated thyroid carcinoma as compared to only 0-9% of WDTC (142). About half of the patients with anaplastic cancer have a previous or coexistent differentiated thyroid carcinoma with evidence of de-differentiation from more

differentiated tumors and this is often associated with loss of TP53 tumor suppressor protein variants (143) . The re-introduction of the wild type p53 into ATC cell lines results in the re-differentiation of ATC with a markedly impaired tumorigenic potential (144).

2.6.1.2 Follicular thyroid carcinoma

PAX8-PPAR γ: The fusion of the PAX8 gene with the PPARγ gene arises due to a (2;3)(q13;p25) translocation resulting in strong over-expression of the chimeric PAX8-PPARγ protein (105). The resultant fusion protein can probably function as a dominant-negative suppressor of PPARγ-induced gene transcription which confers anti-apoptotic properties (145). Alternatively, the fusion product can disrupt PAX8 transcriptional activity resulting in the deregulation of expression of its thyroid-specific target genes, like thyroglobulin, thyroperoxidase, and sodium-iodide symporter. PAX8-PPARγ accelerates cell growth, reduces apoptosis and permits anchorage-independent, contact uninhibited growth in a thyroid cell line (146). PAX8-PPARγ rearrangement has been found in 30-40% of FTC, 38% of FVPTC, 2-13% of follicular adenomas, and with lower prevalence in oncocytic carcinomas (105). Tumors expressing PAX8/PPARγ rearrangements occur at a younger age. The resultant tumors are small in size with a solid appearance or nests and frequently have vascular invasion (105, 147).

RAS: Members of the RAS family transmit signals originating from tyrosine kinase membrane receptors to a cascade of MAPK to activate the transcription of target genes involved in cell proliferation, survival, and apoptosis (148). RAS signaling through

downstream ERK and AKT pathways stimulate epithelial to mesenchymal transition in various cells (149). Constitutive activation of H-RAS, N-RAS, and K-RAS, as a result of mutations has been reported as markers for aggressive thyroid cancer behavior. The point mutations have been identified in codon 12, 13 or 61 for H-RAS, N-RAS and K-RAS, in codon 61 for N-RAS and H-RAS mutations and in codon 12/13 of K-RAS (150). RAS mutations occur in approximately 10-20% of papillary cancers, 25-30% of PDTC, 40-50% of ATC and 40-50% of FTC (105). These data suggest that RAS is involved in both thyroid cancer initiation and progression. The above mentioned RAS mutations are present in 20-40% of follicular adenoma, 40-50% of FTC, and 10-20% of follicular variant PTC, and are associated with a reduction in local lymph node metastasis in favor of more distant metastases (151).

2.6.1.3 Medullary thyroid carcinoma

The receptor tyrosine kinase, encoded by RET proto oncogene, is normally expressed in developing neural crest derived tissues, including thyroid C cells. Germ line or somatic point mutations close to the transmembrane or in the tyrosine kinase (TK) region of RET contribute to thyroid C-cell carcinogenesis. RET interaction with members of the glial-derived neurotrophic factor (GDNF) family of ligands leads to dimerization of RET and activation of its tyrosine kinase activity. Downstream signaling events lead to growth and survival signals that are controlled by receptor occupancy and crosstalk with other ligand-receptor systems. RET mutations cause ligand-independent receptor dimerization

or constitutively activate kinase activity independent of RET dimerization. Germ line point mutations are seen in multiple endocrine neoplasia type II (MEN II).

2.6.2 MicroRNAs and thyroid cancer

MicroRNAs represent a class of endogenous small noncoding RNAs of 20-24 nucleotides that regulate gene expression at the post-transcriptional level, thereby regulating major cellular processes, including proliferation, differentiation, mobility and apoptosis (142). About 70 nucleotides long precursor microRNAs are further processed by the Dicer enzyme to produce shorter mature sequences about 21-24 nucleotides. MiR expression profiles were reported to have high diagnostic value in distinguishing thyroid cancer types. Microarray profiling is a technique that has been used to systematically detect the differential expression of microRNAs in cancer and control samples, but different melting temperatures of short-length microRNAs and the high sequence homology between microRNA family members can lead to false positive microarray results (152).

When compared with normal thyroid tissue, 32% of miRs were found to be consistently up-regulated and 38% were down-regulated in thyroid cancer (153). In PTC, seven miRs (miR-221, -222, -146, -21, -155, -181a, and -181b) were found to be up-regulated compared with the normal thyroid, with the highest up-regulation of miR-221, -222, and -181b. They were together termed as PTC-7-miR. The fact that miR-221 is also up-regulated in unaffected thyroid tissue of several PTC patients implicates that miR-221 may be involved in early events of thyroid carcinogenesis (154). Up-regulation of miR-

211 and miR-222 has been inversely correlated with the down-regulation of Kit receptor and CDKN1B (p27^{Kip1}) protein, a key regulator of cell cycle progression (155). Cell lines transfected with miR-221, -222, and -21 are known to have lower levels of thyroid hormone receptor-β (THRB), an important tumor suppressor gene (156). MiR-221 and miR-222 were found at the highest levels in BRAF- and RAS-positive tumors and in tumors with no known mutations. Highest expression of miR-146b was detected in PTC with RAS mutations (153). In FTC, miR-196, -197, -328, -346 are up-regulated, whereas miR-339 is reported to be over-expressed in oncocytic variants of FTC (153). Down-regulation of miR-30d, -125b, -26a, -30a-5p, -138 and up-regulation of the miR-17-92 cluster is seen in ATC (157). In MTC, 10 specific microRNAs (miR-9, miR-10a, miR-124a, miR-127, miR-129, miR-137, miR-154, miR-224, miR-323, and miR-370) have been reported to be up-regulated (153). MiR-200, a key factor of the epithelial phenotype, is considered as a therapeutic target to reduce the rates of invasive and metastatic thyroid carcinomas (158).

2.7   *Diagnosis*

2.7.1   Clinical features

Almost half of all thyroid cancers present as asymptomatic thyroid nodules and less than 1% of them are hyperthyroid. In North America, 4-7% of all adults have palpable thyroid nodules. With the increasing use of high resolution ultrasound, 19-60% of the population have been found to have ultrasound detectable nodules (43, 159). Only 5-10% of all thyroid nodules are malignant (160), but as many as 30-50% of the thyroid nodules identified after childhood radiation are found to be malignant (55). Benign nodules are seen

more frequently in women in the 20-40 years age group and thyroid nodules are five times more common in women (160). Solitary thyroid nodules in males younger than 14 years or older than 65 years of age are suspicious for malignancy.

Symptoms of thyroid cancer are due to local, regional or distant disease. A rapidly enlarging nodule could be malignant, although hemorrhage in a benign nodule can also present in the same way. Other local effects of expanding thyroid nodules and local invasion include hoarseness of voice due to pressure-mediated vocal cord palsy or infiltration of the recurrent laryngeal nerve, which runs in close proximity to the thyroid gland. Tracheal compression can result in stridor and tracheal invasion can manifest as hemoptysis. Dysphagia can indicate esophageal compression. Metastatic disease could present with cervical lymphadenopathy (regional metastasis) or distant metastases usually to the lungs (PTC) or bone (FTC).

2.7.2 Ultrasonography

Advances in the ultrasound technology have made it the imaging procedure of choice for thyroid nodules. Ultrasonography assists in discerning solid from cystic nodule and dominant nodules and multi-nodular goiters from solitary nodules. It also helps to identify features of malignancy such as micro-calcifications, hypo-echogenecity of a solid nodule, intra-nodular hyper-vascularity, taller than wide on transverse view and infiltrative margins or extra-thyroidal extensions (ETE). According to the 2015 American Thyroid Association (ATA) guidelines, solid hypoechoic nodules or solid hypoechoic components

of a partially cystic nodule with one or more features like irregular margins (infiltrative, micro-lobulated), micro-calcifications, taller than wide shape, rim calcifications with small extrusive soft tissue component or evidence of ETE are highly suspicious (>70–90% risk of malignancy). Hypoechoic solid nodules with smooth margins without ETE, taller than wide shape or micro-calcifications are intermediately suspicious (10–20% risk of malignancy). FNAB is recommended for nodules ≥ 1 cm in the largest dimension that have high or intermediately suspicious sonographic features. An isoechoic or hyperechoic solid nodule, or partially cystic nodule with eccentric solid areas, without micro-calcification, irregular margin or ETE, or taller than wide shape have low suspicion of malignancy (5–10% risk of malignancy) and FNAB is recommended for such nodules ≥1.5 cm. Spongiform or partially cystic nodules without any of the suspicious sonographic features described above have very low suspicion (<3% risk of malignancy) and FNA is considered at size ≥2 cm and observation without FNA is also a reasonable option. Purely cystic nodules (no solid component) are likely benign (<1% risk of malignancy) and a biopsy is not recommended (12).

Ultrasonography can be used to identify and characterize cervical lymphadenopathy by their rounded shape, hypo-echogenicity, loss of fatty hilus, peripheral vascularity, calcification and cystic changes in a lymph node (161). Ultrasound guided FNAB is recommended for cervical lymph nodes that are sonographically suspicious for thyroid cancer. Ultrasound can also be used as a guide to localize nodule for fine-needle aspiration biopsy (FNAB) and for targeting the solid areas in a solid cystic nodule.

2.7.3 FDG-PET /CT scan

PET/CT scan involves the injection of a molecule containing a positron emitter radionuclide. These radionuclides are usually produced by a particle accelerator such as a cyclotron. The subsequently emitted radiation is detected by a scanner that can be incorporated into a CT image. Fluorine-18 (18F or ^{18}F) with a half-life of 110 minutes is usually tagged to a glucose analogue (2-deoxy-d-glucose) to produce Fluorodeoxyglucose (FDG) or Fludeoxyglucose (^{18}F). The uptake of FDG by tissues is an indicator of tissue glucose uptake and closely correlates with glucose metabolism in the tissue. The radioactivity uptake by tissues can be analysed semi-quantitatively and is expressed as Standardized Uptake Value (SUV):

SUV= Radioactivity concentration (Ci/mL) / (Injected dose/ Body mass)(mCi/kg)

The volume of interest in PET scan is divided into voxels and the maximum single-voxel SUV is called SUVmax. It is important to distinguish between SUVmax and peak SUV that is defined as the average SUV within a 1 cm^3 sphere centred in the highest uptake region of the tumor. Average SUV over the entire volume of interest is defined as the mean SUV. Metabolic tumor volume is the sum of estimated volumes of voxels with increased uptake (MTV; global MTV =volume of voxels with SUV > threshold SUV). Total lesion glycolysis (TLG) is the sum of the product of each lesion's MTV and the corresponding mean SUV over lesions within that MTV (TLG; global TLG = MTV x mean SUV) (162-164).

Estimation of SUV has its own limitations (165). As FDG uptake by metabolically active tissue continues over time, tumor SUV will rise rapidly initially and continue to rise over at least several hours (time dependence), making it challenging to compare SUVs from one study to another, thereby making it difficult to assess the treatment response over a period of time if identical protocols are not used (166). SUVmax is more reliable and reproducible than mean SUV because of the challenge of contouring the tumor (167). Contouring of tumors is dependent on resolution of tomography (lower resolution image will have lower SUVmax) as well as background noise. As a bright voxel in the region of interest may give a spurious high SUVmax value it is less reliable in noisy images (168). Resolution depends primarily on the intrinsic resolution of the scanner, reconstruction filtering, and reconstruction matrix size. Even though intrinsic resolution is around 5 mm, most modern PET systems can reliably estimate SUVmax of lesions at least 10–12 mm in size. Smaller lesions appear less intense on PET scan than their true intensity because of limited resolution of the system. Recovery coefficient (RC) method can be used for partial volume correction of PET images, as described earlier (169). A RC of 1.0 indicates correctly displayed activity, whereas a value of 0.5 indicates that the displayed activity is only 50% of true activity.

Body habitus and high blood sugar can also influence the SUV values. As FDG does not distribute uniformly, especially in adipose tissue, obese patients have relatively more FDG available for uptake into tumors, which could give falsely high SUV values. FDG and glucose use the same uptake system, and consequently, high levels of glucose

competes and inhibits FDG uptake into tissue. Thus, SUV values tend to be lower if the glucose levels are higher. Correction of SUV by dividing by the glucose level was not found to improve diagnostic accuracy (170). As there is a high risk of missing out cancers if serum glucose is greater than 200 mg/dl, some centers use a small amount of IV regular insulin to lower glucose levels and wait at least one hour for insulin levels to drop back toward baseline before scanning (168).

Non-specific uptake of FDG glucose is often observed in metabolically active tissue such as brain, Waldeyer's ring, heart, vocal cords, orbital muscles, brown fat etc. (171). It is a challenge to distinguish between the increased FDG uptake due to malignant and non-malignant causes. Threshold concept and target to background ratios have been employed for this purpose. A cut off mean SUV of 2.5 was considered to have sensitivity of 92% and a specificity of 90% in distinguishing benign and malignant pulmonary nodules (166). It is imperative to emphasize that there is no abrupt change in the probability of malignancy at a threshold SUV; rather the probability of malignancy rises as the SUVmax exceeds the threshold and decreases as the SUVmax drops below the threshold (168). Inflammation due to treatment, infection or chronic inflammatory diseases can often cause a non-specific increase in FDG uptake and SUV. The FDG uptake also differs from site to site, and a single threshold value may not be valid for all malignancies. Lowe et al. used a visual guideline for comparing solitary pulmonary nodules to the mediastinum. Nodules with uptake greater than mediastinum (i.e., uptake ratio >1.0) were more likely to be malignant (172). The uptake of 18F-FDG in a normal gland is the same as the surrounding soft tissue

33

(171). FDG-PET under TSH stimulation is thought to be more accurate as TSH may stimulate FDG uptake by differentiated thyroid cancer (173, 174)

Incidental FDG uptake in thyroid can be either focal or diffuse and has been reported in 1-2% of patients undergoing FDG-PET or FDG-PET /CT for other reasons (175-177). Diffusely increased uptake in the thyroid has been reported in 0.6-3.3% of patients undergoing FDG-PET or FDG-PET /CT and commonly represents benign disease like thyroiditis (178-180). Focal FDG uptake within the thyroid gland can be associated with 24-36% risk of malignancy, most commonly PTC (181-185). Treglia et al. performed a meta-analysis of 34 studies evaluating incidental focal thyroid uptake detected by FDG-PET /CT (n = 215,057) and found a pooled malignancy risk of 36.2% (95% CI: 33.8–38.6%) (183). In a systematic review performed by Shie et al. on incidental focal thyroid uptake (n = 55,160), 62.1% of patients had benign disease, 33.2% had cancer, and 4.7% of diagnoses were indeterminate nodules (186). PTC was found to be the most prevalent thyroid malignancy (82.2%) among those who had cancer. Similarly, a meta-analysis for detecting recurrent MTC showed a pooled detection rate of 59%. The overall sensitivity was only 20-36.8% when the calcitonin level was lower than 1,000 pg/mL (187-189). The relatively low detection rate of disease in patients with low calcitonin levels is likely a result of a smaller tumor mass or microscopic disease (189). The sensitivity of FDG-PET /CT for MTC recurrence in patients with multiple endocrine neoplasia (MEN) type 2A syndrome was significantly lower (23%) (188). When patients with MEN type 2A syndrome were excluded, overall per-patient sensitivity of FDG-PET /CT for detecting

MTC lesions increased from 44.1-50%. 68Ga-d-Phe(1)-Tyr(3)-octreotide, a PET radiopharmaceutical highly specific for somatostatin receptors, and 18F-dihydroxyphenylalanine have shown promising results in PET imaging in MTC (190, 191). FDG-PET /CT had a sensitivity of 92%, specificity of 80%, positive predictive value (PPV) of 92%, and negative predictive value (NPV) of 80% with an accuracy of 89% for the identification of Hürthle cell thyroid carcinoma (192). When WDTC dedifferentiate, they lose their ability to concentrate iodine, but their ability to concentrate FDG increases (193). ATC lesions, whether primary or metastatic, consistently show high FDG uptake (194).

2.7.4   Fine-needle aspiration biopsy (FNAB)

FNAB is the mainstay in the diagnosis of thyroid cancer and also has a role in sub-typing thyroid malignancies. The accuracy of FNAB has increased with the use of ultrasound guided FNAB. An air-filled 10 cc syringe with its plunger partially retracted is attached to the 25-gauge needle. The nodule is immobilized with the index and middle fingers or thumb of the other hand and the needle is moved back & forth several times with a rapid, gentle, stabbing motion. The needle contents are immediately expelled onto clean glass slides for thin, evenly spread smears (195). At least 2, preferably, 3 punctures are performed to get at least six follicular cell groups; each should have 10-15 cells obtained from at least two aspirates of the nodule to get a diagnostic smear (161). Seven to 10% of FNAB are non-diagnostic and contributing factors to this rate are nodule composition, FNAB technique, and on-site assessment for specimen adequacy (5, 196).

The Bethesda system is currently used to report thyroid cytopathology assessments (4). The six diagnostic categories described in this system are (a) inadequate or non-diagnostic, (b) benign or hyperplastic, (c) atypia of undetermined significance/follicular lesion of undetermined significance, (d) follicular or HCN, (e) suspicious for malignancy, and (f) malignant (4, 5). Approximately 60-70% of all thyroid FNAs reports show benign cytology and these carry a less than 1% risk of malignancy (5). Three to 6% of FNAB are reported as atypia of undetermined significance probably due to poor specimen preparation or the presence of minimal atypical features in a predominantly benign appearing sample (4, 6). Follicular or HCN on FNAB are found in 6-12% FNAB specimens (197-200), and carry a 20-30% risk of malignancy (6). A histological assessment of vascular and/or capsular invasion is required to distinguish a FTC or FVPTC from benign FA (201-203). This is often possible only after examination of paraffin sections post-thyroidectomy. Frozen section is usually inadequate to make this distinction. Specimens suspicious for malignancy on FNAB account for 3-5% of cases. They display some nuclear features of the cancer in a small number of aspirated cells but not in the majority of the sample (4, 5, 204). Surgery is recommended in this group since the risk of malignancy is 50-75% (5). Finally, 3-7% of FNABs are considered malignant and require thyroidectomy, as they display conclusive features of malignancy with a PPV of malignancy in 100% of cases (5).

FNAB samples from indeterminate thyroid nodules can be analyzed further for the identification of molecular markers of malignancy, like BRAF and RAS mutational status or by panels that include multiple genes (205, 206). As no single molecular marker can

definitively prove or rule out malignancy in all indeterminate thyroid nodule, Disease State Commentary from the AACE Thyroid Scientific Committee and a consensus statement from the ATA Surgical Affairs Committee recommends that molecular marker testing on indeterminate FNAB specimens is not intended to replace other sources of information or clinical judgement (12, 207, 208). A seven-gene panel of genetic mutations, miRInform (Asuragen), looks at 17 known genetic alterations in seven validated molecular markers (KRAS, BRAF, HRAS, NRAS, RET/PTC 1, RET/PTC3 and PAX8/PPARγ) and rearrangements (BRAF, RAS, RET/PTC, PAX8/PPAR) (197, 209). Because of its high specificity (86%−100%) and PPV (84%−100%), it has been used as a rule-in test (197, 198, 206, 210-212), but with a low sensitivity (44-100%) (206, 210, 212). Next-generation sequencing (ThyroSeq) of an expanded panel of point mutations, single base insertions/deletions and gene rearrangement overcomes this limitation with a reported sensitivity of 90% (213, 214). A next generation sequencing panel allows for simultaneous sequencing of 284 mutations in AKT1, BRAF, CTNNB1, GNAS (guanine nucleotide binding protein, alpha stimulating), HRAS, KRAS, NRAS, PIK3CA, PTEN, RET, TP53, andTSH receptor genes.

Use of a gene expression classifier, such as the Afirma® Thyroid FNA Analysis (Veracyte) (167 GEC; mRNA expression of 167 genes) categorizes thyroid nodules as either "benign" or "suspicious" by measuring expression of 167 genes via messenger RNA, thereby reducing unnecessary surgery (200, 215). Alexander et al. reported Afirma® gene expression classifier to have 92% sensitivity with a specificity of 52% and NPV of 93%

for "atypia (or follicular lesion) of undetermined clinical significance," "FN or lesion suspicious for FN," or "suspicious cytological findings" to be 95%, 94%, and 85%, respectively (216). With a high sensitivity, it has been suggested as a rule-out test to exclude the possibility of malignancy in indeterminate thyroid nodule.

Immunohistochemical stains, such as galectin-3, have been examined in multiple studies of histologically confirmed thyroid FNA samples with indeterminate cytology, with reports of relatively high rates of specificity (93%), but low sensitivity (78%). The estimated PPV and NPV for cancer detection were 82% and 91%, respectively (217). Nuclear Galectin-3 overexpression along with nuclear phosphoglycerate kinase 1 (PGK1) loss has been suggested to be a highly effective combination for distinguishing malignant from benign thyroid nodules on FNAB (218). Similarly, in a prospective study, immunohistochemical stains for Hector Battifora Mesothelia-1 (HBME-1) has shown a sensitivity, specificity, PPV, and NPV of 78.67%, 84.13%, 85.51%, and 76.81%, respectively (219). These diagnostic tests can run into thousands of dollars and thus, the ATA felt that until an expert consensus review of existing data can be completed, no evidence-based recommendation for or against their use can be made (220).

2.8   *Histopathology of thyroid carcinoma*

Histology is the gold standard for diagnosis and subtyping of thyroid carcinoma. Diagnostic features such as the nuclear atypia, capsular and lympho-vascular invasion, architectural distortion, tumor embolization, and immunohistochemical profile are

available on histopathological examination. Histopathology also provides information on the prognostic features like size, ETE, lymph node positivity and completeness of resection (margin status). WDTC accounts for over 90% of all thyroid malignancies (221) and comprises of papillary, follicular, and Hürthle cell variant of follicular carcinoma in descending order of incidence and carries excellent prognosis (222, 223).

2.8.1 Papillary thyroid carcinoma (PTC)

PTC is the most common type of thyroid cancer. The diagnosis of PTC is based on the nuclear characteristics of the tumor, like having powdery to clear chromatin described as "Orphan Annie eye" nuclei. Cells in PTC appear to have overlapping and small nucleoli, nuclear grooving, an irregular "raisin-like" nuclear membrane and sometimes nuclear pseudo-inclusions (224). The papillary structures of the classic PTC are complex "finger-like" projections with fibro-vascular core. There are several histological variants of classic PTC which include the encapsulated or the more aggressive variants, such as the tall cell, insular, diffuse sclerosing, columnar cell and the follicular variants (FVPTC). The encapsulated variant has a very low metastatic potential. The FVPTC is the most common variant of PTC after the classic PTC. FVPTC displays the same characteristic nuclear features as classic PTC, but has a follicular rather than papillary architecture (224, 225). FVPTC are often difficult to diagnose because of the cytological similarity to follicular adenoma (226). The clinical and genetic differences between classic PTC and FVPTC account for the more aggressive behavior of the FVPTC. It presents with a higher rate of central compartment lymph node metastasis and BRAF mutation (226). Encapsulated

FVPTC has been recently reclassified as non-invasive follicular thyroid neoplasm with papillary-like nuclear features (NIFTP) (227).

The more aggressive variants of PTC include tall cell, insular, diffuse sclerosing, and columnar cell variants. Tall cell variant is usually seen in older males and is associated by vascular and ETE (224). At least 50% of these PTC cells have granular eosinophilic cytoplasm and a height twice that of the width; they carry a poorer prognosis (224, 228, 229). The presence of BRAF mutation in tall cell variants may account for this increased tumor aggressiveness (230). The diffuse sclerosing variant of PTC is usually seen in the young adult females, young children and adolescents who present with diffuse involvement of both thyroid lobes without the formation of a localized mass (231). A dominant nodule is present in about 50% of these cases (231). This thyroid tumor variant often coincides with previous or ongoing lymphocytic thyroiditis and has abundant psammoma bodies (circular and often micro-calcified structures), diffuse stromal fibrosis, dense lymphoid infiltration, extensive squamous metaplasia, and nuclei similar to classic PTC. These tumors appear more aggressive with higher rate of lymph node and pulmonary metastases but do not have increased mortality (224, 231). The columnar cell variant, an infrequent variant of PTC, consists of pseudo-stratified columnar cells with elongated hyper-chromatic nuclei, as well as supra- and sub-nuclear cytoplasmic vacuoles (224). Its encapsulated form does not metastasize, however, the un-encapsulated form of this variant displays a more aggressive behavior (231).

The insular variant consists of well-defined nests of tumor cells with scant cytoplasm and dark, round, monomorphic nuclei, cytological uniformity, hyper-cellularity, and scant colloid (232). These tumors are larger with higher nuclear to cytoplasmic ratio and lack nuclear grooving and intra-nuclear inclusions that are generally seen in classic PTC (232). This is a more aggressive variant of PTC, which is considered by some as a poorly-differentiated form of PTC because this variant still shows radioactive iodine uptake, a process that does not occur in undifferentiated thyroid carcinoma. The insular variant is associated with aggressive features like ETE, lymph node metastasis, distant metastasis, and a poor prognosis (233). As their histological and biological behavior is intermediate between PTC and ATC in aggressiveness, they require more aggressive treatment involving surgery, radioactive iodine (RAI) and external beam radiation in selected cases for gross residual disease.

2.8.2 Follicular thyroid carcinoma (FTC)

FTC typically have micro-follicular architecture with cuboidal cells lining the follicles. They can be well-differentiated with normal follicles, minimal invasion and colloid or poorly-differentiated with solid growth pattern, no follicles, marked nuclear atypia, and extensive vascular and/or capsular invasion (234). The former carries excellent prognosis and the latter has very poor prognosis. Features consistent with PTC, such as psammoma bodies and nuclear changes are typically absent but they can be seen in FVPTC.

FTC are more common in iodine deficient areas with underlying endemic goiters. Based on the extent of capsular invasion they are classified as minimally invasive follicular cancer with microscopic penetration of the tumor capsule without vascular invasion, while diffusely invasive follicular cancer extends beyond the tumor capsule into blood vessels and adjacent thyroid parenchyma (234, 235). Angio-invasive follicular cancer may be associated with distant metastases (236).

2.8.3   Oncocytic (Hürthle cell) carcinoma

Oncocytic (Hürthle cell, or oxyphilic) variants of both papillary and FTC have been identified. Oncocytic variant of PTC is comprised of large polygonal cells, nuclear features characteristic of PTC with prominent central nucleoli and granular eosinophilic cytoplasm (224). The Hürthle cell type of FTC shows focal papillary architecture and presents with a more aggressive clinical course (235). The abundance of mitochondria within the cytoplasm gives it an eosinophilic granularity (224).

2.8.4   Medullary thyroid carcinoma (MTC)

Medullary thyroid carcinoma have neuroendocrine origin and arise from the para-follicular C cells. MTC is characterized by plasmacytoid, spindle/clear cells with neuroendocrine nucleus arranged in organoid or trabecular (in form of rods) shape or in cell nests. Amyloid deposition (thyrocalcitonin) is observed in 60-80% of MTC. On immunohistochemistry, MTC is positive for chromogranin, calcitonin and carcinoembryonic antigen.

2.8.5 Anaplastic thyroid carcinoma (ATC)

Anaplastic thyroid carcinoma are extensively infiltrative and characterized by atypical cells, either spindle, epithelioid, squamoid, giant or osteoclast-like giant cells with abundant atypical mitotic figures and multinucleated cells (41, 114). The spindle cell variants are sometimes arranged in fascicles to resemble sarcoma, while at other times they are arranged to resemble fibrous histiocytoma (52). The giant cell variant is more pleomorphic and has numerous tumor giant cells, whereas the squamoid type is characterized as having irregular configuration and abundant cytoplasm (52). These variants are described as tan white fleshy large tumors with large areas of hemorrhage, high mitotic activity, necrosis, marked invasiveness, and a low rate of apoptosis (237). It has been suggested that well-differentiated thyroid carcinoma may progress towards ATC through de-differentiation of insular variants of PTC or FTC and altered expression of p53 (52). This fact is further supported by co-existing findings of differentiated thyroid cancer in up to 90% of ATC (52).

Upon initial presentation, ATC are usually identified as rapidly growing single nodule or multiple nodules, often over 5 cm, with pressure symptoms and hoarseness (52). The diagnosis of ATC can be accurately confirmed by FNAB in 90% cases (238). Failure of FNAB to diagnose ATC may be due to sampling error. ATC can also be incidentally found in patients who have undergone surgery for a WDTC (52). For 51 ATC patients treated with radiotherapy for local control, the median survival was found to be 7.5 months, versus 1.6 months for patients without local control (239). Since many ATC patients

present with distant metastases, chemotherapy becomes an important player in the multimodal management of ATC. Regardless of the use of monotherapy (doxorubicin) or combination therapies (i.e. cisplatin, bleomycin, melphalan, paclitaxel), the response rates are very disappointing (52). Only a few patients show improvements and patients are not reported to have complete response, often due to development of chemoresistance (52). Cancer cells often utilize the oncofetal nucleoprotein high-mobility group A2 (HMGA2) to gain increased transformative cell plasticity, prevent apoptosis, and to enhance metastasis of chemoresistance (240). A combination of 8 biomarkers: thyroglobulin, bcl-2, MIB-1, E-cadherin, p53, beta-catenin, topoisomerase II-alpha, and vascular endothelial growth factor are reported to successfully distinguish differentiated from anaplastic thyroid tumors (241).

2.9   *Prognostic factors in thyroid cancer*

Prognostic factors determining oncological outcome can be classified as the *patient factors* like age, gender; the *tumor factors* such as histology, grade, tumor size, multifocality, ETE, nuclear atypia, vascular invasion, tumor necrosis, DNA ploidy, lymph nodal and distant metastasis; and the *treatment factors* i.e. completeness of resection, extent of thyroidectomy and adjuvant RAI (15, 18, 20, 21, 27).

2.9.1   Histology

Tumor histology is one of the most important prognostic factors. Prognosis is worst with ATC, followed by insular carcinoma/ PDTC, and MTC. Although ATC is rare with

an age-adjusted annual incidence of 2 per million/year (242), its lethality is highlighted by the fact that out of approximately 1,200 thyroid cancer deaths in the USA in 2006, over 50% of reported thyroid cancer deaths were due to ATC, even though ATC accounts for only 2% of all thyroid carcinomas (41). The aggressive variants of PTC, including tall cell, follicular, columnar cell, and insular variants, carry poor prognosis as compared to the classical PTC. Minimally invasive FTC has better outcome compared to widely invasive PTC.

2.9.2 Age

Age at the onset of WDTC is a critical predictor of patient outcome (47). An age cut-off of 45 years is currently used by WDTC staging guidelines of UICC (18). Patients under this age cut-off are considered stage I, if they have no distant metastasis; and stage II, with distant metastasis. Any metastatic tumor in an older patient (over 45 years) is considered as stage IV disease. Patients above 45 years are considered to have stage III disease if their tumor is larger than 4 cm, has minimal ETE, or regional lymph node metastasis. Other studies have suggested different age cut-offs, ranging from 50 to 60 years (222, 243, 244). Our recent study concluded that the independent influence of age is not obvious until the age of 55 years (49). After the threshold age of 55 years, the DSS was reported to fall with increase in age. An age threshold of 55 years was found to be better than 45 years that is currently used in the TNM staging by us (49, 245). A large multi-institutional study involving 9484 patients from 10 centres in the USA, Canada and Brazil confirmed this observation (246).

2.9.3   Tumor size

The size of the tumor correlates with the prognosis for patients with thyroid carcinoma (18). The larger the tumor size, the more likely is the presence of loco-regional and distant metastases (25). Also, the risk of recurrent disease and cancer-specific mortality increases linearly with tumor size (47). A study by Mazzaferri et al. reported that tumors <1.5 cm in size had a 0.4% 30-year cancer-specific mortality rate as compared to 22% for tumors >4.5 cm (25).

2.9.4   Gender

Mortality rates and recurrence rates are higher among men than women (25, 47). The DSS in WDTC has been reported to be independently influenced by the male gender (49). Males in a population cohort with WDTC had a 50% higher risk of cancer recurrence and double the risk of dying of their cancer as compared to their female counterparts (49).

2.9.5   Lymph node metastasis

Thyroid cancers, especially PTC and MTC, can spread to the lymph nodes in the central compartment (between the two carotid arteries) and the lateral compartments of the neck. At the time of presentation, 15-30% of patients have clinically evident regional lymph node involvement. With the widespread use of ultrasonography, higher rates of lymph node metastasis have been reported (47, 247, 248). The clinical importance of lymph node metastasis is controversial with evidence showing either no difference in survival for patients with or without lymph node metastasis (17, 249), increased risk of recurrence (25,

250), or reduced survival (251). A study of the SEER database concluded that patient age was an important factor influencing survival for patients with lymph node metastasis. The patients aged < 45 years lymph node metastasis had no effect on survival as compared to a 46% increased risk of death for patients in patients older than 45 years (p<0.001) (252).

2.9.6 Extra-thyroidal extension (ETE)

Approximately 30% of PTC extend beyond the thyroid margins into surrounding musculature, recurrent laryngeal nerve, esophagus, or trachea. This is associated with high risk of recurrence (25, 47, 253). These tumors require aggressive surgical resection, radioactive iodine and possibly external beam radiotherapy (254, 255). ETE is also associated with an increased risk for recurrent disease, as well as higher risk of lymph node metastasis and a greater risk of dying of thyroid cancer (25, 256, 257). ETE is considered an important prognostic factor in most of the staging systems for WDTC (Table 1).

2.9.7 Distant metastases

At the initial presentation, 5-10% of patients have distant metastases and an additional 2.5-5% of patients will be found to have distant metastases on initial RAI (47). Fifty percent develop distant metastases in the lungs, 25% only in the bone, 20% have metastases at both sites, and about 5% develop distant metastases to other sites (258, 259). Distant metastasis is one of the strongest determinants of poor survival in WDTC (49).

Table 1: Summary of prognostic factor and staging systems for thyroid cancer.

Prognostic variable	EORTC (1979)	NTCTCS (1998)	TNM (2009)	AMES (1988)	Ohio State Univ (1994)	MSKCC (1995)	Univ of Muntser (1997)	MDA/UAB (2000)	AGES (1987)	Univ. of Chicago (1990)	MACIS (1993)	Murcia (2000)
Reference	(14)	(15)	(18)	(19)	(25)	(26)	(261)	(260)	(16)	(23)	(17)	(27)
Age	×	×	×	×	-	×	-	×	×	-	×	×
Sex	×	-	-	×	-	-	-	-	-	-	-	-
Size	-	×	×	×	×	×	×	-	×	-	×	×
Histology	×	×	-	-	-	×	-	-	-	-	-	×
Grade	×	×	-	-	-	-	-	-	×	-	×	×
Mutifocality	×	Number of foci	×	-	Number of foci	-	-	-	×	-	-	-
Extrathyroid extension	×	×	×	×	-	×	-	-	×	×	×	×
Lymph node metastasis	-	×	×	-	-	-	-	-	-	×	-	-
Distant metastasis	×	×	×	×	×	×	×	×	×	×	×	×
Incomplete resection	-	-	-	-	-	-	-	-	-	-	×	-
Histological type	All histological types			WDTC						Only PTC		

48

Multitudes of risk stratification systems (Table 1) have considered distant metastasis as an important prognostic factor for WDTC (14-19, 21, 23-28, 260, 261). Metastatic PTC patients have over 50% mortality (258, 259, 262). Survival is better in younger patients, patients with microscopic disease, and patients with iodine-avid tumors (258, 262, 263). An age threshold of 45 years is currently used by the American Joint Committee on Cancer (AJCC)/Union Internationale Contre le Cancer (UICC) system for stage grouping of WDTC (18). Based on the TNM staging system, WDTC patients younger than 45 years with distant metastasis are considered as stage II, whereas WDTC patients $\geq$ 45 years of age with distant metastasis are considered to be stage IVC.

2.10   Staging/ prognostic scoring system for thyroid cancer

Various staging/ risk stratification systems are developed to aid in prognostication of thyroid cancer patients, predicting risk of death from thyroid cancer, and in making decisions on post thyroidectomy adjuvant therapy. For the risk of recurrence, patients are stratified into three categories depending on certain criteria that could account for increased risk of recurrence and death of disease (161). Low-risk patients have no lymph node or distant metastases or <5 micro-metastases; fully resected macroscopic tumors; no tumor invasion of loco-regional tissues or structures; no aggressive histology (i.e. tall cell or insular variant) or vascular invasion or; no ^{131}I uptake outside the thyroid bed (161, 264). Intermediate-risk patients have microscopic invasion of tumor into the peri-thyroidal soft tissues at initial surgery; cervical lymph node metastases < 3 cm or >5 micro-metastases or ^{131}I uptake outside the thyroid bed (265); tumor with aggressive histology (columnar,

tall cell or insular variants) or vascular invasion (>4 foci in FTC) (161). <u>High-risk patients</u> have macroscopic tumor invasion, aggressive histology, incomplete tumor resection, lymph nodes > 3 cm in size or distant metastases, and telomerase reverse transcriptase (TERT) and BRAF mutation (161).

2.10.1 European Organization for Research and Treatment of Cancer (EORTC)

European Organization for Research and Treatment of Cancer (EORTC) was one of the earliest prognostic scoring system that was based on Weibull survival model, developed after a multivariable analysis of 507 patients from 23 European hospitals for staging all histologic types of thyroid carcinoma (14).

Total score = Patient's age +12 if male +10 if poorly differentiated FTC +10 if invasion of the thyroid capsule +15 if one distant metastasis +30 if 2 or more distant metastases +10 if medullary +45 if the principal or associated cell type is anaplastic.

Risk groups: Group 1 = score < 50   Group 2 = score 50–65   Group 3 = score 66–83

Group 4 = score 84–108   Group 5 = score >108

2.10.2 Mayo Clinic (AGES or Age, Grade, Extent, Size)

The AGES scoring system was developed from a multivariable analysis of more than 14,200 patient-years' experience in 860 PTC patients at Mayo Clinic (16).

Total score = 0.05 x age in years (if aged $\geq$40) or + 0 (if aged<40) +1 (if tumor grade 2) or +3 (if tumor grade 3 or 4) +1 (if ETE) +3 (if distant spread) + 0.2 x tumor size (maximum diameter in cm)

Risk groups: Group 1 = score <4.00   Group 2 = score 4.01–4.99

Group 3 = score 5.00–5.99   Group 4 = score $\geq$ 6

2.10.3 Lahey Clinic (AMES or Age, Metastases, Extent, Size)

The AMES staging system was developed from a cohort of 814 patients with differentiated thyroid cancer using age and size as categorical variables. Different age cut-off were used for risk stratification in men (41 years) and women (51 years) (19).

Risk groups:

Low-risk group: a) Young patients (men<41years, women<51years), no distant metastases

b) Older patients with intra-thyroidal papillary cancer or minor tumor capsular involvement follicular carcinoma, tumor size < 5 cm, no distant metastases

High-risk group: a) All patients with distant metastases

b) All older patients with major capsular involvement papillary cancer or major capsular involvement follicular carcinoma and tumor size $\geq$ 5 cm

2.10.4 University of Chicago (Clinical Class)

The Clinical Class system was developed from a cohort of 269 PTC patients with average follow-up period of 12 years from the time of diagnosis. It is one of the few systems where age is not included in the classification, despite being a significant factor in multivariable analysis (23)

Classes: Class I: Patients have disease limited to the thyroid gland

Class II   Patients have loco-regional lymph node involvement

Class III: Patients have extra-thyroidal tumor invasion

Class IV: Patients have distant metastases

2.10.5 Karolinska Hospital and Institute (DAMES or DNA ploidy, Age, Metastases, Extent, Size)

Addition of nuclear DNA content to the AMES risk-group classification for PTC was found to add prognostic value to the existing AMES risk-group classification. Nuclear DNA content was measured both on the fine needle aspiration material and the surgical specimen in 73 patients with primary or recurrent PTC (21). This staging system however, does not assign a risk group to low risk AMES group with aneuploid tumors.

Risk groups:

Low risk: Patients in AMES low risk group and had euploid tumors

Intermediate risk: Patients in AMES high risk group and had euploid tumors

High risk   Patients in AMES high risk group and had aneuploid tumors

2.10.6 Mayo Clinic (MACIS or Metastases, Age, Complete resection, Invasion, Size)

MACIS was developed as an alternative to AGES at the Mayo Clinic, using a cohort of 1779 patients of PTC because the tumor grade is not often available at most centers (17).

Total score = 3.1 (if aged $\leq$39 years), or 0.08 x age (if aged $\geq$ 40 years), + 0.3 x tumor size in cm, +1 (if not completely resected), +1 (if locally invasive), +3 (if distant metastases)

Risk groups: Group 1 = <6.0   Group 2 = 6.0–6.99

              Group 3 = 7.0–7.99   Group 4 = > 8.0

2.10.7 University of Bergen (SAG or Sex, Age, Grade)

SAG staging was developed by the retrospective analysis 173 consecutive patients with PTC by combining sex and age of the patient and histologic grade based on nuclear atypia, tumor necrosis, and vascular invasion (22).

Total score = 1 (if male) + 1 (if aged $\geq$70 years) + 1 (if any one of the 3 microscopic features, such as vascular invasion, marked nuclear atypia and tumor necrosis are present)

Risk groups: SAG I = score is 1   SAG II = score is 2   SAG III = score is 3

2.10.8 Ohio State University (OSU)

The Ohio State University staging system was based on the multivariable analysis of tumor size, lymph node involvement, multifocality, local tumor invasion, and distant metastases in 1355 patients with papillary and FTC (25).

Stages: Stage 1: Primary tumor smaller than 1.5 cm in diameter

   Stage 2: Primary tumor 1.5–4.4 cm, or presence of cervical lymph node

           metastases, or more than 3 intra-thyroidal foci of tumor

   Stage 3: Primary tumor at least 4.5 cm or presence of ETE.

   Stage 4: Primary tumor with distant metastases

2.10.9 Noguchi Thyroid Clinic (Noguchi)

Based on multivariable analysis of 2192 PTC patients with mean follow-up of 12.5 years, patients were divided into 3 risk groups (excellent, intermediate, or poor) based on gender, age, tumor size, ETE, and gross lymph node metastases. The independent significant factors for the male sex were age and gross lymph node metastases, whereas for the female sex, they were age, gross lymph node metastases, tumor size, and ETE (24). Risk groups are described separately for men and women:

Men:

Excellent group: All patients up to 45 years of age and patients without gross nodal metastasis up to 60 years of age.

Intermediate group: Patients without gross nodal metastasis over age 60 and patients aged 45 to 55 with gross nodal metastasis.

Poor group: Patients over 55 with gross nodal metastasis.

Women:

Excellent group: All patients up to age 50 and patients age 50 to 55 without metastasis.

Intermediate group: Patients age 50 to 55 without gross nodal metastasis, patients over age 65 with primary tumor less than 30 mm in maximum diameter, and patients with gross nodal metastasis at 50 to 55 years of age.

Poor group: Remaining patients.

2.10.10 Memorial Sloan Kettering (Grade, Age, Metastases, Extent, Size or GAMES)

Based on the outcome of consecutive series of 1038 previously untreated patients with differentiated carcinoma of thyroid treated at Memorial Sloan Kettering Cancer Center, an age of 45 years and tumor size of 4 cm were considered as the cut-off points for continuous variables for risk stratification (26).

Risk groups:

Low risk: Age <45, no distant metastases, tumor size <4 cm and PTC on histology

Intermediate risk: Age <45, distant metastases, tumor size >4 cm or FTC on histology

                   Age $\geq$ 45, no distant metastases, tumor < 4 cm and PTC on histology

High risk: Age $\geq$ 45, distant metastases, tumor size >4 cm or FTC on histology

2.10.11 University of Münster (Münster)

This system is based on analysis of primary tumor and distant metastasis in 500 WDTC (almost 40% patients had FTC) with median follow-up of 5.6 years (261) .

T1: tumor size =1 cm   T2: size 1–4 cm   T3: size >4, limited to thyroid

T4: any size beyond capsule   M0, no distant metastases   M1, distant metastases

Risk groups: Low risk = T1–3 and M0   High risk = T4 or M1

2.10.12 National Thyroid Cancer Treatment Cooperative Study (NTCTCS)

This staging system was validated prospectively on 1607 patients recruited from 14 U.S. institutions. For PTC, significant factors include age, size, ETE, and metastases. For FTC, they include age, size, metastases, and poor differentiation. Parameters selected in

this system were age, tumor size, tumor type, ETE, lymph node, and distant metastases. Several factors tended to predominate in the assignment of tumor stage for each histologic type (15). Stage is determined by the highest stage determined by the following clinico-pathological factors:

Factors	Histology			
	PTC		FTC	
Age	<45 years	≥ 45 years	<45 years	≥ 45 years
Tumor size (cm)				
<1 cm	I	I	I	II
1–4 cm	I	II	I	III
>4 cm	II	III	II	III
Tumor description				
Microscopic multifocal	I	II	I	III
Macroscopic multifocal	I	II	II	III
Microscopic extra-thyroidal	I	II	I	III
Macroscopic extra-thyroidal	II	III	II	III
Poor differentiation	Not available	Not available	III	III
Metastases				
Cervical lymph node	I	III	I	III
Distant	III	IV	III	IV

MTC

C-cell hyperplasia	I
Tumor size < 1 cm	II
Tumor size ≥ 1 cm or positive cervical lymph nodes	III
Extra glandular invasion or extra cervical metastases	IV

ATC	IV

2.10.13 University of Alabama and M.D. Anderson (UAB &MDA)

This risk grouping was developed using a regression model obtained from a retrospective study on 208 patients with WDTC from two US institutions (260).

Risk groups:

Low-risk = patients <50 years of age without distant metastases

Intermediate risk = patients > 50 years of age without distant metastases

High-risk = patients of any age with distant metastases

The risk groups are further subdivided based on the tumor size (≤3 cm and >3 cm)

2.10.14 Virgen de la Arrixaca University at Murcia (Murcia)

This system calculates prognostic index based on 4 prognostic factors obtained from univariate and multivariate analyses on a cohort of 200 PTC patients (27).

Prognostic index = (3 x age score) + (2 x size score) + (6 x spread score) + (2 x histologic variant score)

Age score: 1 if aged <50 years,   2 if aged $\geq$50 years

Size score: 1 if tumor size from 1–4 cm,   2 if tumor size >4 cm

Spread score: 1 if intra-thyroidal,   2 if extra-thyroidal

Histologic variant score: 1 if well-differentiated, FVPTC or diffuse sclerosis variant,

                 2 if solid or tall-cell variant PTC,   3 if poorly differentiated PTC

Risk groups: Low risk = index <18 Medium risk = index 18–22 High risk = index >22

2.10.15 Cancer Institute Hospital in Tokyo (CIH)

This system uses 4 prognostic parameters: age, distant metastases, ETE, and large nodal metastases. These parameters were derived from a multivariate analysis of 604 PTC patients with mean follow-up of 10.6 years for stratification into two risk groups (28).

Risk groups: High risk: Patients of any age with distant metastasis or patients 50 years or older with $\geq$3 cm nodal metastasis and/or ETE

Low risk: Those who did not meet the high-risk criteria

2.10.16 Ankara Oncology Training and Research Hospital in Turkey (Ankara)

This system classifies patients into 4 risk groups that were identified by the logistic regression equation, and developed from a cohort of 347 WDTC patients (20).

Pre-treatment score: exp [(0.2 x tumor size) + (1 if age >45 years) + (0.5 if angioinvasion) + (1 if distant metastasis)]

Post-treatment score: exp [(0.2 x tumor size) + (0.8 if age >45 years) + (0.7 if

angioinvasion) + (0.6 if distant metastasis) + (0.9 if total/near total

thyroidectomy) + (0.7 if use of adjuvant radioiodine)]

Pre-treatment probability of cancer-specific mortality (P) = (score)/ (1+score)

Risk groups: Very-low risk- $P \leq 55\%$

Low risk- P from 56%- 85%

High risk- P from 86%- 95%

Very high risk- $P \geq 96\%$

Post-treatment risk groups were not defined

2.10.17 UICC/AJCC TNM Staging (Tumor, node, metastasis)

The TNM staging system, first described in the 1940s, takes into account the anatomic extent of the primary tumor (T), the involvement of regional lymph nodes (N), and distant metastasis (M). It allows standardized information gathering and sharing as well as quantification of the cancer burden and possible prediction of the oncological outcome. According to the current TNM classification of malignant tumors (7th Edition), the staging of thyroid cancer International Classification of Diseases for Oncology (ICD-O C73) is unique as the patient's age and histological tumor type determine the stage of disease in addition to the T category, N category, and M category (18).

T-   Primary Tumor

Tx -   Primary tumor cannot be assessed

T0 -   No evidence of primary tumor

T1 -   Primary tumor ≤2 cm in greatest dimension and limited to the thyroid

(T1a ≤ 1cm; T1b 1-2 cm in greatest dimension, both limited to the thyroid)

T2 -   Primary tumor >2 and ≤4 cm in greatest dimension and limited to the thyroid

T3 -   Primary tumor >4 cm in greatest dimension, limited to the thyroid or any tumor

with minimal extra-thyroid extension (sternothyroid muscle/ peri-thyroidal tissue)

T4a-   Any tumor extending beyond the thyroid capsule to invade subcutaneous soft

tissues, larynx, trachea, esophagus, or recurrent laryngeal nerve

Intra-thyroidal anaplastic thyroid carcinoma - surgically resectable

T4b -   Any tumor invading prevertebral fascia or encasing the carotid / mediastinal vessels

Extra-thyroidal anaplastic thyroid carcinoma - surgically unresectable

N-   Regional Lymph Nodes

Nx -   Regional lymph nodes cannot be assessed

N0 -   No evidence of regional lymph nodes

N1a - Metastasis to level VI nodes (pretracheal, paratracheal, and prelaryngeal/

Delphian)

N1b - Metastasis to unilateral, bilateral or contralateral cervical, retropharyngeal or

superior mediastinal nodes

M-   Distant Metastasis

M0 -   No distant metastasis

M1 -   Distant metastasis

Stage Groupings

Papillary or Follicular

Stage	Patient age <45y	Patient age ≥45y
I	Any T, Any N, M0	T1, N0, M0
II	Any T, Any N, M1	T2, N0, M0
III		T3, N0, M0
		T1-3, N1a, M0
IVA		T4a, Any N, M0
		T1-3, N1b, M0
IVB		T4b, Any N, M0
IVC		Any T, Any N, M1

Medullary (Any age)

Stage	
I	T1, N0, M0
II	T2-3, N0, M0
III	T1-3, N1a, M0
IVA	T4a, Any N, M0
	T1-3, N1b, M0
IVB	T4b, Any N, M0
IVC	Any T, Any N, M1

Anaplastic (Any age)

Stage

IVA   T4a, Any N, M0

IVB   T4b, Any N, M0

IVC   Any T, Any N, M1

The existence of multiple risk stratification systems for predicting outcome of thyroid cancer indicates that none is universally acceptable, and a prognostic system to predict individualized patient's risk rather than the stratified group risk is required.

2.11 Treatment

Most thyroid cancers are treated with radical intent and carry excellent prognosis after appropriate treatment. Surgery, either hemi or total thyroidectomy with or without lymph node dissection is the mainstay of treatment for most thyroid cancer. Radioactive iodine is an effective adjuvant treatment for high risk WDTC.

2.11.1 Thyroidectomy

Surgery in the form of either a hemi-thyroidectomy or a total thyroidectomy, with or without adjuvant radioactive iodine, is the treatment of choice for most thyroid carcinoma. For low risk WDTC that are intra-thyroidal, micro-invasive, unifocal, and less than 1 cm in size (micro-carcinoma), hemi-thyroidectomy is a safe option. For node negative WDTC, 1-4 cm in size, options of both hemi-thyroidectomy and total

thyroidectomy exist. For WDTC $\geq$ 4cm, with ETE or bilateral disease, with cervical lymph node or distant metastasis, lympho-vascular invasion, prior irradiation to head and neck, familial thyroid cancer, a total thyroidectomy is usually recommended (12). Advocates of total thyroidectomy cite the incidence of 30-87.5% of occult papillary carcinomas in the contralateral lobe (266, 267) and 7-10% chance of recurrence in the opposite lobe (268) as evidences to support the recommendation of total thyroidectomy. Lower recurrence rates and possibly increased survival after total thyroidectomy (269), facilitation of earlier detection of recurrent or metastatic carcinoma with radio-iodine & thyroglobulin and the possibility of treatment of recurrent or metastatic carcinoma with radio-iodine (268) are the other considerations to recommend total thyroidectomy. Surgical complications after thyroid cancer surgery include hemorrhage, wound infection, superior or recurrent laryngeal nerve palsy resulting in vocal cord malfunction (unilateral or bilateral in 1-2% cases), hypocalcaemia (transient or permanent in 3-5% patients) and rarely pneumothorax. Therapeutic level VI neck dissection or central compartment lymph node dissection (CCND) is indicated for patients with clinical or radiological evidence of central or lateral neck lymph nodes. Prophylactic CCND (unilateral or bilateral) may be done in PTC with no clinical evidence of lymph node metastasis in the central compartment of the neck, especially for T3/ T4 cancers. CCND is not indicated for small (T1 or T2), non-invasive, clinically node-negative PTC and most follicular cancers. MTC is treated with total thyroidectomy and elective CCND. A formal therapeutic neck dissection is recommended for all node positive (N1b) thyroid cancer. The majority of patients with ATC are unsuitable for surgery at the time of diagnosis due to significant extension of the tumor

beyond the thyroid gland, thereby making any meaningful resection impossible and dangerous (52). However, some patients with localized disease not affecting surrounding vital structures, where complete resection of the ATC is possible, can have prolonged survival after surgery and adjuvant treatment (52).

TSH suppression results in a 27% reduction in risk of adverse outcome in WDTC. Total TSH suppression (TSH level= 0.1-0.5 mU/L) is recommended for high risk patients, whereas low risk patients need only partial TSH suppression (TSH level= 0.5-2.0 mU/L). Careful monitoring of TSH levels is essential especially in post-menopausal females and elderly with pre-existing cardiac ailment. A starting dose of levothyroxine is 2 µg/ kg / day (age <60 years) or 1.6-1.8 µg/ kg / day (age ≥ 60 years), which is adjusted based on TSH level on follow-up.

2.11.2 Adjuvant treatment

After surgical removal of the thyroid in patients with WDTC, RAI (in the form of ^{131}I) is administered to destroy any residual thyroid tissue and for subsequent detection of loco-regional and/or metastatic disease (270). As adjuvant therapy, radioactive iodine helps to decrease the risk of recurrence and mortality by destroying suspected metastatic disease. It is also used for salvage treatment of any persistent or recurrent disease as therapeutic RAI therapy (161). Indications of RAI treatment include advanced TNM stage, presence of lymph node metastasis, ETE, and incomplete resection (271). Unstimulated thyroglobulin measurement performed after total thyroidectomy can be used to assess the

need for adjuvant RAI in WDTC, thereby sparing some patients from potential side effects of RAI, such as sialadenitis, lacrimal gland injury, and infertility (12, 272-274). For a low risk or low to intermediate risk patient, 30 milliCurie (mCi) is adequate, for intermediate risk patients an additional 150 mCi is recommended and for known structural residual disease 150-200 mCi (100-150 mCi for patients >70 years) is used (12).

External beam radiotherapy (XRT) has a limited role in the treatment of WDTC. The sequence of external beam XRT and RAI therapy depends on the volume of gross residual disease and RAI uptake. Patients with localized residual disease or with non-radioiodine concentrating de-differentiated carcinoma are candidates for adjuvant radiation. In ATC, external beam XRT is used either in an adjuvant or palliative setting for loco-regional control of the disease. Surgery followed by combined chemo-radiation is recommended for ATC patients with localized disease. Radiation is used as a palliative measure to prevent death by asphyxiation and possibly to increase survival by a few months (52). Radiotherapy alone is also sometimes used as a palliative measure to increase local control and short-term patient survival (239). In MTC, radiation treatment is of limited use and is restricted to patients with residual disease or in a palliative setting.

2.11.3 Targeted therapy

Targeted therapies are emerging treatment modalities for thyroid cancer. A common feature of many thyroid cancers is increased vascularization with elevated expression of VEGF as compared to the normal tissue. Drugs with anti-angiogenic

properties (Sorafenib, Sunitinib, Axitinib, and Pazopanib) are chosen for targeting the

vascular endothelial growth factor tyrosine kinase receptors (VEGFRs). The response rate

to targeted inhibition has been reported to be low and it is attributed to compensatory

signaling pathways that can rescue tumor growth (275). Other molecular targets in thyroid

cancer include the epidermal growth factor receptor (EGFR) that is targeted by Gefitinib,

the platelet-derived growth factor receptor (PDGFR) targeted by Pazopanib and Axitinib,

c-Kit targeted by Axitinib, or RAF and RET that are targeted by Sorafenib. Gene therapy,

aimed at transcription factors TTF-1 and PAX8 (involved in the transcriptional activation

of thyroid-specific genes, such as Tg and NIS), can improve the ability of ATC cells to

uptake radioiodine (41, 114). PDGFRα has been reported to mediate nodal metastases in

papillary thyroid cancer by driving the epithelial-mesenchymal transition (276). Recently

published results of the DECISION trial showed significant improvement ($p<0.001$) in

progression-free survival with Sorafenib (10.8 months) as compared with placebo (5.8

months) in patients with progressive radioactive iodine-refractory differentiated thyroid

cancer (277). Our recent work identified the receptor of advanced glycation end products

(RAGE)/Dia-1 signaling system as a mediator for the pro-migratory response of

extracellular S100A4 in human thyroid cancer which may become a suitable therapeutic

target to reduce local invasion and metastasis (278).

2.12 *Follow-up*

The efficacy of treatments is assessed by measuring serum Tg levels. Tg is a

prohormone of T4 and T3 and is synthesized by follicular cells of the thyroid and stored in

colloid. Small amounts of Tg are released into the serum with the release of T4 and T3. Tg is used as a marker for WDTC management and for the detection of residual/recurrent disease. Residual Tg after ^{131}I therapy may be indicative of persistent malignancy (270). Determinants of serum Tg concentrations are the mass of residual thyroid tissue; the presence of thyroid injury either due to thyroiditis or interventions such as FNAB, thyroidectomy or RAI therapy; and magnitude of TSH receptor stimulation (i.e. endogenous TSH, recombinant human TSH, serum human chorionic gonadotropin, TSH receptor antibodies associated with autoimmune thyroid disease) (279). Anti-Tg antibodies may also interfere with the detection of serum Tg level and result in falsely low levels, thereby limiting the accuracy of this assay. This is especially true for patients with autoimmune diseases where levels of anti-Tg antibodies may be higher than normal (280). Approximately 10% of the general population have anti-Tg antibodies compared to 20% for WDTC patients (281).

Serum Tg levels prior to surgery are not a reliable indicator of thyroid cancer because both normal and malignant thyroid cells release Tg. Since serum Tg is cleared with a half-life of 30 hours, it is expected to be undetectable if the patient is cured after total thyroidectomy and RAI ablation (279). However, it may take up to one year or longer for the levels to fall below the detection threshold (282). The detection threshold of most serum Tg assays was 0.8 ng/mL earlier. This has improved to 0.1 ng/mL or less with the newer available assays (283, 284). The sensitivity of Tg assay improves when Tg levels are measured after TSH stimulation either after thyroid hormone withdrawal or administration

of recombinant human TSH (rhTSH). Suppressed Tg <0.2 ng/ml, stimulated Tg <1 ng/ml and negative scanning qualify as excellent treatment response with 1-4% chance of recurrence and <1% risk of disease specific death. Suppressed Tg 0.2-1ng/ml, stimulated Tg <10 ng/ml with non-specific imaging and stable /declining anti-Tg Ab is considered indeterminate response with 15-20% chance of identification of structural disease on follow-up and <1% risk of disease specific death. Suppressed Tg ≥1ng/ml, stimulated Tg <10ng/ml, negative imaging and rising anti-Tg antibody titer is labelled as biochemical incomplete response with 20% chance of identification of structural disease on follow-up and <1% risk of disease specific death. At least 30% of biochemical incomplete responses resolve spontaneously and 20% achieve this after additional therapy. Structural/ functional evidence of disease at any Tg level with or without anti-Tg antibody is taken as structural incomplete response with 50-85% of the patients continuing to have persistent disease despite treatment. The risk of disease specific death is 11% with lymph node metastasis and 50% with distant metastasis. The target TSH level for patients with excellent or indeterminate response is 0.5-2mU/L (low-intermediate risk group) and 0.1-0.5mU/L (high risk patient). For patients with biochemical incomplete response TSH target is 0.1-0.5mU/L and TSH<0mU/L for those with structural incomplete response (12). The benefits of TSH suppression should be weighed against the risk of atrial fibrillation or tachycardia, osteoporosis or osteopenia, especially in post-menopausal women > 60 years of age.

Serum Tg is an important indicator for the requirement of radioactive remnant ablation (RRA) therapy after total thyroidectomy for patients with well-differentiated

thyroid carcinoma. The need for RRA therapy post total thyroidectomy is highly debatable. The ATA, the European Thyroid Association, and the British Thyroid Association have set different guidelines as to which PTC patients should receive residual remnant ablation therapy based on the risk of persistent disease or for developing recurrent disease (161, 264, 285). Thyroglobulin has no role in follow-up of ATC and MTC. Serum calcitonin is a good tumor marker for follow-up of MTC.

2.13   Summary of literature and objectives of this study

To summarize, thyroid cancer represents a group of different histological types with diverse clinical behaviour. Most thyroid cancers arise from follicular cells. The process of carcinogenesis is associated with a number of genetic alterations. Fine needle aspiration biopsy (FNAB) and ultrasonography play pivotal roles in the diagnosis of thyroid cancer. However, the sub-classification of a FN/HCN on FNAB remains a challenge. FDG-PET /CT scan of FN/HCN have been used for this purpose with variable success. Predicting the oncological outcome of thyroid cancer is an exciting field of research but developing a model that fits the different histological types and incorporates the patient, tumor and treatment variables remains a daunting task.

The objectives of this study were to evaluate the efficacy of FDG-PET/CT in predicting the risk of malignancy in FN/HCN and to perform an epidemiological analysis of prognostic markers in thyroid cancers for developing prognostic models to predict oncological outcome of thyroid cancer based on the individual's prognostic factors.

Chapter III

Materials and Methods

3.1   Assessment of the diagnostic role of FDG-PET /CT

3.1.1   Study group

The prospective arm of this study, approved by the Research Ethics Board at the University of Manitoba (Ethics reference number: H2010:056), included 47 consecutive consenting patients with 50 FN/HCN, >5mm in size, seen in the Thyroid clinic, CancerCare Manitoba from July 2013 to December 2015. The minimum sample size (N=44) was calculated for a power of 0.80 with alpha of 0.05, based on 20% risk of malignancy in FN/HCN nodules and 39% risk of malignancy in FDG-PET positive indeterminate nodules (7, 11). All patients had a prior ultrasonography and ultrasound guided FNAB showing FN/HCN. Histopathology results were considered as the gold standard for diagnosis(286).

3.1.2   FDG-PET/CT : Technique and calculations

A FDG-PET/CT scan was performed pre-operatively. All patients were asked to fast for 4 to 6 hours prior to the administration of F-18 FDG injection. To minimize the examination time and substantially reduce the radiation exposure, only a half-dose of FDG (185 MBq) was administered and patients were scanned in two bed positions (neck and superior mediastinum). The acquisition time was increased from 3 to 5 minutes per bed position. A standard acquisition protocol for the 3D-mode Biograph-16 (Siemens; Malvern, PA) PET/CT scanner was used for all patients. Helical CT was acquired with 3 to 5mm section thickness, as described earlier (287). All scans were reported by a single

observer blinded to the surgical and pathologic findings. Tumor diameter, as reported on histopathology, was used as a guide to contour the region of interest on FDG- PET/CT. FDG uptake by the thyroid nodules were expressed as SUVmax. As the background FDG uptake by the non-nodular thyroid was about 2.5, MTV and TLG were calculated for 30 lesions with SUVmax $\geq$2.5. MTV is defined as total tumor volume with an SUV of 2.5 or greater. TLG was calculated as (mean SUV) $\times$ (MTV).

The RC method for partial volume correction of PET images was used, as described earlier (169). To generate a correction curve, the NEMA/IEC body phantom was imaged (http://www.spect.com/pub/NEMA_IEC_Body_Phantom_Set.pdf), which has 6 spherical inserts ranging in diameter from10-37 mm. The contrast between the spheres and the background region was 3.93. This phantom was imaged 5 times using the thyroid protocol. For each scan, SUVmax was measured in the spherical lesion and the average of the 5 values for each sphere was taken. The ratio of the difference of the average SUVmax for each sphere and its background activity to the difference of the average SUVmax for the largest sphere (37 mm) and its background activity was plotted against the sphere size. An exponential curve was fitted to the data to calculate the RC for the sphere diameter. This method assumes that the thyroid nodule of interest is a perfect sphere.

$$Recovery\ Coefficient = \frac{Measured\ maximum\ activity - Background\ activity}{Known\ activity - Background\ activity}$$

$$Partial\ volume\ corrected\ activity = (Measured\ maximum\ activity - Background\ activity)/(Recovery\ Coefficient) + Background\ activity$$

3.1.3 Statistical methods

The demographic and FDG-PET/CT characteristics of FA and HCA were recorded. The data were managed and analyzed using SPSS for Windows version 23·0 (SPSS Inc., Chicago, IL). After checking for normality assumption, the mean and standard deviation were used to express normally distributed data (such as the size of nodule), which were compared by analysis of variance (ANOVA). The median with interquartile range (IQR) was used for non-normally distributed data (i.e. the SUV). Inter-group comparison of non-normally distributed data was made by Mann-Whitney nonparametric analysis. χ^2 test with Yates' correction was used to compare categorical variables. A p-value <0.05 (two-sided) was considered to indicate statistical significance and 95% CI were used to express reliability in the estimates.

Receiver operating characteristic (ROC) curve analysis of SUVmax and the area under the curve (AUROC) were used to assess discrimination between follicular and HCA. Youden index was used to identify the optimal cut-off SUVmax for the purpose (288). Sensitivity, specificity, PPV, NPV and test efficiency (accuracy) were used as measures to describe the effectiveness of FDG-PET /CT. A true positive was defined as the instance where the FDG-PET /CT made a positive prediction and this coincided with a positive histopathology. A false positive was an event where FDG-PET /CT made a positive prediction and the subject had a negative result on histopathology. A true negative was defined as the occurrence where the FDG-PET /CT gave a negative prediction and the subject had a negative result in the histopathology. A false negative represented a situation

where FDG-PET /CT made a negative prediction but the histopathology showed a positive result.

Sensitivity: Sensitivity of a FDG-PET /CT is the percentage of all patients with thyroid cancer present who have a positive FDG-PET /CT.

$$\frac{\text{True positive}}{\text{True positive + False negative}} \times 100\%$$

Specificity: Specificity of a FDG-PET /CT is the percentage of all patients without thyroid cancer who have a negative FDG-PET /CT.

$$\frac{\text{True negative}}{\text{False positive + True negative}} \times 100\%$$

Positive Predictive Value (PPV): The percent of all positive FDG-PET /CTs that are true positives.

$$\frac{\text{True positive}}{\text{True positive + False positive}} \times 100\%$$

Negative Predictive Value (NPV): The percent of all negative FDG-PET /CTs that are true negatives.

$$\frac{\text{True negative}}{\text{False negative + True negative}} \times 100\%$$

Test Efficiency: The efficiency of a test is the percentage of times that a test gives the correct answer compared to the total number of tests.

$$\frac{\text{True positive + True negative}}{\text{True positive + True negative + False positive + False negative}} \times 100\%$$

73

3.2 Epidemiological analysis of prognostic markers in thyroid cancer

3.2.1 Establishment of the Manitoba thyroid cancer cohort

This study involved a review of electronic and paper records of a population-based cohort (the Manitoba thyroid cancer cohort) of all 2306 consecutive thyroid cancers diagnosed in 2296 patients in Manitoba, Canada from January 1, 1970 to December 31, 2010 and identified from the Manitoba Cancer Registry. The Manitoba Cancer Registry is a member of the North American Association of Central Cancer Registries. Ethics approval for this study was obtained from the Research Ethics Board at the University of Manitoba (Ethics reference number: H2008:057). Individual electronic and paper records of diagnosis and treatment of this cohort were reviewed at CancerCare Manitoba. CancerCare Manitoba is the tertiary cancer care center for the province of Manitoba with a catchment population of about 1.2 million and Manitoba Cancer Registry as a part of it. The primary source of diagnostic information included 2148 pathology reports, 80 discharge summaries, 56 autopsy records, 18 operative reports, and 4 death certificates.

Patient demographics, extent of disease at initial presentation, the treatment modalities employed, pathology details, cancer recurrences during the follow-up, and the final oncological status as of January 1, 2015, were recorded. All patients, who migrated out of province (considered lost to follow-up) during the study period, were censored at that point in time. Patients that were initially diagnosed by autopsy or death certificate were excluded from survival analyses. All cases were re-staged according to the AJCC/ UICC staging for thyroid cancer (7th edition, 2009) (18). The topography and histology were re-

coded by WHO International Classification of Diseases for Oncology (3rd Edition) codes and the disease, signs and symptoms were re-coded by International Classification of Diseases (10th Edition) codes to ensure uniformity. The pathology and treatment details of 683 (29.6%) were independently reviewed for accuracy as a part of a collaborative staging project.

3.2.2 Epidemiological analysis of oncological outcomes

The data were managed and analyzed using SPSS for Windows version 23·0 (SPSS Inc., Chicago, IL). ANOVA was used to compare group means and categorical data were compared using the Pearson chi-square test with continuity correction as appropriate. A p-value <0.05 (two-sided) was considered to indicate statistical significance and 95% CI were used to express reliability in the estimates. Bonferroni correction was used to reduce the chances of obtaining false-positive results (type I errors) when multiple pair wise tests were performed on a single set of data. The patient characteristics, the extent of disease at presentation and the tumor histology were recorded along with the treatment modalities, the patterns of failure and the final oncological outcome. Age standardized incidence rate was calculated by direct method (289). Age specific incidence rates were initially calculated by using the age distributions of the newly diagnosed thyroid cancers cases in the Province of Manitoba and that of the provincial population for each year obtained from the Manitoba Health's Population Registry, Manitoba Bureau of Statistics and Statistics Canada. Age-specific mortality rates calculated above were then multiplied with the number of persons in each age group of the 1991 standard Canadian population to get the

expected deaths for each age group. The number of expected deaths from all age groups were added together to obtain the total number of expected deaths. Finally the age-adjusted mortality rates were calculated by dividing with the total number of expected deaths with the standard population.

Relapse free survival (RFS) and DSS were estimated by the Kaplan-Meier product limit method and the effect of individual prognostic factors on survival was assessed by using the log rank test. After checking for normality assumption, the mean and standard deviation were used to express normally distributed data (such as age of the patients) and median with inter-quartile range (IQR) were used for non-normally distributed data (i.e. tumor size and follow-up). Multivariable analyses were performed with Cox Proportional Hazards models to assess the independent effect of prognostic factors on DSS after testing for the proportional hazard assumption. The effects of age at diagnosis, gender, tumor size, ETE, lymph node metastasis, distant metastasis, the histological type, treatment modalities and the presence of post-treatment gross residual disease on the ten year probability of relapse and death by disease were evaluated by competing risk regression analysis to assess the competing influence of other causes of mortality, such as the deaths due to a second primary tumor or non-cancer deaths, using STATA version 12 (StataCorp. TX, USA). (290). Cumulative incidence function (CIF) was used to describe the probability of relapse and death using a proportional hazards regression model to directly model the sub-distribution of a competing risk (291). After excluding 60 thyroid cancers that were detected either at autopsy (56 patients) or by death certificate (4 patients) and 10 patients

with familial MTC, 2226 patients were included in the proportional hazards regression model for competing risks analysis for deaths due to thyroid cancer. Similarly, 1977 patients who had complete resection of their thyroid cancer without any macroscopic post-treatment residual disease were included in the proportional hazards regression model for competing risks analysis of relapse of thyroid cancer.

3.2.3 Development and validation of the Manitoba thyroid prognostic nomogram

The data from the Manitoba thyroid cancer cohort were used to develop prognostic nomograms. Based on the weighted relative importance of individual prognostic factors on the 10 year risk of relapse and death from disease, prognostic nomograms were developed as described earlier (292). The period of diagnosis was also included to produce estimates for the nomograms based on a more recent cohort. Analyses were conducted using R version 2.13.2 (www.r-project.org). The R packages cmprsk10, Design, and QHScrnomo were used for modeling and developing the nomograms. Restricted cubic splines were used for the continuous variable of age. The default setting for 4 knots was used for RFS, and the default setting for 3 knots was used for DSS. Twenty imputations were produced with the multivariable imputation by chained equations (mice) package for missing values among predictor variables. The models were internally cross-validated by calibration (calibration curve) and discrimination (c-index or AUROC) using QHScrnomo. Calibration curves and concordance indexes were produced using only one of the 20 complete datasets after multiple imputations. Discrimination is the ability of a model to separate subject outcomes between the predicted probability and the response. The

response is defined as the proportion of all evaluable ordered patient pairs for which predictions and outcomes are concordant (293, 294). If there is complete concordance between the predicted probability and the actual response, c-index is 1 (ideal).

3.2.4 Comparison with existing staging/risk stratification systems for thyroid cancer

The strength of our thyroid prognostic nomogram was compared with 12 other commonly used staging/risk stratification systems, to predict the risk of death from thyroid cancer in a population-based thyroid cancer cohort. For this purpose, 60 patients who were initially diagnosed by autopsy or death certificate, 76 patients with ATC with extremely high case fatality rate (CFR), and 10 familial medullary thyroid cancers (MTC) where the oncological outcome is largely determined by their specific gene mutations, were excluded from this study. One hundred and twenty three patients who did not have treatment with radical intent and 38 patients who were followed up in the Manitoba health care system for less than a year were also excluded. Individual electronic and paper records of the remaining 1989 patients from the Manitoba thyroid cancer cohort were reviewed and 1900 patients were selected for this study on whom there was adequate information on patient demographics, tumor characteristics and completeness of tumor resection required for staging by 12 commonly used staging/risk stratification systems (222).

R version 3.2.2 was used to analyze the data, using the packages of Hmisc to construct restricted cubic splines, and the packages of riskRegression and prodlim to run competing risk models. Restricted cubic splines were used to account for the non-linear

relationship between age and the outcomes, using the default 3 knots. The discrimination capability of the models were evaluated by c-index at 10 years. C-indices were produced using only one of the 20 complete datasets after multiple imputations. Akaike information criterion (AIC) was used to compare different prognostic models that are used for stage grouping/risk stratification of thyroid cancer. AIC is defined as $AIC = -2LL + 2m$, where LL is the maximized log-likelihood and m is the number of parameters in the model (degrees of freedom) (295, 296). Delta AIC was calculated to compare the models. It is defined as $Delta\ AIC\ (\Delta_i) = AIC_i - minAIC$, where AIC_i is the AIC value for model i and min AIC is the AIC value of the best model identified by the lowest AIC (297). The model with smallest AIC value is considered the best amongst the compared models.

3.2.5 Development and validation of web-based computerized prognostic model

In order to establish a web-based computerized prognostic model, a 50% random sample was drawn from the study population to be used for the model development (N=1161) and the model was validated on the remaining patients (N=1135). The prognostic factors (covariates) were tested for confounders/ multi-collinearity, interactions and transformations. Cox proportional hazard model was used to develop the model using the development sample. The ROC curves were used to evaluate the accuracy of the developed Cox proportional hazard model in predicting the long-term DSS beyond the first year. The AUROC curves of both the development and the validation samples were compared to assess the accuracy of the model.

3.2.6 External validation of the Manitoba prognostic model

The electronic and paper records of 1454 patients with differentiated thyroid cancers treated and followed up at the London Health Sciences Centre, London, Ontario, Canada for a median follow-up of 7.0 years (IQR= 4.8-10.7) were analyzed after obtaining the ethics approval for this study from the Research Ethics Boards and completion of Data sharing agreement between CancerCare Manitoba and London Health Sciences Centre. Patient demographics, extent of disease at initial presentation, the treatment modalities employed, pathology details, cancer recurrences during the follow-up, and the final oncological status as of March 1, 2016 were recorded. To circumvent the challenge of changes in staging system over the study time period, uniform restaging of all cancers was done according to the UICC staging for thyroid cancer (7th edition, 2010) (18). The topography and histology were re-coded by WHO International Classification of Diseases for Oncology (3rd Edition) codes and the disease, signs and symptoms were re-coded by International Classification of Diseases (10th Edition) codes to ensure uniformity. DSS was estimated by the Kaplan-Meier product limit method. The validation analysis was based on contrasting these survival probabilities against the true state of DSS, employing ROC curve analysis.

3.2.7 Prognostic importance of distant metastasis in TNM staging

In order to analyse the prognostic importance of distant metastasis in stage grouping by the TNM classification, 2018 electronic and paper charts, including pathology and operative reports, 56 discharge summaries, and 44 autopsy records, were reviewed and 215

patients with Stage II WDTC and 61 patients with distant metastasis (M1) were identified. Details involving patient demographics, extent of disease at presentation, treatment, pathology, recurrences of cancer, and the final outcome status as of July 1, 2015, were recorded. As the TNM staging system has evolved over time, all cases were restaged using the TNM criteria of AJCC/ UICC staging for thyroid cancer (7th Edition, 2009) to ensure uniformity.

Recurrences were defined as the presence of clinical and/or radiological/biochemical evidence of disease. The Kaplan-Meier product limit method was used to estimate RFS and DSS and log rank test was used to compare survival between groups. Multivariable analyses were performed with Cox proportional hazard models to evaluate the independent impact of various prognostic factors on the DSS and RFS of our population-based cohort, after confirming the proportional hazard assumption.

Chapter IV

Results

4.1 Assessment of the diagnostic role of FDG-PET /CT

Forty seven consecutive, consenting, patients with 50 FN/HCN, diagnosed by FNAB, were recruited in the prospective arm of this study. The mean age of patients in this group was 58.7 ± 12.8 years and 72% of the patients were females. On final histopathology, there were 23 follicular adenoma, 8 HCA, 11 papillary carcinomas, 6 follicular variant of papillary carcinomas and 2 follicular carcinomas. In all, 19 (38%) nodules were malignant. HCN were identifiable by pre-operative FNAB in 6 (75%) cases. The mean size of the thyroid nodule was 2.6 ± 1.3 cm with 4 micro-carcinomas (tumor size=7.0-8.5 mm).

4.1.1 Diagnostic role of FDG-PET /CT

The median SUVmax value of all thyroid nodules in the study group was 3.45 (IQR= 0-7.58). The patients' age (p=0.14) and gender (p=0.43) as well as the median SUVmax (p= 0.10) of benign and malignant nodules were not significantly different. However, the malignant nodules were significantly smaller (p= 0.01) than the benign ones (Table 2). All 31 benign thyroid nodule measured >10 mm in size. Median MTV was 4.70 (IQR=1.71-19.95) and median TLG was 20.75 (IQR=4.87-FF101.03) for lesions with SUV>3.0. There was insignificant difference in MTV (p=0.116) and TLG (p=0.187) of benign and malignant follicular neoplasms. All 4 micro-carcinomas in this cohort had SUVmax over 3.5 (range=3.6-5.9).

Table 2: Patient demographics and characteristics of benign and malignant follicular / Hürthle cell neoplasms.

	Benign (N=31)	Malignant(N=19)	p-value
Mean age	60.9±12.8	55.3±12.3	0.13
Gender (Male: Female)	9:22	4:15	0.74
Mean size of the nodule	2.9±1.3 cm	2.0±1.1 cm	0.01
Median SUVmax	2.60; IQR= 0-7.60	4.60; IQR= 3.40-7.65	0.10

Of 31 benign follicular neoplasms, all HCA and 12 (52%) FA showed increased focal FDG uptake. SUVmax of HCA was significantly higher (p<0.001) than that of FA. All HCA showed focally increased FDG uptake with median SUVmax of 9.3 (IQR= 6.9-19.9). No significant difference was observed in the age (p=0.48) and gender (p=0.52) of the patients, and in the size of FA and HCA (p=0.79) (Table 3).

Table 3: Characteristics of follicular and Hürthle cell adenomas.

	FA (N=23)	HCA (N=8)	p-value
Mean age	59.8±13.6	63.5±9.4	0.48
Gender (Male : Female)	8:14	1:6	0.52
Mean size of the nodule	2.8±1.3 cm	3.2±1.2 cm	0.79
Median SUVmax	2.2; IQR= 0-3.0	9.3; IQR= 6.9-19.9	<0.001

Increased focal FDG uptake had 100% (95% CI: 56-100%) sensitivity, specificity of 49% (95% CI: 27-69%), PPV of 37% (95% CI: 17-61%), and NPV of 100% (95% CI:

80-100%) for identifying HCA, with a low overall accuracy of 60%. Youden index indicated SUVmax of 5 to be the best cut-off for discriminating between FA and HCA, with AUROC of 0.90 (95% CI: 0.79-1.00; p=0.001). With this cut-off, FDG-PET /CT had a sensitivity of 88% (95% CI: 47-99%), specificity of 87% (95% CI: 65-97%), PPV of 70% (95% CI: 35-92%), and NPV of 95% (95% CI: 74-99%), with an overall accuracy of 87% (Table 4).

Table 4: FDG-PET/CT findings in follicular and Hürthle cell adenomas (SUVmax cut-off for FDG-PET positivity =5).

	HCA	FA	Total
FDG-PET positive	7	3	10
FDG-PET negative	1	20	21
Total	8	23	31

Similarly, focally increased FDG uptake by thyroid nodule had a sensitivity of 89% (95% CI: 65-98%), specificity of 35% (95% CI: 19-54%), PPV of 46% (95% CI: 30-63%), and NPV of 85% (95% CI: 54-97%) for diagnosing malignant FN/HCN. With this criteria, the overall accuracy of FDG-PET /CT was low at 56%. As all HCA were observed to show high SUV, we excluded them from further analysis. After excluding HCA, the AUROC for discriminating benign from malignant nodules was 0.79 (95% CI: 0.63-0.94; p=0.002), with 3.25 as the best SUVmax cut-off for the purpose (Table 5). FDG-PET /CT had a sensitivity of 79% (95% CI: 54-93%), specificity of 83% (95% CI: 60-94%), PPV of 79% (95% CI: 54-93%), and NPV of 83% (95% CI: 60-94%), with an improved overall

accuracy was 81% with this SUVmax cut-off. Figure 4 highlights the difference between

the SUVmax of benign and malignant non-Hürthle cell FN expressed as (p=0.003).

Table 5: FDG-PET/CT findings in benign and malignant thyroid nodules (SUVmax cut-

off for FDG-PET positivity =3.25).

	Carcinoma positive	Carcinoma negative	Total
FDG-PET positive	15	12*	27
FDG-PET negative	4	19	23
Total	19	31	50

* Includes 8 HCA
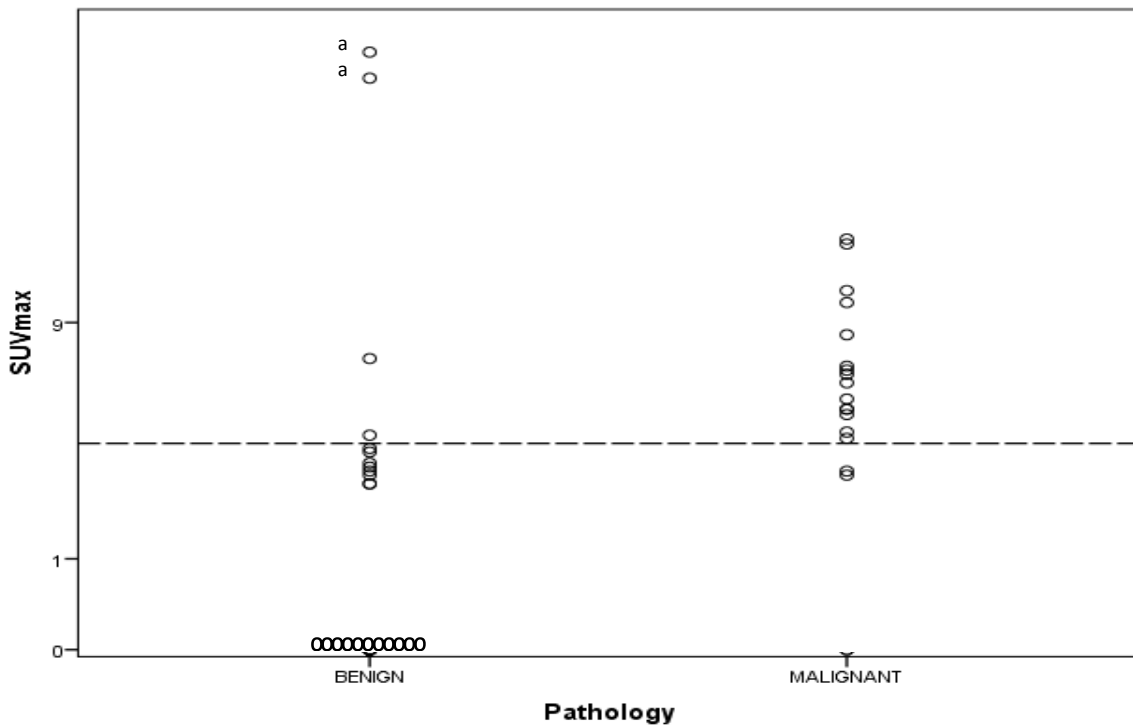
Figure 4: Scatter plot of SUVmax in benign and malignant non-Hürthle cell FN.
Y-axis shows the SUVmax on a logarithmic scale with the reference line indicating
SUVmax = 3.25. SUVmax was undetectable (SUVmax= 0) in 2 malignant and 11 benign
neoplasms.
a   Two benign FN were outliers with SUVmax of 54.0 and 65.0

Smaller lesions appear less intense on PET scan than their true intensity because of limited resolution of the system. As 4 nodules were < 1cm in their maximum diameter, partial volume correction by RC method was applied to minimize the risk of underestimating their SUVmax. Assuming that the thyroid nodule of interest is a perfect sphere, the NEMA/IEC body phantom, with 6 spherical inserts ranging in diameter from10-37 mm, was imaged 5 times using the thyroid protocol. The difference between the SUVmax and the background for each scan was recorded and the mean of these values for each of the spheres was calculated (Table 6).

Table 6: Calculation of recovery coefficient (RC)

Diameter	Scan 1	Scan 2	Scan 3	Scan 4	Scan 5	Mean	RC
37 mm	4.29	4.15	4.26	4.32	4.28	4.26	1
28 mm	4.32	4.14	4.36	4.29	4.27	4.276	1.004
22 mm	3.74	4.09	4.28	4.09	3.87	4.014	0.942
17 mm	3.83	3.65	3.66	3.7	3.41	3.65	0.857
13 mm	2.45	3.58	2.56	2.44	2.72	2.75	0.646
10 mm	1.48	1.64	1.55	1.92	1.9	1.698	0.398

The ratio of the average difference of the SUVmax for each sphere and its background activity to the difference of the average SUVmax for the largest sphere (37 mm) and its background activity was then computed (RC). An exponential curve was fitted to the data (Figure 5). It was used to calculate RC for the thyroid nodules using their size (diameter) assuming that the nodules are perfect spheres.
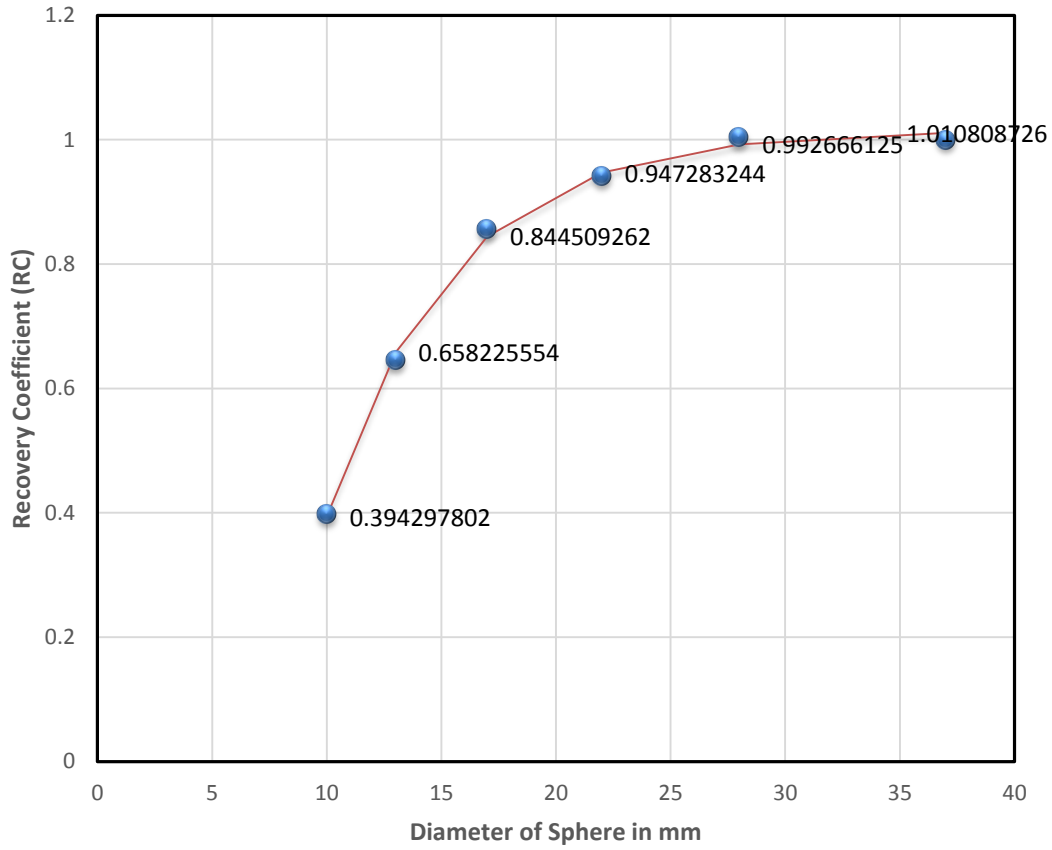
Figure 5: Exponential curve fit to the data for calculation of recovery coefficent. A recovery coefficient of 1.0, indicates correctly displayed activity, whereas a value of 0.5 indicates that the displayed activity is only 50% of true activity. As the curve shows a sharp decline towards 0 for spheres (lesions) < 10 mm, less than 40% of the true activity of these lesions is displayed.

When the recovery coefficient was plotted against the sphere diameter, it showed a sharp decline towards 0 for lesions < 10 mm (Figure 5). Consequently the partial volume correction for lesions was reliable only between 10 and 25 mm. As all 4 PTC with diameter < 10 mm had SUVmax >3.25, partial volume corrected SUVmax did not change the classification of these lesions. Partial volume correction of SUVmax did have any significant influence on the characterization of benign and malignant follicular neoplasms by FDG-PET/CT

4.2   Epidemiological analysis of prognostic markers in thyroid cancer

4.2.1   The Manitoba thyroid cancer cohort

In total, 2306 thyroid cancers were observed in Manitoba in 2296 patients from 1970-2010. Nine patients had a synchronous second primary tumor of a different histology along with PTC (follicular-3, Hürthle cell-3, medullary-2, poorly differentiated-1), while one patient had a metachronous second papillary carcinoma in the contra-lateral thyroid lobe 25 years after initial management. The Manitoba thyroid cancer cohort includes 570 (24.8%) males and 1726 (75.2%) females with a mean age ($\pm$ standard deviation) of 49 ± 18 years.

According to the 2011 census, the population of Manitoba was recorded at 1,208,268. There was an average population increase of 0.56%/ year from 1970 level of 988,245. The number of newly diagnosed thyroid cancers increased from 22 in 1970 to 122 in 2010, and the ASIR per 100,000 for thyroid cancer from 2.52 (95% CI: 1.57-3.83) in 1970 to 9.37 (95% CI:7.65-11.08) in 2010 (Figure 6). The ASIR per 100,000 rose from 0.72 (95% CI: 1.57-3.83) in 1970 to 4.94 (95% CI: 3.35-7.03) in 2010 for males and the respective rates for females went up from 4.28 (95% CI: 2.56-6.71) to 13.75 (95% CI: 10.96-17.04). The ASIR per 100,000 for ATC fell from 0.11 (95% CI: 0.05-0.19) during 1970-1980 to 0.05 (95% CI: 0.02-0.11) in 2001-2010 for both sexes and the respective rates for PTC went up from 0.93 (95% CI: 0.75-1.15) to 6.64 (95% CI: 6.17-7.11). The mean age of patients at the time of diagnosis, median tumor size and the tumor stage at presentation showed statistically non-significant change (p>0.05, NS) over the past four

decades (Table 7). Thyroid cancers ≤ 10mm (micro-carcinoma) represented 23.4% of all

thyroid cancers and this proportion did not change significantly (p=0.87) during the study

period. In all, T1 tumors were seen in 978 (32.6%) patients, T2 in 597 (26%), T3 in 468

(20.4%) and T4 in 246 (10.7%) patients. In 7 (0.3%) patients a primary tumor was either

not identified or could not be staged.
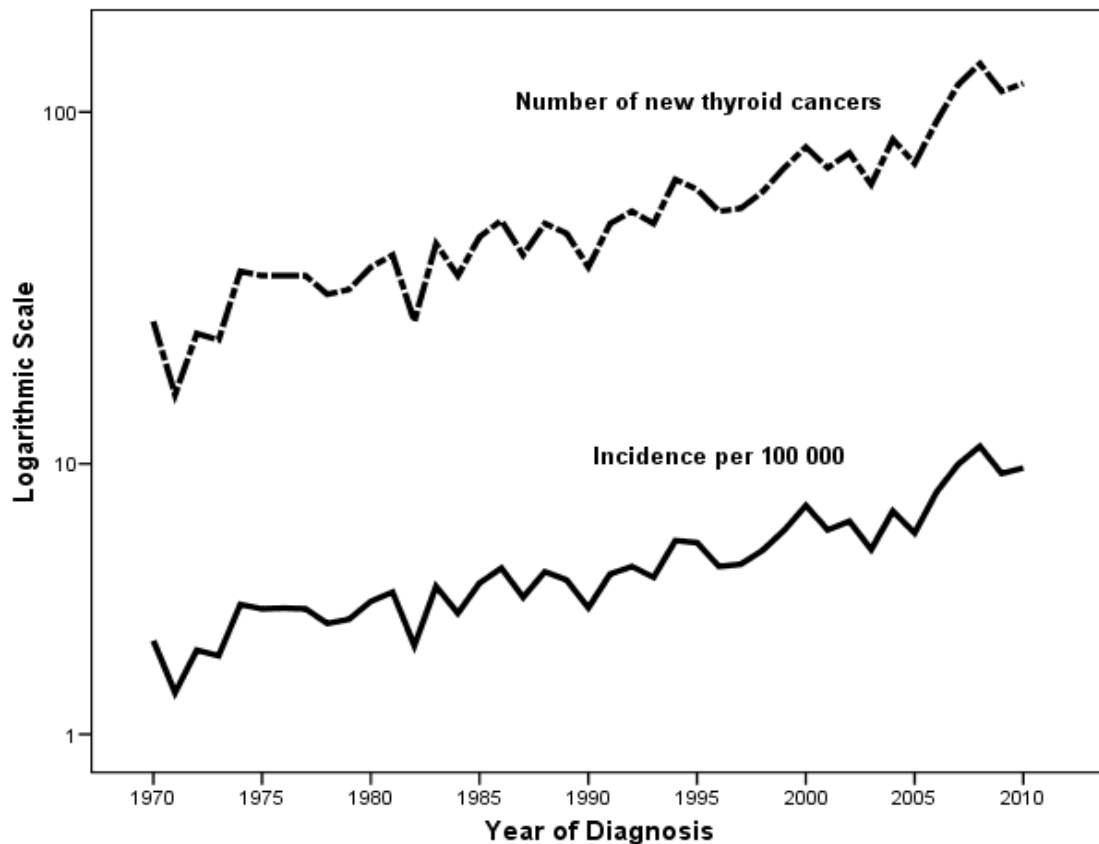
Figure 6: Trend of newly diagnosed thyroid cancers in Manitoba, Canada
Age standardized incidence rate per 100,000 (ASIR) and actual number of new cancers
have steadily increased over past 4 decades (1970-2010). The curves appear parallel to
each other as the population of the Province of Manitoba has not changed very substantially
over this time period. Y-axis shows numbers on a logarithmic scale.

Table 7: Clinical characteristics of thyroid cancer by decade of presentation.

		1970-1980 (N=331)	1981-1990 (N=410)	1991-2000 (N=594)	2001-2010 (N=971)	p-value
Mean age in years		49.3±18.4	47.5±18.6	48.0±18.7	49.1±17.0	0.14(NS)
Gender ratio (Female : Male)		2.5:1	2.8:1	3.6:1	3:1	0.45(NS)
Median tumor size (IQR)		19.9 (15-22)mm	20 (20-25)mm	21 (20-24)mm	20 (19-22)mm	0.44(NS)
Tumor size distribution	≤1cm	75 (22.6%)	117 (28.5%)	153 (25.8%)	242 (24.9%)	0.54(NS)
	1-2cm	110 (33.2%)	93 (22.7%)	143 (24.1%)	247 (25.5%)	0.47(NS)
	2-4cm	108 (32.6%)	152 (37.0%)	197 (33.1%)	310 (31.9%)	0.63(NS)
	> 4cm	38 (11.6%)	48 (11.8%)	101 (17.0%)	172 (17.7%)	0.53(NS)
TNM stage	I	207 (62.6%)	280 (68.4%)	380 (64.0%)	610 (62.8%)	0.82(NS)
	II	23 (6.9%)	34 (8.3%)	62 (10.4%)	120 (12.4%)	0.61(NS)
	III	32 (9.7%)	52 (12.6%)	62 (10.4%)	125 (12.9%)	0.38(NS)
	IV	69 (20.8%)	44 (10.7%)	90 (15.2%)	116 (11.9%)	0.24(NS)
Total thyroidectomy		94 (28.4%)	159 (38.9%)	293 (49.3%)	691 (71.2%)	<0.001
Adjuvant radioactive iodine		36 (10.9%)	79 (19.3%)	177 (29.8%)	603 (62.1%)	0.004
Histology	Papillary	192 (58.0%)	278 (67.8%)	459 (77.3%)	834 (85.9%)	<0.001
	Follicular	86 (26.0%)	70 (17.1%)	62 (10.4%)	50 (5.1%)	<0.001
	Hürthle Cell	3 (0.9%)	24 (5.9%)	22 (3.7%)	36 (3.7%)	0.008
	Poorly differentiated	9 (2.7%)	1 (0.2%)	3 (0.5%)	3 (0.3%)	<0.001
	Medullary	17 (5.1%)	24 (5.9%)	17 (2.9%)	21 (2.2%)	0.003
	Anaplastic	19 (5.7%)	9 (2.2%)	24 (4.0%)	20 (2.1%)	0.046
	Unspecified*	5 (1.5%)	4 (1%)	7 (1.2%)	7 (0.7%)	0.62(NS)
Median follow up in months (95% C.I)		419.4 (409.9-428.9)	304.9(296.2-313.7)	188.4(182.5-194.3)	68.5 (65.4-71.6)	<0.001
10 year DSS (N=2296)		85.4 (82.9-90.0)%	92.2 (89.1-94.5)%	89.3(86.5-91.6)%	95.6 (90.5-96.6)%	<0.001
Post treatment 10 year RFS (N=2065)		86.6 (81.1-90.6)%	88.9 (85.1-91.8)%	88.1(84.7-90.6)%	91.9 (89.2-94.1)%	0.18(NS)

*Carcinoma not otherwise specified

At the time of diagnosis, 544 (23.7%) patients had lymph node involvement in the neck and 90 (3.9%) patients had evidence of distant metastasis. Multifocal thyroid cancers were observed in 742 (32.3%) patients and gross ETE of tumor in 480 (20.9%) cases. Total thyroidectomy was performed in 55.1% of all patients and in 54.3% of patients with WDTC. In all, 34.8% patients had adjuvant radioactive iodine and 73% of the patients with WDTC who had total thyroidectomy received adjuvant RAI. Most patients with unresectable macroscopic residual disease in the neck at the time of surgery following total thyroidectomy or those at a high risk of disease recurrence, such as patients with T3/T4 tumors, regional and distant metastasis, received radioactive iodine for differentiated thyroid cancer. Complete surgical excision of gross tumor was achieved in 96.1% cases. Use of external beam radiation therapy was limited to unresectable macroscopic residual disease. The distribution of T stage (p=0.50), N stage (p=0.27) and M stage (p=0.61) and the proportion of patients with multifocal disease (p=0.26), gross ETE of tumor (p=0.66) or with complete excision of tumor (p=0.40) remained unchanged during the study period.

PTC was the most common histological type and the proportion of PTC steadily increased from 58.0% (1970-1980) to 85.9% (2000-2010). Most of the thyroid cancers were classical PTC (46.9%), followed by follicular variant (24.2%), encapsulated (2.3%), and micro-invasive (1.6%) variants. Sclerosing, solid, tall cell and columnar cell variants together accounted for only 1.9% of all thyroid cancers. During the same period, the proportion of all thyroid cancers that were diagnosed as FVPTC increased from 12.4% to

32.9% (Table 7), whereas the proportion of FTC fell from 26% to 5.1% (p<0.001) and anaplastic carcinoma from 5.7% to 2.1% (p<0.001) (Figure 7).
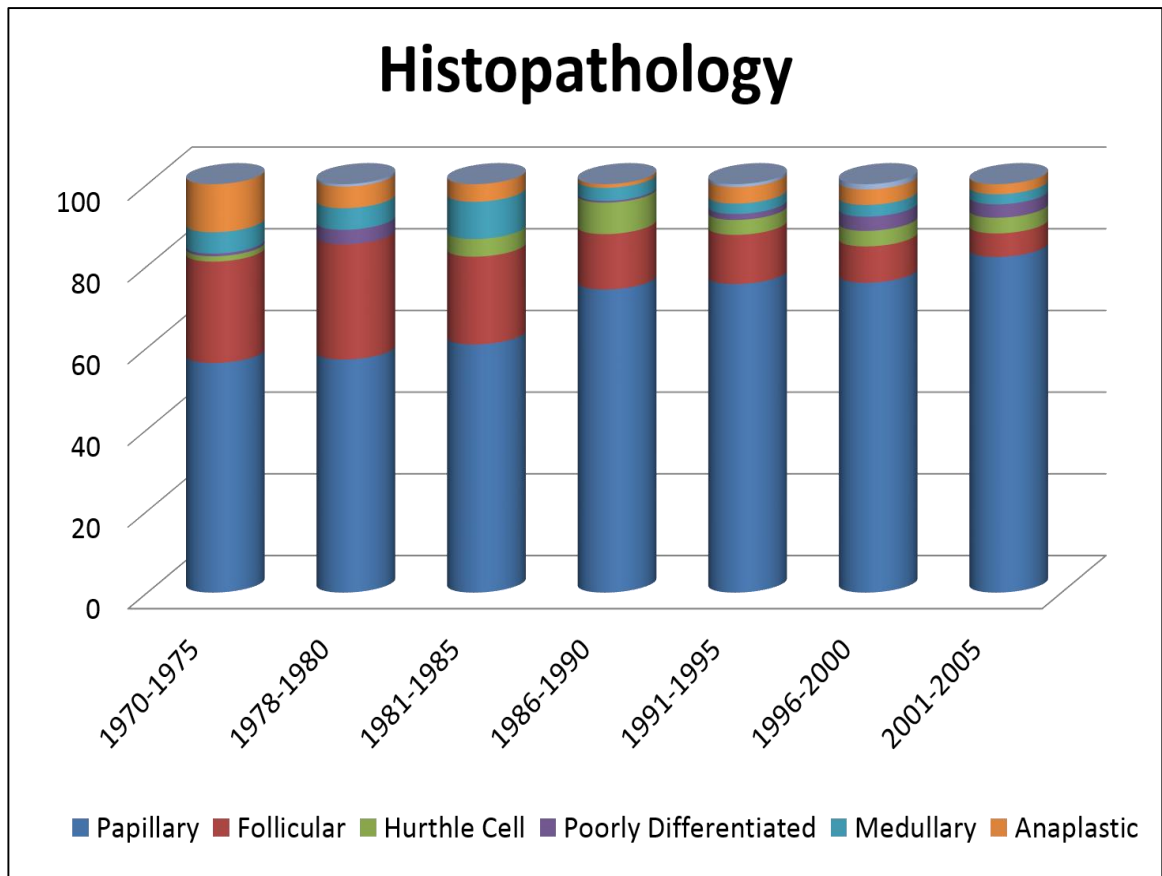
Figure 7: Changing patterns of histopathology of thyroid cancer in Manitoba.
The chart shows a steady increase in the proportion of PTC and a decline in the proportion of FTC to ATC. Unclassified differentiated carcinoma represents the top light blue portion. The actual number of PTC also rose from 86 (1970-1975) to 516 (2006-2010), whereas that of FTC decreased from 37 to 28 and ATC from 18 to 12 during the same time period.

The proportion of MTC has remained nearly unchanged over this period. The proportion of the patients undergoing total thyroidectomy increased by two and a half times between 1970-1980 and 2001-2010 (p<0.001), while those receiving adjuvant radioactive iodine increased by over five times (p=0.004).

92

4.2.2 Epidemiological analysis of oncological outcomes

Oncological outcomes of treatment with curative intent were assessed in the 2065 patients who underwent primary surgical treatment after excluding cases that were diagnosed only on autopsy or death report (n=60), those who died before surgery (n=64), and non-surgical candidates (n=35). Those who refused treatment (n=24) or had their primary surgery or follow-up performed in another province/country (n=48) were also excluded. Seventy eight (3.8%) patients had post-surgery macroscopic residual disease and they were excluded from the model to predict the risk of relapse. During the median follow-up of 10.5 years (IQR=4.8-18.8 years), 200 (9.7%) patients had clinical/radiological evidence of recurrent disease after at least 6 months following an initial successful treatment. The recurrences were in the residual thyroid lobe or thyroid bed in 23 (11.5%) cases, in the central compartment of neck in 64 (32%), in the lateral compartment of neck in 44 (22%), at a distant metastatic site in 54 (27%), and at multiple sites in 15 (7.5%) cases. RFS after 10 years of radical treatment was 89.3% (95% CI: 87.7-90.8%) and 90.5% of all recurrences were observed during this period (69.5% within first 5 years). Ten year RFS has not changed significantly over the last four decades (Table 7).

In all, 201 patients died from thyroid cancer (CFR -8.8%) and 76% of all thyroid cancer related deaths were observed within 10 years (54.9% within first 5 years). The CFR for different histological types of thyroid cancer is summarized in Table 8. Of all deaths due to thyroid cancer, 63 (31.3%) had papillary carcinoma, 60 (29.9%) anaplastic, 24

(11.9%) follicular, 21 (10.4%) medullary, 15 (7.5%) Hürthle cell, 8 (4%) poorly differentiated, and 10 (5%) had unspecified thyroid carcinoma.

Table 8: Case fatality rate and survival by histological types of thyroid cancers.

Histological Type	CFR	10 year DSS (95% CI)	10 year RFS (95% CI)
Papillary (N=1763)	3.6%	96.8 (95.7-97.7)%	87.7 (85.9-89.4)%
Follicular (N=268)	9.0%	91.5 (87.0-94.5)%	87.3 (82.4-91.0)%
Hürthle Cell (N=85)	17.6%	81.4 (69.7-89.0)%	69.8 (57.9-79.0)%
Medullary (N=79)	26.6%	77.6 (65.4-85.9)%	27.3 (6.5-53.9)%
Poorly differentiated (N=39)	31.2%	74.1 (28.9-93.0)%	52.0 (38.5-63.9)%
Anaplastic (N=72)	83.3%	7.3 (2.4-15.9)%	1.4 (0.1-6.7)%

Tumor histology had a very significant impact on the DSS and RFS (Table 8). PTC had the best DSS rates (96.8% at 10 years and 94.6% at 20 years), whereas only 7.3% with anaplastic cancer survived for 10 years. The DSS of the Manitoba thyroid cancer cohort by Kaplan-Meier product limit method, over the last four decades, is shown in Figure 8. The 10 year thyroid cancer specific survival (DSS) of the Manitoba thyroid cancer cohort (N=2296) was 91.8% (95% CI: 90.5-92.9%) which improved significantly from 85.4% (1970-1980) to 95.6% (2001-2010) (Table 7). The factors responsible for this improvement in DSS were investigated by a multivariable analysis by competing risk hazard model.
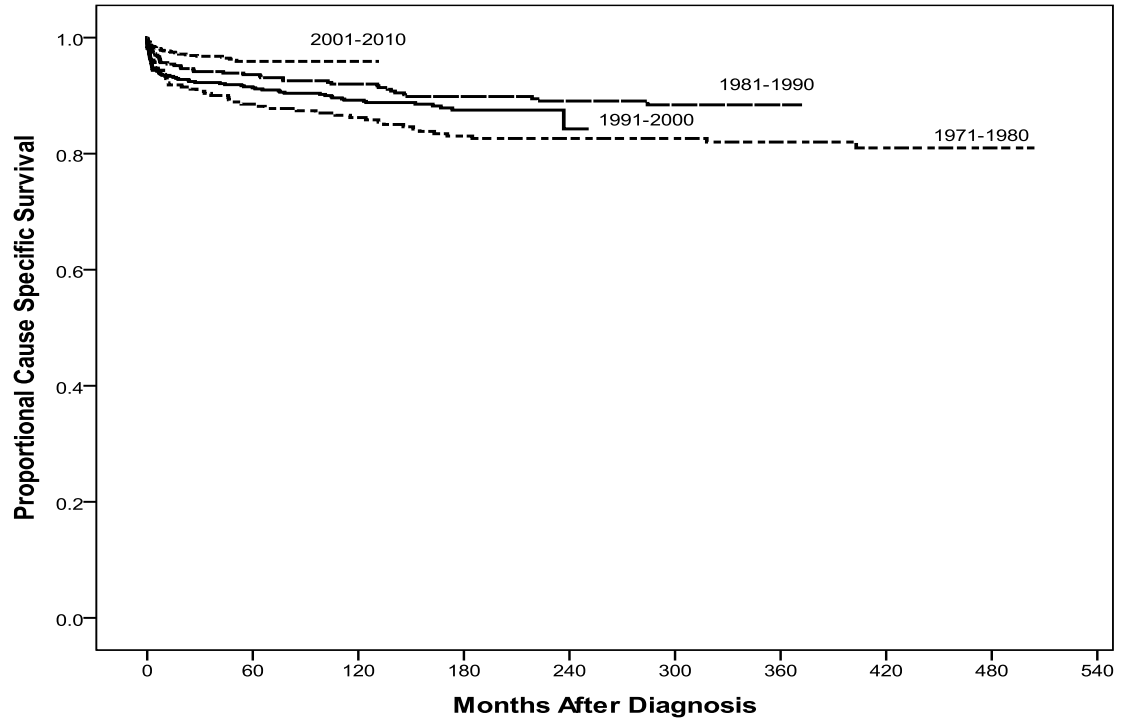
Figure 8: The disease specific survival of the Manitoba thyroid cancer cohort.
Ten-year DSS as calculated by Kaplan-Meier method shows a steady improvement from
85.4% to 95.6% from 1971-1980 to 2001-2010. Y-axis shows proportion of patients
surviving at any point in time.

In view of a lengthy follow-up of over 40 years and low disease specific mortality
of thyroid cancer, CIF by competing risk regression analysis was performed. Figure 9
shows an 8.1% reduction (from 12.6 to 4.5%) in death due to thyroid cancer after 5 years
of follow-up. It is evident that there was a statistically significant difference between the
risk of dying from thyroid cancer between the decades of 1970s and 1980s, and this
remained statistically unchanged between the 1980s and the 1990s. There was a further
reduction in thyroid cancer related mortality in the 2000s.
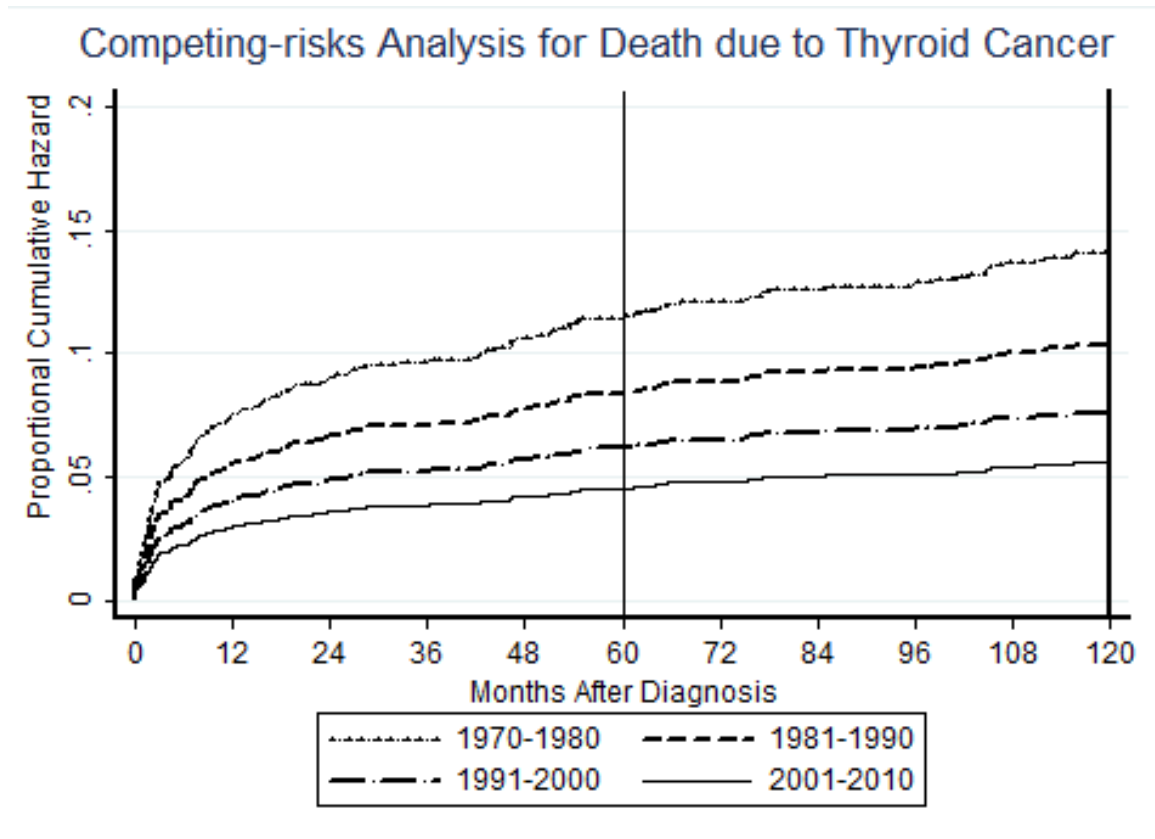
Figure 9: Cumulative incidence of death from thyroid cancer over 10 years after diagnosis. Cumulative incidence of death has been calculated by competing risk analysis. Values of proportional cumulative hazard of along the Y-axis shows the total number of deaths from thyroid cancer at any point in time after treatment. Vertical line at 60 months shows a reduction in death due to thyroid cancer after 5 years of follow-up, from 12.6% (1970-1980) to 4.5% (2001-2010).

Multivariable analysis by Cox proportional hazard model is shown in Table 9. The DSS was adversely influenced independently by non-papillary histology, especially anaplastic histology (HR=8.7; 95% CI:5.2-14.5; p< 0.001), male gender (HR=1.8;95% CI:1.3-2.5; p= 0.001), TNM stage III (HR=2.30; 95% CI:1.00-5.29, p= 0.05), and stage IV (HR=8.37; 3.99-17.54, p< 0.001), incomplete surgical resection (HR=2.4; 95% CI:1.4-4.2, p= 0.002) and age at diagnosis (HR=1.05 per year; 95% CI:1.03-1.06; p< 0.001).

Table 9: Multivariable analysis by Cox proportional hazard models for independent influence

of prognostic factors on disease specific survival.

Prognostic Factor		Hazard Ratio (95% CI)
Age at the time of diagnosis (per year)		1.05 (1.03-1.06), p<0.001
Gender (Male versus Female)		1.79 (1.28-2.51), p=0.001
Extent of Thyroidectomy (Hemi versus Total)		0.991 (0.60-1.64), p=0.971 (NS)
Completeness of resection (Incomplete versus complete)		2.40 (1.37-4.19), p=0.002
Adjuvant Radioactive iodine (RAI versus no RAI)		1.59 (0.91-2.79), p=0.101 (NS)
AJCC TNM stage grouping	Stage I	1.00 (reference)
	Stage II	1.94 (0.78-4.84), p=0.155 (NS)
	Stage III	2.30 (1.00-5.29), p= 0.05
	Stage IV	8.37 (3.99-17.54), p< 0.001
Histology	Papillary	1.00 (reference)
	Anaplastic	8.66 (5.18-14.49), p< 0.001
	Medullary	2.62 (1.48-4.66), p= 0.001
	Hürthle	2.23 (1.21-4.14), p= 0.010
	Follicular	1.76 (1.01-3.09), p=0.047
Decade of diagnosis	1970-1980	1.00 (reference)
	1981-1990	0.92 (0.56-1.53), p=0.753 (NS)
	1991-2000	1.40 (0.91-2.17), p=0.126 (NS)
	2001-2010	0.65 (0.40-1.08), p=0.096 (NS)

Each of these factors, except for the histology, has remained unchanged during the study period (Table 7). The extent of thyroidectomy, use of adjuvant RAI, or the decade of diagnosis did not have any significant independent influence on DSS in multivariable analysis (Table 9).

4.2.3   Development and validation of the Manitoba thyroid prognostic nomogram

As the CFR of ATC was extremely high and the 10 year DSS and RFS were very poor (Table 8), the multivariable analyses for competing risks of death and relapse was performed again, but restricted to non-ATC. The behavior of familial MTC is largely determined by their specific gene mutations. Therefore, the familial MTC (N=10) were excluded from multivariable analysis. On multivariable analysis, the patient's age and gender; T,N and M stages; histological type; presence of distant metastasis; and post-treatment macroscopic residual disease were important determinants of cumulative incidence of death due to thyroid cancer (Table 10). The competing risk sub-hazard model confirmed these observations of Cox regression analysis (Table 9).

Lymph node positivity had a very significant impact ($p<0.001$) on the cumulative incidence of relapses after complete resection of macroscopic disease (Table 11) but not on the incidence of deaths from thyroid cancer ($p=0.063$) (Table 10). The extent of thyroidectomy did not have any independent impact on the risk of dying from cancer and adjuvant radioactive iodine showed collinearity with total thyroidectomy. Consequently, both of these parameters were not included in the nomogram. Age showed a very

interesting non-monotonic relationship of age with relapse of thyroid cancer but a linear relation with the risk of deaths from thyroid cancer. After controlling for other factors, the risk of thyroid cancer relapse was found to be at minimum at 40 years. It showed a trend to increase from this base line in both younger and older patients.

Table 10: Prognostic factors influencing cumulative incidence of death from thyroid cancer in proportional hazards regression for sub-distribution of competing risks (N= 2226).

Prognostic factors	Sub-hazard ratio (SHR)	95% C.I	p-value
Age (10-year increments)	1.67	1.47 - 1.91	p<0.001
Gender (Male Vs Female)	2.195	1.49 - 3.24	p<0.001
Histology			
Histology (Medullary Vs Papillary)	4.219	2.40 - 7.42	p<0.001
Histology (Follicular Vs Papillary)	1.122	0.67 - 1.89	p=0.664
Distant Metastasis	8.462	4.86 - 14.75	p<0.001
T Stage			
T4Vs T1	3.439	1.73 - 6.83	p<0.001
T3 Vs T1	2.580	1.30 - 5.04	p=0.007
T2 Vs T1	1.519	0.74 - 3.13	p=0.257
Post-treatment Residual Disease	2.412	1.40 - 4.15	p=0.001
Regional lymph node involvement	2.212	0.97-5.03	p=0.063
Extent of thyroidectomy (Total Vs Hemi)	1.521	0.86-1.41	p=0.151

Table 11: Prognostic factors influencing cumulative incidence of thyroid cancer relapse in proportional hazards regression for sub-distribution of competing risks (N= 1977).

Prognostic factors	Sub-hazard ratio (SHR)	95% C.I	p-value
Age[a] (0-35 years)	0.952	0.92 - 0.98	p=0.002
Age'[a] (>50 years)	1.118	0.99 - 1.25	p=0.053
Age"[a] (35-50 years)	0.788	0.55 - 1.13	p=0.195
Gender (Male Vs Female)	1.607	1.16 - 2.22	p=0.004
Histology			
Medullary Vs Papillary	2.371	1.39 - 4.05	p=0.002
Hürthle/Poorly diff. Vs Papillary	2.651	1.51 - 4.64	p=0.001
Follicular Vs Papillary	0.768	0.43 - 1.37	p=0.370
Distant Metastasis	11.593	5.00 - 26.90	p<0.001
Regional lymph node involvement	2.414	1.68 - 3.47	p<0.001
T Stage			
T4Vs T1	2.728	1.52 - 4.89	p=0.001
T3 Vs T1	2.372	1.62 - 3.47	p<0.001
T2 Vs T1	1.189	0.77 - 1.83	p=0.432
Extent of thyroidectomy (Hemi Vs Total)	0.803	0.56 - 1.12	P=0.221

[a] Non-monotonic relationship of age with relapse of thyroid cancer

Based on the subhazard ratio of independent prognostic factors, we constructed nomograms to predict the risks of death and relapse of thyroid cancer (Figure 10).
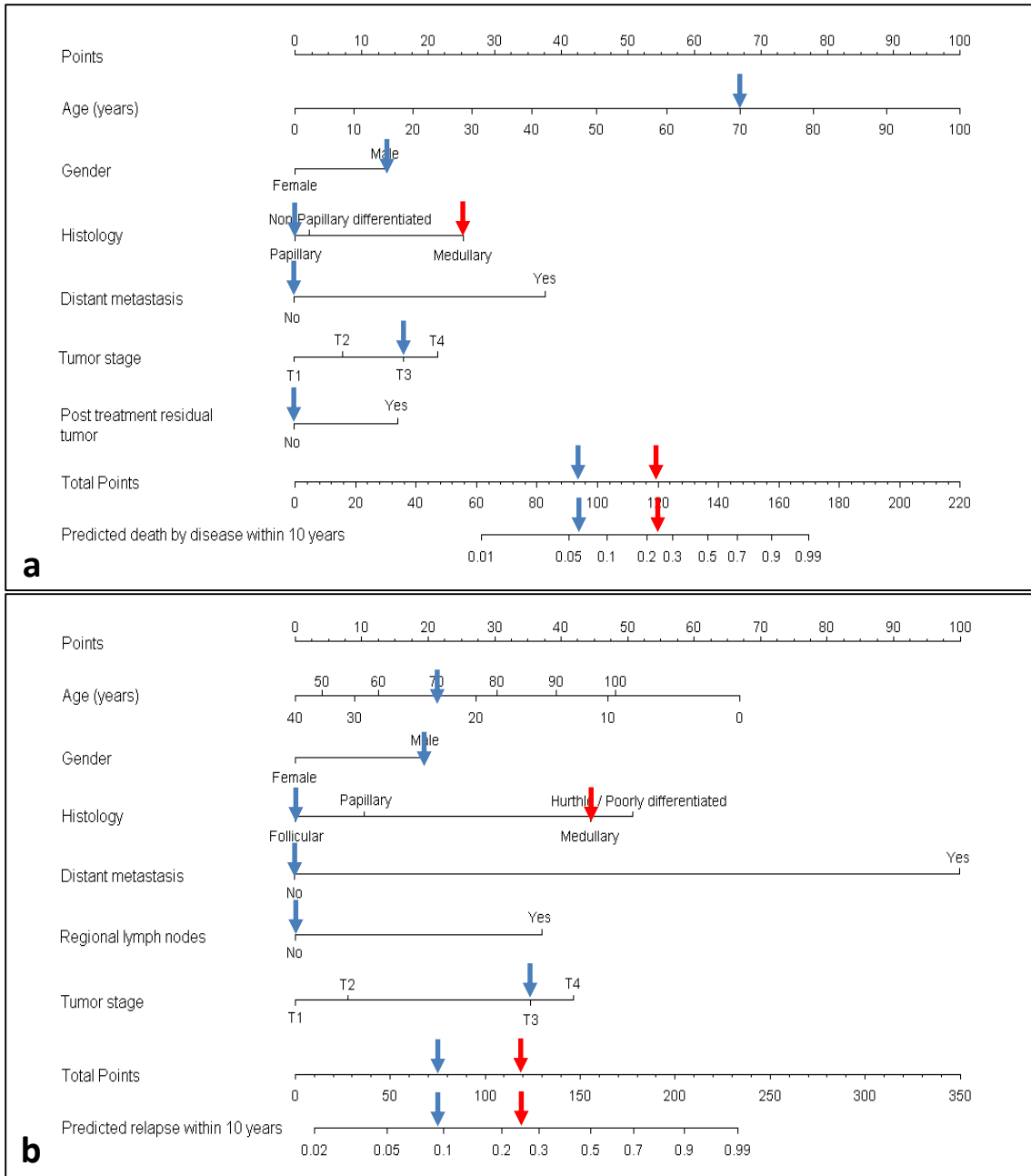
Figure 10: Thyroid cancer prognostic nomograms to predict the risks of (a) death and (b) relapse from thyroid cancer.

Blue arrows show that a 70-year old male patient, who underwent complete resection of a T3N0M0 PTC, without any evidence of residual disease [94 points on risk of thyroid cancer death nomogram (a) and 75 points on risk of relapse nomogram (b)], had a 6% predicted risk of death 9% and predicted risk of relapse from thyroid cancer within 10 years after treatment. If the same patient had MTC (red arrows) instead of PTC, he would have a 25% predicted risk of relapse and 24% predicted risk of death over the same time period.

Figure 10 shows that a 70-year old (21 points) male (19 points) patient, who underwent complete resection of a T3 (35 points) N0 (0 point) M0 (0 point) PTC (0 point), had a 9% predicted risk of relapse of thyroid cancer (Figure 10b; blue arrows indicate a total of 75 points), and a 6% predicted risk of death from thyroid cancer within 10 years of treatment [Figure 10a; blue arrows indicate a total of 94 points for age(67 points) male gender (12 points) and T3 tumor (15 points)]. If the same patient had MTC (red arrows) instead of PTC, he would have a 25% predicted risk of relapse (119 points; Figure 10b) and 24% predicted risk of death over the same time period (119 points; Figure 10b). Further, if the same patient had T3 PTC with pulmonary metastasis (100 additional points for the risk of relapse and 38 additional points for the risk of death from thyroid cancer), these nomograms would predict 68% risk of relapse and 40% predicted risk of death from thyroid cancer within 10 years following treatment.

Discrimination is the ability of a model to separate subject outcomes between the predicted probability and the observed response. Our model had a high c-index for predicting the risks of thyroid cancer related death (0.92) and relapse of thyroid cancer (0.76), indicating an excellent discrimination capability, where the c-index of 1 is ideal. The marginal estimate was plotted against the model average predictive probability as calibration plots and most of the predictions fell on the 45-degree diagonal line (Figures 11a & b).
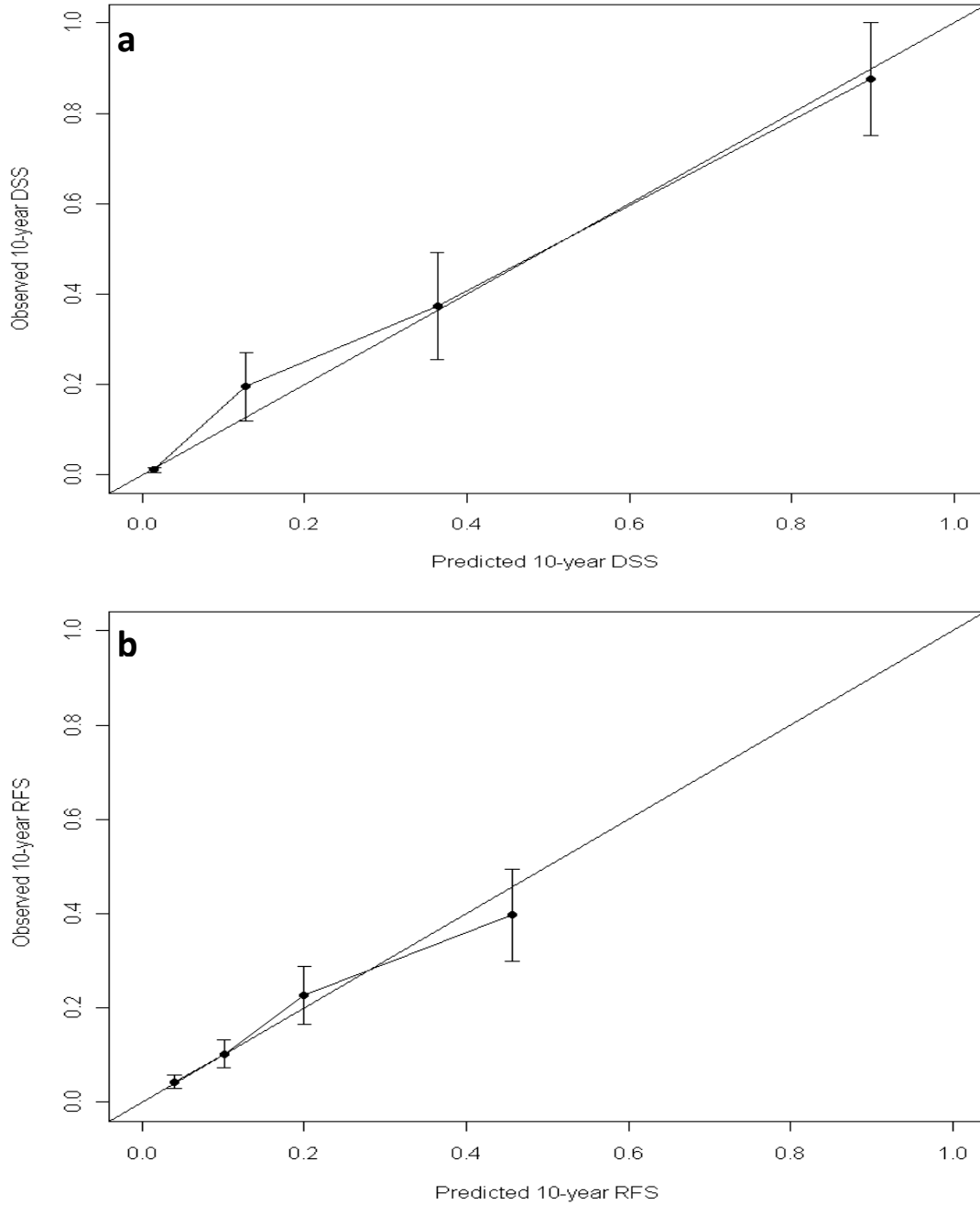
Figure 11: Calibration plots for predicting the risk of thyroid cancer related (b) deaths and (a) relapses.
The calibration plots show observed survival plotted against the predicted survival. An ideal calibration curve falls on the 45-degree diagonal line. The calibration curves were very close to the diagonal showing that most of the predictions were either close to or on the 45-degree diagonal line suggesting good calibration.

4.2.4   Comparison with existing staging/risk stratification systems for thyroid cancer

The Manitoba thyroid prognostic model was compared with 12 existing staging system in a subset of 1900 patients (450 males and 1450 females), who had a follow-up of 22,287 patient-years. The mean age of the patients was 47 ± 17 years and PTC was the most commonly observed histological type in 1533 (80.7%) patients, followed by follicular carcinoma (FTC) in 193 (10.2%) patients, Hürthle cell in 70 (3.7%), poorly differentiated carcinoma in 39 (2.1%), and medullary carcinoma in 65 (3.4%) patients. TNM classification as well as stage/class/risk group distribution of patients with non-ATC, WDTC and PTC is summarized in Table 12.

Table 12: Stage distribution for different staging/risk stratification systems.

Staging	Group	Papillary (N=1533)	Differentiated (N=1796)	Non-Anaplastic (N=1900)
T category	T1	756 (49.32%)	821 (45.71%)	855 (45.00%)
	T2	398 (25.96%)	505 (28.12%)	532 (28.00%)
	T3	310 (20.22%)	388 (21.60%)	414 (21.79%)
	T4	69 (4.50%)	82 (4.57%)	99 (5.21%)
N category	N0	1127 (73.52%)	1371 (76.34%)	1431 (75.32%)
	N1	406 (26.48%)	425 (23.66%)	469 (24.68%)
M category	M0	1509 (98.43%)	1764 (98.22%)	1858 (97.79%)
	M1	24 (1.57%)	32 (1.78%)	42 (2.21%)
Tumor, Node, Metastases	Stage I	1086 (70.84%)	1213 (67.54%)	1213 (65.21%)
	Stage II	148 (9.65%)	210 (11.69%)	210 (12.00%)

(AJCC-TNM) Classification 7th Edition	Stage III	181 (11.81%)	230 (12.81%)	230 (12.89%)
	Stage IV	118 (7.70%)	143 (7.96%)	143 (9.89%)
National Thyroid Cancer Treatment Cooperative Study (NTCTCS)	Stage I	781 (50.95%)	801 (44.60%)	801 (42.68%)
	Stage II	443 (28.90%)	510 (28.40%)	510 (27.47%)
	Stage III	292 (19.05%)	460 (25.61%)	460 (26.95%)
	Stage IV	17 (1.11%)	25 (1.39%)	25 (2.89%)
European Organization for Research and Treatment of Cancer (EORTC)	Group 1	784 (51.14%)	887 (49.39%)	887 (48.21%)
	Group 2	410 (26.74%)	477 (26.56%)	477 (26.42%)
	Group 3	261 (17.03%)	321 (17.87%)	349 (18.37%)
	Group 4	76 (4.96%)	106 (5.90%)	127 (6.68%)
	Group 5	2 (0.13%)	5 (0.28%)	6 (0.32%)
Mayo Clinic (Age, Grade, Extent, Size or AGES)	Group 1	571 (37.25%)	648 (36.08%)	Not Applicable
	Group 2	379 (24.72%)	411 (22.88%)	
	Group 3	342 (22.31%)	416 (23.16%)	
	Group 4	241 (15.72%)	321 (17.87%)	
Virgen de la Arrixaca University at Murcia (Murcia)	Low risk	1173 (76.52%)	1348 (75.06%)	Not Applicable
	Medium risk	325 (21.20%)	403 (22.44%)	
	High risk	35 (2.28%)	45 (2.51%)	
Mayo Clinic (Metastases, Age, Completeness of Resection, Invasion, Size or MACIS)	Group 1	1261 (82.26%)	1430 (79.62%)	Not Applicable
	Group 2	152 (9.92%)	194 (10.80%)	
	Group 3	64 (4.17%)	90 (5.01%)	

	Group 4	56 (3.65%)	82 (4.57%)	
University of Chicago *(Clinical Class)*	Class 1	923 (60.21%)	1083 (60.30%)	Not Applicable
	Class 2	225 (14.68%)	231 (12.86%)	
	Class 3	361 (23.55%)	450 (25.06%)	
	Class 4	24 (1.57%)	32 (1.78%)	
Ohio State University (OSU)	Stage 1	433 (28.25%)	456 (25.39%)	Not Applicable
	Stage 2	715 (46.64%)	859 (47.83%)	
	Stage 3	361 (23.55%)	449 (25.00%)	
	Stage 4	24 (1.57%)	32 (1.78%)	
University of Müntser *(Müntser)*	Low risk	1449 (94.52%)	1694 (94.32%)	Not Applicable
	High risk	84 (5.48%)	102 (5.68%)	
University of Alabama and M.D. Anderson (UAB & MDA)	Low risk	901 (58.77%)	1024 (57.02%)	Not Applicable
	Intermediate risk	608 (39.66%)	740 (41.20%)	
	High risk	24 (1.57%)	32 (1.78%)	
Lahey Clinic (Age, Metastases, Extent, Size or AMES)	Low risk	1341 (87.48%)	1547 (86.14%)	Not Applicable
	High risk	192 (12.52%)	249 (13.86%)	
Memorial Sloan Kettering (Grade, Age, Metastases, Extent, Size or GAMES)	Low risk	633 (41.29%)	633 (35.24%)	Not Applicable
	Intermediate risk	773 (50.42%)	871 (48.50%)	
	High risk	127 (8.28%)	292 (16.26%)	
Relapse free survival at 20 years		86.0%	86.0%	84.3%
Disease specific survival at 20 years		94.9%	93.4%	92.7%

Total thyroidectomy was performed in 1047 patients (55.1%) and 982 patients (54.7%) with differentiated thyroid cancers; 717 (73.0%) of these received adjuvant radioactive iodine. Sixty (3.2%) patients had post-treatment residual disease. All patients of WDTC, who had unresectable macroscopic residual disease in the neck following total thyroidectomy or those, who were at a high risk of disease recurrence, i.e. those with T3/T4 tumors, regional and distant metastasis, received RAI. Use of external beam radiation therapy was limited to unresectable macroscopic residual disease. During the median follow-up of 11.59 years (inter-quartile range= 7.13-19.24 years), 181 (9.53%) patients had clinical/radiological evidence of recurrent disease after at least 6 months following an initial successful treatment. During the course of follow-up, 106 (5.6%) patients died of their disease.

Degree of freedom (m) and -2 log likelihood (-2LL) obtained by using competing risk analysis were used to calculate AIC, Delta AIC, and concordance indices for different staging systems in predicting the risk of death from PTC (Table 13), differentiated thyroid cancers of follicular cell origin (Table 14), and all non-ATC (Table 15). The thyroid prognostic nomogram model had the lowest AICs and highest concordance indices for risk of death from non-ATC (AIC=1161.82, c-index=0.944), differentiated thyroid cancers of follicular cell origin (AIC=822.43, c-index=0.941) and PTC (AIC=451.64, c-index=0.947), suggesting it to be the best among the compared models. In terms of AIC, TNM-AJCC Classification was the next best model for predicting risk of death from all

non-ATC and MACIS was the next best model for differentiated thyroid cancers of follicular cell origin and more specifically for PTC.

Table 13: AIC, Delta AIC, Akaike weight, and Evidence Ratio for risk of death from papillary thyroid carcinoma for various staging systems.

Staging system	AIC[1]	Δ_i[2]	C- Index
Nomogram	471.6354	0	0.947
MACIS	480.053	8.417	0.904
AMES	506.3923	34.757	0.908
Clinical Class	511.4453	39.810	0.910
OSU	511.4632	39.828	0.905
NTCTCS	511.7387	40.103	0.920
Münster	517.1069	45.472	0.849
EORTC	523.1761	51.541	0.797
UAB & MDA	528.926	57.291	0.845
AGES	529.3788	57.743	0.906
TNM Classification	530.1004	58.465	0.892
GAMES	547.2368	75.601	0.882
Murcia	559.8731	88.238	0.850

---

[1] $AIC = -2LL + 2m$
[2] $\Delta_i = AIC_i - minAIC$

Table 14: AIC, Delta AIC, Akaike weight, and Evidence Ratio for risk of death from differentiated thyroid carcinoma for various staging systems.

Staging system	AIC	Δ_i	C- Index
Nomogram	8224342	0	0.941
MACIS	8580169	355827	0.889
AMES	8994295	769953	0.842
Clinical Class	8909118	684776	0.866
OSU	8924191	699849	0.876
NTCTCS	8853948	629606	0.888
Münster	9134634	910292	0.782
EORTC	9206111	981769	0.830
UAB & MDA	9322623	1098281	0.783
AGES	9211526	987184	0.864
TNM Classification	9051132	82679	0.865
GAMES	9498399	1274057	0.856
Murcia	9791918	1567576	0.776

Table 15: AIC, Delta AIC, Akaike weight, and Evidence Ratio for risk of death from non-anaplastic thyroid carcinoma for various staging system

Staging system	AIC	Δ_i	C- Index
Nomogram	1161819	0	0.944
TNM Classification	1276576	114757	0.873
NTCTCS	1282011	120192	0.883
EORTC	1320669	15885	0.842

4.2.5 Development and validation of web-based computerized prognostic model

A web-based computerized model (*www.survivalcurves.net*) to predict cancer survival for thyroid cancer was developed that uses the prognostic factors i.e. age, gender, TNM stage, histology from the Cox proportional hazard model to plot survival curves for thyroid cancers. For this purpose, two randomly selected development and validation samples were used. These samples were similar to each other in terms of the age and gender distribution, even though slightly higher proportion of female patients were randomly selected in the validation sample. Their follow-up duration was also comparable (Table 16).

Table 16: Development and validation samples for web-based prognostic model.

	Development Sample (N=1161)	Validation Sample (N=1135)	p-value
Age in years	48.5 ± 17.7	48.7 ± 18.3	0.882
Female Gender	819 (73.2%)	823 (76.9%)	0.052
Follow-up in years	12.8 ± 10.1	12.5 ± 9.7	0.397

On multivariable analysis by the Cox proportional hazard model restricted to the development sample, the DSS was independently influenced by the age at diagnosis, male gender completeness of resection, and tumor histology as well as by their T, N and M stages (Table 17). ` For the long-term disease-specific survival of thyroid cancer, the presence of distant metastasis was the most important factor influencing DSS (HR=10.4; p<0.001), followed by anaplastic histology (HR=8.8; p<0.001).

110

Table 17: Cox Proportional Hazard Model for development sample.

Variable	Hazard Ratio	95% (CI)	p-value
Age at diagnosis in years	1.07	(1.04, 1.09)	<0.001
Gender (Male vs. female)	3.0	(1.6, 5.8)	0.001
Histological type			0.001
Follicular vs. Papillary	2.4	(0.8, 7.2)	
Hürthle Cell vs. papillary	3.0	(1.2, 7.7)	
Poorly differentiated/ Medullary vs. Papillary	6.3	(2.5, 15.8)	
Anaplastic vs. Papillary	8.4	(2.1, 33.2)	
T stage			0.078
T2 vs. T1	1.5	(0.5, 5.0)	
T3 vs. T1	3.8	(1.3, 11.1)	
T4a vs. T1	3.8	(1.0, 14.0)	
T4b vs. T1	3.3	(0.8, 13.7)	
N stage			0.043
N1a vs. N0	3.6	(1.4, 9.3)	
N1b vs. N0	4.0	(1.8, 8.9)	
M stage (M1 vs. M0)	13.6	(5.0, 37.0)	<0.001
Completeness of resection	2.8	(1.1,7.0)	0.025

ROC curves were used to evaluate the Cox proportional hazard model developed for predicting long-term DSS beyond the first year (Figures 12).
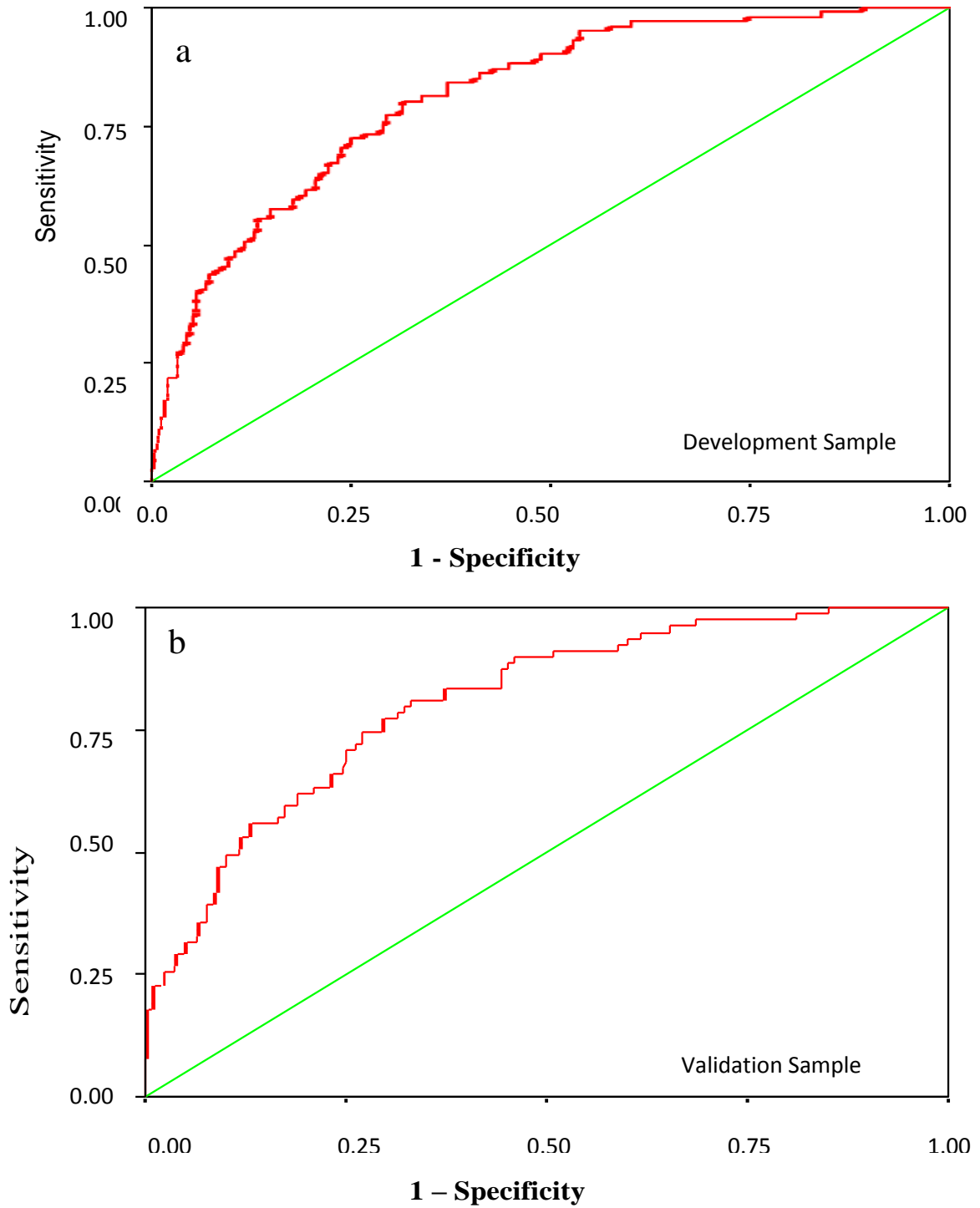
Figure 12: ROC curve for (a) development and (b) validation samples.
Sensitivity is plotted against 1-specificity on a unity square to indicate both sensitivity and specificity of the model. The ROC curves are far from the chance diagonals and never actually touch it. The AUROC is 0.87 for development and 0.82 for validation samples.

112

The ROC curves show that the Cox proportional hazard model, for the validation sample (Figures 12b), had similar prediction capability of the long-term survival as the Cox proportional hazard model developed from the development sample (Figures 12a). The area under curve was 0.87 (95% CI: 0.83-0.92) for development and 0.82 (95% CI: 0.77-0.87) for validation samples. The large area under the curve (>0.80) indicates good accuracy (validity). The 95% CI did not include the chance probability (0.50). The CIs were quite narrow (<0.10), which indicates good reliability (precision) of the estimate. For both samples, the ROC curves were far from the chance diagonals and never actually touched it.

Figure 13 shows the screenshots of the web pages with survival curves and 95% CI plotted to show three case scenarios of 10-year DSS probability of a 70-year old male. After complete surgical resection of T3N0M0 PTC, the likelihood of 10-year DSS would be 94% (95% CI: 90-97%). In the presence of distant metastasis (T3N0M1 PTC) his 10-year DSS probability would be only 61% (95% CI: 46-79%). If the same patient had T3N0M0 MTC, the likelihood of 10-year DSS would be 74% (95% CI: 63-87%). This web-based model offers the option of adding 95% CI to the DSS curve. The orange and purple curves on either side of the blue DSS curve represent the upper and lower limits of 95% CI. The survival probability at any time point up to 30 years can be obtained by moving the cursor along the curve. The corresponding points on the two outer curves (orange and purple) represent the 95% CI. This model is freely available online for exclusive use by healthcare professionals.
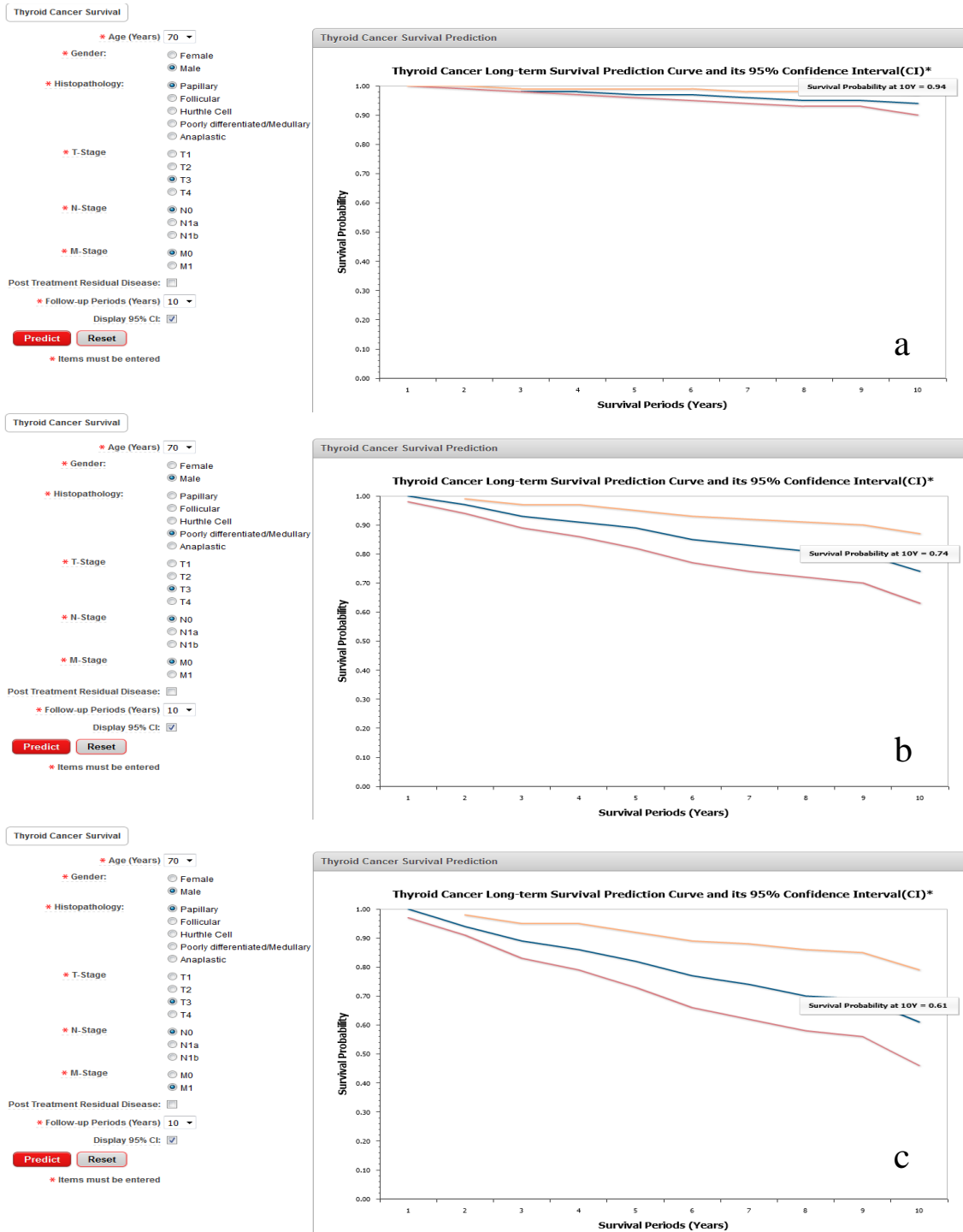
Figure 13: Disease specific survival of a 70-year old male with (a) T3N0M0 PTC (b) T3N0M0 MTC (c) T3N0M1 PTC.
The orange and purple curves on either side of the blue DSS curve represent the upper and lower limits of 95% CI.

4.2.6 External validation of the Manitoba prognostic model

The web-based Manitoba prognostic model was further validated on an independent external cohort that included 1454 thyroid cancer patients treated and followed up at London Health Sciences Centre for a total of 12273 patient-years. The cohort has 305 (21.0%) males and 1149 (79.0%) females with a mean age ($\pm$ standard deviation) of 45.7$\pm$14.5 years. PTC was seen in 1349 (92.8%) patients and FTC in 102 (7.0%). Three (0.2%) had PDTC. Histology had a significant impact on survival (p<0.001) (Figure 14). At the time of diagnosis, 350(24.1%) patients had cervical lymph node involvement and 36 (2.5%) patients had evidence of distant metastasis. Gross ETE of tumor were observed in 284 (19.5%) patients. Complete surgical resection was attempted and achieved in 1263 (86.9%) cases and 1236 (85.0%) patients received adjuvant RAI.
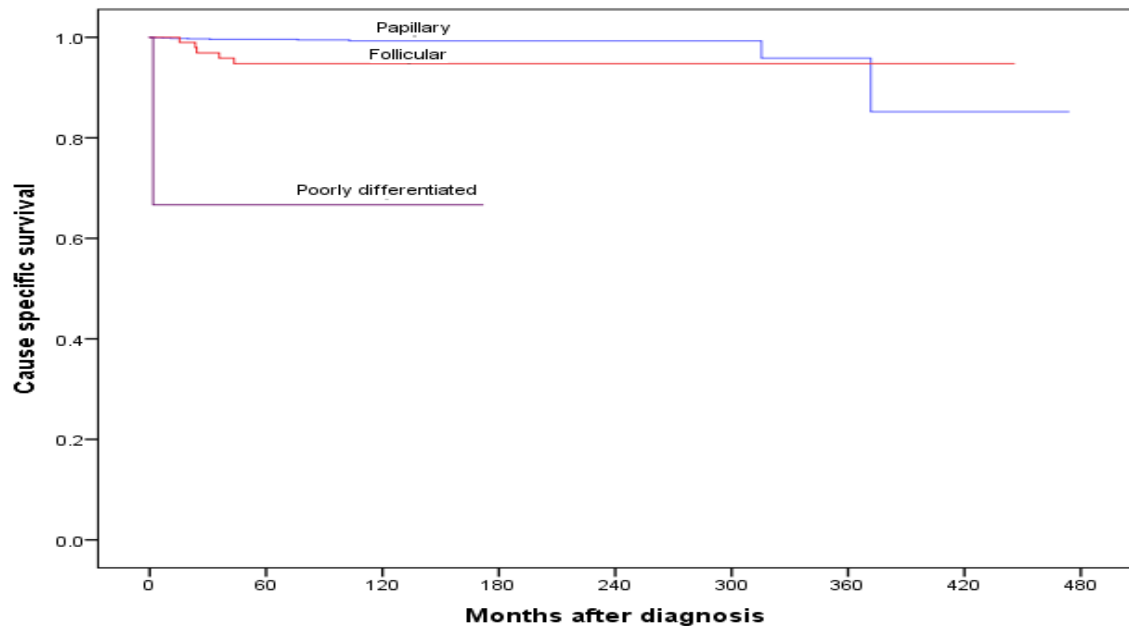
Figure 14: Disease specific survival of London, ON cohort, based on the histology. DSS was calculated by Kaplan-Meier method. Ten-year DSS was 99.1% for PTC, 94.9% for FTC, and 66.8% for PDTC. PDTC had a significantly lower DSS (p<0.001) as compared to FTC and PTC.

According to UICC-TNM classification, 987 (67.9%) patients had stage I disease, 186 (12.8%) had stage II, 197(13.5%) had stage III disease and 76 (5.2%) had stage IV disease. Eight (0.6%) cases did not have adequate information to ensure proper staging. During a median follow-up of 7.0 years (IQR= 4.8-10.7), 167 (11.5%) patients had clinical/radiological evidence of recurrent disease and at the last follow-up 116 (8.0%) were alive with disease, whereas 15 (1%) patients had died due to their thyroid cancer. Five-year DSS was 99.4% and 10-year DSS was 98.9%. The Manitoba prognostic model, was validated on an independent external cohort of thyroid cancer patients with a c-index (AUROC) = 0.96 (Figure 15). This indicated excellent discrimination and a very narrow 95% CI (0.93-0.97), indicated a very good reliability.

Area Under the Curve 0.96 (95% CI=0.93, 0.99)
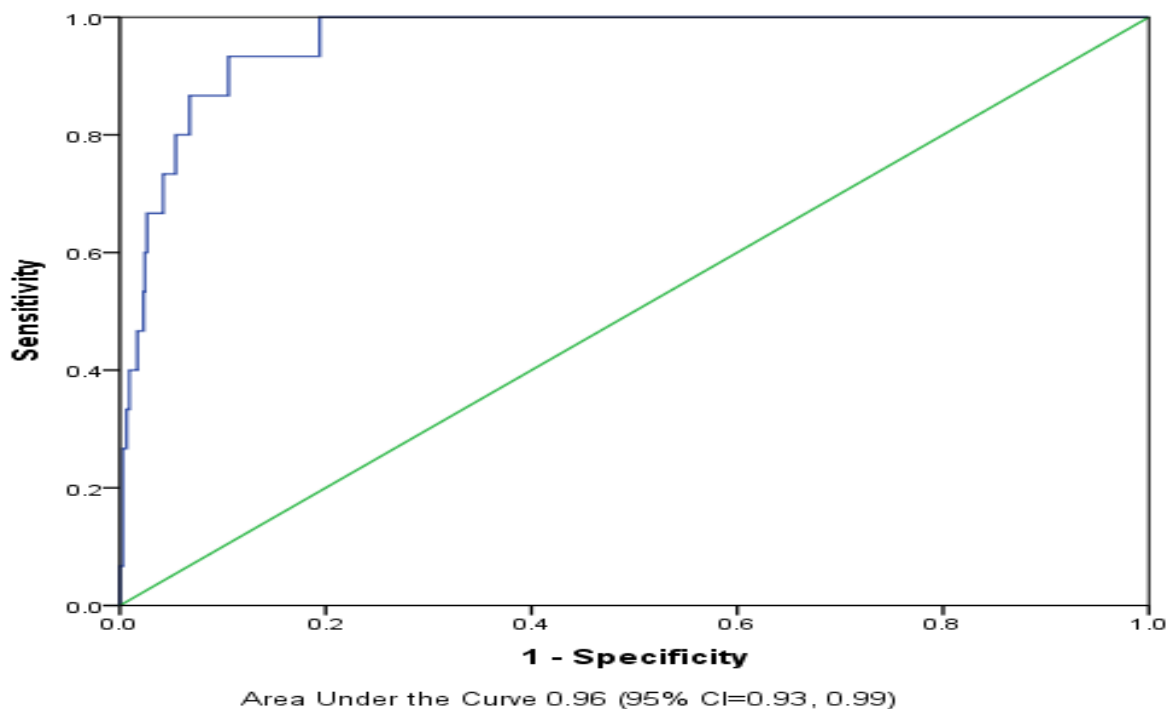
Figure 15: ROC curve showing predicted and actual disease specific survival.
The ROC curve of external validation using the London, ON cohort is very far from the chance diagonal and never actually touches it. The AUROC is 0.96 (95% CI: 0.93-0.97).

116

4.2.7 Prognostic importance of distant metastasis in TNM staging

Our population cohort of 2118 consecutive WDTC patients showed that the DSS of stage II metastatic carcinoma was very similar to stage IVB (p=0.530, NS) and IVC (p=0.127, NS) (Figure 16).
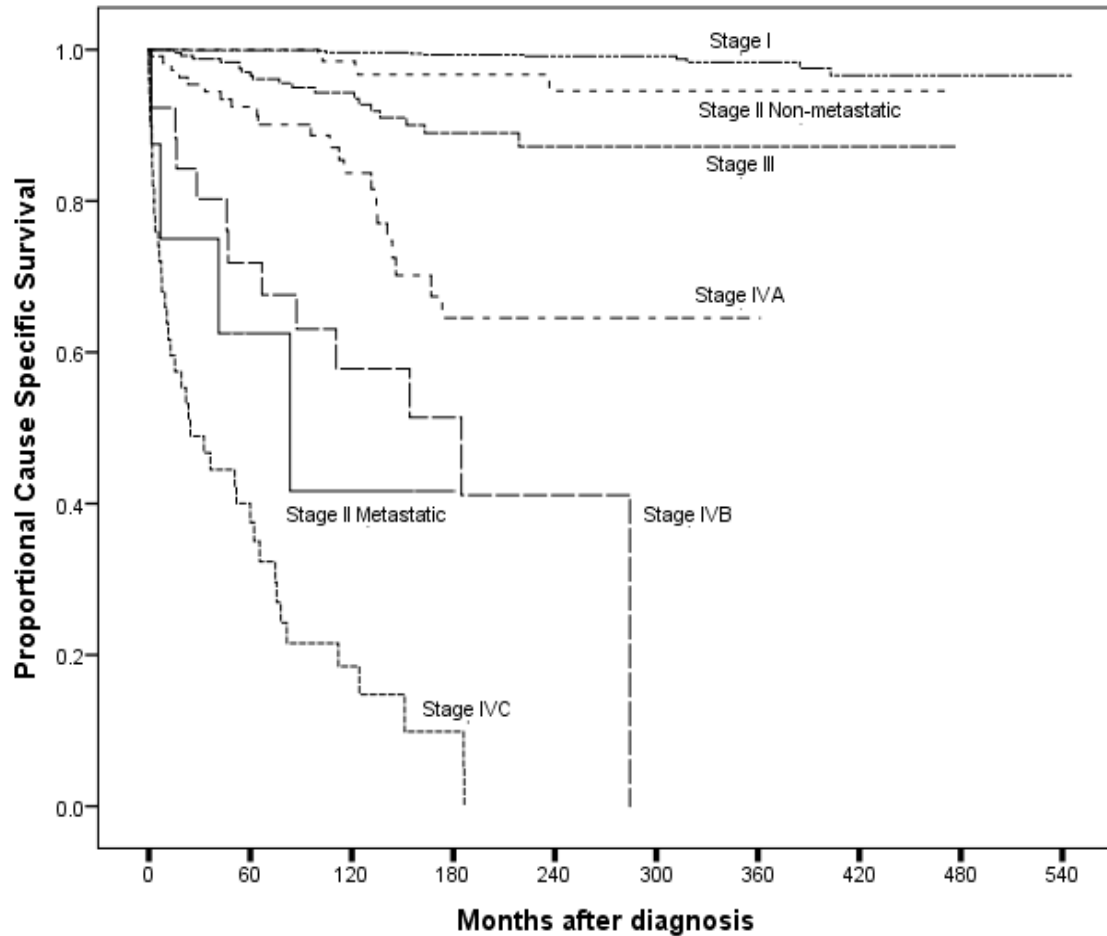
Figure 16: Disease specific survival of WDTC in the Manitoba thyroid cancer cohort. DSS of metastatic WDTC in patients <45 years (stage II metastatic) is intermediate between stages IVB and IVC (metastatic WDTC in patients ≥ 45 years). It was significantly different from non-metastatic WDTC in patients ≥ 45 years (stage II metastatic). DSS was calculated by Kaplan-Meier method. Y-axis shows proportion of patients surviving at any point in time.

A subset analysis was done on 215 stage II WDTC patients with the mean age of 58.0 ± 11.8 years and 164 (76.3%) patients were females. The median tumor size was 30mm (IQR= 25-35mm) and 209 (97.2%) patients had T2 tumor; 2 (0.9%) had T1, 1 (0.5%) T3 tumor, and 3 (1.4%) had T4 tumor. Eight (3.7%) patients had metastatic WDTC and 5 (2.3%) were node positive. One hundred fifty two (70.7%) patients had papillary carcinoma, followed by 40 (18.6%) follicular carcinoma, and 23 (10.7%) had Hürthle cell carcinoma. Total thyroidectomy was performed in 108 (50.2%) and 47(21.9%) received adjuvant radioactive iodine treatment.

During a median follow-up of 134.3 months (IQR= 80.7-211.6 months), 19 (8.8%) patients had recurrent or persistent disease. At the time of last contact, 142 (66%) patients were alive without any evidence of disease and 3 (1.4%) with disease. Nine (4.2%) had died due to the disease, 17 (7.9%) due to a second primary cancer and 44 (20.4%) due to other causes. The demographics and clinical presentation of metastatic and non-metastatic stage II WDTC were significantly different (Table 18). A similar proportion of patients had PTC and total thyroidectomy in both groups. However, there was a significant difference (p< 0.001) in the DSS and the RFS of metastatic and non-metastatic stage II WDTC (Table 18). Metastatic and non-metastatic stage II WDTC had a 15 year DSS of 41.7% and 96.7%, respectively.

Cox proportional hazard model to assess the independent influence of various prognostic factors on oncological outcome of stage II WDTC showed a 52 times higher

risk of death in metastatic stage II WDTC as compared to non-metastatic stage II WDTC, and a 17 times higher risk of death was seen in males as compared to the females (Table 19).

Table 18: Clinical characteristics and oncological outcome of non-metastatic and metastatic stage II well differentiated thyroid carcinoma (N=215).

	T2N0M0 (patient age≥45 years) (N=207)	Any T, any N, M1 (patient age<45 years) (N=8)	p-value
Mean Age	58.9 ± 11.0 years	34.9 ± 7.7 years	<0.001
Gender (F:M)	4:1	1:3	0.001
Papillary thyroid carcinoma	69.6%	100%	NS
T2 tumor	100%	25%	<0.001
Lymph node involvement (N+)	0%	50.0%	<0.001
Distant metastasis (M1)	0%	100%	<0.001
Total thyroidectomy	50.5%	75.0%	NS
Radioactive iodine	38.2%	75.0%	0.027
Extra-thyroidal spread	0%	37.5%	<0.001
Complete resection	99%	75%	0.002
Recurrence or residual disease	5.8%	87.5%	<0.001
Dead of disease	2.4%	50%	<0.001
10 year RFS	93.3%	12.5%	<0.001
15 year DSS	96.7%	41.7%	<0.001

Table 19: Multivariable analysis by Cox proportional hazard model for independent influence of prognostic factors on disease specific survival of stage II well differentiated thyroid carcinoma (N=215).

Prognostic Factor	Hazard Ratio (95% CI)
Distant Metastasis (M stage)	52.28 (7.49-365.93), p< 0.001
Gender (Male versus Female)	16.77 (2.81-99.94), p=0.002
Completeness of resection (Incomplete versus complete)	p=0.057(NS*)
Age at the time of diagnosis (per year)	p=0.147(NS)
Extent of thyroidectomy (Hemi versus Total)	p=0.373(NS)
Adjuvant Radioactive Iodine (RAI versus no RAI)	p=0.417(NS)
Lymph node involvement (N stage)	p=0.524(NS)
Histology (Hürthle cell vs others)	p=0.795(NS)
Primary Tumor (T Stage)	p=0.859(NS)

The Manitoba thyroid cancer cohort contains 106 metastatic thyroid cancer cases that includes 61 metastatic WDTC (2.9% of all WDTC) with a mean age of 65.4 ± 16.1 years and 30 (49.2%) female patients. Forty three (70.5%) patients had papillary carcinoma, 14(23.0%) follicular carcinoma, and 4 (6.5%) had Hürthle cell carcinoma. There were significantly higher proportions of PTC and female patients in the < 45 years age group (Table 20). As expected stage IVC patients were significantly older than stage II. Eleven (18.0%) patients had T1 tumor, 10 (16.4%) had T2, 19 (31.2%) T3 tumor whereas 21 (34.4%) had T4 tumor.

Table 20: Clinical characteristics and outcome of metastatic stage WDTC (n=61).

	Stage II (Any T, any N, M1) (N=8)	Stage IVC (Any T, any N, M1) (N=53)	p-value
Age	34.9 ± 7.7 years	70.3 ± 11.1 years	<0.001
Gender (F:M)	1:3	1:1	<0.001
PTC	100%	57.4%	0.020
T1/T2 tumor	50%	31.1%	NS*
T3/T4 tumor	50%	68.9%	NS
Lymph node involvement	50.0%	55.7%	NS
Total thyroidectomy	75.0%	84.2%	NS
Radioactive iodine	75.0%	68.4%	NS
Extra-thyroidal spread	37.5%	32.1%	NS
Complete resection	75%	66.7%	NS
Post-treatment persistence	87.5%	93.0%	NS
Dead of disease	50%	78.9%	NS
10 year RFS	12.5%	4.7%	NS
15 year DSS	41.7%	9.9%	NS

Fifty three (86.9%) patients showed signs of clinical, radiological or biochemical evidence of recurrent or persistent disease. At the time of the last follow-up 3 (4.9%) patients were alive without any evidence of disease and 7 (11.5%) were alive with disease. In the meantime, 46 (75.4%) patients had died because of WDTC, and 5 (8.2%) due to

121

other causes. There was no difference in the DSS (p=0.127) and RFS (p=0.591) of the two groups. To assess the independent influence of prognostic factors on DSS of metastatic WDTC, multivariable analysis was performed by Cox proportional hazard model. It showed no difference between metastatic stage II and stage IVC WDTC (Table 21). Adjuvant radioactive iodine reduced the risk of death from metastatic WDTC by 80%. Males with metastatic WDTC were 6.3 times more likely to die of their disease as compared to their female counterpart. Incomplete resection and Hürthle cell histology were the other two independent determinants of survival in metastatic WDTC (Table 21).

Table 21: Multivariable analysis by Cox proportional hazard model for independent influence of prognostic factors on DSS of metastatic WDTC (N=61).

Prognostic Factor	Hazard Ratio (95% CI)
TNM stage IV vs TNM stage II	p=0.874(NS)
Gender (Male versus Female)	6.33(1.91-20.91), p=0.002
Adjuvant Radioactive Iodine (RAI versus no RAI)	0.190 (0.07-0.54), p=0.002
Histology (Hürthle cell vs others)	8.87 (1.08-72.55), p=0.042
Completeness of resection (Incomplete versus complete)	3.43 (1.17-10.07), p=0.025
Primary Tumor (T Stage)	p=0.187(NS)
Age at the time of diagnosis (per year)	p=0.354(NS)
Extent of thyroidectomy (Hemi versus Total)	p=0.553(NS)
Lymph node involvement (N stage)	p=0.831(NS)

4.3   Summary of results

I did not find any significant difference between the benign and malignant nodules in terms of the patients' age and gender, median SUVmax, MTV and TLG. However there was a very significant difference between the SUVmax of HCA and FA. All HCA but only half of the FA showed increased focal FDG uptake (298). As all HCA were observed to show high SUV, after excluding HCA, the AUROC for discriminating benign from malignant nodules was 0.79 (95% CI: 0.63-0.94; p=0.002), with 3.25 as the best SUVmax cut-off for the purpose. FDG-PET /CT had a sensitivity of 79% (95% CI: 54-93%), specificity of 83% (95% CI: 60-94%), PPV of 79% (95% CI: 54-93%), and NPV of 83% (95% CI: 60-94%), with an overall accuracy of 81% (286). Partial volume correction of SUVmax of 4 PTC with diameter < 10 mm did not change the classification of these lesions as all these lesions had SUVmax >3.25 (true positive). All benign lesions were > 10mm in diameter and partial volume correction of SUVmax did not have any significant influence on their characterization.

This work has resulted in establishment of the Manitoba thyroid cancer cohort, a unique cohort of 2306 thyroid cancers with a median follow-up 11.5 years and comprehensive information about the demographics, staging and treatment of these patients. The ASIR of thyroid cancer from 2.52 in 1970 to 9.37 in 2010, even though the proportion of micro carcinoma, mean age of patients at the time of diagnosis, median tumor size and the tumor stage at presentation did not show any statistically significant change. The proportion of the patients undergoing total thyroidectomy increased by two and a half

times between 1970-1980 and 2001-2010, while those receiving adjuvant radioactive iodine increased by over five times, but both of them did not have any significant influence on DSS. During the same period, the proportion of all thyroid cancers that were diagnosed as FVPTC increased from 12.4% to 32.9%, whereas the proportion of FTC fell from 26% to 5.1% (p<0.001) and anaplastic carcinoma from 5.7% to 2.1%. The increase in proportion of PTC and decrease in ATC has resulted in significantly improved 10-year DSS from 85.4% (1970-1980) to 95.6% (2001-2010) with a 64.3% reduction in death due to thyroid cancer (from 12.6 to 4.5%) after 5 years of follow-up (71).

The oncological outcome of the Manitoba thyroid cancer cohort was used to develop and validate the thyroid prognostic nomogram and web-based prognostic model for predicting oncological outcomes of thyroid cancer (29, 299). Discrimination (c- index) is the ability of a model to separate subject outcomes between the predicted probability and the observed response. The Manitoba thyroid cancer prognostic model had a high c-index for predicting the risks of thyroid cancer related death (0.92) and relapse of thyroid cancer (0.76), indicating an excellent discrimination capability, where the c-index of 1 is ideal. The marginal estimate was plotted against the model average predictive probability as calibration plots and most of the predictions fell on the 45-degree diagonal line (29). This model compares favorably with the existing staging/risk stratification systems (299). The thyroid prognostic nomogram model had the lowest AICs and highest concordance indices for risk of death from non-ATC (AIC=1161.82, c-index=0.944), differentiated thyroid cancers of follicular cell origin (AIC=822.43, c-index=0.941) and PTC (AIC=451.64, c-

index=0.947), suggesting it to be the best among the compared models. In terms of AIC, TNM-AJCC Classification was the next best model for predicting risk of death from all non-ATC and MACIS was the next best model for differentiated thyroid cancers of follicular cell origin and more specifically for PTC (299).

The Manitoba prognostic model was successfully adapted as a web-based model. The AUROC was similar for development [0.87 (95% CI: 0.83-0.92)] for and 0.82 (95% CI: 0.77-0.87) for validation samples. The Manitoba prognostic model was validated on an independent external cohort of thyroid cancer patients from London, Ontario with a c-index of 0.96 (0.93-0.97). The large area under the curve (>0.80) indicates good discrimination (validity) and the 95% CIs were quite narrow (<0.10) indicating good reliability (precision).

The prognostic importance of age and distant metastasis in TNM staging were critically analyzed using the Manitoba thyroid cancer cohort. Cox proportional hazard model to assess the independent influence of various prognostic factors on oncological outcome of stage II WDTC showed a 52 times higher risk of death in metastatic stage II WDTC as compared to non-metastatic stage II WDTC and there was no difference between metastatic stage II and stage IVC WDTC (300).

Chapter V

Discussion

5.1   Assessment of the diagnostic role of FDG-PET /CT

The incidence of thyroid adenoma on autopsy specimens has been reported to be 3-4.3% (301, 302). FNAB and ultrasonography are the mainstays in the diagnosis of thyroid cancer. However, differentiation between benign and malignant FN remains a challenge for both ultrasound and FNAB. Fifteen to 30% of the thyroid lesions that are reported as FN/HCN on FNAB are ultimately malignant (7). FDG-PET/CT scan has been used for this purpose with variable success. The purpose of this study was to evaluate if FDG-PET/CT can aid in distinguishing benign from malignant FN/HCN. If the malignant potential of a FN/HCN could be predicted by FDG-PET scan, a single stage total thyroidectomy can be undertaken and a second surgery after initial hemi-thyroidectomy could be avoided. This would save healthcare dollars and spare patients of the stress and risks associated with a second surgery. Diagnostic role of FDG-PET scan in thyroid nodules have been studied extensively (303-310).

Almost 1.5-2.1% of thyroid nodules are hyper-metabolic on FDG-PET scans (175, 183-185). The metabolic activity of the thyroid nodule is expressed in terms of SUV. Various studies have considered different criteria for PET positivity, ranging from any focal increased uptake in the region of the thyroid nodule above background (303, 304, 309, 310) to different SUVmax cut-offs ranging from 2 to 7 (184, 305, 307, 311). However, some studies did not find a SUVmax cut-off to be a definite predictor for malignancy (312).

Area under the SUVmax curve of > 175.5 or a heterogeneity factor of FDG uptake >2.751 have also been considered to define FDG-PET positivity (308, 313). According to an earlier meta-analysis, 1 in 3 FDG-PET positive thyroid nodules were reported to be malignant with higher mean SUVmax (6.9) as compared to the benign ones (4.8) ($p<0.001$) (177). A more recent meta-analysis included 7 studies, of which 5 were prospective. The cancer prevalence in the study cohort was 26% (314). No significant difference was found between the median SUVmax of benign and thyroid nodules, as has also been reported earlier (306). In this study group, increased focal FDG uptake by thyroid nodules (irrespective of the SUVmax) had a high sensitivity of 89% (95% CI: 65-98%) and specificity of 35% (95% CI: 19-54%) for detecting cancer, similar to those reported in the two meta-analysis: 89.0% (95% CI: 79.0%-95.0%) & 55.0% (95% CI: 48.0%-62.0%) (314), and 95% (95% CI: 86%-99%) & 48% (95% CI: 40%-56%) (11), respectively.

The diagnostic role of FDG-PET scan in thyroid nodules has been constrained by the high false positivity associated with FDG uptake by benign thyroid nodules (303-310). The meta-analyses, however, did not consider HCN separate from other FN, even though, in the pooled data, all HCN showed high FDG uptake (11, 314). Increased FDG uptake in Hürthle cells and poorly differentiated components have been reported earlier to be independent predictors of high (≥ 5) SUVmax (184). Intense FDG uptake was found in HCA (median SUVmax = 9.3). Increased FDG uptake by benign HCN (13, 315) can often be mistaken for malignancy (false positive). As 75% of the HCA could be identified by a preoperative FNAB, all FDG-positive thyroid nodules should undergo preoperative FNAB.

Hürthle cells, also known as oncocytes or Askanazy cells comprise over 75% of the cells in HCN (13, 316). A Hürthle cell is an oxyphilic variant of follicular cell which has granular cytoplasm due to abundant intra-cytoplasmic mitochondria (317). These intra-cytoplasmic mitochondria probably account for intense FDG uptake by HCN. HCN can be divided into three groups: oncocytic adenoma (HCA), oncocytic cancer (Hürthle cell carcinoma), and oncocytic infiltration (Hürthle cell nests) (13). No age and gender difference or a difference in the nodule size was found between the patients with FA and HCA, but all (100%) HCA showed increased focal FDG uptake as compared to only half (52%) of FA (298). Oncocytic cells are also seen in the parathyroid, that can give rise to PET positive oncocytic parathyroid adenoma (318).

It is important to consider HCA as a cause of increased focal FDG uptake alongside with primary or secondary malignancies in thyroid. A FDG-PET positive indeterminate thyroid neoplasm is more likely to be a HCA than a FA. Malignancy needs to be ruled out particularly in the nodules without Hürthle cell features (FN). HCA should also be suspected in the case of increased focal FDG uptake in the thyroid on staging FDG-PET scans for extra-thyroidal malignancies besides primary or metastatic disease in thyroid. SUVmax of HCA was found to be significantly higher (p<0.001) than that of FA, with SUVmax of 5 to be the best cut-off for discriminating between FA and HCA with excellent accuracy. The overall accuracy of FDG-PET/CT improved from 60% to 87 %, by using this cut-off SUVmax, rather than any increased focal uptake as the criterion of PET positivity. The specificity also improved from 49% to 87%, and PPV from 37% to 70%.

Although it is a unique prospective study of its type, the number of subjects recruited are modest and independent validation of SUVmax cut-off of 5 is recommended.

Selecting an appropriate cut-off value for any diagnostic test is challenging, as lowering the cut-off improves the sensitivity of the test; but does so at the expense of specificity. However, this will increase the number of false positives and lower its PPV, which in this case may result in unnecessary thyroidectomies. On the other hand, if the cut-off is set too high to make the test more specific, the test can miss some thyroid cancers (lower NPV) but will avoid unnecessary thyroidectomies. Ideally, a cut-off with best overall accuracy should be considered. Based on the ROC curve analysis the SUVmax of 3.25 was identified as the optimal cut-off value to discriminate between benign and malignant nodules (Figure 4), which is slightly higher than the recommended cut-off of 2.05 reported in the recent meta-analysis. The cut-off SUVmax of 3.25 offers a much higher specificity as compared to the meta-analysis (83% vs 42%) (314). The use of SUVmax cut-off of 3.25 and exclusion of HCN improves the overall accuracy of FDG-PET /CT to 81% from 56% obtained by using increased focal FDG uptake and 60% reported in meta-analysis (11). The FDG-PET /CT with a PPV 79% (95% CI: 54-93%), observed in this study was much higher than 39% (95% CI: 31-47%) reported in the meta-analysis (11).

To the best of my knowledge, this is probably the first study that prospectively looked at the impact of intense focal FDG uptake by HCA (false positivity) as a cause for

lower specificity and PPV of FDG-PET in discriminating benign and malignant indeterminate thyroid nodules (298). A cut-off SUVmax of 3.25 provided a higher accuracy with reasonably high sensitivity, specificity, PPV and NPV for predicting malignancy in FDG-PET positive non-Hürthle cell FN, as compared to any increased focal FDG uptake by thyroid nodules. FDG-PET/CT has been reported to offer a cost advantage in diagnosing malignant FN as compared to the alternatives of diagnostic thyroidectomy or molecular markers (319). The lack of any significant difference between the TLG and MTV of benign and malignant neoplasms rules out the possibility of using them as a marker of malignancy.

One of the limitations of this study is our inability to correlate the FDG-PET/CT findings with the molecular markers recommended for consideration in indeterminate thyroid nodules by the current ATA guidelines (12). The other challenge is the accurate calculation of SUVmax in sub-centimetre nodules due to partial volume effects which was corrected by the recovery coefficient method (169). It is unlikely that partial volume effect of sub-centimeter lesions had any significant impact on the FDG-PET results as all 4 sub-centimeter lesions were PTC with SUVmax > 3.25 (true positives) and partial volume correction did not make any substantial difference to the results, as has been reported before (320, 321). To compensate for the potential confounding effect of the reduced dose of FDG (185 MBq), employed to decrease the radiation exposure, the acquisition time was increased by 60% from 3 minutes to 5 minutes.

5.2 Epidemiological analysis of prognostic markers in thyroid cancer

5.2.1 The Manitoba thyroid cancer cohort

According to the Canadian Cancer Statistics, thyroid cancer has the fastest increase in the incidence of all cancers, with age standardized incidence increasing at the rate of 6.8% per year in males (1998-2007) and 6.9% per year in females (2002-2007). However, the 10-year relative survival ratio in 2004-2006 was 97% (95% CI: 96-98%) (289, 322). Similar trends have been reported globally (323-334). By direct method, the ASIR of thyroid cancer per 100,000 Canadians has increased from 1.1 in 1970-1972 to 6.1 in 2012 for males, and from 3.3 to 22.2 for females during the same period (289, 335). The life time probability of developing a thyroid cancer for a Canadian female has increased from 1 in 71 (in 2011) to 1 in 60 (in 2014) and for Canadian males from 1 in 223 (in 2011) to 1 in 193 (in 2014) (3, 42).

The risk of death from thyroid cancer for Canadian males also has decreased from 1 in 1,937 to 1 in 1538 during the same time period (3, 42). It is the most common cancer of adolescent and young women (15-29 years age group) and second most common cancer in 30-49 years age group (42, 336). Over 90% of the thyroid cancers are either follicular or papillary carcinoma, often termed as WDTC and carry excellent prognosis. Age of the patient at the time of diagnosis has a significant impact on oncological outcome of both WDTC and MTC (49, 337). Surgery is the mainstay of treatment of non-ATC and post-treatment gross residual disease is considered to be an important prognostic factor for both differentiated and MTC (25, 338).

A cohort is a population group, or subset thereof, that is followed over a period of time. The members of the cohort, based on defined criteria, share common experience which in this study was the diagnosis of thyroid cancer in the province of Manitoba (71). By virtue of residence in the same province, this study cohort was expected to share similar risk of exposure and get similar standard of medical care in the publicly funded health care system of the province. The incidence trends of thyroid cancers in the US were reported by using the SEER database, which is robust but it has its inherent limitations in terms of coverage, coding reliability, patient migration to an area that is not covered by SEER and limited information on the treatment details of the patients (71). These limitations make it difficult to interpret the time trend in treatment of thyroid cancer and its influence on thyroid cancer related survival. Due to the excellent treatment outcome of most thyroid cancers, randomized controlled trials to assess treatment response will require prohibitively large sample sizes and resources and are not readily feasible (339). A population-based cohort with low attrition rates, such as ours (only 2.1 % loss to follow-up over 40 years), is probably the best possible model to study the time trends in thyroid cancer survival. As all members of the cohort received the same treatment, that was the standard of care for their era, and their medical records were individually reviewed for accuracy and completeness. Thus, the study cohort was a reliable and stable model to study the trends and factors influencing survival of patients with thyroid cancer (71).

This study shows that the incidence of thyroid cancer in the province of Manitoba has increased by 373% from 1970 to 2010. This has resulted largely from an increase in

the number of PTC (Table 1). The proportion of cancers classified as FVPTC has almost

tripled from 12.4% to 32.9%, and this has also contributed to the increase in the proportion

of PTC (71). At the same time, the proportion of FTC has decreased from 26% to 5.1%,

possibly due to a change in the criteria for diagnosing papillary carcinoma after 1988,

whereby, all lesions with typical cytological features (ground-glass nuclei, nuclear

grooves, and psammoma bodies) were classified as papillary carcinoma even if they did

not show papillae (340). Thus, many erstwhile FTC are rechristened as FVPTC. During

the last four decades, the 10 year DSS has improved from 85.4% to 95.6%, whereas the 10

year RFS has remained relatively stable (86.6% to 91.9%) (71).

In 2014, thyroid cancers (N=6,000) were expected to account for 3.1% of all

cancers (N=191,300) in Canada (42). The number of newly diagnosed thyroid cancer in

the province of Manitoba has increased by over three-fold in the last four decades which is

congruent with reports from Canada and other countries (71, 323-333). However, this

increase in study cohort has not been restricted to the smaller thyroid cancers as reported

earlier (323, 325, 328, 334). An increase in the number of thyroid cancers of all sizes was

observed, which is a true increase in the incidence of thyroid cancer in Manitoba and cannot

be explained only by over diagnosis of a subclinical disease (71). The cause for this

increase is likely multi-factorial due to iodine deficiency, radiation exposure, long standing

goiters and family history (67, 341-344). The shift in histological pattern of thyroid cancer

has also been reported from other regions (345). The decrease in proportion of anaplastic

carcinoma could be a result of more aggressive treatment of goiters and differentiated

thyroid cancers by thyroidectomies before they could undergo anaplastic transformation (71). The proportion of tumors > 2 cm in our cohort is higher than that reported earlier (3, 328, 346), because of strict criteria in Manitoba for performing fine needle biopsy of thyroid. Most of the micro-carcinomas in this study were incidentally detected in thyroidectomy or autopsy specimens. Even before the introduction of the ATA guidelines (161), which recommend threshold sizes of >1cm (hypoechoic solid nodule), 1.5cm (iso- or hyper-echoic solid nodule), 1.5–2cm (mixed cystic–solid nodule with suspicious features) and ≥2.0 cm (mixed cystic–solid nodule without suspicious features) in a low risk patient without cervical lymphadenopathy or micro-calcification, radiologist and surgeons were very conservative in their approach to thyroid nodules. This is also reflected by a large proportion of patients (44.9%) having less than a total thyroidectomy (71).

5.2.2 Epidemiological analysis of oncological outcomes

During 1970-2010, the DSS for thyroid cancer has steadily improved by. The cumulative incidence of death due to thyroid cancer fell by 8.1%, whereas the RFS for patients treated with radical intent has remained unchanged (Table 7). This improvement is not because of an increase in the proportion of early stage disease or smaller tumors in recent years, as evidenced by stable tumor size and stage of thyroid cancers at presentation (Table 7). Although both total thyroidectomy and adjuvant radioactive iodine treatment have been used more often during the recent time (Table 7), they did not have any significant impact on DSS (Table 9). More aggressive treatment of early stage disease did not result in a significantly better disease control, as reflected by a stable RFS during this

period. Therefore, aggressive use of adjuvant radioactive iodine should be judiciously balanced against the treatment related morbidities and the risk of developing second primary cancer.

On multivariable analysis, DSS was negatively influenced by non-papillary tumor histology, male gender, advanced tumor stage, incomplete surgical resection and older age at diagnosis (Table 9). Patient demographics, completeness of surgery, and initial cancer stage have not changed significantly in this study cohort (Table 7). However, there has been a marked change in the relative proportion of various types of thyroid cancer diagnosed over this time period. The proportion of PTC has increased from 58% (1970-1980) to 85.9% (2000-2010) and the proportion of anaplastic cancers fell from 5.7% (1970-1980) to 2.1% (2001-2010) (71). As PTC has the best survival rates (96.8% at 10 years) and ATC has the worst (7.3% survival at 10 years), the opposite trend in the relative incidence of papillary and ATC is most likely responsible for the improved outcome of thyroid cancer (Tables 6 & 7). After controlling for other independent prognostic factors influencing DSS of thyroid cancer in a multivariable model, there was no difference in the DSS of thyroid cancer observed over the last four decades (Table 9).

A time span of four decades is both a strength and a limitation of this study as the diagnostic criteria, staging, and treatment recommendations have evolved over time. To circumvent this challenge, uniform re-staging of all cancers was done using the 2009 AJCC/UICC Cancer staging system for thyroid cancer. Additionally, as a part of

collaborative staging project, the pathology and treatment details of 683 (29.6%) cases were independently reviewed for accuracy and topography, and histology were re-coded by WHO International Classification of Diseases for Oncology (3rd Edition) codes (29, 71).

5.2.3 Development and validation of the Manitoba prognostic nomogram

The use of numerous age based prognostic scoring systems for predicting outcome of thyroid cancer signifies that none is universally acceptable (29). Moreover, most of these staging systems are valid only for WDTC (16-28) and more specifically for PTC (16, 17, 21-24, 26-28). Prognostic scoring systems (17-20, 22, 25, 27, 28) require lengthy calculations of prognostic scores that make individualized risk prediction quite arduous. Various risk stratification systems (19, 21, 23-26, 28) are easier to use in the clinics but they provide stratified group risk estimates rather than individualized patient's risk. ATA proposed a staging system (12, 161) to predict risk of recurrence in low, intermediate and high risk groups of WDTC, categorized on the basis of regional and distant metastases, completeness of resection, loco-regional tumor invasion at initial surgery, aggressive histology, ^{131}I uptake outside the thyroid bed on the whole body RAI scan.

Although thyroid cancers represent a conglomerate of different histological types with varying outcomes, the prognostic factors independently influencing the risks of relapse and death are similar for most non-ATC as outlined in Tables 9 and 10. The feasibility of outcome predictions at 5, 10 and 20 years in the nomograms was explored.

Nomograms combine multiple independent variables to predict an outcome using the prognostic weight of each variable in calculating the probability of such an outcome. Prognostic nomogram can be developed for a variety of clinical outcomes, such as survival (overall or disease-specific), and the probability of developing loco-regional recurrence or metastasis. An ideal nomogram should be reliable, widely applicable and also easy to use. A 10-year time frame for oncological outcome prediction was opted for as most of the non-ATC are indolent and a five-year period is very short to detect late recurrences and deaths from thyroid cancer. Over 30% of relapses and 45% of deaths from thyroid cancers were observed after five years, whereas, over 90% of thyroid cancer relapses and over three quarters of death from thyroid cancers were observed within first 10 years after diagnosis and treatment. Although an oncological outcome prediction at 20 years would have been ideal, it becomes less reliable as the median follow-up of the cohort is 10.5 years. The clinically relevant prognostic factors which independently influence the incidences of relapse and deaths from thyroid cancers, i.e. tumor stage (T), distant metastasis (M), age and gender of the patient, tumor histology, were incorporated to construct an easy to use nomogram. Post-treatment gross residual disease was an important factor only for the prediction of death from thyroid cancer. Understandably, the patients with residual tumor were excluded from the regression model to predict thyroid cancer relapse as the quantification of macroscopic residual disease could be very subjective and variable. Lymph node metastasis predicted higher risk of future disease relapse but it did not alter the risk of dying from thyroid cancer, indicating a successful salvage of regional recurrences in most of the cases.

Prognostic nomograms use the experience of a large group of patients to predict an individual's prognosis based on the individual's characteristics. The likelihood of a reliable prediction depends on the robustness of the model and its representativeness. The Manitoban population (our cohort) is a mix of different ethnic groups from all over the world because of the ongoing immigrations over the years. It is very likely that the nomograms apply to other populations also, but this needs to be demonstrated. The source of information was quite reliable as the individual medical records were reviewed for their accuracy and completeness. The period of diagnosis was used to produce estimates for the nomograms to minimize the impact of time dependent changes in treatment practices, if any (29). Larger databases, such as the SEER database are robust, but they have the inherent limitations in terms of coverage, coding reliability, patient migration to an area that is not covered by SEER and availability of limited information on the treatment details of the patients.

Yang et al. proposed nomograms based on SEER data to predict five and 10 year mortality related to thyroid cancer, other cancers and other causes (38). However, these nomograms do not take into consideration the presence of post-treatment residual disease which is a known prognostic factor for both WDTC and MTC (17, 338). T-stage was used to quantify the extent of primary tumor, incorporating both the size and the ETE, rather than classifying the extent as local, regional and distant. Regional disease could signify either an extension into adjacent tissue or to the regional lymph node(s). In the latter case, the nodal disease figures twice in their nomogram, both in the extent of tumor as well as in

the lymph node involvement. It does not include gender (sex) of the patient in nomogram to predict the probability of death from thyroid cancer, even though its impact on cumulative incidence of thyroid cancer deaths in their study was very significant (p< 0.001). The other two nomograms published by Yang et al. deal with death from other cancers and non-cancer deaths where thyroid cancer does not have a major role (38). The Manitoba thyroid cancer population cohort offsets these limitations that are inherent to the nature of SEER database, like the lack of information on relapses that precludes the development of nomogram to predict this important oncological outcome (29). The Manitoba prognostic nomogram, that predicts cumulative incidence of relapse of thyroid cancer, shows a very interesting, non-monotonic relationship between age of the patients and relapse (Figure 9). There was a bimodal relationship (scales wrap around) between relapse and age of the patients. The higher rate of relapse at younger age does not lead to higher deaths from thyroid cancer in younger patients (29). Moreover, the lymph node involvement, an important determinant of risk of relapse, is more often observed in pediatric patients that tend to have more relapses (62).

Prognostic modeling has some limitations as the oncological outcome collected over a long period of time could have been influenced by the changes in the treatment and follow-up recommendations. However, in this study cohort more aggressive treatment by total thyroidectomy with adjuvant radioactive iodine has not resulted in any significant increase in the risk of relapse as long as there was no residual disease (Table 11). Consequently, the treatment modalities were not included in the nomogram. An

improvement in the survival of the Manitoba thyroid cancer cohort over the last four decades independent of change in the tumor size or treatment modalities was reported earlier (71). The prognostic factors, that influenced the DSS, have remained largely unaltered during the study period (71). Thus, the time period of this study is unlikely to have any independent influence on the nomograms. Some differences such as follicular versus papillary histology and T1 versus T2 tumor stage were not statistically significant, but were incorporated in the nomogram because of their overall importance. To maintain homogeneity of data across the study period, only clinically and radiologically detectable disease relapses were considered as recurrences. Thus, the relapse prediction by the nomogram is valid only for those thyroid cancers that are treated with curative intent with no clinical/radiological evidence of residual disease as outlined in the model (29). Isolated hyper-thyroglobulinemia or molecular markers like BRAF (347) were not considered as independent prognostic factors because they were not a part of the standard clinical care in a large proportion of the cohort and their independent impact without discernable disease is contentious. MTC represents a diverse group of cancers with specific gene mutation determining the prognosis of familial MTC. In the Manitoba thyroid cancer cohort 10 (12.6%) MTC patients had familial MTC and were excluded from the models to develop nomograms. Therefore, these nomograms are appropriate for use with sporadic MTC and not for familial MTC (29).

The Manitoba thyroid cancer nomograms had very good concordance indices of 0.92 (thyroid cancer deaths) and 0.76 (thyroid cancer relapses); where 0.5 is the worst

(complete random prediction) and 1.0 is the best score (perfect prediction). Calibration is the other ability of the model to make unbiased estimates of outcome. On the calibration plot, most of the predictions fell on the 45-degree diagonal line suggesting good calibration.

In view of the prolonged course of most thyroid cancers, it is possible that other causes of mortality, unrelated to thyroid cancer, could result in an over-estimation of thyroid cancer deaths, as determined by the Kaplan Meir method. Consequently, competing risk regression was used to obtain unbiased estimation of cumulative incidence of deaths resulting from thyroid cancer. A competing risk is an event the occurrence of which either precludes or changes the probability of the occurrence of another event of interest (348). In this study deaths due to second primary cancer and non-cancer deaths were treated as competing risks. As the covariate effects cannot be assessed by the CIF, a sub-distribution hazard approach is used for multivariable analysis. Sub-distribution hazards account for competing events by altering the risk set of the subjects. For calculation of DSS by the Kaplan-Meier product limit method, the risk set decreases each time a subject is censored because of death from another cause. However, these subjects remain in the risk set in competing risk analysis and are censored only after all the events have taken place. Cox proportional hazards model makes no such assumptions about the baseline, but assumes non-informative censoring (censoring of individual subjects are not related to the probability of an event occurring) and proportional hazard function (hazard functions are proportional over time). Thus, merely checking for the proportional hazards assumption does not eliminate the possible bias introduced by competing risks. In dealing with a cohort

141

with long follow-up, where a subject is at least at an equal risk of dying from another cause as dying from thyroid cancer, competing risk with sub-distribution hazard is likely to give a more realistic risk of death.

5.2.4   Comparison with existing staging/risk stratification systems for thyroid cancer

The numerous prognostic scoring systems for thyroid cancer are either valid only for WDTC (16-28), more specifically for PTC (16, 17, 21-24, 26-28), or require lengthy calculations of prognostic scores (17-20, 22, 25, 27, 28) that make individualized risk prediction quite arduous. The thyroid prognostic nomogram combines multiple independent variables to predict the risk of death from thyroid cancer of individual patients with thyroid cancer by using the prognostic weights (points) assigned to each variable (29). It had a very good calibration with the calibration curve close to the diagonal. It had excellent discrimination demonstrated by high c-index (0.92), where 0.5 is the worst (complete random prediction) and 1.0 is the best score (perfect prediction). AIC and c-index were used to compare the Manitoba thyroid cancer model with 12 other high ranking models from an earlier comparison (222). Five other models (20-22, 24, 28), that required additional unavailable information for staging, were excluded from this comparison.

The Manitoba thyroid cancer prognostic nomogram model incorporates age, gender, histology and post-treatment residual disease in addition to the T, N, and M categories, which were found to be independent prognostic factors determining oncological outcome of thyroid cancer (29). The advantages of this model include its applicability to

all non-ATC and incorporation of TNM categories in addition to other prognostic factors, which makes it comprehensive but still simple to use.

AIC was developed in the early 1970s to provide an objective tool for choosing between different competing models and lower AIC values suggest relative superiority (295-297). The model for thyroid prognostic nomogram had the lowest AICs for non-ATC, differentiated thyroid cancers of follicular cell origin and PTC for predicting risk of death from thyroid cancer. The AIC value on its own can be misinterpreted, as there is no value of statistical significance associated with it. As it is a relative comparison of various statistical models, it is only as good as the data from the model that generate it (349). Delta AIC (Δ_i) is used to quantify the support for alternative models as compared to the best model. In general, a value of $\Delta_i < 2$ suggests substantial evidence in favor of the alternative model, values between 3 and 7 indicate the alternative model has considerably less support, whereas $\Delta_i > 10$ indicates that the alternative model is very unlikely (297). Δ_i for the next best alternative model (MACIS) for PTC was 8.42, DTC (MACIS) was 35.58, and for non-ATC (AJCC-TNM) was 114.76, thereby suggesting a low to extremely low likelihood of any of these alternative models being more valid as compared to the Manitoba thyroid cancer prognostic nomogram. This difference was most pronounced in non-ATC followed by differentiated thyroid cancer because of higher number of deaths in these patients as compared to PTC. Although the nomogram model performed better than the alternative staging systems, some of the staging systems (such as MACIS for papillary and differentiated thyroid cancer) also demonstrated good discrimination, even though they

project group risk rather than individual risk. PVE (proportion of variation explained) has previously been used to compare staging classifications (222). As PVE favor more complex models by not accounting for the additional degrees of freedom, PVE would be more biased towards TNM classification and the nomogram model than the simpler staging classifications. AIC would penalize these more complex models by accounting for additional degrees of freedom and make them less favorable.

In absence of a randomized control trial, a large population-based cohort with low attrition rates, like ours, is probably the best possible model to study the oncological outcomes of thyroid cancer like the relapses and the deaths. The Manitoba thyroid cancer cohort is a mix of different ethnicity because a large proportion of immigrant population. The source of information was quite reliable as the individual medical records were reviewed for their accuracy and completeness. However, as the competing risk model for the Manitoba thyroid cancer prognostic nomogram was developed from the Manitoba thyroid cancer cohort, the source of data for comparison of different staging system in this study, there is a possibility of selection bias (299).

5.2.5   Development and validation of web-based computerized prognostic model
Although the Manitoba thyroid cancer prognostic nomogram was internally and externally validated and compared with other existing prognostic scoring systems (29, 299) with excellent concordance indices, paper-based nomograms offer limited portability and accessibility in the clinical setting. In a busy clinical practice, the use of a paper nomogram

to calculate the estimated DSS of a patient is both cumbersome and time consuming. The other limitation of a paper-based nomogram is its ability to predict the likelihood of death due to thyroid cancer at only a single time point (at 10 years for Manitoba nomogram).

The numerical probability of survival of an individual patient at any time point in the follow-up period is based on the behavior of the rest of the patients in the cohort with matching criteria. As the possible combinations of these risk factors for any given time period are virtually unlimited which warrants a computerized web-based model to plot the survival curve for any given set of risk factors and for any given time point. Computerized prognostic models enable continuous estimation of the probability of a particular outcome, such as death. As the planned use of the model is to predict the survival probabilities at different time points based on a given set of covariates it does not, unlike a nomogram, have a cut-off time point for DSS prediction.

A computerized web-based model was developed to overcome the limitations of paper nomogram and is freely available online (*www.survivalcurves.net*) for external validation. The strength of using computerized prognostic models lies in the fact that they combine the prognostic weight of multiple independent variables in calculating the probability of death from thyroid cancer. The risk of death from thyroid cancer obtained by competing risk model could not be plotted and incorporated into a web-based model because of limitation of available statistical packages. To overcome this limitation, a validated Cox proportional hazard model was used for the online survival prediction. This

program plots a real-time survival curve over a period of time for an individual's risk factors.

The sensitivity and the specificity of the web-based survival probabilities (validation) were evaluated against the true DSS status (gold standard). The ROC curve was plotted with sensitivity against 1-specificity on a unity square (0.0 -1.0). The ROC curve is an indicator of both sensitivity and specificity of the model. The areas under the curves (0.81) show the predictive strength and the validity of the models. The tight CI of the areas under the curves confirm the strength of the model to accurately predict DSS. This model has been internally and externally validated. However, it would be authenticated further by validation at multiple institutions. The web-based model is available for global use and offers the option of adding 95% CI to the DSS curve. The corresponding points on the two curves on either side of the survival curve represent 95% CI.

For a prognostic model to be widely used in clinical practice, it is important that it is easily available and easy to use as a knowledge transfer tool. It is also important that the end user is able to understand and interpret the results that are generated by the model. The disclaimer states that "this Website is intended for use by health care providers (physician, nurses, researcher, administrators, etc.) only as an applied research tool for the utility of Cox's proportional Hazard models in cancer survival prediction. Due to the need for the understanding of the scientific terms to be used in interpreting the models, non-health care

providers are not supposed to be using this website". It further states that "the survival prediction is based on a mathematical model that was generated and internally validated on the Manitoba thyroid cancer patients and was also externally validated on an independent thyroid cancer cohort in Canada. However, the model does not take into consideration co-morbidity (coexisting diseases or conditions) and other risk factors not included in the model. Therefore, the resulting predictions are only specific to death from thyroid cancer and not the overall death from any cause, but still could be liable to errors and do not, in anyway, claim 100% certainty or accuracy".

5.2.6   External validation of the Manitoba prognostic model

The ROC curve was used to evaluate the sensitivity and the specificity of the model-based survival probabilities (test) against the true (known) DSS status (gold standard). On external validation of the Manitoba prognostic model with an independent cohort of 1454 patients from London, Ontario, Canada, the AUROC of 0.96 indicates excellent discrimination (c-index). A narrow 95% CI (0.93-0.97) indicates a very good reliability of prediction. If the ROC curve runs away from the chance diagonal on the left side and never touches it, it indicates good predictability. The larger the AUROC (ranges from 0.0 to 1.0), with its 95% CI not including the chance probability (0.50), the better is the accuracy of the model. All these criteria are met by the curve shown in Figure 15. The limitation of this cohort was a small number of patients (15) dying from thyroid cancer during the follow-up period.

The Manitoba thyroid cancer prognostic nomogram model was also independently externally validated at the University of Hong Kong for predicting 10-year DSS in a cohort of 849 PTC patients with ≥7 years follow-up. Age at diagnosis, tumor size, tumor multifocality (defined ≥2 tumor foci in ipsilateral lobe), nodal status, and distant metastases were found to be significant independent factors in this cohort for both 5- and 10-year DSS and an alternative nomogram was proposed. However, there was no statistically significant difference in the discrimination and accuracy between the two nomograms even though both the development and validation samples of the Hong Kong nomogram were drawn from the same cohort, giving it an advantage (350) .

5.2.7 Prognostic importance of distant metastasis in TNM staging

WDTC represent a group of unique cancers with the age of the patient at diagnosis being an important determinant of prognosis. The widely adopted TNM classification uses discrete cut-off age of 45 years for risk stratification (18) though its validity has been questioned in various studies (49, 245, 246). An attempt was made to compare the demographical characteristics and the oncological outcomes of the two age groups of stage II WDTC patients and to compare the oncological outcome of metastatic WDTC in patients younger and older than 45 years to see if there was any difference between these two groups. As it is evident from Table 18, the presentation of metastatic and non-metastatic stage II cancers was significantly different in terms of their clinical presentation and oncological outcome. Both DSS and RFS were significantly different between the two groups and a significantly higher proportion of patients with metastatic stage II WDTC

died of their disease. This strongly suggests that the metastatic and non-metastatic stage II WDTC are very different entities grouped together. In an earlier study that compared TNM stages in patients in different age groups, younger patients had an 11-fold increase in mortality between stages I and II, whereas there was no difference for older patients (351). It also showed a difference between the two age-based subgroups of stage II WDTC. The SEER database has inherent limitations in terms of coverage, coding reliability, patient migration to an area that is not covered by the SEER and availability of limited information on the treatment details of the patients. A Swedish study had earlier failed to show any difference in the odds of death from WDTC between metastatic and non-metastatic WDTC (352). On multivariable analysis, presence of distant metastasis was the single most important prognostic predictor of the oncological outcome of stage II WDTC and the presence of distant metastasis at diagnosis accorded a 52 fold increase in the hazard of death from WDTC (Table 19).

Distant metastasis is considered to be an important prognostic factor in determining the oncological outcome of WDTC in numerous prognostic scoring/staging systems. Metastatic WDTC have been variably staged as stages II (18), III (15) or IV (15, 18, 23, 25) by different staging systems. Similarly, different risk stratification systems also have staged metastatic WDTC as high risk (19, 26, 260, 261) or intermediate risk WDTC (26). The comparison of clinical presentation and oncological outcome of metastatic WDTC in patients < or ≥ 45 years (Table 20) does not show any significant difference between these two groups apart from increased proportion of female patients and PTC in younger patients

149

(stage II). There were statistically insignificant differences between the recurrence rates, risk of death from disease as well as DSS and RFS between stage II (M1) vs stage IVC WDTC. Stage of presentation (stage II vs stage IVC) had no influence on the DSS that was significantly lower for males, incomplete resection and Hürthle cell histology. Adjuvant radioactive iodine significantly reduced the risk of death from WDTC.

The cohort of WDTC was followed over a span of four decades, with 42.5% patients having at least 15 years of follow-up. As a result the DSS is presented for WDTC cohort at 15 years. RFS is presented at 10 year as all treatment failures in metastatic WDTC and 95% of those in stage II WDTC took place within 10 years. The major limitation of this study is the number of metastatic stage II WDTC (N= 8), however, the 55% difference in the DSS between metastatic and non-metastatic stage II WDTC renders a post-hoc power of 98.7% to this study with α=0.05.

5.3 Impact and future directions

This is probably the first study that has prospectively looked at the impact of intense focal FDG uptake by HCA (false positivity) as a cause for lower specificity and PPV of FDG-PET in discriminating benign and malignant indeterminate thyroid nodules (286, 298). A cut-off SUVmax of 3.25 provides a higher accuracy with reasonably high sensitivity, specificity, PPV and NPV for predicting malignancy in FDG-PET positive non Hürthle cell FN, as compared to any increased focal FDG uptake by thyroid nodules or a cut-off of 2.05, as suggested by an earlier meta-analysis, with a much higher specificity

150

(83% vs 42%) (314). This finding is of great clinical importance as the benign HCA often mimic a thyroid cancer in terms of increased uptake of FDG. As 75% of HCA could be identified by FNAB in this study, there is a possibility of ruling them out preoperatively as the potential cause of increased FDG uptake (298). If over 75% of the cells in a FDG-positive, incidentally detected, asymptomatic FN are Hürthle cells they can potentially be observed under close surveillance. On the contrary, 4 out of 5 FDG-positive, Hürthle cell negative FN are likely malignant and should undergo surgical excision. Commercially available diagnostic molecular markers (200, 206, 207, 210, 213-215) are not available in Manitoba for FNAB specimen to compare the FDG-PET/CT findings with the molecular markers. Attempts were made to compare the mIR profile of FA, FVPTC and FTC but lack of adequate numbers of FTC made it impossible to draw any meaningful conclusions. In future, attempts will be made to correlate FDG-PET/CT findings with the molecular markers that are recommended for consideration in indeterminate thyroid nodules by the current ATA guidelines (12)

This work has resulted in establishment of the Manitoba thyroid cancer cohort of 2306 thyroid cancers with a median follow-up 11.5 years and comprehensive information about patients demographics, staging and treatment details (71). This unique, large, population-based cohort does not have the inherent limitations of SEER database in terms of coverage, coding reliability, patient migration to an area that is not covered by SEER and limited information on the treatment details of the patients. A 373% increase was observed in the incidence of thyroid cancer (71), which was not restricted to only the

micro-carcinoma as reported earlier (323, 325, 328, 334). As the tumor size has remained unchanged for last 40 years, the increase in the incidence of thyroid cancer in Manitoba cannot be explained by only over diagnosis of early cancer. During this period the cumulative incidence of death due to thyroid cancer fell by 8.1%, whereas the RFS for patients treated with radical intent has remained unchanged. This change was independent of any change in the stage distribution or treatment modalities. However, it was linked to decreasing proportion of ATC (71).

The prognostic importance of age and distant metastasis in the TNM staging of WDTC was assessed by using the Manitoba thyroid cancer cohort. A 55% difference in 15-year DSS of metastatic and non-metastatic stage II WDTC was observed in this study that needs to be confirmed in a large multi-institutional study with a larger number of metastatic stage II WDTC (300). Both these findings have the potential of changing the existing TNM stage grouping of thyroid cancer. This cohort was also used by two of my students for re-evaluation of the age based TNM staging of thyroid cancer and led to the proposal of using a more appropriate age cut-off age of 55 years for age-based stratification (49, 245). These findings were validated by an international multi-institutional study, where 1900 cases (20% of the total study group) were contributed from this cohort (246). I will add another 761 thyroid cancer patients from 2011 and 2015 to this cohort, as obtained from the Manitoba Cancer Registry to examine the validity of the recently proposed terminology by ATA to classify response to therapy and their clinical implications on this updated large cohort of over 3000 patients.

Development and validation of novel Manitoba prognostic model models for predicting oncological outcome of thyroid cancer was another important contribution of this work (29). This model compares favorably with the existing staging/risk stratification systems (299). The Manitoba prognostic model was successfully adapted as a web-based model with very good c-index and has been externally validated using the independent data shared by the London Health Sciences Centre, London, Ontario. Lang and Wong at the University of Hong Kong have also externally validated the Manitoba prognostic nomogram independently in predicting 10-year DSS (350). The web-based model is able to predict outcome of patients with different histological types of thyroid cancer after they have survived for a year. This is because ATC has a very high mortality in the first year after diagnosis. This readily available, easy to use web-based model provides portability with the ease of calculation. It has a potential of becoming a knowledge transfer tool to be used in the clinical practice.

Although the Manitoban population (our cohort) is a mix of different ethnic groups from all over the world because of the ongoing immigrations over the years, independent validation in the target population is recommended prior to its clinical use. We hope to validate this model on a German cohort from the University of Münster in the near future. In Canada, members of **CAN**ADA-Wide Study on **T**hyroid **C**ancer: Presentation, Treatment and Outcomes of Thyroid Cancer in Canada - Epidemiological Description and Relation to Socio-demographic Determinants (**CAN-TC**) have expressed interest in the external validation of the nomogram in different provinces across Canada.

Chapter VI

Conclusions

The goal of this study was to evaluate the efficacy of FDG-PET/CT scan for predicting the risk of malignancy in FNs diagnosed by fine needle aspiration and to develop prognostic models to predict the individualized oncological outcome of thyroid cancer based on the individual's demographic and tumor related prognostic parameters.

FDG-PET /CT was found to be of help in differentiating benign and malignant non-Hürthle cell thyroid nodules. As HCA show significantly higher FDG uptake as compared to FA and thus, they can often masquerade as malignant thyroid nodule (298). A cut-off SUVmax of 3.25 was found to enhance the accuracy of FDG-PET /CT in identifying cancers in non-Hürthle cell indeterminate thyroid nodules (286). Clubbing HCN with other indeterminate thyroid nodules in the past led to low specificity and PPV reported in two meta-analyses as all HCA showed increased FDG uptake (false positive).

The epidemiological analysis of prognostic markers for thyroid cancer was performed with the aim of developing a model to predict the oncological outcomes in terms of risk of thyroid cancer relapse and death from thyroid cancer. A population-based Manitoba thyroid cancer cohort was established. It included all 2306 consecutive thyroid cancers diagnosed in 2296 patients in Manitoba, Canada, from January 1, 1970 to December 31, 2010. A true 3.73 fold increase in the age standardized incidence of thyroid cancer in the province of Manitoba was observed over the last 4 decades. This cannot be

attributed only to the over-diagnosis of subclinical disease alone (71). The median tumor size and the proportion of micro-carcinoma in Manitoba have remained unchanged over the last four decades. The proportion of total thyroidectomy and radioactive iodine have increased over time, however, both of these did not have any significant impact on DSS. A 10.2% improvement in DSS of thyroid cancer, over the last 40 years in the Manitoba population-based thyroid cancer cohort, was observed to be independent of early diagnosis or use of more aggressive treatment modalities. The major factor contributing to this improvement in survival was the increasing proportion of PTC and a corresponding decrease in ATC. Since outcomes for the former are usually excellent whereas outcomes for the latter are typically dismal, the increase in proportion of PTC has resulted in improved oncological outcome of thyroid cancer.

The prognostic role of age and distant metastasis on TNM stage grouping was analyzed. The oncological outcome of patients with metastatic stage II WDTC was very different from that of non-metastatic stage II WDTC. The outcome of metastatic disease in younger patient (stage II) was very similar to that in older patients with similar disease burden (stage IVC). Staging all metastatic WDTC as stage IV irrespective of the age of the patient is strongly advocated (300).

Unique nomograms to predict the likelihood of relapse and death from thyroid cancer in an individual patient were developed with good calibration and discrimination capabilities. These nomograms were internally cross-validated and compared with the

existing staging/risk scoring system (29, 299). The thyroid prognostic nomogram model was better than the other compared models in predicting risk of death from thyroid cancer in a population-based thyroid cancer cohort.

For a prognostic model to be used in the clinical practice, it is important that it is readily available, and easy to use as a knowledge transfer tool. To facilitate this, the model to predict thyroid cancer specific survival was adapted as a web-based thyroid cancer survival prediction model which predicts the survival of an individual patient based on the DSS of similar patients in the Manitoba thyroid cancer cohort. The Manitoba thyroid cancer prognostic model was externally validated in an independent cohort of patient from London, Ontario, Canada with good accuracy and reliability. The approach offers a framework that can be adapted for developing similar prognostic models for other cancers.

Chapter VII

Literature Cited

1. Parkin DM, Bray F, Ferlay J, Pisani P. Global cancer statistics, 2002. CA Cancer J Clin. 2005;55(2):74-108.

2. Canadian Cancer Society's Advisory Committee on Cancer Statistics. Canadian Cancer Statistics 2015 - Special Topic Predictions of the Future Burden of Cancer in Canada. [S.l.]: Canadian Cancer Society; 2015. Available from: http://myaccess.library.utoronto.ca/login?url=http://site.ebrary.com/lib/utoronto/Top?id=11070588.

3. Canadian Cancer Society., Statistics Canada., Public Health Agency of Canada., Canadian Electronic Library (Firm). Canadian cancer statistics 2011 featuring colorectal cancer. Toronto, Ont.: Canadian Cancer Society; 2011. Available from: http://myaccess.library.utoronto.ca/login?url=http://site.ebrary.com/lib/utoronto/Top?id=10471043.

4. Layfield LJ, Cibas ES, Gharib H, Mandel SJ. Thyroid aspiration cytology: current status. CA Cancer J Clin. 2009;59(2):99-110.

5. Langer JE, Baloch ZW, McGrath C, Loevner LA, Mandel SJ. Thyroid nodule fine-needle aspiration. Semin Ultrasound CT MR. 2012;33(2):158-65.

6. Baloch ZW, LiVolsi VA, Asa SL, Rosai J, Merino MJ, Randolph G, et al. Diagnostic terminology and morphologic criteria for cytologic diagnosis of thyroid lesions: a synopsis of the National Cancer Institute Thyroid Fine-Needle Aspiration State of the Science Conference. Diagn Cytopathol. 2008;36(6):425-37.

7. Cibas ES, Ali SZ. The Bethesda System for Reporting Thyroid Cytopathology. Thyroid. 2009;19(11):1159-65.

8. Grant CS, Barr D, Goellner JR, Hay ID. Benign Hurthle cell tumors of the thyroid: a diagnosis to be trusted? World J Surg. 1988;12(4):488-95.

9. Thompson NW, Dunn EL, Batsakis JG, Nishiyama RH. Hurthle cell lesions of the thyroid gland. Surg Gynecol Obstet. 1974;139(4):555-60.

10. McLeod MK, Thompson NW, Hudson JL, Gaglio JA, Lloyd RV, Harness JK, et al. Flow cytometric measurements of nuclear DNA and ploidy analysis in Hurthle cell neoplasms of the thyroid. Arch Surg. 1988;123(7):849-54.

11. Vriens D, de Wilt JH, van der Wilt GJ, Netea-Maier RT, Oyen WJ, de Geus-Oei LF. The role of [18F]-2-fluoro-2-deoxy-d-glucose-positron emission tomography in thyroid nodules with indeterminate fine-needle aspiration biopsy: systematic review and meta-analysis of the literature. Cancer. 2011;117(20):4582-94.

12. Haugen BR, Alexander EK, Bible KC, Doherty GM, Mandel SJ, Nikiforov YE, et al. 2015 American Thyroid Association Management Guidelines for Adult Patients with Thyroid Nodules and Differentiated Thyroid Cancer: The American Thyroid Association Guidelines Task Force on Thyroid Nodules and Differentiated Thyroid Cancer. Thyroid. 2016;26(1):1-133.

13. Zandieh S, Pokieser W, Knoll P, Sonneck-Koenne C, Kudlacek M, Mirzaei S. Oncocytic adenomas of thyroid-mimicking benign or metastatic disease on 18F-FDG-PET scan. Acta Radiol. 2015;56(6):709-13.

14. Byar DP, Green SB, Dor P, Williams ED, Colon J, van Gilse HA, et al. A prognostic index for thyroid carcinoma. A study of the E.O.R.T.C. Thyroid Cancer Cooperative Group. Eur J Cancer. 1979;15(8):1033-41.

15. Sherman SI, Brierley JD, Sperling M, Ain KB, Bigos ST, Cooper DS, et al. Prospective multicenter study of thyroiscarcinoma treatment: initial analysis of staging and outcome. National Thyroid Cancer Treatment Cooperative Study Registry Group. Cancer. 1998;83(5):1012-21.

16. Hay ID, Grant CS, Taylor WF, McConahey WM. Ipsilateral lobectomy versus bilateral lobar resection in papillary thyroid carcinoma: a retrospective analysis of surgical outcome using a novel prognostic scoring system. Surgery. 1987;102(6):1088-95.

17. Hay ID, Bergstralh EJ, Goellner JR, Ebersold JR, Grant CS. Predicting outcome in papillary thyroid carcinoma: development of a reliable prognostic scoring system in a cohort of 1779 patients surgically treated at one institution during 1940 through 1989. Surgery. 1993;114(6):1050-7.

18. Sobin LH, Gospodarowicz MK, Wittekind C, International Union against Cancer. TNM classification of malignant tumours. 7th ed. Chichester, West Sussex, UK ; Hoboken, NJ: Wiley-Blackwell; 2010. xx, 310 p. p.

19. Cady B, Rossi R. An expanded view of risk-group definition in differentiated thyroid carcinoma. Surgery. 1988;104(6):947-53.

20. Yildirim E. A model for predicting outcomes in patients with differentiated thyroid cancer and model performance in comparison with other classification systems. J Am Coll Surg. 2005;200(3):378-92.

21. Pasieka JL, Zedenius J, Auer G, Grimelius L, Hoog A, Lundell G, et al. Addition of nuclear DNA content to the AMES risk-group classification for papillary thyroid cancer. Surgery. 1992;112(6):1154-9.

22. Akslen LA. Prognostic importance of histologic grading in papillary thyroid carcinoma. Cancer. 1993;72(9):2680-5.

23. DeGroot LJ, Kaplan EL, McCormick M, Straus FH. Natural history, treatment, and course of papillary thyroid carcinoma. J Clin Endocrinol Metab. 1990;71(2):414-24.

24. Noguchi S, Murakami N, Kawamoto H. Classification of papillary cancer of the thyroid based on prognosis. World J Surg. 1994;18(4):552-7.

25. Mazzaferri EL, Jhiang SM. Long-term impact of initial surgical and medical therapy on papillary and follicular thyroid cancer. Am J Med. 1994;97(5):418-28.

26. Shaha AR, Loree TR, Shah JP. Intermediate-risk group for differentiated carcinoma of thyroid. Surgery. 1994;116(6):1036-40.

27. Sebastian SO, Gonzalez JM, Paricio PP, Perez JS, Flores DP, Madrona AP, et al. Papillary thyroid carcinoma: prognostic index for survival including the histological variety. Arch Surg. 2000;135(3):272-7.

28. Sugitani I, Kasai N, Fujimoto Y, Yanagisawa A. A novel classification system for patients with PTC: addition of the new variables of large (3 cm or greater) nodal

160

metastases and reclassification during the follow-up period. Surgery. 2004;135(2):139-48.

29.   Pathak KA, Mazurat A, Lambert P, Klonisch T, Nason RW. Prognostic nomograms to predict oncological outcome of thyroid cancers. J Clin Endocrinol Metab. 2013;98(12):4768-75.

30.   Brennan MF, Kattan MW, Klimstra D, Conlon K. Prognostic nomogram for patients undergoing resection for adenocarcinoma of the pancreas. Ann Surg. 2004;240(2):293-8.

31.   Kattan MW, Karpeh MS, Mazumdar M, Brennan MF. Postoperative nomogram for disease-specific survival after an R0 resection for gastric carcinoma. J Clin Oncol. 2003;21(19):3647-50.

32.   Kattan MW, Yu C, Salomon L, Vora K, Touijer K, Guillonneau B. Development and validation of preoperative nomogram for disease recurrence within 5 years after laparoscopic radical prostatectomy for prostate cancer. Urology. 2011;77(2):396-401.

33.   Mariani L, Miceli R, Kattan MW, Brennan MF, Colecchia M, Fiore M, et al. Validation and adaptation of a nomogram for predicting the survival of patients with extremity soft tissue sarcoma using a three-grade system. Cancer. 2005;103(2):402-8.

34.   Sorbellini M, Kattan MW, Snyder ME, Reuter V, Motzer R, Goetzl M, et al. A postoperative prognostic nomogram predicting recurrence for patients with conventional clear cell renal cell carcinoma. J Urol. 2005;173(1):48-51.

35. Lachance JA, Choudhri AF, Sarti M, Modesitt SC, Jazaeri AA, Stukenborg GJ. A nomogram for estimating the probability of ovarian cancer. Gynecol Oncol. 2011;121(1):2-7.

36. Klar M, Jochmann A, Foeldi M, Stumpf M, Gitsch G, Stickeler E, et al. The MSKCC nomogram for prediction the likelihood of non-sentinel node involvement in a German breast cancer population. Breast Cancer Res Treat. 2008;112(3):523-31.

37. Hoang T, Xu R, Schiller JH, Bonomi P, Johnson DH. Clinical model to predict survival in chemonaive patients with advanced non-small-cell lung cancer treated with third-generation chemotherapy regimens based on eastern cooperative oncology group data. J Clin Oncol. 2005;23(1):175-83.

38. Yang L, Shen W, Sakamoto N. Population-based study evaluating and predicting the probability of death resulting from thyroid cancer and other causes among patients with thyroid cancer. J Clin Oncol. 2013;31(4):468-74.

39. Kondo T, Ezzat S, Asa SL. Pathogenetic mechanisms in thyroid follicular-cell neoplasia. Nature reviews Cancer. 2006;6(4):292-306.

40. Suh I, Vriens MR, Guerrero MA, Griffin A, Shen WT, Duh QY, et al. Serum thyroglobulin is a poor diagnostic biomarker of malignancy in follicular and Hurthle-cell neoplasms of the thyroid. Am J Surg. 2010;200(1):41-6.

41. O'Neill JP, Power D, Condron C, Bouchier-Hayes D, Walsh M. Anaplastic thyroid cancer, tumorigenesis and therapy. Irish journal of medical science. 2010;179(1):9-15.

42. Canadian Cancer Society's Advisory Committee on Cancer Statistics. Canadian Cancer Statistics 2014 - Special Topic Skin Cancers. [S.l.]: Canadian Cancer Society; 2014. Available from: http://myaccess.library.utoronto.ca/login?url=http://site.ebrary.com/lib/utoronto/Top?id=10901270.

43. Vander JB, Gaston EA, Dawber TR. The significance of nontoxic thyroid nodules. Final report of a 15-year study of the incidence of thyroid malignancy. Ann Intern Med. 1968;69(3):537-40.

44. Tunbridge WM, Evered DC, Hall R, Appleton D, Brewis M, Clark F, et al. The spectrum of thyroid disease in a community: the Whickham survey. Clin Endocrinol (Oxf). 1977;7(6):481-93.

45. Mandel SJ. A 64-year-old woman with a thyroid nodule. JAMA. 2004;292(21):2632-42.

46. Hegedus L. Clinical practice. The thyroid nodule. N Engl J Med. 2004;351(17):1764-71.

47. Sipos JA, Mazzaferri EL. Thyroid cancer epidemiology and prognostic variables. Clin Oncol (R Coll Radiol). 2010;22(6):395-404.

48. Schmid KW. [Molecular pathology of thyroid tumors]. Pathologe. 2010;31 Suppl 2:229-33.

49. Mazurat A, Torroni A, Hendrickson-Rebizant J, Benning H, Nason RW, Pathak KA. The age factor in survival of a population cohort of well-differentiated thyroid cancer. Endocr Connect. 2013;2(3):154-60.

50. Dean DS, Gharib H. Epidemiology of thyroid nodules. Best Pract Res Clin Endocrinol Metab. 2008;22(6):901-11.

51. Giusti F, Falchetti A, Franceschelli F, Marini F, Tanini A, Brandi ML. Thyroid cancer: current molecular perspectives. J Oncol. 2010;2010:351679-.

52. Are C, Shaha AR. Anaplastic thyroid carcinoma: biology, pathogenesis, prognostic factors, and treatment approaches. Ann Surg Oncol. 2006;13(4):453-64.

53. Hill AB. The Environment and Disease: Association or Causation? Proc R Soc Med. 1965;58:295-300.

54. Schneider AB, Recant W, Pinsky SM, Ryo UY, Bekerman C, Shore-Freedman E. Radiation-induced thyroid carcinoma. Clinical course and results of therapy in 296 patients. Annals of internal medicine. 1986;105(3):405-12.

55. Goldman ND, Coniglio JU, Falk SA. Thyroid cancers. I. Papillary, follicular, and Hurthle cell. Otolaryngol Clin North Am. 1996;29(4):593-609.

56. Wingren G, Hallquist A, Hardell L. Diagnostic X-ray exposure and female papillary thyroid cancer: a pooled analysis of two Swedish studies. European journal of cancer prevention : the official journal of the European Cancer Prevention Organisation. 1997;6(6):550-6.

57. Yue J, Lu H, Liu J, Berwick M, Shen Z. Filamin-A as a marker and target for DNA damage based cancer therapy. DNA Repair (Amst). 2012;11(2):192-200.

58. Ron E, Lubin JH, Shore RE, Mabuchi K, Modan B, Pottern LM, et al. Thyroid cancer after exposure to external radiation: a pooled analysis of seven studies. Radiat Res. 1995;141(3):259-77.

59.   Ron E. Childhood cancer--treatment at a cost. J Natl Cancer Inst. 2006;98(21):1510-1.

60.   Memon A, Godward S, Williams D, Siddique I, Al-Saleh K. Dental x-rays and the risk of thyroid cancer: a case-control study. Acta oncologica. 2010;49(4):447-53.

61.   Inskip PD, Ekbom A, Galanti MR, Grimelius L, Boice JD, Jr. Medical diagnostic x rays and thyroid cancer. J Natl Cancer Inst. 1995;87(21):1613-21.

62.   Gorlin JB, Sallan SE. Thyroid cancer in childhood. Endocrinol Metab Clin North Am. 1990;19(3):649-62.

63.   Williams ED, Abrosimov A, Bogdanova T, Demidchik EP, Ito M, LiVolsi V, et al. Morphologic characteristics of Chernobyl-related childhood papillary thyroid carcinomas are independent of radiation exposure but vary with iodine intake. Thyroid. 2008;18(8):847-52.

64.   Williams D. Twenty years' experience with post-Chernobyl thyroid cancer. Best Pract Res Clin Endocrinol Metab. 2008;22(6):1061-73.

65.   Williams D. Radiation carcinogenesis: lessons from Chernobyl. Oncogene. 2008;27 Suppl 2:S9-18.

66.   Bosetti C, Negri E, Kolonel L, Ron E, Franceschi S, Preston-Martin S, et al. A pooled analysis of case-control studies of thyroid cancer. VII. Cruciferous and other vegetables (International). Cancer Causes Control. 2002;13(8):765-75.

67.   Galanti MR, Hansson L, Bergstrom R, Wolk A, Hjartaker A, Lund E, et al. Diet and the risk of papillary and follicular thyroid carcinoma: a population-based case-control study in Sweden and Norway. Cancer Causes Control. 1997;8(2):205-14.

68. Dal Maso L, Bosetti C, La Vecchia C, Franceschi S. Risk factors for thyroid cancer: an epidemiological review focused on nutritional factors. Cancer Causes Control. 2009;20(1):75-86.

69. Peterson E, De P, Nuttall R. BMI, diet and female reproductive factors as risks for thyroid cancer: a systematic review. PloS one. 2012;7(1):e29177.

70. Malandrino P, Scollo C, Marturano I, Russo M, Tavarelli M, Attard M, et al. Descriptive epidemiology of human thyroid cancer: experience from a regional registry and the "volcanic factor". Frontiers in endocrinology. 2013;4:65.

71. Pathak KA, Leslie WD, Klonisch TC, Nason RW. The changing face of thyroid cancer in a population-based cohort. Cancer Med. 2013;2(4):537-44.

72. Haymart MR, Repplinger DJ, Leverson GE, Elson DF, Sippel RS, Jaume JC, et al. Higher serum thyroid stimulating hormone level in thyroid nodule patients is associated with greater risks of differentiated thyroid cancer and advanced tumor stage. J Clin Endocrinol Metab. 2008;93(3):809-14.

73. Fiore E, Vitti P. Serum TSH and risk of papillary thyroid cancer in nodular thyroid disease. J Clin Endocrinol Metab. 2012;97(4):1134-45.

74. Chiu HK, Sanda S, Fechner PY, Pihoker C. Correlation of TSH with the risk of paediatric thyroid carcinoma. Clinical endocrinology. 2012;77(2):316-22.

75. Mijovic T, How J, Pakdaman M, Rochon L, Gologan O, Hier MP, et al. Body mass index in the evaluation of thyroid cancer risk. Thyroid. 2009;19(5):467-72.

76. Clavel-Chapelon F, Guillas G, Tondeur L, Kernaleguen C, Boutron-Ruault M-C. Risk of differentiated thyroid cancer in relation to adult weight, height and body shape over life: the French E3N cohort. Int J Cancer. 2010;126(12):2984-90.

77. Guarino V, Castellone MD, Avilla E, Melillo RM. Thyroid cancer and inflammation. Mol Cell Endocrinol. 2010;321(1):94-9102.

78. Meinhold CL, Ron E, Schonfeld SJ, Alexander BH, Freedman DM, Linet MS, et al. Nonradiation risk factors for thyroid cancer in the US Radiologic Technologists Study. Am J Epidemiol. 2010;171(2):242-52.

79. Tita P, Ambrosio MR, Scollo C, Carta A, Gangemi P, Bondanelli M, et al. High prevalence of differentiated thyroid carcinoma in acromegaly. Clinical endocrinology. 2005;63(2):161-7.

80. Ruchala M, Skiba A, Gurgul E, Uruski P, Wasko R, Sowinski J. The occurrence of thyroid focal lesions and a need for fine needle aspiration biopsy in patients with acromegaly due to an increased risk of thyroid cancer. Neuro endocrinology letters. 2009;30(3):382-6.

81. Gullu BE, Celik O, Gazioglu N, Kadioglu P. Thyroid cancer is the most common cancer associated with acromegaly. Pituitary. 2010;13(3):242-8.

82. Baris D, Gridley G, Ron E, Weiderpass E, Mellemkjaer L, Ekbom A, et al. Acromegaly and cancer risk: a cohort study in Sweden and Denmark. Cancer Causes Control. 2002;13(5):395-400.

83. Ng AK, Kenney LB, Gilbert ES, Travis LB. Secondary malignancies across the age spectrum. Semin Radiat Oncol. 2010;20(1):67-78.

84.	Burgess JR, Duffield A, Wilkinson SJ, Ware R, Greenaway TM, Percival J, et al. Two families with an autosomal dominant inheritance pattern for papillary carcinoma of the thyroid. J Clin Endocrinol Metab. 1997;82(2):345-8.

85.	Hemminki K, Eng C, Chen B. Familial risks for nonmedullary thyroid cancer. J Clin Endocrinol Metab. 2005;90(10):5747-53.

86.	Ishikawa Y, Sugano H, Matsumoto T, Furuichi Y, Miller RW, Goto M. Unusual features of thyroid carcinomas in Japanese patients with Werner syndrome and possible genotype-phenotype relations to cell type and race. Cancer. 1999;85(6):1345-52.

87.	Elisei R, Cosci B, Romei C, Bottici V, Renzini G, Molinaro E, et al. Prognostic significance of somatic RET oncogene mutations in sporadic medullary thyroid cancer: a 10-year follow-up study. J Clin Endocrinol Metab. 2008;93(3):682-7.

88.	Takano T. Fetal cell carcinogenesis of the thyroid: a hypothesis for better understanding of gene expression profile and genomic alternation in thyroid carcinoma. Endocrine journal. 2004;51(6):509-15.

89.	Takano T. Fetal cell carcinogenesis of the thyroid: a modified theory based on recent evidence. Endocrine journal. 2014;61(4):311-20.

90.	Vogelstein B, Fearon ER, Hamilton SR, Kern SE, Preisinger AC, Leppert M, et al. Genetic alterations during colorectal-tumor development. The New England journal of medicine. 1988;319(9):525-32.

91.	Nowell PC. The clonal evolution of tumor cell populations. Science. 1976;194(4260):23-8.

92. Parameswaran R, Brooks S, Sadler GP. Molecular pathogenesis of follicular cell derived thyroid cancers. International journal of surgery. 2010;8(3):186-93.

93. Karunamurthy A, Panebianco F, S JH, Vorhauer J, Nikiforova MN, Chiosea S, et al. Prevalence and phenotypic correlations of EIF1AX mutations in thyroid nodules. Endocrine-related cancer. 2016;23(4):295-301.

94. Xu B, Ghossein R. Genomic Landscape of poorly Differentiated and Anaplastic Thyroid Carcinoma. Endocrine pathology. 2016;27(3):205-12.

95. Kunstman JW, Juhlin CC, Goh G, Brown TC, Stenman A, Healy JM, et al. Characterization of the mutational landscape of anaplastic thyroid cancer via whole-exome sequencing. Human molecular genetics. 2015;24(8):2318-29.

96. Cancer Genome Atlas Research N. Integrated genomic characterization of papillary thyroid carcinoma. Cell. 2014;159(3):676-90.

97. Zhang W, Liu HT. MAPK signal pathways in the regulation of cell proliferation in mammalian cells. Cell research. 2002;12(1):9-18.

98. Riesco-Eizaguirre G, Gutierrez-Martinez P, Garcia-Cabezas MA, Nistal M, Santisteban P. The oncogene BRAF V600E is associated with a high risk of recurrence and less differentiated papillary thyroid carcinoma due to the impairment of Na+/I- targeting to the membrane. Endocrine-related cancer. 2006;13(1):257-69.

99. Riesco-Eizaguirre G, Santisteban P. Molecular biology of thyroid cancer initiation. Clin Transl Oncol. 2007;9(11):686-93.

100. Wang Y, Hou P, Yu H, Wang W, Ji M, Zhao S, et al. High prevalence and mutual exclusivity of genetic alterations in the phosphatidylinositol-3-kinase/akt pathway in thyroid tumors. J Clin Endocrinol Metab. 2007;92(6):2387-90.

101. Ricarte-Filho JC, Ryder M, Chitale DA, Rivera M, Heguy A, Ladanyi M, et al. Mutational profile of advanced primary and metastatic radioactive iodine-refractory thyroid cancers reveals distinct pathogenetic roles for BRAF, PIK3CA, and AKT1. Cancer research. 2009;69(11):4885-93.

102. Hou P, Liu D, Shan Y, Hu S, Studeman K, Condouris S, et al. Genetic alterations and their relationship in the phosphatidylinositol 3-kinase/Akt pathway in thyroid cancer. Clin Cancer Res. 2007;13(4):1161-70.

103. Garcia-Rostan G, Camp RL, Herrero A, Carcangiu ML, Rimm DL, Tallini G. Beta-catenin dysregulation in thyroid neoplasms: down-regulation, aberrant nuclear expression, and CTNNB1 exon 3 mutations are markers for aggressive tumor phenotypes and poor prognosis. Am J Pathol. 2001;158(3):987-96.

104. Chung K-W, Suh I, OH C. Molecular Biology of Thyroid Cancer. In: Hubbard J IW, Lo C-Y editor. Endocrine Surgery. London: Springer; 2009. p. 97-110.

105. Nikiforov YE. Molecular diagnostics of thyroid tumors. Arch Pathol Lab Med. 2011;135(5):569-77.

106. Grieco M, Santoro M, Berlingieri MT, Melillo RM, Donghi R, Bongarzone I, et al. PTC is a novel rearranged form of the ret proto-oncogene and is frequently detected in vivo in human thyroid papillary carcinomas. Cell. 1990;60(4):557-63.

107. Santoro M, Melillo RM, Carlomagno F, Fusco A, Vecchio G. Molecular mechanisms of RET activation in human cancer. Ann N Y Acad Sci. 2002;963:116-21.

108. Trovisco V, Soares P, Preto A, Castro P, Maximo V, Sobrinho-Simoes M. Molecular genetics of papillary thyroid carcinoma: great expectations. Arq Bras Endocrinol Metabol. 2007;51(5):643-53.

109. Bounacer A, Wicker R, Caillou B, Cailleux AF, Sarasin A, Schlumberger M, et al. High prevalence of activating ret proto-oncogene rearrangements, in thyroid tumors from patients who had received external radiation. Oncogene. 1997;15(11):1263-73.

110. Gilfillan CP. Review of the genetics of thyroid tumours: diagnostic and prognostic implications. ANZ J Surg. 2010;80(1-2):33-40.

111. Ciampi R, Knauf JA, Kerler R, Gandhi M, Zhu Z, Nikiforova MN, et al. Oncogenic AKAP9-BRAF fusion is a novel mechanism of MAPK pathway activation in thyroid cancer. J Clin Invest. 2005;115(1):94-9101.

112. Lee J-H, Lee E-S, Kim Y-S. Clinicopathologic significance of BRAF V600E mutation in papillary carcinomas of the thyroid: a meta-analysis. Cancer. 2007;110(1):38-46.

113. Kebebew E, Weng J, Bauer J, Ranvier G, Clark OH, Duh Q-Y, et al. The prevalence and prognostic value of BRAF mutation in thyroid cancer. Ann Surg. 2007;246(3):466-70.

114. DeLellis RA. Pathology and genetics of thyroid carcinoma. J Surg Oncol. 2006;94(8):662-9.

115. Xing M, Westra WH, Tufano RP, Cohen Y, Rosenbaum E, Rhoden KJ, et al. BRAF mutation predicts a poorer clinical prognosis for papillary thyroid cancer. J Clin Endocrinol Metab. 2005;90(12):6373-9.

116. Fugazzola L, Puxeddu E, Avenia N, Romei C, Cirello V, Cavaliere A, et al. Correlation between B-RAFV600E mutation and clinico-pathologic parameters in papillary thyroid carcinoma: data from a multicentric Italian study and review of the literature. Endocrine-related cancer. 2006;13(2):455-64.

117. Kimura ET, Nikiforova MN, Zhu Z, Knauf JA, Nikiforov YE, Fagin JA. High prevalence of BRAF mutations in thyroid cancer: genetic evidence for constitutive activation of the RET/PTC-RAS-BRAF signaling pathway in papillary thyroid carcinoma. Cancer research. 2003;63(7):1454-7.

118. Nikiforova MN, Kimura ET, Gandhi M, Biddinger PW, Knauf JA, Basolo F, et al. BRAF mutations in thyroid tumors are restricted to papillary carcinomas and anaplastic or poorly differentiated carcinomas arising from papillary carcinomas. J Clin Endocrinol Metab. 2003;88(11):5399-404.

119. Begum S, Rosenbaum E, Henrique R, Cohen Y, Sidransky D, Westra WH. BRAF mutations in anaplastic thyroid carcinoma: implications for tumor origin, diagnosis and treatment. Modern pathology : an official journal of the United States and Canadian Academy of Pathology, Inc. 2004;17(11):1359-63.

120. Fukushima T, Suzuki S, Mashiko M, Ohtake T, Endo Y, Takebayashi Y, et al. BRAF mutations in papillary carcinomas of the thyroid. Oncogene. 2003;22(41):6455-7.

121. Puxeddu E, Moretti S, Elisei R, Romei C, Pascucci R, Martinelli M, et al. BRAF(V599E) mutation is the leading genetic event in adult sporadic papillary thyroid carcinomas. J Clin Endocrinol Metab. 2004;89(5):2414-20.

122. Soares P, Trovisco V, Rocha AS, Lima J, Castro P, Preto A, et al. BRAF mutations and RET/PTC rearrangements are alternative events in the etiopathogenesis of PTC. Oncogene. 2003;22(29):4578-80.

123. Trovisco V, Vieira de Castro I, Soares P, Maximo V, Silva P, Magalhaes J, et al. BRAF mutations are associated with some histological types of papillary thyroid carcinoma. The Journal of pathology. 2004;202(2):247-51.

124. Kim KH, Kang DW, Kim SH, Seong IO, Kang DY. Mutations of the BRAF gene in papillary thyroid carcinoma in a Korean population. Yonsei medical journal. 2004;45(5):818-21.

125. Davies H, Bignell GR, Cox C, Stephens P, Edkins S, Clegg S, et al. Mutations of the BRAF gene in human cancer. Nature. 2002;417(6892):949-54.

126. Pratilas CA, Taylor BS, Ye Q, Viale A, Sander C, Solit DB, et al. (V600E)BRAF is associated with disabled feedback inhibition of RAF-MEK signaling and elevated transcriptional output of the pathway. Proc Natl Acad Sci U S A. 2009;106(11):4519-24.

127. Elisei R, Ugolini C, Viola D, Lupi C, Biagini A, Giannini R, et al. BRAF(V600E) mutation and outcome of patients with papillary thyroid carcinoma: a 15-year median follow-up study. J Clin Endocrinol Metab. 2008;93(10):3943-9.

128. Lupi C, Giannini R, Ugolini C, Proietti A, Berti P, Minuto M, et al. Association of BRAF V600E mutation with poor clinicopathological outcomes in 500 consecutive cases of papillary thyroid carcinoma. J Clin Endocrinol Metab. 2007;92(11):4085-90.

129. Koperek O, Kornauth C, Capper D, Berghoff AS, Asari R, Niederle B, et al. Immunohistochemical detection of the BRAF V600E-mutated protein in papillary thyroid carcinoma. Am J Surg Pathol. 2012;36(6):844-50.

130. Tang KT, Lee CH. BRAF mutation in papillary thyroid carcinoma: pathogenic role and clinical implications. Journal of the Chinese Medical Association : JCMA. 2010;73(3):113-28.

131. Cohen Y, Rosenbaum E, Clark DP, Zeiger MA, Umbricht CB, Tufano RP, et al. Mutational analysis of BRAF in fine needle aspiration biopsies of the thyroid: a potential application for the preoperative assessment of thyroid nodules. Clin Cancer Res. 2004;10(8):2761-5.

132. Knauf JA, Sartor MA, Medvedovic M, Lundsmith E, Ryder M, Salzano M, et al. Progression of BRAF-induced thyroid cancer is associated with epithelial-mesenchymal transition requiring concomitant MAP kinase and TGFβ signaling. Oncogene. 2011;30(28):3153-62.

133. Weier H-UG, Ito Y, Kwan J, Smida J, Weier JF, Hieber L, et al. Delineating chromosomal breakpoints in radiation-induced papillary thyroid cancer. Genes (Basel). 2011;2(3):397-419.

134. Bounacer A, Schlumberger M, Wicker R, Du-Villard JA, Caillou B, Sarasin A, et al. Search for NTRK1 proto-oncogene rearrangements in human thyroid tumours originated after therapeutic radiation. Br J Cancer. 2000;82(2):308-14.

135. Georgescu MM. PTEN Tumor Suppressor Network in PI3K-Akt Pathway Control. Genes & cancer. 2010;1(12):1170-7.

136. Torres J, Pulido R. The tumor suppressor PTEN is phosphorylated by the protein kinase CK2 at its C terminus. Implications for PTEN stability to proteasome-mediated degradation. The Journal of biological chemistry. 2001;276(2):993-8.

137. Al-Khouri AM, Ma Y, Togo SH, Williams S, Mustelin T. Cooperative phosphorylation of the tumor suppressor phosphatase and tensin homologue (PTEN) by casein kinases and glycogen synthase kinase 3beta. J Biol Chem. 2005;280(42):35195-202.

138. Nagy R, Ganapathi S, Comeras I, Peterson C, Orloff M, Porter K, et al. Frequency of germline PTEN mutations in differentiated thyroid cancer. Thyroid. 2011;21(5):505-10.

139. Paes JE, Ringel MD. Dysregulation of the phosphatidylinositol 3-kinase pathway in thyroid neoplasia. Endocrinol Metab Clin North Am. 2008;37(2):375-87.

140. Lane DP. Cancer. A death in the life of p53. Nature. 1993;362(6423):786-7.

141. Taccaliti A, Silvetti F, Palmonella G, Boscaro M. Anaplastic thyroid carcinoma. Frontiers in endocrinology. 2012;3:84.

142. Fabian MR, Sonenberg N, Filipowicz W. Regulation of mRNA translation and stability by microRNAs. Annu Rev Biochem. 2010;79:351-79.

143. Moretti F, Nanni S, Farsetti A, Narducci M, Crescenzi M, Giuliacci S, et al. Effects of exogenous p53 transduction in thyroid tumor cells with different p53 status. J Clin Endocrinol Metab. 2000;85(1):302-8.

144. Moretti F, Farsetti A, Soddu S, Misiti S, Crescenzi M, Filetti S, et al. p53 re-expression inhibits proliferation and restores differentiation of human thyroid anaplastic carcinoma cells. Oncogene. 1997;14(6):729-40.

145. Kroll TG, Sarraf P, Pecciarini L, Chen CJ, Mueller E, Spiegelman BM, et al. PAX8-PPARgamma1 fusion oncogene in human thyroid carcinoma [corrected]. Science. 2000;289(5483):1357-60.

146. McIver B, Grebe SK, Eberhardt NL. The PAX8/PPAR gamma fusion oncogene as a potential therapeutic target in follicular thyroid carcinoma. Current drug targets Immune, endocrine and metabolic disorders. 2004;4(3):221-34.

147. Dwight T, Thoppe SR, Foukakis T, Lui WO, Wallin G, Hoog A, et al. Involvement of the PAX8/peroxisome proliferator-activated receptor gamma rearrangement in follicular thyroid tumors. J Clin Endocrinol Metab. 2003;88(9):4440-5.

148. Barbacid M. ras genes. Annu Rev Biochem. 1987;56:779-827.

149. Giehl K. Oncogenic Ras in tumour progression and metastasis. Biol Chem. 2005;386(3):193-205.

150. Garcia-Rostan G, Zhao H, Camp RL, Pollan M, Herrero A, Pardo J, et al. ras mutations are associated with aggressive tumor phenotypes and poor prognosis in thyroid cancer. J Clin Oncol. 2003;21(17):3226-35.

151. Nikiforov YE, Nikiforova MN. Molecular genetics and diagnosis of thyroid cancer. Nature reviews Endocrinology. 2011;7(10):569-80.

152. Carter WB, Tourtelot JB, Savell JG, Lilienfeld H. New treatments and shifting paradigms in differentiated thyroid cancer management. Cancer Control. 2011;18(2):96-9103.

153. Nikiforova MN, Tseng GC, Steward D, Diorio D, Nikiforov YE. MicroRNA expression profiling of thyroid tumors: biological significance and diagnostic utility. J Clin Endocrinol Metab. 2008;93(5):1600-8.

154. He H, Jazdzewski K, Li W, Liyanarachchi S, Nagy R, Volinia S, et al. The role of microRNA genes in papillary thyroid carcinoma. Proc Natl Acad Sci U S A. 2005;102(52):19075-80.

155. Visone R, Pallante P, Vecchione A, Cirombella R, Ferracin M, Ferraro A, et al. Specific microRNAs are downregulated in human thyroid anaplastic carcinomas. Oncogene. 2007;26(54):7590-5.

156. Jazdzewski K, Boguslawska J, Jendrzejewski J, Liyanarachchi S, Pachucki J, Wardyn KA, et al. Thyroid hormone receptor beta (THRB) is a major target gene for microRNAs deregulated in papillary thyroid carcinoma (PTC). The Journal of clinical endocrinology and metabolism. 2011;96(3):E546-53.

157. Menon MP, Khan A. Micro-RNAs in thyroid neoplasms: molecular, diagnostic and therapeutic implications. J Clin Pathol. 2009;62(11):978-85.

158. Braun J, Hoang-Vu C, Dralle H, Huttelmaier S. Downregulation of microRNAs directs the EMT and invasive potential of anaplastic thyroid carcinomas. Oncogene. 2010;29(29):4237-44.

159. Mazzaferri EL. Management of a solitary thyroid nodule. N Engl J Med. 1993;328(8):553-9.

160. Campbell JP, Pillsbury HC, 3rd. Management of the thyroid nodule. Head Neck. 1989;11(5):414-25.

161. Cooper DS, Doherty GM, Haugen BR, Hauger BR, Kloos RT, Lee SL, et al. Revised American Thyroid Association management guidelines for patients with thyroid nodules and differentiated thyroid cancer. Thyroid. 2009;19(11):1167-214.

162. Larson SM, Erdi Y, Akhurst T, Mazumdar M, Macapinlac HA, Finn RD, et al. Tumor Treatment Response Based on Visual and Quantitative Changes in Global Tumor Glycolysis Using PET-FDG Imaging. The Visual Response Score and the Change in Total Lesion Glycolysis. Clin Positron Imaging. 1999;2(3):159-71.

163. Bai B, Bading J, Conti PS. Tumor quantification in clinical positron emission tomography. Theranostics. 2013;3(10):787-801.

164. Vanderhoek M, Perlman SB, Jeraj R. Impact of the definition of peak standardized uptake value on quantification of treatment response. J Nucl Med. 2012;53(1):4-11.

165. Boellaard R, Krak NC, Hoekstra OS, Lammertsma AA. Effects of noise, image resolution, and ROI definition on the accuracy of standard uptake values: a simulation study. J Nucl Med. 2004;45(9):1519-27.

166. Lowe VJ, DeLong DM, Hoffman JM, Coleman RE. Optimum scanning protocol for FDG-PET evaluation of pulmonary malignancy. J Nucl Med. 1995;36(5):883-7.

167. Lee JR, Madsen MT, Bushnel D, Menda Y. A threshold method to improve standardized uptake value reproducibility. Nucl Med Commun. 2000;21(7):685-90.

168. Graham MM. Quantitation of PET Data in Clinical Practice. In: Shreve P, Townsend WD, editors. Clinical PET-CT in Radiology: Integrated Imaging in Oncology. New York, NY: Springer New York; 2011. p. 61-6.

169. Srinivas SM, Dhurairaj T, Basu S, Bural G, Surti S, Alavi A. A recovery coefficient method for partial volume correction of PET images. Ann Nucl Med. 2009;23(4):341-8.

170. Paquet N, Albert A, Foidart J, Hustinx R. Within-patient variability of (18)F-FDG: standardized uptake values in normal tissues. J Nucl Med. 2004;45(5):784-8.

171. Bogsrud TV, Lowe VJ, Hay ID. PET-CT of Thyroid Cancer. In: Shreve P, Townsend WD, editors. Clinical PET-CT in Radiology: Integrated Imaging in Oncology. New York, NY: Springer New York; 2011. p. 209-25.

172. Lowe VJ, Hoffman JM, DeLong DM, Patz EF, Coleman RE. Semiquantitative and visual analysis of FDG-PET images in pulmonary abnormalities. J Nucl Med. 1994;35(11):1771-6.

173. Moog F, Linke R, Manthey N, Tiling R, Knesewitsch P, Tatsch K, et al. Influence of thyroid-stimulating hormone levels on uptake of FDG in recurrent and metastatic differentiated thyroid carcinoma. J Nucl Med. 2000;41(12):1989-95.

174. Deichen JT, Schmidt C, Prante O, Maschauer S, Papadopoulos T, Kuwert T. Influence of TSH on uptake of [18F]fluorodeoxyglucose in human thyroid cells in vitro. Eur J Nucl Med Mol Imaging. 2004;31(4):507-12.

175. Pagano L, Sama MT, Morani F, Prodam F, Rudoni M, Boldorini R, et al. Thyroid incidentaloma identified by (1)(8)F-fluorodeoxyglucose positron emission tomography with CT (FDG-PET/CT): clinical and pathological relevance. Clin Endocrinol (Oxf). 2011;75(4):528-34.

176. Nishimori H, Tabah R, Hickeson M, How J. Incidental thyroid "PETomas": clinical significance and novel description of the self-resolving variant of focal FDG-PET thyroid uptake. Can J Surg. 2011;54(2):83-8.

177. Soelberg KK, Bonnema SJ, Brix TH, Hegedus L. Risk of malignancy in thyroid incidentalomas detected by 18F-fluorodeoxyglucose positron emission tomography: a systematic review. Thyroid. 2012;22(9):918-25.

178. Kurata S, Ishibashi M, Hiromatsu Y, Kaida H, Miyake I, Uchida M, et al. Diffuse and diffuse-plus-focal uptake in the thyroid gland identified by using FDG-PET: prevalence of thyroid cancer and Hashimoto's thyroiditis. Ann Nucl Med. 2007;21(6):325-30.

179. Karantanis D, Bogsrud TV, Wiseman GA, Mullan BP, Subramaniam RM, Nathan MA, et al. Clinical significance of diffusely increased 18F-FDG uptake in the thyroid gland. J Nucl Med. 2007;48(6):896-901.

180. Chen W, Parsons M, Torigian DA, Zhuang H, Alavi A. Evaluation of thyroid FDG uptake incidentally identified on FDG-PET/CT imaging. Nucl Med Commun. 2009;30(3):240-4.

181. Choi JY, Lee KS, Kim HJ, Shim YM, Kwon OJ, Park K, et al. Focal thyroid lesions incidentally identified by integrated 18F-FDG PET/CT: clinical significance and improved characterization. J Nucl Med. 2006;47(4):609-15.

182. Yi JG, Marom EM, Munden RF, Truong MT, Macapinlac HA, Gladish GW, et al. Focal uptake of fluorodeoxyglucose by the thyroid in patients undergoing initial disease staging with combined PET/CT for non-small cell lung cancer. Radiology. 2005;236(1):271-5.

183. Treglia G, Bertagna F, Sadeghi R, Verburg FA, Ceriani L, Giovanella L. Focal thyroid incidental uptake detected by (1)(8)F-fluorodeoxyglucose positron emission tomography. Meta-analysis on prevalence and malignancy risk. Nuklearmedizin. 2013;52(4):130-6.

184. Bertagna F, Treglia G, Piccardo A, Giovannini E, Bosio G, Biasiotto G, et al. F18-FDG-PET/CT thyroid incidentalomas: a wide retrospective analysis in three Italian centres on the significance of focal uptake and SUV value. Endocrine. 2013;43(3):678-85.

185. Kim H, Kim SJ, Kim IJ, Kim K. Thyroid incidentalomas on FDG PET/CT in patients with non-thyroid cancer - a large retrospective monocentric study. Onkologie. 2013;36(5):260-4.

186. Shie P, Cardarelli R, Sprawls K, Fulda KG, Taur A. Systematic review: prevalence of malignant incidental thyroid nodules identified on fluorine-18 fluorodeoxyglucose positron emission tomography. Nucl Med Commun. 2009;30(9):742-8.

187. Skoura E, Rondogianni P, Alevizaki M, Tzanela M, Tsagarakis S, Piaditis G, et al. Role of [(18)F]FDG-PET/CT in the detection of occult recurrent medullary thyroid cancer. Nucl Med Commun. 2010;31(6):567-75.

188. Skoura E, Datseris IE, Rondogianni P, Tsagarakis S, Tzanela M, Skilakaki M, et al. Correlation between Calcitonin Levels and [(18)F]FDG-PET/CT in the Detection of Recurrence in Patients with Sporadic and Hereditary Medullary Thyroid Cancer. ISRN Endocrinol. 2012;2012:375231.

189. Ong SC, Schoder H, Patel SG, Tabangay-Lim IM, Doddamane I, Gonen M, et al. Diagnostic accuracy of 18F-FDG PET in restaging patients with medullary thyroid carcinoma and elevated calcitonin levels. J Nucl Med. 2007;48(4):501-7.

190. Beuthien-Baumann B, Strumpf A, Zessin J, Bredow J, Kotzerke J. Diagnostic impact of PET with 18F-FDG, 18F-DOPA and 3-O-methyl-6-[18F]fluoro-DOPA in recurrent or metastatic medullary thyroid carcinoma. Eur J Nucl Med Mol Imaging. 2007;34(10):1604-9.

191. Koukouraki S, Strauss LG, Georgoulias V, Eisenhut M, Haberkorn U, Dimitrakopoulou-Strauss A. Comparison of the pharmacokinetics of 68Ga-DOTATOC and [18F]FDG in patients with metastatic neuroendocrine tumours scheduled for 90Y-DOTATOC therapy. Eur J Nucl Med Mol Imaging. 2006;33(10):1115-22.

192. Plotkin M, Hautzel H, Krause BJ, Schmidt D, Larisch R, Mottaghy FM, et al. Implication of 2-18fluor-2-deoxyglucose positron emission tomography in the follow-up of Hurthle cell thyroid cancer. Thyroid. 2002;12(2):155-61.

193. Feine U, Lietzenmayer R, Hanke JP, Wohrle H, Muller-Schauenburg W. [18FDG whole-body PET in differentiated thyroid carcinoma. Flipflop in uptake patterns of 18FDG and 131I]. Nuklearmedizin. 1995;34(4):127-34.

194. Treglia G, Muoio B, Giovanella L, Salvatori M. The role of positron emission tomography and positron emission tomography/computed tomography in thyroid tumours: an overview. Eur Arch Otorhinolaryngol. 2013;270(6):1783-7.

195. Suen KC. Fine-needle aspiration biopsy of the thyroid. CMAJ : Canadian Medical Association journal = journal de l'Association medicale canadienne. 2002;167(5):491-5.

196. Degirmenci B, Haktanir A, Albayrak R, Acar M, Sahin DA, Sahin O, et al. Sonographically guided fine-needle biopsy of thyroid nodules: the effects of nodule characteristics, sampling technique, and needle size on the adequacy of cytological material. Clin Radiol. 2007;62(8):798-803.

197. Cantara S, Capezzone M, Marchisotta S, Capuano S, Busonero G, Toti P, et al. Impact of proto-oncogene mutation detection in cytological specimens from thyroid nodules improves the diagnostic accuracy of cytology. J Clin Endocrinol Metab. 2010;95(3):1365-9.

198. Moses W, Weng J, Sansano I, Peng M, Khanafshar E, Ljung BM, et al. Molecular testing for somatic mutations improves the accuracy of thyroid fine-needle aspiration biopsy. World J Surg. 2010;34(11):2589-94.

199. Ferraz C, Eszlinger M, Paschke R. Current state and future perspective of molecular diagnosis of fine-needle aspiration biopsy of thyroid nodules. J Clin Endocrinol Metab. 2011;96(7):2016-26.

200. Chudova D, Wilde JI, Wang ET, Wang H, Rabbee N, Egidio CM, et al. Molecular classification of thyroid nodules using high-dimensionality genomic data. J Clin Endocrinol Metab. 2010;95(12):5296-304.

201. Gharib H, Goellner JR. Fine-needle aspiration biopsy of the thyroid: an appraisal. Ann Intern Med. 1993;118(4):282-9.

202. Gharib H. Changing concepts in the diagnosis and management of thyroid nodules. Endocrinol Metab Clin North Am. 1997;26(4):777-800.

203. Brander A, Viikinkoski P, Tuuhea J, Voutilainen L, Kivisaari L. Clinical versus ultrasound examination of the thyroid gland in common clinical practice. J Clin Ultrasound. 1992;20(1):37-42.

204. Schlinkert RT, van Heerden JA, Goellner JR, Gharib H, Smith SL, Rosales RF, et al. Factors that predict malignant thyroid lesions when fine-needle aspiration is "suspicious for follicular neoplasm". Mayo Clin Proc. 1997;72(10):913-6.

205. Ohori NP, Nikiforova MN, Schoedel KE, LeBeau SO, Hodak SP, Seethala RR, et al. Contribution of molecular testing to thyroid fine-needle aspiration cytology of "follicular lesion of undetermined significance/atypia of undetermined significance". Cancer cytopathology. 2010;118(1):17-23.

206. Nikiforov YE, Steward DL, Robinson-Smith TM, Haugen BR, Klopper JP, Zhu Z, et al. Molecular testing for mutations in improving the fine-needle aspiration diagnosis of thyroid nodules. J Clin Endocrinol Metab. 2009;94(6):2092-8.

207. Bernet V, Hupart KH, Parangi S, Woeber KA. AACE/ACE disease state commentary: molecular diagnostic testing of thyroid nodules with indeterminate cytopathology. Endocr Pract. 2014;20(4):360-3.

208. Ferris RL, Baloch Z, Bernet V, Chen A, Fahey TJ, 3rd, Ganly I, et al. American Thyroid Association Statement on Surgical Application of Molecular Profiling for Thyroid Nodules: Current Impact on Perioperative Decision Making. Thyroid. 2015;25(7):760-8.

209. Filicori F, Keutgen XM, Buitrago D, AlDailami H, Crowley M, Fahey TJ, 3rd, et al. Risk stratification of indeterminate thyroid fine-needle aspiration biopsy specimens based on mutation analysis. Surgery. 2011;150(6):1085-91.

210. Nikiforov YE, Ohori NP, Hodak SP, Carty SE, LeBeau SO, Ferris RL, et al. Impact of mutational testing on the diagnosis and management of patients with

cytologically indeterminate thyroid nodules: a prospective analysis of 1056 FNA samples. J Clin Endocrinol Metab. 2011;96(11):3390-7.

211. Ohori NP, Schoedel KE. Variability in the atypia of undetermined significance/follicular lesion of undetermined significance diagnosis in the Bethesda System for Reporting Thyroid Cytopathology: sources and recommendations. Acta Cytol. 2011;55(6):492-8.

212. Beaudenon-Huibregtse S, Alexander EK, Guttler RB, Hershman JM, Babu V, Blevins TC, et al. Centralized molecular testing for oncogenic gene mutations complements the local cytopathologic diagnosis of thyroid nodules. Thyroid. 2014;24(10):1479-87.

213. Nikiforov YE, Carty SE, Chiosea SI, Coyne C, Duvvuri U, Ferris RL, et al. Highly accurate diagnosis of cancer in thyroid nodules with follicular neoplasm/suspicious for a follicular neoplasm cytology by ThyroSeq v2 next-generation sequencing assay. Cancer. 2014;120(23):3627-34.

214. Nikiforova MN, Wald AI, Roy S, Durso MB, Nikiforov YE. Targeted next-generation sequencing panel (ThyroSeq) for detection of mutations in thyroid cancer. J Clin Endocrinol Metab. 2013;98(11):E1852-60.

215. Duick DS, Klopper JP, Diggans JC, Friedman L, Kennedy GC, Lanman RB, et al. The impact of benign gene expression classifier test results on the endocrinologist-patient decision to operate on patients with thyroid nodules with indeterminate fine-needle aspiration cytopathology. Thyroid. 2012;22(10):996-1001.

216. Alexander EK, Kennedy GC, Baloch ZW, Cibas ES, Chudova D, Diggans J, et al. Preoperative diagnosis of benign thyroid nodules with indeterminate cytology. The New England journal of medicine. 2012;367(8):705-15.

217. Bartolazzi A, Orlandi F, Saggiorato E, Volante M, Arecco F, Rossetto R, et al. Galectin-3-expression analysis in the surgical selection of follicular thyroid nodules with indeterminate fine-needle aspiration cytology: a prospective multicentre study. Lancet Oncol. 2008;9(6):543-9.

218. Ralhan R, Veyhl J, Chaker S, Assi J, Alyass A, Jeganathan A, et al. Immunohistochemical Subcellular Localization of Protein Biomarkers Distinguishes Benign from Malignant Thyroid Nodules: Potential for Fine-Needle Aspiration Biopsy Clinical Application. Thyroid. 2015;25(11):1224-34.

219. Franco C, Martinez V, Allamand JP, Medina F, Glasinovic A, Osorio M, et al. Molecular markers in thyroid fine-needle aspiration biopsy: a prospective study. Appl Immunohistochem Mol Morphol. 2009;17(3):211-5.

220. Hodak SP, Rosenthal DS, American Thyroid Association Clinical Affairs C. Information for clinicians: commercially available molecular diagnosis testing in the evaluation of thyroid nodule fine-needle aspiration specimens. Thyroid. 2013;23(2):131-4.

221. Clark OH. Predictors of thyroid tumor aggressiveness. West J Med. 1996;165(3):131-8.

222. Lang BH-H, Lo C-Y, Chan W-F, Lam K-Y, Wan K-Y. Staging systems for papillary thyroid carcinoma: a review and comparison. Ann Surg. 2007;245(3):366-78.

223. Nixon IJ, Ganly I, Patel S, Palmer FL, Whitcher MM, Tuttle RM, et al. The impact of microscopic extrathyroid extension on outcome in patients with clinical T1 and T2 well-differentiated thyroid cancer. Surgery. 2011;150(6):1242-9.

224. Khanafshar E, Lloyd RV. The spectrum of papillary thyroid carcinoma variants. Adv Anat Pathol. 2011;18(1):90-7.

225. Hagag P, Hod N, Kummer E, Cohenpour M, Horne T, Weiss M. Follicular variant of papillary thyroid carcinoma: clinical-pathological characterization and long-term follow-up. Cancer J. 2006;12(4):275-82.

226. Gupta S, Ajise O, Dultz L, Wang B, Nonaka D, Ogilvie J, et al. Follicular variant of papillary thyroid cancer: encapsulated, nonencapsulated, and diffuse: distinct biologic and clinical entities. Arch Otolaryngol Head Neck Surg. 2012;138(3):227-33.

227. Nikiforov YE, Seethala RR, Tallini G, Baloch ZW, Basolo F, Thompson LD, et al. Nomenclature Revision for Encapsulated Follicular Variant of Papillary Thyroid Carcinoma: A Paradigm Shift to Reduce Overtreatment of Indolent Tumors. JAMA Oncol. 2016;2(8):1023-9.

228. Ghossein RA, Leboeuf R, Patel KN, Rivera M, Katabi N, Carlson DL, et al. Tall cell variant of papillary thyroid carcinoma without extrathyroid extension: biologic behavior and clinical implications. Thyroid. 2007;17(7):655-61.

229. LiVolsi VA. Papillary carcinoma tall cell variant (TCV): a review. Endocrine pathology. 2010;21(1):12-5.

230. Salajegheh A, Petcu EB, Smith RA, Lam AKY. Follicular variant of papillary thyroid carcinoma: a diagnostic challenge for clinicians and pathologists. Postgrad Med J. 2008;84(988):78-82.

231. Albores-Saavedra J, Wu J. The many faces and mimics of papillary thyroid carcinoma. Endocrine pathology. 2006;17(1):1-18.

232. Silver CE, Owen RP, Rodrigo JP, Rinaldo A, Devaney KO, Ferlito A. Aggressive variants of papillary thyroid carcinoma. Head Neck. 2011;33(7):1052-9.

233. Rufini V, Salvatori M, Fadda G, Pinnarelli L, Castaldi P, Maussier ML, et al. Thyroid carcinomas with a variable insular component: prognostic significance of histopathologic patterns. Cancer. 2007;110(6):1209-17.

234. Collini P, Sampietro G, Rosai J, Pilotti S. Minimally invasive (encapsulated) follicular carcinoma of the thyroid gland is the low-risk counterpart of widely invasive follicular carcinoma but not of insular carcinoma. Virchows Arch. 2003;442(1):71-6.

235. D'Avanzo A, Treseler P, Ituarte PH, Wong M, Streja L, Greenspan FS, et al. Follicular thyroid carcinoma: histology and prognosis. Cancer. 2004;100(6):1123-9.

236. Baloch ZW, LiVolsi VA. Prognostic factors in well-differentiated follicular-derived carcinoma and medullary thyroid carcinoma. Thyroid. 2001;11(7):637-45.

237. Basolo F, Pollina L, Fontanini G, Fiore L, Pacini F, Baldanzi A. Apoptosis and proliferation in thyroid carcinoma: correlation with bcl-2 and p53 protein expression. Br J Cancer. 1997;75(4):537-41.

238. Ain KB. Anaplastic thyroid carcinoma: behavior, biology, and therapeutic approaches. Thyroid. 1998;8(8):715-26.

239. Levendag PC, De Porre PM, van Putten WL. Anaplastic carcinoma of the thyroid gland treated by radiation therapy. Int J Radiat Oncol Biol Phys. 1993;26(1):125-8.

240. Hombach-Klonisch S, Natarajan S, Thanasupawat T, Medapati M, Pathak A, Ghavami S, et al. Mechanisms of therapeutic resistance in cancer (stem) cells with emphasis on thyroid cancer cells. Front Endocrinol (Lausanne). 2014;5:37.

241. Wiseman SM, Griffith OL, Deen S, Rajput A, Masoudi H, Gilks B, et al. Identification of molecular markers altered during transformation of differentiated into anaplastic thyroid carcinoma. Arch Surg. 2007;142(8):717-27; discussion 27-9.

242. Green LD, Mack L, Pasieka JL. Anaplastic thyroid cancer and primary thyroid lymphoma: a review of these rare thyroid malignancies. J Surg Oncol. 2006;94(8):725-36.

243. Lang BH, Lo CY, Chan WF, Lam KY, Wan KY. Prognostic factors in papillary and follicular thyroid carcinoma: their implications for cancer staging. Ann Surg Oncol. 2007;14(2):730-8.

244. Kim S, Wei JP, Braveman JM, Brams DM. Predicting outcome and directing therapy for papillary thyroid carcinoma. Arch Surg. 2004;139(4):390-4; discussion 3-4.

245. Hendrickson-Rebizant J, Sigvaldason H, Nason RW, Pathak KA. Identifying the most appropriate age threshold for TNM stage grouping of well-differentiated thyroid cancer. Eur J Surg Oncol. 2015;41(8):1028-32.

246. Nixon IJ, Wang LY, Migliacci JC, Eskander A, Campbell MJ, Aniss A, et al. An International Multi-Institutional Validation of Age 55 Years as a Cutoff for Risk Stratification in the AJCC/UICC Staging System for Well-Differentiated Thyroid Cancer. Thyroid. 2016;26(3):373-80.

247. Kouvaraki MA, Shapiro SE, Fornage BD, Edeiken-Monro BS, Sherman SI, Vassilopoulou-Sellin R, et al. Role of preoperative ultrasonography in the surgical management of patients with thyroid cancer. Surgery. 2003;134(6):946-54.

248. Stulak JM, Grant CS, Farley DR, Thompson GB, van Heerden JA, Hay ID, et al. Value of preoperative ultrasonography in the surgical management of initial and reoperative papillary thyroid cancer. Arch Surg. 2006;141(5):489-94.

249. Bhattacharyya N. A population-based analysis of survival factors in differentiated and medullary thyroid carcinoma. Otolaryngol Head Neck Surg. 2003;128(1):115-23.

250. Ito Y, Higashiyama T, Takamura Y, Miya A, Kobayashi K, Matsuzuka F, et al. Risk factors for recurrence to the lymph node in papillary thyroid carcinoma patients without preoperatively detectable lateral node metastasis: validity of prophylactic modified radical neck dissection. World J Surg. 2007;31(11):2085-91.

251. Podnos YD, Smith D, Wagman LD, Ellenhorn JDI. The implication of lymph node metastasis on survival in patients with well-differentiated thyroid cancer. Am Surg. 2005;71(9):731-4.

252. Zaydfudim V, Feurer ID, Griffin MR, Phay JE. The impact of lymph node involvement on survival in patients with papillary and follicular thyroid carcinoma. Surgery. 2008;144(6):1070-7.

253. Gemsenjager E, Heitz PU, Seifert B, Martina B, Schweizer I. Differentiated thyroid carcinoma. Follow-up of 264 patients from one institution for up to 25 years. Swiss Med Wkly. 2001;131(11-12):157-63.

254. Chiang F-Y, Lin J-C, Lee K-W, Wang L-F, Tsai K-B, Wu C-W, et al. Thyroid tumors with preoperative recurrent laryngeal nerve palsy: clinicopathologic features and treatment outcome. Surgery. 2006;140(3):413-7.

255. McCaffrey JC. Evaluation and treatment of aerodigestive tract invasion by well-differentiated thyroid carcinoma. Cancer Control. 2000;7(3):246-52.

256. Jukkola A, Bloigu R, Ebeling T, Salmela P, Blanco G. Prognostic factors in differentiated thyroid carcinomas and their implications for current staging classifications. Endocrine-related cancer. 2004;11(3):571-9.

257. Lee S-H, Lee S-S, Jin S-M, Kim J-H, Rho Y-S. Predictive factors for central compartment lymph node metastasis in thyroid papillary microcarcinoma. Laryngoscope. 2008;118(4):659-62.

258. Durante C, Haddy N, Baudin E, Leboulleux S, Hartl D, Travagli JP, et al. Long-term outcome of 444 patients with distant metastases from papillary and follicular

thyroid carcinoma: benefits and limits of radioiodine therapy. J Clin Endocrinol Metab. 2006;91(8):2892-9.

259. Lee J, Soh E-Y. Differentiated thyroid carcinoma presenting with distant metastasis at initial diagnosis clinical outcomes and prognostic factors. Ann Surg. 2010;251(1):114-9.

260. Beenken S, Roye D, Weiss H, Sellers M, Urist M, Diethelm A, et al. Extent of surgery for intermediate-risk well-differentiated thyroid cancer. Am J Surg. 2000;179(1):51-6.

261. Lerch H, Schober O, Kuwert T, Saur HB. Survival of differentiated thyroid carcinoma studied in 500 patients. J Clin Oncol. 1997;15(5):2067-75.

262. Benbassat CA, Mechlis-Frish S, Hirsch D. Clinicopathological characteristics and long-term outcome in patients with distant metastases from differentiated thyroid cancer. World J Surg. 2006;30(6):1088-95.

263. Sampson E, Brierley JD, Le LW, Rotstein L, Tsang RW. Clinical management and outcome of papillary and follicular (differentiated) thyroid cancer presenting with distant metastasis at diagnosis. Cancer. 2007;110(7):1451-6.

264. Schlumberger M, Pacini F, Wiersinga WM, Toft A, Smit JWA, Sanchez Franco F, et al. Follow-up and management of differentiated thyroid carcinoma: a European perspective in clinical practice. Eur J Endocrinol. 2004;151(5):539-48.

265. Bachelot A, Cailleux AF, Klain M, Baudin E, Ricard M, Bellon N, et al. Relationship between tumor burden and serum thyroglobulin level in patients with papillary and follicular thyroid carcinoma. Thyroid. 2002;12(8):707-11.

266. Hirabayashi RN, Lindsays. Carcinoma of the thyroid gland: a statistical study of 390 patients. J Clin Endocrinol Metab. 1961;21:1596-610.

267. Russell CF, Van Heerden JA, Sizemore GW, Edis AJ, Taylor WF, ReMine WH, et al. The surgical management of medullary thyroid carcinoma. Ann Surg. 1983;197(1):42-8.

268. Soh EY, Clark OH. Surgical considerations and approach to thyroid cancer. Endocrinol Metab Clin North Am. 1996;25(1):115-39.

269. Mazzaferri EL. Treating differentiated thyroid carcinoma: where do we draw the line? Mayo Clin Proc. 1991;66(1):105-11.

270. Van Nostrand D. The benefits and risks of I-131 therapy in patients with well-differentiated thyroid cancer. Thyroid. 2009;19(12):1381-91.

271. Vaisman A, Orlov S, Yip J, Hu C, Lim T, Dowar M, et al. Application of post-surgical stimulated thyroglobulin for radioiodine remnant ablation selection in low-risk papillary thyroid carcinoma. Head Neck. 2010;32(6):689-98.

272. Sawka AM, Orlov S, Gelberg J, Stork B, Dowar M, Shaytzag M, et al. Prognostic value of postsurgical stimulated thyroglobulin levels after initial radioactive iodine therapy in well-differentiated thyroid carcinoma. Head Neck. 2008;30(6):693-700.

273. Solans R, Bosch JA, Galofre P, Porta F, Rosello J, Selva-O'Callagan A, et al. Salivary and lacrimal gland dysfunction (sicca syndrome) after radioiodine therapy. J Nucl Med. 2001;42(5):738-43.

274. Silberstein EB. Reducing the incidence of 131I-induced sialadenitis: the role of pilocarpine. J Nucl Med. 2008;49(4):546-9.

275. Antonelli A, Fallahi P, Ferrari SM, Ruffilli I, Santini F, Minuto M, et al. New targeted therapies for thyroid cancer. Curr Genomics. 2011;12(8):626-31.

276. Ekpe-Adewuyi E, Lopez-Campistrous A, Tang X, Brindley DN, McMullen TP. Platelet derived growth factor receptor alpha mediates nodal metastases in papillary thyroid cancer by driving the epithelial-mesenchymal transition. Oncotarget. 2016.

277. Brose MS, Nutting CM, Jarzab B, Elisei R, Siena S, Bastholt L, et al. Sorafenib in radioactive iodine-refractory, locally advanced or metastatic differentiated thyroid cancer: a randomised, double-blind, phase 3 trial. Lancet. 2014;384(9940):319-28.

278. Medapati MR, Dahlmann M, Ghavami S, Pathak KA, Lucman L, Klonisch T, et al. RAGE Mediates the Pro-Migratory Response of Extracellular S100A4 in Human Thyroid Cancer Cells. Thyroid. 2015;25(5):514-27.

279. Spencer CA, Wang CC. Thyroglobulin measurement. Techniques, clinical benefits, and pitfalls. Endocrinol Metab Clin North Am. 1995;24(4):841-63.

280. Spencer CA, Lopresti JS. Measuring thyroglobulin and thyroglobulin autoantibody in patients with differentiated thyroid cancer. Nat Clin Pract Endocrinol Metab. 2008;4(4):223-33.

281. Spencer CA, Takeuchi M, Kazarosyan M, Wang CC, Guttler RB, Singer PA, et al. Serum thyroglobulin autoantibodies: prevalence, influence on serum thyroglobulin measurement, and prognostic significance in patients with differentiated thyroid carcinoma. J Clin Endocrinol Metab. 1998;83(4):1121-7.

282. Ozata M, Suzuki S, Miyamoto T, Liu RT, Fierro-Renoy F, DeGroot LJ. Serum thyroglobulin in the follow-up of patients with treated differentiated thyroid cancer. J Clin Endocrinol Metab. 1994;79(1):98-9105.

283. Smallridge RC, Meek SE, Morgan MA, Gates GS, Fox TP, Grebe S, et al. Monitoring thyroglobulin in a sensitive immunoassay has comparable sensitivity to recombinant human tsh-stimulated thyroglobulin in follow-up of thyroid cancer patients. J Clin Endocrinol Metab. 2007;92(1):82-7.

284. Schlumberger M, Hitzel A, Toubert ME, Corone C, Troalen F, Schlageter MH, et al. Comparison of seven serum thyroglobulin assays in the follow-up of papillary and follicular thyroid cancer patients. J Clin Endocrinol Metab. 2007;92(7):2487-95.

285. Paschke R, Hegedus L, Alexander E, Valcavi R, Papini E, Gharib H. Thyroid nodule guidelines: agreement, disagreement and need for future research. Nat Rev Endocrinol. 2011;7(6):354-61.

286. Pathak KA, Goertzen AL, Nason RW, Klonisch T, Leslie WD. A prospective cohort study to assess the role of FDG-PET in differentiating benign and malignant follicular neoplasms. Annals of Medicine and Surgery. 2016;12:27-31.

287. Bybel B, Greenberg ID, Paterson J, Ducharme J, Leslie WD. Increased F-18 FDG intestinal uptake in diabetic patients on metformin: a matched case-control analysis. Clin Nucl Med. 2011;36(6):452-6.

288. Fluss R, Faraggi D, Reiser B. Estimation of the Youden Index and its associated cutoff point. Biom J. 2005;47(4):458-72.

289. Canadian Cancer Society., Statistics Canada., Public Health Agency of Canada., Canadian Electronic Library (Firm). Canadian cancer statistics 2012. Toronto, Ont.: Canadian Cancer Society; 2012. Available from: http://myaccess.library.utoronto.ca/login?url=http://site.ebrary.com/lib/utoronto/Top?id=10585841.

290. RJ G. A class of k-sample tests for comparing the cumulative incidence of a competing risk. Ann Stat. 1988;16:1141-54.

291. Fine JP GR. A proportional hazards model for the subdistribution of a competing risk. J Am Stat Assoc. 1999;94:496-509.

292. Iasonos A, Schrag D, Raj GV, Panageas KS. How to build and interpret a nomogram for cancer prognosis. J Clin Oncol. 2008;26(8):1364-70.

293. Harrell FE, Lee KL, Mark DB. Multivariable prognostic models: issues in developing models, evaluating assumptions and adequacy, and measuring and reducing errors. Stat Med. 1996;15(4):361-87.

294. Wolbers M, Koller MT, Witteman JCM, Steyerberg EW. Prognostic models with competing risks: methods and application to coronary risk prediction. Epidemiology. 2009;20(4):555-61.

295. Akaike H. Information Theory and an Extension of the Maximum Likelihood Principle. In: Parzen E, Tanabe K, Kitagawa G, editors. Selected Papers of Hirotugu Akaike. New York, NY: Springer New York; 1998. p. 199-213.

296. Everitt B. The Cambridge dictionary of statistics. 3rd ed. Cambridge: Cambridge University Press; 2006. ix, 432 p. p.

297. MAZEROLLE MJ. APPENDIX 1: Making sense out of Akaike's Information Criterion (AIC): its use and interpretation in model selection and inference from ecological data: Université Laval, Québec, Québec; 2004.

298. Pathak KA, Klonisch T, Nason RW, Leslie WD. FDG-PET characteristics of Hurthle cell and follicular adenomas. Ann Nucl Med. 2016.

299. Pathak KA, Lambert P, Nason RW, Klonisch T. Comparing a thyroid prognostic nomogram to the existing staging systems for prediction risk of death from thyroid cancers. Eur J Surg Oncol. 2016.

300. Pathak KA, Klonisch TC, Nason RW. Stage II differentiated thyroid cancer: A mixed bag. J Surg Oncol. 2016;113(1):94-7.

301. Silverberg SG, Vidone RA. Adenoma and carcinoma of the thyroid. Cancer. 1966;19(8):1053-62.

302. Bisi H, Fernandes VS, de Camargo RY, Koch L, Abdo AH, de Brito T. The prevalence of unsuspected thyroid pathology in 300 sequential autopsies, with special reference to the incidental carcinoma. Cancer. 1989;64(9):1888-93.

303. de Geus-Oei LF, Pieters GF, Bonenkamp JJ, Mudde AH, Bleeker-Rovers CP, Corstens FH, et al. 18F-FDG PET reduces unnecessary hemithyroidectomies for thyroid nodules with inconclusive cytologic results. Journal of nuclear medicine : official publication, Society of Nuclear Medicine. 2006;47(5):770-5.

304. Deandreis D, Al Ghuzlan A, Auperin A, Vielh P, Caillou B, Chami L, et al. Is (18)F-fluorodeoxyglucose-PET/CT useful for the presurgical characterization of

thyroid nodules with indeterminate fine needle aspiration cytology? Thyroid. 2012;22(2):165-72.

305. Hales NW, Krempl GA, Medina JE. Is there a role for fluorodeoxyglucose positron emission tomography/computed tomography in cytologically indeterminate thyroid nodules? Am J Otolaryngol. 2008;29(2):113-8.

306. Kim JM, Ryu JS, Kim TY, Kim WB, Kwon GY, Gong G, et al. 18F-fluorodeoxyglucose positron emission tomography does not predict malignancy in thyroid nodules cytologically diagnosed as follicular neoplasm. J Clin Endocrinol Metab. 2007;92(5):1630-4.

307. Kresnik E, Gallowitsch HJ, Mikosch P, Stettner H, Igerc I, Gomez I, et al. Fluorine-18-fluorodeoxyglucose positron emission tomography in the preoperative assessment of thyroid nodules in an endemic goiter area. Surgery. 2003;133(3):294-9.

308. Smith RB, Robinson RA, Hoffman HT, Graham MM. Preoperative FDG-PET imaging to assess the malignant potential of follicular neoplasms of the thyroid. Otolaryngology--head and neck surgery : official journal of American Academy of Otolaryngology-Head and Neck Surgery. 2008;138(1):101-6.

309. Traugott AL, Dehdashti F, Trinkaus K, Cohen M, Fialkowski E, Quayle F, et al. Exclusion of malignancy in thyroid nodules with indeterminate fine-needle aspiration cytology after negative 18F-fluorodeoxyglucose positron emission tomography: interim analysis. World J Surg. 2010;34(6):1247-53.

310. Sebastianes FM, Cerci JJ, Zanoni PH, Soares J, Jr., Chibana LK, Tomimori EK, et al. Role of 18F-fluorodeoxyglucose positron emission tomography in preoperative assessment of cytologically indeterminate thyroid nodules. The Journal of clinical endocrinology and metabolism. 2007;92(11):4485-8.

311. Munoz Perez N, Villar del Moral JM, Muros Fuentes MA, Lopez de la Torre M, Arcelus Martinez JI, Becerra Massare P, et al. Could 18F-FDG-PET/CT avoid unnecessary thyroidectomies in patients with cytological diagnosis of follicular neoplasm? Langenbecks Arch Surg. 2013;398(5):709-16.

312. Kim SJ, Kim BH, Jeon YK, Kim SS, Kim IJ. Limited diagnostic and predictive values of dual-time-point 18F FDG PET/CT for differentiation of incidentally detected thyroid nodules. Ann Nucl Med. 2011;25(5):347-53.

313. Kim SJ, Chang S. Predictive value of intratumoral heterogeneity of F-18 FDG uptake for characterization of thyroid nodules according to Bethesda categories of fine needle aspiration biopsy results. Endocrine. 2015;50(3):681-8.

314. Wang N, Zhai H, Lu Y. Is fluorine-18 fluorodeoxyglucose positron emission tomography useful for the thyroid nodules with indeterminate fine needle aspiration biopsy? A meta-analysis of the literature. J Otolaryngol Head Neck Surg. 2013;42:38.

315. Wiesner W, Engel H, von Schulthess GK, Krestin GP, Bicik I. FDG PET-negative liver metastases of a malignant melanoma and FDG PET-positive hurthle cell tumor of the thyroid. Eur Radiol. 1999;9(5):975-8.

316. Barnabei A, Ferretti E, Baldelli R, Procaccini A, Spriano G, Appetecchia M. Hurthle cell tumours of the thyroid. Personal experience and review of the literature. Acta Otorhinolaryngol Ital. 2009;29(6):305-11.

317. Maximo V, Sobrinho-Simoes M. Hurthle cell tumours of the thyroid. A review with emphasis on mitochondrial abnormalities with clinical relevance. Virchows Arch. 2000;437(2):107-15.

318. Paul A, Villepelet A, Lefevre M, Perie S. Oncocytic parathyroid adenoma. Eur Ann Otorhinolaryngol Head Neck Dis. 2015;132(5):301-3.

319. Vriens D, Adang EM, Netea-Maier RT, Smit JW, de Wilt JH, Oyen WJ, et al. Cost-effectiveness of FDG-PET/CT for cytologically indeterminate thyroid nodules: a decision analytic approach. J Clin Endocrinol Metab. 2014;99(9):3263-74.

320. Vesselle H, Turcotte E, Wiens L, Schmidt R, Takasugi JE, Lalani T, et al. Relationship between non-small cell lung cancer fluorodeoxyglucose uptake at positron emission tomography and surgical stage with relevance to patient prognosis. Clin Cancer Res. 2004;10(14):4709-16.

321. Menda Y, Bushnell DL, Madsen MT, McLaughlin K, Kahn D, Kernstine KH. Evaluation of various corrections to the standardized uptake value for diagnosis of pulmonary malignancy. Nucl Med Commun. 2001;22(10):1077-81.

322. Ellison LF, Wilkins K. An update on cancer survival. Health Rep. 2010;21(3):55-60.

323. Enewold L, Zhu K, Ron E, Marrogi AJ, Stojadinovic A, Peoples GE, et al. Rising thyroid cancer incidence in the United States by demographic and tumor characteristics, 1980-2005. Cancer Epidemiol Biomarkers Prev. 2009;18(3):784-91.

324. Jung KW, Park S, Kong HJ, Won YJ, Lee JY, Seo HG, et al. Cancer statistics in Korea: incidence, mortality, survival, and prevalence in 2009. Cancer Res Treat. 2012;44(1):11-24.

325. Grodski S, Brown T, Sidhu S, Gill A, Robinson B, Learoyd D, et al. Increasing incidence of thyroid cancer is due to increased pathologic detection. Surgery. 2008;144(6):1038-43.

326. Burgess JR, Tucker P. Incidence trends for papillary thyroid carcinoma and their correlation with thyroid surgery and thyroid fine-needle aspirate cytology. Thyroid. 2006;16(1):47-53.

327. Colonna M, Guizard AV, Schvartz C, Velten M, Raverdy N, Molinie F, et al. A time trend analysis of papillary and follicular cancers as a function of tumour size: a study of data from six cancer registries in France (1983-2000). Eur J Cancer. 2007;43(5):891-900.

328. Davies L, Welch HG. Increasing incidence of thyroid cancer in the United States, 1973-2002. JAMA. 2006;295(18):2164-7.

329. Yu G-P, Li JC-L, Branovan D, McCormick S, Schantz SP. Thyroid cancer incidence and survival in the national cancer institute surveillance, epidemiology, and end results race/ethnicity groups. Thyroid. 2010;20(5):465-73.

330. Leenhardt L, Grosclaude P, Cherie-Challine L. Increased incidence of thyroid carcinoma in france: a true epidemic or thyroid nodule management effects? Report from the French Thyroid Cancer Committee. Thyroid. 2004;14(12):1056-60.

331. Lubina A, Cohen O, Barchana M, Liphshiz I, Vered I, Sadetzki S, et al. Time trends of incidence rates of thyroid cancer in Israel: what might explain the sharp increase. Thyroid. 2006;16(10):1033-40.

332. Smailyte G, Miseikyte-Kaubriene E, Kurtinaitis J. Increasing thyroid cancer incidence in Lithuania in 1978-2003. BMC Cancer. 2006;6:284-.

333. Fahey TJ, Reeve TS, Delbridge L. Increasing incidence and changing presentation of thyroid cancer over a 30-year period. Br J Surg. 1995;82(4):518-20.

334. Kent WDT, Hall SF, Isotalo PA, Houlden RL, George RL, Groome PA. Increased incidence of differentiated thyroid carcinoma and detection of subclinical disease. CMAJ. 2007;177(11):1357-61.

335. Liu S, Semenciw R, Ugnat AM, Mao Y. Increasing thyroid cancer incidence in Canada, 1970-1996: time trends and age-period-cohort effects. Br J Cancer. 2001;85(9):1335-9.

336. Canadian Cancer Society., Statistics Canada., Public Health Agency of Canada., Canadian Electronic Library (Firm). Canadian cancer statistics 2009 special topic : cancer in adolescents and young adults. Toronto, Ont.: Canadian Cancer Society; 2009. Available from: http://myaccess.library.utoronto.ca/login?url=http://site.ebrary.com/lib/utoronto/Top?id=10391008.

337. Roman S, Lin R, Sosa JA. Prognosis of medullary thyroid carcinoma: demographic, clinical, and pathologic predictors of survival in 1252 cases. Cancer. 2006;107(9):2134-42.

338. Brierley J, Tsang R, Simpson WJ, Gospodarowicz M, Sutcliffe S, Panzarella T. Medullary thyroid cancer: analyses of survival and prognostic factors and the role of radiation therapy in local control. Thyroid. 1996;6(4):305-10.

339. Carling T, Carty SE, Ciarleglio MM, Cooper DS, Doherty GM, Kim LT, et al. American Thyroid Association design and feasibility of a prospective randomized controlled trial of prophylactic central lymph node dissection for papillary thyroid carcinoma. Thyroid. 2012;22(3):237-44.

340. Hedinger CE, Williams ED, Sobin LH. Histological typing of thyroid tumours. 2nd ed. Berlin ; New York: Springer-Verlag; 1988. xii, 66 p. p.

341. Fincham SM, Ugnat AM, Hill GB, Kreiger N, Mao Y. Is occupation a risk factor for thyroid cancer? Canadian Cancer Registries Epidemiology Research Group. J Occup Environ Med. 2000;42(3):318-22.

342. Fraker DL. Radiation exposure and other factors that predispose to human thyroid neoplasia. Surg Clin North Am. 1995;75(3):365-75.

343. Haselkorn T, Bernstein L, Preston-Martin S, Cozen W, Mack WJ. Descriptive epidemiology of thyroid cancer in Los Angeles County, 1972-1995. Cancer Causes Control. 2000;11(2):163-70.

344. Sont WN, Zielinski JM, Ashmore JP, Jiang H, Krewski D, Fair ME, et al. First analysis of cancer incidence and occupational radiation exposure based on the National Dose Registry of Canada. Am J Epidemiol. 2001;153(4):309-18.

345. Han JM, Bae Kim W, Kim TY, Ryu JS, Gong G, Hong SJ, et al. Time trend in tumour size and characteristics of anaplastic thyroid carcinoma. Clin Endocrinol (Oxf). 2012;77(3):459-64.

346. Busco S, Giorgi Rossi P, Sperduti I, Pezzotti P, Buzzoni C, Pannozzo F. Increased incidence of thyroid cancer in Latina, Italy: a possible role of detection of subclinical disease. Cancer Epidemiol. 2013;37(3):262-9.

347. Wang TS, Sosa JA. Thyroid gland: Can a nomogram predict death in patients with thyroid cancer? Nat Rev Endocrinol. 2013;9(4):192-3.

348. Gooley TA, Leisenring W, Crowley J, Storer BE. Estimation of failure probabilities in the presence of competing risks: new representations of old estimators. Statistics in medicine. 1999;18(6):695-706.

349. Wagenmakers EJ, Farrell S. AIC model selection using Akaike weights. Psychon Bull Rev. 2004;11(1):192-6.

350. Lang BH, Wong CK. Validation and Comparison of Nomograms in Predicting Disease-Specific Survival for Papillary Thyroid Carcinoma. World J Surg. 2015;39(8):1951-8.

351. Tran Cao HS, Johnston LE, Chang DC, Bouvet M. A critical analysis of the American Joint Committee on Cancer (AJCC) staging system for differentiated

thyroid carcinoma in young patients on the basis of the Surveillance, Epidemiology, and End Results (SEER) registry. Surgery. 2012;152(2):145-51.

352. Lundgren CI, Hall P, Dickman PW, Zedenius J. Clinically significant prognostic factors for differentiated thyroid carcinoma: a population-based, nested case-control study. Cancer. 2006;106(3):524-31.

Appendix

Papers published

1. **Pathak KA**, Klonisch T, Nason RW, Leslie WD. A prospective cohort study to assess the role of FDG-PET in differentiating benign and malignant follicular neoplasms. Ann Med Surg. 2016;12:27-31. (Role: Corresponding author)

2. **Pathak KA**, Lambert P, Nason RW, Klonisch T. Comparing a thyroid prognostic nomogram to the existing staging systems for prediction risk of death from thyroid cancers. Eur J Surg Oncol. 2016 Oct; 42(10):1491-6.

3. **Pathak KA**, Klonisch T, Nason RW, Leslie WD. FDG-PET characteristics of Hürthle cell and follicular adenomas. Ann Nucl Med. 2016 Aug; 30(7):506-9.

4. **Pathak KA**, Klonisch T, Nason RW. Stage II differentiated thyroid cancer: A mixed bag. J Surg Oncol. 2016 Jan; 113(1):94-7.

5. **Pathak KA,** Mazurat A, Lambert P, Klonisch T, Nason RW. Prognostic nomograms to predict treatment outcomes of thyroid cancer Clin Endocrinol Metab. 2013 Dec;98(12):4768-75.

6. **Pathak KA,** Leslie WD, Klonisch TC, Nason RW. The changing face of thyroid cancer in a population-based cohort. Cancer Medicine 2013; 2:537–544.

7. Hendrickson-Rebizant J, Sigvaldason H, Nason RW, **Pathak KA**. Identifying the most appropriate age threshold for TNM stage grouping of well-differentiated thyroid cancer. Eur J Surg Oncol. 2015 Aug; 41(8):1028-32.

8. Mazurat A, Torroni A, Hendrickson-Rebizant J, Benning H, Nason RW, **Pathak KA.** The age factor in survival of a population cohort of well-differentiated thyroid cancer. Endocr Connect. 2013 Sep 23; 2(3):154-60.

9. Nixon IJ, Wang LY, Migliacci JC, Eskander A, Campbell MJ, Aniss A, Morris L, Vaisman F, Corbo R, Momesso D, Vaisman M, Carvalho A, Learoyd D, Leslie WD, Nason RW, Kuk D, Wreesmann V, Morris L, Palmer FL, Ganly I, Patel SG, Singh B, Tuttle RM, Shaha AR, Gönen M, **Pathak KA**, Shen WT, Sywak M, Kowalski L, Freeman J, Perrier N, Shah JP. An International Multi-Institutional Validation of Age 55 Years as a Cutoff for Risk Stratification in the AJCC/UICC Staging System for Well-Differentiated Thyroid Cancer. Thyroid. 2016 Mar; 26(3):373-80.

10. Medapati M, Dahlmann M, Ghavami S, **Pathak KA**, Lucman L, Klonisch T, Hoang-Vu C, Stein U, Hombach-Klonisch S. RAGE mediates the pro-migratory response of extracellular S100A4 in human thyroid cancer cells. Thyroid 2015 May;25(5):514-27

11. Hombach-Klonisch S, Natarajan S, Thanasupawat T, Medapati M, **Pathak KA**, Ghavami S, Klonisch T. Mechanisms of therapeutic resistance in cancer (stem) cells with emphasis on thyroid cancer cells. Front Endocrinol (Lausanne). 2014 Mar 25;5:37

CrossMark

A prospective cohort study to assess the role of FDG-PET in differentiating benign and malignant follicular neoplasms

K. Alok Pathak [a, c, *], Andrew L. Goertzen [b], Richard W. Nason [a], Thomas Klonisch [c], William D. Leslie [b]

[a] Division of Surgical Oncology, Cancer Care Manitoba & University of Manitoba, Winnipeg Canada
[b] Section of Nuclear Medicine, Department of Radiology, University of Manitoba, Winnipeg Canada
[c] Department of Human Anatomy and Cell Science, University of Manitoba, Winnipeg Canada

HIGHLIGHTS

- Earlier meta-analyses have not considered Hürthle cell neoplasm separate from other follicular neoplasm.
- Hürthle cell neoplasm are known to show high FDG uptake.
- FDG-PET/CT can help in differentiating benign and malignant non-Hürthle cell thyroid nodules.
- A cut-off SUVmax of 3.25 enhances the accuracy of FDG-PET/CT in identifying cancers in thyroid nodules.

ARTICLE INFO

ABSTRACT

Background: Follicular and Hürthle cell neoplasms are diagnostic challenges. This prospective study was designed to evaluate the efficacy of [18F]-2-fluoro-2-deoxy-d-glucose (FDG) positron emission tomography/computed tomography (PET/CT) in predicting the risk of malignancy in follicular/Hürthle cell neoplasms.

Materials and methods: Fifty thyroid nodules showing follicular/Hürthle cell neoplasm on prior ultrasonography guided fine needle aspiration cytology (FNAC) were recruited into this study. A FDG-PET/CT scan, performed for neck and superior mediastinum, was reported by a single observer, blinded to the surgical and pathology findings. Receiver operating characteristic (ROC) curve analysis of maximum standardized uptake value (SUVmax) and the area under the curve (AUROC) were used to assess discrimination between benign from malignant nodules. Youden index was used to identify the optimal cut-off SUVmax for diagnosing malignancy. Sensitivity, specificity, predictive values and overall accuracy were used as measures of performance.

Results: Our study group comprises of 31 benign and 19 malignant thyroid nodules. After excluding all Hürthle cell adenomas, the AUROC for discriminating benign and malignant non-Hürthle cell neoplasms was 0.79 (95% CI, 0.64–0.94; p = 0.001); with SUVmax of 3.25 as the best cut-off for the purpose. PET/CT had sensitivity of 79% (95% CI, 54–93%), specificity of 83% (95% CI, 60–94%), positive predictive value (PPV) of 79% (95% CI, 54–93%), and negative predictive value (NPV) of 83% (95% CI, 60–94%). The overall accuracy was 81%.

Conclusions: FDG-PET/CT can help in differentiating benign and malignant non-Hürthle cell neoplasms. SUVmax of 3.25 was found to be the best for identifying malignant non-Hürthle cell follicular neoplasms.

1. Introduction

Follicular and Hürthle cell neoplasms are diagnostic challenges

for pathologists both on fine needle aspiration cytology (FNAC) and frozen sections, as comprehensive assessment of thyroid nodule for capsular invasion is required for diagnosis [1]. This often requires a

diagnostic hemi-thyroidectomy and a subsequent completion thy-roidectomy (second surgery) for the patients with malignancy diagnosed on paraffin sections. If the malignant neoplasms could be differentiated from benign adenomas preoperatively, these pa-tients could directly undergo one-stage total thyroidectomy. This would avoid a second surgery, treatment delays and additional health care costs.

[18F]-2-fluoro-2-deoxy-d-glucose (FDG) positron emission to-mography/computed tomography (PET/CT) scan has been used to discriminate benign and malignant follicular/Hürthle cell neo-plasms earlier with variable results and is not recommended for routine evaluation of thyroid nodules with indeterminate cytology [2,3]. This prospective study was designed to evaluate the efficacy of FDG-PET/CT scan in predicting the risk of malignancy in inde-terminate follicular neoplasms.

2. Material and methods

2.1. Study cohort

This prospective study, approved by Research Ethics Board at the University of Manitoba (H2010:056), included 47 consecutive consenting patients with 50 follicular/Hürthle cell neoplasms, >5 mm in size, seen in the Thyroid clinic from July 2013 to December 2015, at a comprehensive cancer care centre associated with the University teaching hospital. In all, 49 patients were screened for this study and 2 patients did not consent for FDG-PET/CT scan. The minimum sample size (N = 44) was calculated for a power of 0.80 with alpha of 0.05, based on 20% risk of malignancy in follicular neoplasm nodules and 39% risk of malignancy in FDG-PET positive indeterminate nodules [2,4].

All patients had a prior ultrasonography and ultrasound guided FNAC showing follicular/Hürthle cell neoplasms. A FDG-PET/CT scan was performed pre-operatively; for which, all patients were asked to fast for 4—6 h prior to administration of F-18 FDG injection. To minimize the examination time and substantially reduce the radiation exposure, only a half-dose of FDG (185 MBq) was administered and patients were scanned in a single bed position (neck and superior mediastinum). The acquisition time was increased by 60% (from 3 to 5 minutes per bed position) to compensate for the reduced dose. A standard acquisition protocol for the 3D-mode Biograph-16 (Siemens; Malvern, PA) PET/CT scanner was used for all patients. Helical CT was acquired with 3- to 5-mm section thickness, as described earlier [5]. All scans were reported by a single observer who was blinded to the surgical and pathologic findings. Recovery coefficient method for partial volume correction of PET images was used, as described earlier [6]. Meta-bolic tumor volume is the sum of estimated volumes of voxels with increased uptake (MTV; global MTV = volume of voxels with SUV > threshold SUV). MTV is defined as total tumor volume with SUVmax of 2.5 or greater. Total lesion glycolysis is the sum of the product of each lesion's MTV and the corresponding mean SUV over lesions within that MTV (TLG; global TLG = MTV × mean SUV) [7—9]. MTV and TLG were calculated for 30 lesions with SUVmax ≥ 2.5. Histopathology results were considered as the gold standard for diagnosis.

The patient characteristics, FDG-PET/CT scan findings, and the tumor histology were recorded. The data were managed and analyzed using SPSS for Windows version 23·0 (SPSS Inc., Chicago, IL). After checking for normality assumption, the mean and stan-dard deviation were used to express normally distributed data (such as the age and the size of nodule), which were compared by analysis of variance (ANOVA). The median with interquartile range (IQR) was used for non-normally distributed data (such as the standardized FDG uptake value). Inter-group comparison of non-normally distributed data was made by Mann-Whitney nonpara-metric analysis. χ^2 test was used to compare categorical variables. A p-value <0.05 (two-sided) was considered to indicate statistical significance and 95% confidence intervals (95% CI) were used to express reliability in the estimates.

Receiver operating characteristic (ROC) curve analysis of maximum standardized uptake value (SUVmax) and area under the curve (AUROC) were used to assess discrimination between benign from malignant nodules. Youden index was used to identify the optimal cut-off SUVmax for diagnosing malignancy [10]. Sensi-tivity, specificity, positive predictive value (PPV), negative predic-tive value (NPV) and overall accuracy were used as measures of performance of FDG-PET/CT.

3. Results

The mean age of the patients in our study cohort was 58.7 ± 12.8 years and 72% of them were females. There were 23 follicular ad-enomas, 8 Hürthle cell adenomas, 11 papillary carcinomas, 6 follicular variant of papillary carcinomas and 2 follicular carci-nomas. In all, 19 (38%) nodules were malignant. Hürthle cell neo-plasms were identifiable by pre-operative FNAC in 6 (75%) cases. The mean size of the thyroid nodule was 2.6 ± 1.3 cm and there were 4 micro-carcinomas (tumor size = 7.0—8.5 mm). The patients' age (p = 0.14) and gender (p = 0.43) as well as the median SUVmax (p = 0.10) of benign and malignant nodules were not significantly different (Table 1) however, the malignant nodules were signifi-cantly smaller (p = 0.01) than the benign ones. The median SUV-max value of all thyroid nodules in the study cohort was 3.45 (IQR = 0—7.58) and the SUVmax distribution of the benign and malignant nodules is shown in Fig. 1. All 4 micro-carcinomas in this cohort had SUVmax over 3.25 (range = 3.6—5.9). The SUVmax did not change significantly by partial volume correction (p = 0.55). Median MTV was 4.70 (IQR = 1.71—19.95) and median TLG was 20.75 (IQR = 4.87—101.03) for lesions with SUVmax > 2.5. However, there was no statistically significant difference in MTV (p = 0.116) and TLG (p = 0.187) of benign and malignant follicular neoplasms. All Hürthle cell adenomas showed intense FDG uptake with SUV-max between 3.4 and 33.5 and median SUVmax of 9.3 (IQR = 6.9—19.9).

FDG-PET findings of benign and malignant neoplasms were significantly different (p = 0.003), as summarized in Table 2. Focal increased FDG uptake by thyroid nodule had sensitivity of 89% (95% CI, 65—98%), specificity of 35% (95% CI, 19—54%), PPV of 46% (95% CI, 30—63%), and NPV of 85% (95% CI, 54—97%) for diagnosing follic-ular/Hürthle cell neoplasms. The overall accuracy of FDG-PET/CT was 56%. After excluding Hürthle cell adenomas, the AUROC was

Table 1
Patient demographics and characteristics of benign and malignant follicular/Hürthle cell neoplasms.

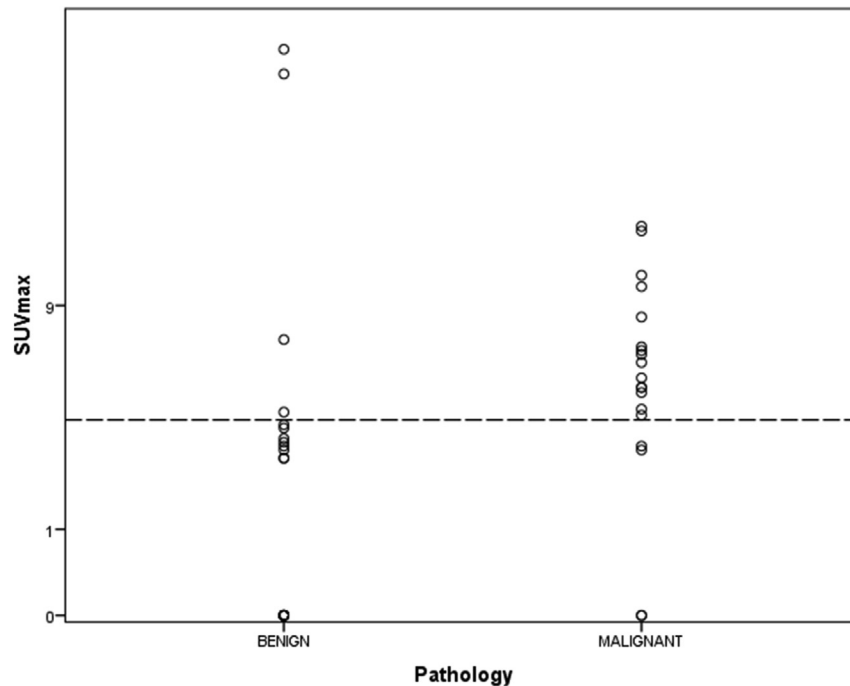|	Benign (N = 31)	Malignant (N = 19)	p-value
Mean age	60.9 ± 12.8	55.3 ± 12.3	0.13
Gender (Male:Female)	9:22	4:15	0.74
Mean size of the nodule	2.9 ± 1.3 cm	2.0 ± 1.1 cm	0.01
Median SUVmax	2.55; IQR = 0—7.60	4.60; IQR = 3.40—7.65	0.10

Fig. 1. Scatter plot of SUVmax in benign and malignant non-Hürthle cell follicular neoplasm. Y-axis shows the SUVmax on logarithmic scale (base 10) with reference (dashed) line indicating SUVmax = 3.25. SUVmax was undetectable in 2 malignant and 11 benign neoplasms (SUVmax = 0).

Table 2
FDG-PET/CT findings in follicular neoplasm.

	Carcinoma positive	Carcinoma negative	Total
FDG-PET positive	15	4[a]	19
FDG-PET negative	4	19	23
Total	19	31	42

[a] Excludes 8 Hürthle cell adenomas.

0.79 (95% CI, 0.63–0.94; p = 0.002) for discriminating benign from malignant nodules with 3.25 as the best SUVmax cut-off for the purpose. FDG-PET/CT had sensitivity of 79% (95% CI, 54–93%), specificity of 83% (95% CI, 60–94%), PPV of 79% (95% CI, 54–93%), and NPV of 83% (95% CI, 60–94%) with an improved overall accuracy was 81% with this SUVmax cut off.

4. Discussion

Although FNAC and ultrasonography are the mainstays of diagnosis of thyroid cancer, the differentiation between benign and malignant follicular neoplasms remains a challenge both on ultrasound and FNAC. Fifteen to 30% of the thyroid lesions that are reported as follicular neoplasm on FNAC are ultimately malignant [4]. The diagnostic role of FDG-PET scan in diagnosing malignant thyroid nodules has been studied earlier also with variable conclusions [11–18]. According to an earlier systematic review, 1 in 3 FDG-PET positive thyroid nodules was reported to be malignant with significantly higher (p < 0.001) mean SUVmax (6.9) as compared to the benign ones (4.8) [19]. We did not find any significant difference between the median SUVmax of benign and malignant thyroid nodules, as has also been reported earlier [14].

The metabolic activity of the thyroid nodule is expressed in terms of SUVmax. Various studies have considered different criteria for PET positivity; ranging from any focal increased uptake in the region of the thyroid nodule above background [11,12,17,18] to different SUVmax cut-offs ranging from 2 to 7 [13,15,20,21].

However, some studies did not find a SUVmax cut-off to be a definite predictor for malignancy [22]. Area under SUVmax curve >175.5 or the heterogeneity factor of FDG uptake >2.751 have also been considered to define FDG-PET positivity [16,23]. In our study group increased focal FDG uptake by thyroid nodules (irrespective of the SUVmax) had a high sensitivity of 89% (95% CI, 65–98%) and specificity of 35% (95% CI, 19–54%) for detecting cancer, similar to those reported in the two meta-analysis: 89.0% (95% CI, 79.0%–95.0%) & 55.0% (95% CI, 48.0%–62.0%) [24], and 95% (95% CI, 86%–99%) & 48% (95% CI, 40%–56%) [2], respectively. Selecting an appropriate cut-off value for any diagnostic test is challenging, as lowering the cut-off improves the sensitivity of the test; but does so at the cost of specificity. However, this will increase the number of false positives and lower its PPV, which in this case may result in unnecessary thyroidectomies. On the other hand, if the cut-off is set too high to make the test more specific, the test can miss some thyroid cancers (lower NPV) but will avoid unnecessary thyroidectomies. Ideally a cut-off with best overall accuracy should be considered. Based on the ROC analysis the SUVmax of 3.25 was identified as the optimal cut-off value to discriminate between benign and malignant nodules, which is slightly higher than the recommended cut-off of 2.05 reported in the recent meta-analysis, with much higher specificity (83% vs 42%) [24].

The meta-analyses, however, did not consider Hürthle cell neoplasm separate from other follicular neoplasm, even though all Hürthle cell neoplasm, in the pooled data, showed high FDG uptake [2,24]. We also found intense FDG uptake in Hürthle cell adenomas (median SUVmax = 9.3). Increased FDG uptake in Hürthle cells and poorly differentiated components have been reported earlier to be independent predictive factors of high (≥5) SUVmax [20]. Increased FDG uptake by benign Hürthle cell neoplasms [25,26] can often be mistaken for malignancy (false positive). We have recently reported the difference in PET characteristics of follicular and Hürthle cell adenomas [1]. The use of SUVmax cut-off of 3.25 and exclusion of Hürthle cell neoplasms improves the overall accuracy of FDG-PET/CT to 81% from 56% obtained by the use of increased

focal FDG uptake and 60% reported in meta-analysis [2]. The FDG-PET/CT with a PPV 79% (95% CI, 54–93%), observed in this study was much higher than 39% (95% CI, 31%–47%) reported in the meta-analysis [2].

To the best of our knowledge, this is the first study which prospectively looked into the impact of intense focal FDG uptake by benign Hürthle cell neoplasms (false positivity), as a cause for lower specificity and PPV of FDG-PET in identifying malignant follicular neoplasms. We found that a cut-off SUVmax of 3.25 provided a higher accuracy with reasonably high sensitivity, specificity, PPV and NPV for predicting malignancy in FDG-PET positive non Hürthle cell follicular neoplasms, as compared to any increased focal FDG uptake by thyroid nodule. The limitation of this study, that we can envision, is the lack of correlation of FDG-PET/CT findings with the molecular markers [27–30], that are recommended for consideration in indeterminate thyroid nodules by the current American Thyroid Association Guidelines [3]. FDG-PET/CT has been reported to offer cost advantage in diagnosing malignant follicular neoplasm as compared to the alternatives of diagnostic thyroidectomy or molecular markers [31]. Use of only a half-dose of FDG could be a potential confounding factor however the same dose was used for all the patients. Further, to compensate for the reduced dose of FDG (185 MBq) to reduce the radiation exposure, the acquisition time was increased by 60%.

To conclude, FDG-PET/CT can help in differentiating benign and malignant non-Hürthle cell thyroid nodules. A cut-off SUVmax of 3.25 enhances the accuracy of FDG-PET/CT in identifying cancers in thyroid nodules. A larger multi-centre study is recommended to confirm these conclusions.

Ethical approval

Research Ethics Board, University of Manitoba (H2010:056).

Source of funding

None.

Author contribution

Kumar A. Pathak: Study design, data collections, data analysis, writing.
Andrew Goertzen: Data analysis, writing.
Richard W Nason: Study design, writing.
Thomas Klonisch: Study design, writing.
William D Leslie: Study design, data collections, data analysis, writing.

Conflicts of interest

None.

Consent

All patients signed informed consent approved by the Research Ethics Board, University of Manitoba.

Guarantor

Kumar A. Pathak.

References

[1] K.A. Pathak, T. Klonisch, R.W. Nason, W.D. Leslie, FDG-PET characteristics of Hurthle cell and follicular adenomas, Ann. Nucl. Med. 30 (7) (2016) 506–509.

[2] D. Vriens, J.H. de Wilt, G.J. van der Wilt, R.T. Netea-Maier, W.J. Oyen, L.F. de Geus-Oei, The role of [18F]-2-fluoro-2-deoxy-d-glucose-positron emission tomography in thyroid nodules with indeterminate fine-needle aspiration biopsy: systematic review and meta-analysis of the literature, Cancer 117 (20) (2011) 4582–4594.

[3] B.R. Haugen, E.K. Alexander, K.C. Bible, G.M. Doherty, S.J. Mandel, Y.E. Nikiforov, et al., 2015 American thyroid association management guidelines for adult patients with thyroid nodules and differentiated thyroid cancer: the American thyroid association guidelines task force on thyroid nodules and differentiated thyroid cancer, Thyroid 26 (1) (2016) 1–133.

[4] E.S. Cibas, S.Z. Ali, The bethesda system for reporting thyroid cytopathology, Thyroid 19 (11) (2009) 1159–1165.

[5] B. Bybel, I.D. Greenberg, J. Paterson, J. Ducharme, W.D. Leslie, Increased F-18 FDG intestinal uptake in diabetic patients on metformin: a matched case-control analysis, Clin. Nucl. Med. 36 (6) (2011) 452–456.

[6] S.M. Srinivas, T. Dhurairaj, S. Basu, G. Bural, S. Surti, A. Alavi, A recovery co-efficient method for partial volume correction of PET images, Ann. Nucl. Med. 23 (4) (2009) 341–348.

[7] S.M. Larson, Y. Erdi, T. Akhurst, M. Mazumdar, H.A. Macapinlac, R.D. Finn, et al., Tumor treatment response based on visual and quantitative changes in global tumor glycolysis using PET-FDG imaging. The visual response score and the change in total lesion glycolysis, Clin. Positron Imaging 2 (3) (1999) 159–171.

[8] B. Bai, J. Bading, P.S. Conti, Tumor quantification in clinical positron emission tomography, Theranostics 3 (10) (2013) 787–801.

[9] M. Vanderhoek, S.B. Perlman, R. Jeraj, Impact of the definition of peak standardized uptake value on quantification of treatment response, J. Nucl. Med. 53 (1) (2012) 4–11.

[10] R. Fluss, D. Faraggi, B. Reiser, Estimation of the Youden Index and its associated cutoff point, Biom. J. 47 (4) (2005) 458–472.

[11] L.F. de Geus-Oei, G.F. Pieters, J.J. Bonenkamp, A.H. Mudde, C.P. Bleeker-Rovers, F.H. Corstens, et al., 18F-FDG PET reduces unnecessary hemithyroidectomies for thyroid nodules with inconclusive cytologic results. Journal of nuclear medicine: official publication, Soc. Nucl. Med. 47 (5) (2006) 770–775.

[12] D. Deandreis, A. Al Ghuzlan, A. Auperin, P. Vielh, B. Caillou, L. Chami, et al., Is (18)F-fluorodeoxyglucose-PET/CT useful for the presurgical characterization of thyroid nodules with indeterminate fine needle aspiration cytology? Thyroid 22 (2) (2012) 165–172.

[13] N.W. Hales, G.A. Krempl, J.E. Medina, Is there a role for fluorodeoxyglucose positron emission tomography/computed tomography in cytologically indeterminate thyroid nodules? Am. J. Otolaryngol. 29 (2) (2008) 113–118.

[14] J.M. Kim, J.S. Ryu, T.Y. Kim, W.B. Kim, G.Y. Kwon, G. Gong, et al., 18F-fluorodeoxyglucose positron emission tomography does not predict malignancy in thyroid nodules cytologically diagnosed as follicular neoplasm, J. Clin. Endocrinol. Metab. 92 (5) (2007) 1630–1634.

[15] E. Kresnik, H.J. Gallowitsch, P. Mikosch, H. Stettner, I. Igerc, I. Gomez, et al., Fluorine-18-fluorodeoxyglucose positron emission tomography in the preoperative assessment of thyroid nodules in an endemic goiter area, Surgery 133 (3) (2003) 294–299.

[16] R.B. Smith, R.A. Robinson, H.T. Hoffman, M.M. Graham, Preoperative FDG-PET imaging to assess the malignant potential of follicular neoplasms of the thyroid, Otolaryngol. Head Neck Surg. Off. J. Am. Acad. Otolaryngol. Head Neck Surg. 138 (1) (2008) 101–106.

[17] A.L. Traugott, F. Dehdashti, K. Trinkaus, M. Cohen, E. Fialkowski, F. Quayle, et al., Exclusion of malignancy in thyroid nodules with indeterminate fine-needle aspiration cytology after negative 18F-fluorodeoxyglucose positron emission tomography: interim analysis, World J. Surg. 34 (6) (2010) 1247–1253.

[18] F.M. Sebastianes, J.J. Cerci, P.H. Zanoni, J. Soares Jr., L.K. Chibana, E.K. Tomimori, et al., Role of 18F-fluorodeoxyglucose positron emission tomography in preoperative assessment of cytologically indeterminate thyroid nodules, J. Clin. Endocrinol. Metab. 92 (11) (2007) 4485–4488.

[19] K.K. Soelberg, S.J. Bonnema, T.H. Brix, L. Hegedus, Risk of malignancy in thyroid incidentalomas detected by 18F-fluorodeoxyglucose positron emission tomography: a systematic review, Thyroid 22 (9) (2012) 918–925.

[20] F. Bertagna, G. Treglia, A. Piccardo, E. Giovannini, G. Bosio, G. Biasiotto, et al., F18-FDG-PET/CT thyroid incidentalomas: a wide retrospective analysis in three Italian centres on the significance of focal uptake and SUV value, Endocrine 43 (3) (2013) 678–685.

[21] N. Munoz Perez, J.M. Villar del Moral, M.A. Muros Fuentes, M. Lopez de la Torre, J.I. Arcelus Martinez, P. Becerra Massare, et al., Could 18F-FDG-PET/CT avoid unnecessary thyroidectomies in patients with cytological diagnosis of follicular neoplasm? Langenbecks Arch. Surg. 398 (5) (2013) 709–716.

[22] S.J. Kim, B.H. Kim, Y.K. Jeon, S.S. Kim, I.J. Kim, Limited diagnostic and predictive values of dual-time-point 18F FDG PET/CT for differentiation of incidentally detected thyroid nodules, Ann. Nucl. Med. 25 (5) (2011) 347–353.

[23] S.J. Kim, S. Chang, Predictive value of intratumoral heterogeneity of F-18 FDG uptake for characterization of thyroid nodules according to Bethesda categories of fine needle aspiration biopsy results, Endocrine 50 (3) (2015) 681–688.

[24] N. Wang, H. Zhai, Y. Lu, Is fluorine-18 fluorodeoxyglucose positron emission tomography useful for the thyroid nodules with indeterminate fine needle aspiration biopsy? A meta-analysis of the literature, J. Otolaryngol. Head Neck Surg. 42 (2013) 38.

[25] S. Zandieh, W. Pokieser, P. Knoll, C. Sonneck-Koenne, M. Kudlacek, S. Mirzaei, Oncocytic adenomas of thyroid-mimicking benign or metastatic disease on

18F-FDG-PET scan, Acta Radiol. 56 (6) (2015) 709–713.

[26] W. Wiesner, H. Engel, G.K. von Schulthess, G.P. Krestin, I. Bicik, FDG PET-negative liver metastases of a malignant melanoma and FDG PET-positive hurthle cell tumor of the thyroid, Eur. Radiol. 9 (5) (1999) 975–978.

[27] Y.E. Nikiforov, D.L. Steward, T.M. Robinson-Smith, B.R. Haugen, J.P. Klopper, Z. Zhu, et al., Molecular testing for mutations in improving the fine-needle aspiration diagnosis of thyroid nodules, J. Clin. Endocrinol. Metab. 94 (6) (2009) 2092–2098.

[28] M.N. Nikiforova, A.I. Wald, S. Roy, M.B. Durso, Y.E. Nikiforov, Targeted next-generation sequencing panel (ThyroSeq) for detection of mutations in thyroid cancer, J. Clin. Endocrinol. Metab. 98 (11) (2013) E1852–E1860.

[29] A. Bartolazzi, F. Orlandi, E. Saggiorato, M. Volante, F. Arecco, R. Rossetto, et al., Galectin-3-expression analysis in the surgical selection of follicular thyroid nodules with indeterminate fine-needle aspiration cytology: a prospective multicentre study, Lancet Oncol. 9 (6) (2008) 543–549.

[30] E.K. Alexander, G.C. Kennedy, Z.W. Baloch, E.S. Cibas, D. Chudova, J. Diggans, et al., Preoperative diagnosis of benign thyroid nodules with indeterminate cytology, N. Engl. J. Med. 367 (8) (2012) 705–715.

[31] D. Vriens, E.M. Adang, R.T. Netea-Maier, J.W. Smit, J.H. de Wilt, W.J. Oyen, et al., Cost-effectiveness of FDG-PET/CT for cytologically indeterminate thyroid nodules: a decision analytic approach, J. Clin. Endocrinol. Metab. 99 (9) (2014) 3263–3274.

Comparing a thyroid prognostic nomogram to the existing staging systems for prediction risk of death from thyroid cancers

K.A. Pathak [a,b,*], P. Lambert [a], R.W. Nason [a,b], T. Klonisch [b]

[a] CancerCare Manitoba, Winnipeg, Manitoba, Canada
[b] Canada University of Manitoba, Winnipeg, Manitoba, Canada

Abstract

Objective: Thyroid prognostic nomogram can be applied across different histological types for predicting the individualized risk of death from thyroid cancer. The objective of this study was to compare the strength of our recently published thyroid prognostic nomogram with 12 existing staging systems to predict the risk of death from thyroid cancer.
Method: This study included 1900 thyroid cancer patients, from a population based cohort of 2296 patients, on whom adequate staging information was available. Competing risk sub-hazard models were used to compare 12 pre-existing prognostic models with the nomogram model. Their relative strengths for prediction of patients' individualized risks of death from thyroid cancer were compared using Akaike information criterion (AIC), delta AIC, and concordance index. R version 3.2.2 was used to analyze the data.
Results: Our cohort of 450 males and 1450 females included 1796 (93.4%) differentiated thyroid cancers. Amongst the compared models, thyroid prognostic nomogram model appeared to be better than other models for predicting the risk of death from all non-anaplastic thyroid cancer (concordance index = 94.4), differentiated thyroid cancer (concordance index = 94.1) and papillary thyroid cancer (concordance index = 94.7). The difference from next best staging systems was most pronounced in non-anaplastic thyroid cancer (delta AIC = 114.8), followed by differentiated thyroid cancer (delta AIC = 35.6) and papillary thyroid cancer (delta AIC = 8.4).
Conclusions: Thyroid prognostic nomogram model was found to be better than the other models compared for predicting risk of death from thyroid cancer.
© 2016 Elsevier Ltd and British Association of Surgical Oncology/European Society of Surgical Oncology. All rights reserved.

Keywords: Prognosis; Model; Survival; Thyroid neoplasm; TNM

Introduction

Thyroid cancer is the fastest growing cancer in Canadian Cancer Statistics 2015 with an estimated age standardized incidence rate (ASIR) of 14.9/10,000 in 2015. ASIR has been increasing at the rate of 6.3% per year in males since 2001 and by 4.4% per year in females (2005−2010).[1] It is the most common cancer in 15−29 year age group (16% of all cancers) and second most common cancer in 30−49 year age group (10% of all cancers).[1] Various staging/

prognostic scoring systems have been used to predict oncological outcome of thyroid cancer.[2−19] Most of these are applicable only to the differentiated thyroid cancers[6−19] and provide stratified group risks rather than individualized risks. A nomogram, on the other hand, can be applied across different histological types to generate numerical probability of individual's clinical outcome, based on his/her risk assessment. We recently published a thyroid prognostic nomogram with excellent discrimination as demonstrated by high concordance index (0.92) and a very good calibration.[2]

This study was aimed to compare the strength of a thyroid prognostic nomogram with 12 commonly used staging/risk stratification systems, to predict the risk of death from thyroid cancer in a population based thyroid cancer cohort.

* Corresponding author. CancerCare Manitoba, 675 McDermot Avenue, Winnipeg R3E 0V9, Canada. Tel.: +1 204 787 8040; fax: +1 204 7872768.
   E-mail address: apathak@cancercare.mb.ca (K.A. Pathak).

Patients and methods

Study cohort

The Manitoba thyroid cancer cohort consists of all 2306 consecutive thyroid cancers diagnosed in 2296 patients, registered in Manitoba Cancer Registry, from January 1, 1970 to December 31, 2010. Sixty patients who were initially diagnosed by autopsy or death certificate, 76 patients with anaplastic thyroid cancer with extremely high case fatality rate, and 10 familial medullary thyroid cancers (MTC) where the oncological outcome is largely determined by their specific gene mutations, were excluded from this study. We also excluded 123 patients who did not have treatment with radical intent and 38 patients who were followed up in Manitoba health care system for less than a year. We reviewed individual electronic and paper records of the remaining 1989 patients and selected 1900 patients for this study on whom we had adequate information on patient demographics, tumor characteristics and completeness of tumor resection required for staging by 12 commonly used staging/risk stratification systems.[20] Ethics approval for this study was obtained from the Research Ethics Board at the University of Manitoba and the treatment details of these patients were obtained from CancerCare Manitoba, the tertiary cancer care center for the province of Manitoba with a catchment population of about 1.2 million. Patient demographics, extent of disease at initial presentation, the treatment modalities employed, pathology details, cancer recurrences during the follow-up, and the final oncological status as of July 1, 2015 were recorded. All patients who migrated out of province during the study period (considered lost to follow up), were censored at that point in time.

Statistical methods

The patient characteristics, the extent of disease at presentation and the tumor histology were recorded along with the treatment modalities, the patterns of failure and the final oncological outcome. The data were managed using SPSS for Windows version 23·0 (SPSS Inc., Chicago, IL). After checking for normality assumption, the mean and standard deviation were used to express normally distributed data (such as the age) and the median with inter-quartile range (IQR) was used for non-normally distributed data (such as the follow-up). A p-value <0.05 (two-sided) was considered to indicate statistical significance and 95% confidence intervals were used to express reliability in the estimates.

The effects of age at diagnosis, patient's gender, T, N and M categories, the histological type, and the presence of post treatment gross residual disease on the risk of death by disease were evaluated by competing risk analysis[21] to assess the competing influence of other causes of mortality,

such as death due to a second primary tumor or non-cancer deaths. Cumulative incidence function (CIF) was used to describe the probability of death using proportional hazards regression model to directly model the sub-distribution of a competing risk.[22] R version 3.2.2 was used to analyze the data, using the packages of Hmisc to construct restricted cubic splines, and the packages of riskRegression and prodlim to run competing risk models. Restricted cubic splines were used to account for the non-linear relationship between age and the outcomes, using the default 3 knots. The discrimination capability of the models was evaluated by concordance index at 10 years. Concordance indices (c-index) were produced using only one of the 20 complete datasets after multiple imputations.

Akaike information criterion (AIC) was used to compare different prognostic models that are used for stage grouping/risk stratification of thyroid cancer. AIC is defined as $AIC = -2LL + 2m$, where LL is the maximized log-likelihood and m is the number of parameters in the model (degrees of freedom).[23,24] Delta AIC was calculated to compare the models. It is defined as $Delta\ AIC(\Delta_i) = AIC_i - minAIC$, where AIC_i is the AIC value for model i and min AIC is the AIC value of the best model identified by the lowest AIC.[25]

Results

Our study group of 1900 patients (450 males and 1450 females) had a follow up of 22,287 patient-years. The mean age of the patients was 46.99 ± 16.96 years and the papillary thyroid cancer (PTC) was the most commonly observed histological type in 1533 (80.68%) patients, followed by follicular carcinoma (FTC) in 193 (10.16%) patients, Hürthle cell in 70 (3.68%), poorly differentiated carcinoma in 39 (2.05%), and medullary carcinoma in 65 (3.42%) patients. TNM classification as well as stage/class/risk group distribution of patients with non-anaplastic thyroid cancer, differentiated thyroid cancer of follicular cell origin and papillary thyroid cancer is summarized in Table 1. Total thyroidectomy was performed in 1047 patients (55.10%) and 982 patients (54.68%) with differentiated thyroid cancers; 717 (73.01%) of these received adjuvant radioactive iodine. Sixty (3.16%) patients had post treatment residual disease. All patients with unresectable macroscopic residual disease in the neck at the time of surgery following total thyroidectomy or those at a high risk of disease recurrence; such as those with T3/T4 tumors, regional and distant metastasis received radioactive iodine for differentiated thyroid cancer (DTC). Use of external beam radiation therapy was limited to unresectable macroscopic residual disease.

During the median follow up of 11.59 years (inter-quartile range = 7.13–19.24 years), 181 (9.53%) patients had clinical/radiological evidence of recurrent disease after at least 6 months following an initial successful treatment.

Table 1
Stage distribution of thyroid cancer for different staging/risk stratification systems.

Staging	Group	Papillary (N = 1533)	Differentiated (N = 1796)	Non-anaplastic (N = 1900)
T category	T1	756 (49.32%)	821 (45.71%)	855 (45.00%)
	T2	398 (25.96%)	505 (28.12%)	532 (28.00%)
	T3	310 (20.22%)	388 (21.60%)	414 (21.79%)
	T4	69 (4.50%)	82 (4.57%)	99 (5.21%)
N category	N0	1127 (73.52%)	1371 (76.34%)	1431 (75.32%)
	N1	406 (26.48%)	425 (23.66%)	469 (24.68%)
M category	M0	1509 (98.43%)	1764 (98.22%)	1858 (97.79%)
	M1	24 (1.57%)	32 (1.78%)	42 (2.21%)
Tumor, Node, Metastases (AJCC-TNM) Classification 7th Edition	Stage I	1086 (70.84%)	1213 (67.54%)	1213 (65.21%)
	Stage II	148 (9.65%)	210 (11.69%)	210 (12.00%)
	Stage III	181 (11.81%)	230 (12.81%)	230 (12.89%)
	Stage IV	118 (7.70%)	143 (7.96%)	143 (9.89%)
National Thyroid Cancer Treatment Cooperative Study (NTCTCS)	Stage I	781 (50.95%)	801 (44.60%)	801 (42.68%)
	Stage II	443 (28.90%)	510 (28.40%)	510 (27.47%)
	Stage III	292 (19.05%)	460 (25.61%)	460 (26.95%)
	Stage IV	17 (1.11%)	25 (1.39%)	25 (2.89%)
European Organization for Research and Treatment of Cancer (EORTC)	Group 1	784 (51.14%)	887 (49.39%)	887 (48.21%)
	Group 2	410 (26.74%)	477 (26.56%)	477 (26.42%)
	Group 3	261 (17.03%)	321 (17.87%)	349 (18.37%)
	Group 4	76 (4.96%)	106 (5.90%)	127 (6.68%)
	Group 5	2 (0.13%)	5 (0.28%)	6 (0.32%)
Mayo Clinic (Age, Grade, Extent, Size or AGES)	Group 1	571 (37.25%)	648 (36.08%)	Not Applicable
	Group 2	379 (24.72%)	411 (22.88%)	
	Group 3	342 (22.31%)	416 (23.16%)	
	Group 4	241 (15.72%)	321 (17.87%)	
Virgen de la Arrixaca University at Murcia (Murcia)	Low risk	1173 (76.52%)	1348 (75.06%)	Not Applicable
	Medium risk	325 (21.20%)	403 (22.44%)	
	High risk	35 (2.28%)	45 (2.51%)	
Mayo Clinic (Metastases, Age, Completeness of Resection, Invasion, Size or MACIS)	Group 1	1261 (82.26%)	1430 (79.62%)	Not Applicable
	Group 2	152 (9.92%)	194 (10.80%)	
	Group 3	64 (4.17%)	90 (5.01%)	
	Group 4	56 (3.65%)	82 (4.57%)	
University of Chicago (Clinical Class)	Class 1	923 (60.21%)	1083 (60.30%)	Not Applicable
	Class 2	225 (14.68%)	231 (12.86%)	
	Class 3	361 (23.55%)	450 (25.06%)	
	Class 4	24 (1.57%)	32 (1.78%)	
Ohio State University (OSU)	Stage 1	433 (28.25%)	456 (25.39%)	Not Applicable
	Stage 2	715 (46.64%)	859 (47.83%)	
	Stage 3	361 (23.55%)	449 (25.00%)	
	Stage 4	24 (1.57%)	32 (1.78%)	
University of Müntser (Müntser)	Low risk	1449 (94.52%)	1694 (94.32%)	Not Applicable
	High risk	84 (5.48%)	102 (5.68%)	
University of Alabama and M.D. Anderson (UAB & MDA)	Low risk	901 (58.77%)	1024 (57.02%)	Not Applicable
	Intermediate risk	608 (39.66%)	740 (41.20%)	
	High risk	24 (1.57%)	32 (1.78%)	
Lahey Clinic (Age, Metastases, Extent, Size or AMES)	Low risk	1341 (87.48%)	1547 (86.14%)	Not Applicable
	High risk	192 (12.52%)	249 (13.86%)	
Memorial Sloan Kettering (Grade, Age, Metastases, Extent, Size or GAMES)	Low risk	633 (41.29%)	633 (35.24%)	Not Applicable
	Intermediate risk	773 (50.42%)	871 (48.50%)	
	High risk	127 (8.28%)	292 (16.26%)	
Disease free survival at 20 years		86.0%	86.0%	84.3%
Disease specific survival at 20 years		94.9%	93.4%	92.7%

During the course of follow up 106 (5.58%) patients died of their disease. AIC, Delta AIC, and concordance indices were calculated for different staging systems in predicting the risk of death from papillary thyroid cancers (Table 2), differentiated thyroid cancers of follicular cell origin (Table 3), and all non-anaplastic thyroid cancers (Table 4) by using competing risk analysis. The thyroid prognostic nomogram model had the lowest AICs and highest concordance indices for risk of death from non-anaplastic thyroid cancers (AIC = 1161.82, c-index = 94.4), differentiated thyroid cancers of follicular cell origin (AIC = 822.43, c-index = 94.1) and papillary

Table 2
AIC, Delta AIC, Akaike weight, and Evidence Ratio for risk of death from papillary thyroid carcinoma by various staging systems.

Staging system	AIC[a]	Δ_i	Concordance index (%)
Nomogram	471.6354	0	94.7
MACIS	480.053	8.417	90.4
AMES	506.3923	34.757	90.8
Clinical Class	511.4453	39.810	91.0
OSU	511.4632	39.828	90.5
NTCTCS	511.7387	40.103	92.0
Müntser	517.1069	45.472	84.9
EORTC	523.1761	51.541	79.7
UAB & MDA	528.926	57.291	84.5
AGES	529.3788	57.743	90.6
TNM Classification	530.1004	58.465	89.2
GAMES	547.2368	75.601	88.2
Murcia	559.8731	88.238	85.0

[a] $AIC = -2LL + 2m$.

Table 3
AIC, Delta AIC, Akaike weight, and Evidence Ratio for risk of death from differentiated thyroid carcinoma by various staging systems.

Staging system	AIC[a]	Δ_i	Concordance index (%)
Nomogram	822.4342	0	94.1
MACIS	858.0169	35.5827	88.9
AMES	899.4295	76.9953	84.2
Clinical Class	890.9118	68.4776	86.6
OSU	892.4191	69.9849	87.6
NTCTCS	885.3948	62.9606	88.8
Müntser	913.4634	91.0292	78.2
EORTC	920.6111	98.1769	83.0
UAB & MDA	932.2623	109.8281	78.3
AGES	921.1526	98.7184	86.4
TNM Classification	905.1132	82.679	86.5
GAMES	949.8399	127.4057	85.6
Murcia	979.1918	156.7576	77.6

[a] $AIC = -2LL + 2m$.

Table 4
AIC, Delta AIC, Akaike weight, and Evidence Ratio for risk of death from non-anaplastic thyroid carcinoma by various staging system.

Staging system	AIC[a]	Δ_i	Concordance index (%)
Nomogram	1161.819	0	94.4
TNM Classification	1276.576	114.757	87.3
NTCTCS	1282.011	120.192	88.3
EORTC	1320.669	158.85	84.2

[a] $AIC = -2LL + 2m$.

Figure 1. AIC values of various staging systems for risk of death from papillary thyroid carcinoma.

Figure 2. AIC values of various staging systems for risk of death from differentiated thyroid carcinoma.
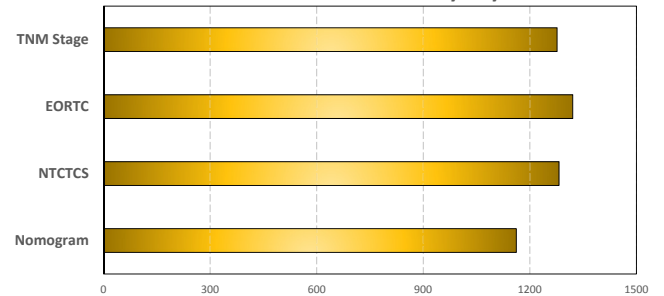
Figure 3. AIC values of various staging systems for risk of death from non-anaplastic thyroid cancers.

thyroid cancers (AIC = 451.64, c-index = 94.7) suggesting it to be the best among the compared models (Figs. 1−3). In terms of AIC, TNM-AJCC Classification was the next best model for predicting risk of death from all non-anaplastic thyroid cancers and MACIS was the next best model for differentiated thyroid cancers of follicular cell origin and more specifically for papillary thyroid cancers.

Discussion

Thyroid cancer is the most common malignant endocrine tumor and in 2015 it is expected to account for 5% of new cancer cases in Canadian females and 1.4% in Canadian males.[1] The use of numerous prognostic scoring systems for predicting oncological outcome of thyroid cancer suggests that none of them is universally acceptable. Most of these staging systems are valid only for DTC[6−19] and more specifically for papillary thyroid cancer.[6−9,16−19]

Prognostic scoring systems[3,6−10] often require lengthy calculations of prognostic scores that make individualized risk prediction quite arduous. American Thyroid Association proposed a staging system[28] on the basis of regional and distant metastases, completeness of resection, locoregional tumor invasion at initial surgery, aggressive histology, ^{131}I uptake outside the thyroid bed on the whole body RAI scan. We recently published thyroid prognostic nomogram by combining multiple independent variables to predict the risk of death from thyroid cancer of individual patients with thyroid cancer by using the prognostic weights (points) assigned to each variable.[2] It had a very good calibration with calibration curve close to the diagonal and excellent discrimination with high c-index (0.92); where 0.5 is the worst (complete random prediction) and 1.0 is the best score (perfect prediction).[2] We used AIC and c-index to compare our model with 12 other highest ranking models from an earlier comparison.[20] Five other models,[9,10,17−19] that required additional unavailable information for staging, were excluded from this comparison.

Our prognostic thyroid nomogram model incorporates age, gender, histology and post treatment residual disease in addition to T, N, M categories which were found to be independent prognostic factors determining oncological outcome of thyroid cancer.[2] The advantages of this model include its applicability to all non-anaplastic thyroid cancers and incorporation of TNM categories in addition to other prognostic factors, which makes it comprehensive but still simple to use. For example, a 70-year old (68 points) male (12 points) patient, who underwent complete resection of a T3 (15 points) N0 (0 point) M0 (0 point) papillary thyroid carcinoma (0 point) without any evidence of residual disease (0 point), gets a sum total of 95 points on the nomogram and has a 7% predicted risk of death from thyroid cancer within 10 years after treatment. If the same patient had medullary thyroid carcinoma (25 additional points) instead of papillary thyroid carcinoma, he would have got a total of 120 points and a 23% predicted risk of death over the same time period. Further, if the same patient had T3 papillary thyroid cancer with pulmonary metastasis (38 additional points), he would have got a total of 133 points and a 48% predicted risk of death from thyroid cancer within 10 years following treatment.

AIC was developed in the early 1970s to provide an objective tool for choosing between different competing models and lower AIC values suggest relative superiority.[23−27] The model for thyroid prognostic nomogram had the lowest AICs for non-anaplastic thyroid cancers, differentiated thyroid cancers of follicular cell origin and papillary thyroid cancers for predicting risk of death from thyroid cancer. The AIC value on its own can be misinterpreted, as there is no value of statistical significance and it is only as good as the data that is used to generate it.[26,27] Delta AIC (Δ_i) is used to quantify the support for alternative models as compared to the best model. In general, a value of $\Delta_i < 2$ suggests substantial evidence in favor of the alternative model, values between 3 and 7 indicate the alternative model has considerably less support, whereas $\Delta_i > 10$ indicates that the alternative model is very unlikely.[25] Δ_i for the next best alternative model (MACIS) for PTC was 8.42, DTC (MACIS) was 35.58, and for non-anaplastic thyroid cancers (AJCC-TNM) was 114.76, thereby suggesting a low to extremely low likelihood of any of these alternative models being more valid as compared to the nomogram. This difference was most pronounced in non-anaplastic thyroid cancer followed by differentiated thyroid cancer because of higher number of deaths in these patients as compared to papillary thyroid cancer.

Although the nomogram model performed better than the alternative staging systems, some of the staging systems (such as MACIS for papillary and differentiated thyroid cancer) also demonstrated good discrimination, even though they project group risk rather than individual risk. PVE (proportion of variation explained) has previously been used to compare staging classifications.[20,29,30] As PVE favor more complex models by not accounting for the additional degrees of freedom, PVE would be more biased towards TNM classification and the nomogram model than the simpler staging classifications. AIC would penalize these more complex models by accounting for additional degrees of freedom and make them less favorable.

In absence of a randomized control trial, a large population based cohort with low attrition rates such as ours (only 2% loss to follow-up over 40 years), is probably the best possible model to study the oncological outcomes of thyroid cancer such as the relapses and the deaths. The Manitoba thyroid cancer cohort is a mix of different ethnicity because of the immigrations over the years. Our source of information was quite reliable as the individual medical records were reviewed for their accuracy and completeness. To ensure consistency, all cancers were uniformly restaged using the 2009 UICC/AJCC classification. As well, treatment recommendations have changed over this time frame with total thyroidectomy and adjuvant RAI becoming more frequent over time. However, these were not shown to significantly influence DSS in our previous study as it was independent of change in the tumor size or treatment modalities.[31] The limitation of AJCC-TNM classification in predicting the oncological outcome of well differentiated thyroid cancer has been reported earlier.[32−34] As the competing risk model for the nomogram was developed from the Manitoba thyroid cancer cohort, the source of data for comparison of different staging system in this study, there is a possibility of selection bias.

To conclude, the thyroid prognostic nomogram model was better than the other compared models in predicting risk of death from thyroid cancer in a population based thyroid cancer cohort. External validation of these results using an independent dataset would be ideal.

Role of funding source

Conflict of interest statement

The authors have nothing to disclose.

Acknowledgments

References

1. Canadian Cancer Society's Steering Committee on Cancer Statistics. *Canadian Cancer Statistics*. Toronto, ON: Canadian Cancer Society; 2015;, p. 16–37.
2. Pathak KA, Mazurat A, Lambert P, Klonisch T, Nason RW. Prognostic nomograms to predict oncological outcome of thyroid cancers. *J Clin Endocrinol Metab* 2013;**98**:4768–75.
3. Byar DP, Green SB, Dor P, et al. A prognostic index for thyroid carcinoma: a study of the EORTC Thyroid Cancer Cooperative Group. *Eur J Cancer* 1979;**15**:1033–41.
4. Sherman SI, Brierley JD, Sperling M, et al. Prospective multicenter study of thyroid carcinoma treatment: initial analysis of staging and outcome. *Cancer* 1998;**83**:1012–21.
5. Sobin L, Gospodarowicz M, Wittekind C. *TNM classification of malignant tumours*. 7th ed. New York: Wiley; 2009;, p. 58–62.
6. Hay ID, Grant CS, Taylor WF, McConahey WM. Ipsilateral lobectomy versus bilateral lobar resection in papillary thyroid carcinoma: a retrospective analysis of surgical outcome using a novel prognostic scoring system. *Surgery* 1987;**102**:1088–95.
7. Hay ID, Bergstralh EJ, Goellner JR, Ebersold JR, Grant CS. Predicting outcome in papillary thyroid carcinoma: development of a reliable prognostic scoring system in a cohort of 1779 patients surgically treated at one institution during 1940 through 1989. *Surgery* 1993;**114**:1050–8.
8. Sebastian SO, Gonzalez JM, Paricio PP, et al. Papillary thyroid carcinoma: prognostic index for survival including the histological variety. *Arch Surg* 2000;**135**:272–7.
9. Akslen LA. Prognostic importance of histologic grading in papillary thyroid carcinoma. *Cancer* 1993;**72**:2680–5.
10. Yildirim E. A model for predicting outcomes in patients with differentiated thyroid cancer and model performance in comparison with other classification systems. *J Am Coll Surg* 2005;**200**:378–92.
11. Mazzaferri EL, Jhiang SM. Long-term impact of initial surgical and medical therapy on papillary and follicular thyroid cancer. *Am J Med* 1994;**97**:418–28.
12. Shaha AR, Loree TR, Shah JP. Intermediate-risk group for differentiated carcinoma of the thyroid. *Surgery* 1994;**116**:1036–41.
13. Lerch H, Schober O, Kuwert T, Saur HB. Survival of differentiated thyroid carcinoma studied in 500 patients. *J Clin Oncol* 1997;**15**: 2067–75.
14. Cady B, Rossi R. An expanded view of risk-group definition in differentiated thyroid carcinoma. *Surgery* 1988;**104**:947–53.
15. Beenken S, Roye D, Weiss H, et al. Extent of surgery for intermediate-risk well-differentiated thyroid cancer. *Am J Surg* 2000;**179**:51–6.
16. DeGroot LJ, Kaplan EL, McCormick M, Straus FH. Natural history, treatment, and course of papillary thyroid carcinoma. *J Clin Endocrinol Metab* 1990;**71**:414–24.
17. Noguchi S, Murakami N, Kawamoto H. Classification of papillary cancer of the thyroid based on prognosis. *World J Surg* 1994;**18**: 552–8.
18. Sugitani I, Kasai N, Fujimoto Y, Yanagisawa A. A novel classification system for patients with PTC: addition of the new variables of large (3cm or greater) nodal metastases and reclassification during the follow-up period. *Surgery* 2004;**135**:139–48.
19. Pasieka JL, Zedenius J, Auer G, et al. Addition of nuclear DNA content to the AMES risk-group classification for papillary thyroid carcinoma. *Surgery* 1992;**112**:1154–60.
20. Lang BH, Lo CY, Chan WF, Lam KY, Wan KY. Staging systems for papillary thyroid carcinoma: a review and comparison. *Ann Surg* 2007;**45**:366–78.
21. Gray RJ. A class of k-sample tests for comparing the cumulative incidence of a competing risk. *Ann Stat* 1988;**16**:1141–54.
22. Fine JP, Gray RJ. A proportional hazards model for the subdistribution of a competing risk. *J Am Stat Assoc* 1999;**94**:496–509.
23. Everitt BS. *The Cambridge Dictionary of statistics*. 3rd ed. Cambridge University Press; 2006;, p. 10.
24. Akaike H. Information theory and an extension of the maximum likelihood principle. In: *Selected papers of Hirotugu Akaike*. Springer; 1998;, p. 199–213.
25. Mazerolle MJ. Appendix 1: making sense out of Akaike's information criterion (AIC): its use and interpretation in model selection and inference from ecological data. *Mouvements et Reproduction des Amphibiens en Tourbières Perturbées* 2004;174–90.
26. Wagenmakers E, Farrell S. AIC model selection using akaike weights. *Psychon Bull Rev* 2004;**11**:192–6.
27. Yang L, Shen W, Sakamoto N. Population-based study evaluating and predicting the probability of death resulting from thyroid cancer and other causes among patients with thyroid cancer. *J Clin Oncol* 2013; **31**:468–74.
28. American Thyroid Association (ATA) Guidelines Taskforce on Thyroid Nodules and Differentiated Thyroid Cancer, Cooper DS, Doherty GM, et al. Revised American Thyroid Association management guidelines for patients with thyroid nodules and differentiated thyroid cancer. *Thyroid* 2009;**19**:1167–214.
29. Brierley JD, Panzarella T, Tsang RW, et al. A comparison of different staging systems. Predictability of patient outcome: thyroid carcinoma as an example. *Cancer* 1997;**79**:2414–23.
30. Passler C, Prager G, Scheuba C, et al. Application of staging systems for differentiated thyroid carcinoma in an endemic goiter region with iodine substitution. *Ann Surg* 2003;**207**:227–34.
31. Pathak KA, Leslie WD, Klonisch TC, Nason RW. The changing face of thyroid cancer in a population based cohort. *Cancer Med* 2013;**2**: 537–44.
32. Mazurat A, Torroni A, Hendrickson-Rebizant J, Benning H, Nason RW, Pathak KA. The age factor in survival of a population cohort of well-differentiated thyroid cancer. *Endocr Connect* 2013 Sep 23;**2**(3):154–60.
33. Hendrickson-Rebizant J, Sigvaldason H, Nason RW, Pathak KA. Identifying the most appropriate age threshold for TNM stage grouping of well-differentiated thyroid cancer. *Eur J Surg Oncol* 2015 Aug;**41**(8): 1028–32.
34. Pathak KA, Klonisch T, Nason RW. Stage II differentiated thyroid cancer: a mixed bag. *J Surg Oncol* 2016 Jan;**113**(1):94–7.

CrossMark

FDG-PET characteristics of Hürthle cell and follicular adenomas

Kumar Alok Pathak[1,2] · Thomas Klonisch[2] · Richard W. Nason[1] · William D. Leslie[3]

Abstract

Objective Follicular (FN) and Hürthle cell neoplasms (HCN) are considered indeterminate on thyroid fine needle aspiration cytology and are preoperative diagnostic challenges. The role of $[^{18}F]$-2-fluoro-2-deoxy-D-glucose (FDG) in characterizing indeterminate thyroid nodules remains equivocal, because of the increased FDG uptake by some benign thyroid nodules. The objective of this study was to compare the FDG positron emission tomography/computerized tomography (PET/CT) characteristics of follicular (FA) and Hürthle cell adenomas (HCA).

Methods Twenty-nine patients with 31 thyroid nodules underwent FDG-PET/CT scans of the neck and superior mediastinum for indeterminate FN/HCN, and were later found to have benign adenomas on final histopathology. All scans were reported by a single observer, who was blinded to the surgical and pathology findings. Receiver operating characteristic (ROC) curve analysis of maximum standardized uptake value (SUV_{max}) and the area under the curve (AUROC) were used to assess discrimination between FA and HCA. Youden index was used to identify the optimal cut-off SUV_{max}. Sensitivity, specificity, predictive values and overall accuracy were used as measures of performance.

Results The mean age of our study cohort was 60.7 ± 12.6 years and 77 % of the patients were females. Age of the patients ($p = 0.48$), their gender ($p = 0.52$), and the size of thyroid nodules ($p = 0.79$) were similar for FA and HCA. Increased focal FDG uptake was observed in 100 % of HCA and 52 % of FA ($p = 0.02$). SUV_{max} of HCA was significantly higher ($p < 0.001$) than that of FA. SUV_{max} of 5 was the best cut-off for discrimination between HCA and FA, with AUROC of 0.90 (95 % CI, 0.79–1.00; $p = 0.001$). With this cut-off, FDG-PET/CT had sensitivity of identifying HCA of 88 % (95 % CI 47–99 %), specificity of 87 % (95 % CI 65–97 %), positive predictive value of 70 % (95 % CI 35–92 %), and negative predictive value of 95 % (95 % CI 74–99 %). The overall accuracy was 87 %.

Conclusions HCA shows significantly higher focal FDG uptake as compared to FA and should always be considered in the differential diagnosis of FDG-PET positive thyroid nodules.

Keywords Thyroid · PET/CT · Imaging · Nuclear · Follicular · Neoplasm

✉ Kumar Alok Pathak
  apathak@cancercare.mb.ca

1 Division of Surgical Oncology, Cancer Care Manitoba, University of Manitoba, ON2048, 675 McDermot Avenue, Winnipeg R3E 0V9, Canada

2 Department of Human Anatomy and Cell Science, University of Manitoba, Winnipeg, Canada

3 Section of Nuclear Medicine, Cancer Care Manitoba, University of Manitoba, Winnipeg, Canada

Introduction

According to the Bethesda classification thyroid nodule cytology of follicular (FN) and Hürthle cell neoplasms (HCN) represent indeterminate cytology [1]. The risk of malignancy ranges from 15 to 30 % with a higher risk associated with Hürthle cell variants [2]. The differentiation between the FN and HCN is often possible only after diagnostic thyroidectomy by identification of predominantly Hürthle cells population on histopathological examination. Hürthle cell adenomas (HCA) are thought to

be more aggressive than follicular adenomas (FA) and may require an expert thyroid pathologist for differentiating it from Hürthle cells carcinoma [5–7]. Oncocytic adenomas can masquerade as metastatic cancers due to increase FDG uptake on PET/CT [3].

The objective of this study was to compare the FDG uptake of HCA and FA of the thyroid. This distinction is important because the intense [^{18}F]-2-fluoro-2-deoxy-D-glucose (FDG) uptake by benign HCA [3, 4] may result in high false positive rates and reduced accuracy of FDG positron emission tomography/computerized tomography (PET/CT) in distinguishing benign from malignant thyroid nodules.

Materials and methods

This prospective study, approved by the University Research Ethics Board, included 31 benign thyroid nodules, >10 mm in size, in 29 consenting patients, who were seen at a comprehensive cancer care centre between July 2013 and December 2015, out of a cohort of 50 indeterminate thyroid nodules, that were assessed by FDG-PET. These nodules were considered indeterminate preoperatively on prior ultrasonography as well as ultrasound guided fine needle aspiration cytology (FNAC), and a FDG-PET/CT scan was performed pre-operatively. All patients were asked to fast for 4–6 h prior to administration of F-18 FDG injection. To minimize the examination time and substantially reduce the radiation exposure, only a half-dose of FDG (185 MBq) was administered and patients were scanned in a single bed position (neck and superior mediastinum) in 3D-mode on a Biograph-16 (Siemens; Malvern, PA, USA) PET/CT scanner. Helical CT was acquired with 3–5 mm section thickness, as previously described [8]. All scans were reported by a single observer who was blinded to the surgical and pathologic findings. Histopathology was considered as the gold standard for diagnosis and all nodules were confirmed to be benign on final histopathology.

The demographic and FDG-PET/CT characteristics of FA and HCA were recorded. The data were managed and analyzed using SPSS for Windows version 23.0 (SPSS Inc., Chicago, IL, USA). After checking for normality assumption, the mean and standard deviation were used to express normally distributed data (such as the size of nodule), which were compared by analysis of variance (ANOVA). The median with interquartile range (IQR) was used for non-normally distributed data (such as the FDG standardized uptake value). Inter-group comparison of non-normally distributed data was made by Mann–Whitney nonparametric analysis. χ^2 test with Yates' correction was used to compare categorical variables. A p value <0.05

(two-sided) was considered to indicate statistical significance and 95 % confidence intervals (95 % CI) were used to express reliability in the estimates.

Receiver operating characteristic (ROC) curve analysis of maximum standardized uptake value (SUV$_{max}$) and area under the curve (AUROC) were used to assess discrimination between follicular and HCA. Youden index was used to identify the optimal cut-off SUV$_{max}$ for this discrimination [9]. Sensitivity, specificity, positive predictive value (PPV), negative predictive value (NPV) and overall accuracy were used as measures of performance of FDG-PET/CT.

Results

Twenty-nine patients with 23 follicular (FA) and 8 Hürthle cell adenomas (HCA) of the thyroid, diagnosed by FNAC, were included in the study. Six out of 8 HCA were identified preoperatively by FNAC. The mean age of our study cohort was 60.7 ± 12.6 years and 77 % of the patients were females. No significant difference was observed in the age ($p = 0.48$) and gender ($p = 0.52$) of the patients, and in the size of thyroid nodules ($p = 0.79$) in FA and HCA groups (Table 1).

The median SUV$_{max}$ value of benign thyroid nodules was 2.60. All (100 %) HCA and 12 (52 %) FA showed increased focal FDG uptake. SUV$_{max}$ of HCA was significantly higher ($p < 0.001$) than that of FA (Fig. 1). Increased focal FDG uptake offered sensitivity of 100 % (95 % CI 56–100 %), specificity of 49 % (95 % CI 27–69 %), positive predictive value (PPV) of 37 % (95 % CI 17–61 %), and negative predictive value (NPV) of 100 % (95 % CI 80–100 %) for identifying HCA with an overall accuracy of 60 %. Youden index indicated SUV$_{max}$ of 5 to be the best cut-off for discriminating between FA and HCA, with AUROC of 0.90 (95 % CI 0.79–1.00; $p = 0.001$). With this cut-off, FDG-PET/CT had sensitivity of 88 % (95 % CI 47–99 %), specificity of 87 % (95 % CI 65–97 %), positive predictive value (PPV) of 70 % (95 % CI 35–92 %), and negative predictive value (NPV) of 95 % (95 % CI 74–99 %) for identifying HCA, with an overall accuracy of 87 % (Table 2).

Discussion

Hürthle cells, also known as oncocytes or Askanazy cells comprise over 75 % of the cells in HCN [3, 10]. Hürthle cells are oxyphillic variant of follicular cells which have granular cytoplasm due to abundant intra-cytoplasmic mitochondria [11]. We did not find any age and gender difference between the patients with FA and HCA or a

Table 1 Patient demographics and characteristics of follicular and Hürthle cell adenomas

	Follicular adenoma ($N = 23$)	Hürthle cell adenoma ($N = 8$)	p value
Mean age	59.8 ± 13.6	63.5 ± 9.4	0.48
Gender (male:female)	8:14	1:6	0.52
Mean size of the nodule	2.8 ± 1.3 cm	3.2 ± 1.2 cm	0.79
Median SUV_{max}	2.2; IQR = 0–3.0	9.3; IQR = 6.9–19.9	<0.001
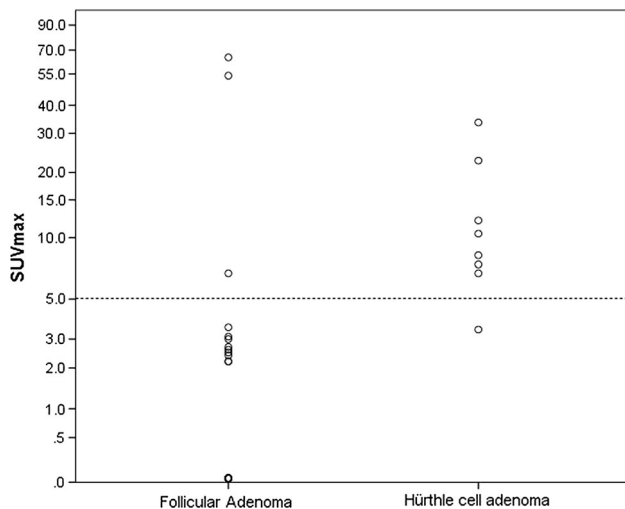
Fig. 1 Scatter plot of maximum standardized uptake value (SUV_{max}) in follicular and Hürthle cell adenomas. *Y* axis shows the SUV_{max} on exponential scale

Table 2 FDG-PET/CT findings in follicular and Hürthle cell adenomas [maximum standardized uptake value (SUV_{max}) cut-off for FDG-PET positivity = 5]

	Hürthle cell adenoma	Follicular adenoma	Total
FDG-PET positive	7	3	10
FDG-PET negative	1	20	21
Total	8	23	31

difference in the nodule size, but all (100 %) HCA showed increased focal FDG uptake as compared to only half (52 %) of FA. The abundant intra-cytoplasmic mitochondria probably accounts for intense FDG uptake by HCN. They can be divided into three groups: oncocytic adenoma (HCA), oncocytic cancer (Hürthle cells carcinoma), and oncocytic infiltration (Hürthle cells nests) [3]. Oncocytic cells are also seen in parathyroid, that can give rise to PET positive oncocytic parathyroid adenoma [12].

The incidence of thyroid adenoma on autopsy specimens has been reported to be 3–4.3 % [13, 14]. Almost 1.5–2.1 % of all thyroid nodules are hyper-metabolic on FDG-PET scans [15–18]. The diagnostic role of FDG-PET scan in thyroid nodules has been constrained by the high false positivity associated with FDG uptake by benign

thyroid nodules [19–26]. Meta-analyses evaluating the role of FDG-PET have not considered the influence of HCN on the accuracy of FDG-PET, even though all HCA showed increased FDG uptake [27, 28]. Increased FDG uptake in Hürthle cells and poorly differentiated components have been reported earlier to be independent predictors of high (≥ 5) SUV_{max} [18]. We found SUV_{max} of HCA to be significantly higher ($p < 0.001$) than that of FA, with SUV_{max} of 5 to be the best cut-off for discriminating between FA and HCA with excellent accuracy. The overall accuracy of FDG- PET/CT improved from 60 to 87 %, by this cut-off SUV_{max} rather than any increased focal uptake as the criterion of PET positivity. The specificity also improved from 49 to 87 %, and PPV from 37 to 70 %. Although it is a unique prospective study of its type, the number of subjects recruited are modest and independent validation of SUV_{max} cut-off of 5 is recommended.

It is important to consider HCA as a cause of increased focal FDG uptake alongside primary or secondary malignancies in thyroid. A FDG-PET positive indeterminate thyroid neoplasm is more likely to be a HCA than a FA. As 75 % of the HCA in this study could be identified by a preoperative FNAC, all FDG-PET positive thyroid nodules should undergo preoperative FNAC preferably under ultrasound guidance. Malignancy needs to be ruled out particularly in the nodules without Hürthle cell features (FN). HCA should also be suspected in case of increased focal FDG uptake in thyroid on staging FDG-PET scan for extra-thyroidal malignancies besides primary or metastatic disease in thyroid.

To conclude, HCA shows significantly higher FDG uptake as compared to FA and thus, they can often masquerade as malignant thyroid nodule. A cut-off SUV_{max} of 5 offers better accuracy for discriminating HCA from FA than merely increased focal FDG uptake.

Compliance with ethical standards

Conflict of interest The authors have no conflict of interest to disclose.

References

1. Layfield LJ, Cibas ES, Gharib H, Mandel SJ. Thyroid aspiration cytology: current status. CA Cancer J Clin. 2009;59:99–110.
2. Cibas ES, Ali SZ. The Bethesda system for reporting thyroid cytopathology. Thyroid. 2009;19:1159–65.

3. Zandieh S, Pokieser W, Knoll P, Sonneck-Koenne C, Kudlacek M, Mirzaei S. Oncocytic adenomas of thyroid-mimicking benign or metastatic disease on ^{18}F-FDG-PET scan. Acta Radiol. 2015;56:709–13.

4. Wiesner W, Engel H, von Schulthess GK, Krestin GP, Bicik I. FDG PET-negative liver metastases of a malignant melanoma and FDG PET-positive Hurthle cell tumor of the thyroid. Eur Radiol. 1999;9:975–8.

5. Grant CS, Barr D, Goellner JR, Hay ID. Benign Hurthle cell tumors of the thyroid: a diagnosis to be trusted? World J Surg. 1988;12:488–95.

6. Thompson NW, Dunn EL, Batsakis JG, Nishiyama RH. Hurthle cell lesions of the thyroid gland. Surg Gynecol Obstet. 1974;139:555–60.

7. McLeod MK, Thompson NW, Hudson JL, Gaglio JA, Lloyd RV, Harness JK, et al. Flow cytometric measurements of nuclear DNA and ploidy analysis in Hurthle cell neoplasms of the thyroid. Arch Surg. 1988;123:849–54.

8. Bybel B, Greenberg ID, Paterson J, Ducharme J, Leslie WD. Increased F-18 FDG intestinal uptake in diabetic patients on metformin: a matched case-control analysis. Clin Nucl Med. 2011;36:452–6.

9. Fluss R, Faraggi D, Reiser B. Estimation of the Youden Index and its associated cutoff point. Biom J. 2005;47:458–72.

10. Barnabei A, Ferretti E, Baldelli R, Procaccini A, Spriano G, Appetecchia M. Hurthle cell tumours of the thyroid. Personal experience and review of the literature. Acta Otorhinolaryngol Ital. 2009;29:305–11.

11. Maximo V, Sobrinho-Simoes M. Hurthle cell tumours of the thyroid. A review with emphasis on mitochondrial abnormalities with clinical relevance. Virchows Arch. 2000;437:107–15.

12. Paul A, Villepelet A, Lefevre M, Perie S. Oncocytic parathyroid adenoma. Eur Ann Otorhinolaryngol Head Neck Dis. 2015;132:301–3.

13. Silverberg SG, Vidone RA. Adenoma and carcinoma of the thyroid. Cancer. 1966;19:1053–62.

14. Bisi H, Fernandes VS, de Camargo RY, Koch L, Abdo AH, de Brito T. The prevalence of unsuspected thyroid pathology in 300 sequential autopsies, with special reference to the incidental carcinoma. Cancer. 1989;64:1888–93.

15. Treglia G, Bertagna F, Sadeghi R, Verburg FA, Ceriani L, Giovanella L. Focal thyroid incidental uptake detected by (1)(8)F-fluorodeoxyglucose positron emission tomography. Meta-analysis on prevalence and malignancy risk. Nuklearmedizin. 2013;52:130–6.

16. Kim H, Kim SJ, Kim IJ, Kim K. Thyroid incidentalomas on FDG PET/CT in patients with non-thyroid cancer—a large retrospective monocentric study. Onkologie. 2013;36:260–4.

17. Pagano L, Sama MT, Morani F, Prodam F, Rudoni M, Boldorini R, et al. Thyroid incidentaloma identified by (1)(8)F-fluorodeoxyglucose positron emission tomography with CT (FDG-PET/CT): clinical and pathological relevance. Clin Endocrinol (Oxf). 2011;75:528–34.

18. Bertagna F, Treglia G, Piccardo A, Giovannini E, Bosio G, Biasiotto G, et al. F18-FDG-PET/CT thyroid incidentalomas: a wide retrospective analysis in three Italian centres on the significance of focal uptake and SUV value. Endocrine. 2013;43:678–85.

19. de Geus-Oei LF, Pieters GF, Bonenkamp JJ, Mudde AH, Bleeker-Rovers CP, Corstens FH, et al. ^{18}F-FDG PET reduces unnecessary hemithyroidectomies for thyroid nodules with inconclusive cytologic results. J Nuclear Med. 2006;47:770–5.

20. Deandreis D, Al Ghuzlan A, Auperin A, Vielh P, Caillou B, Chami L, et al. Is (18)F-fluorodeoxyglucose-PET/CT useful for the presurgical characterization of thyroid nodules with indeterminate fine needle aspiration cytology? Thyroid. 2012;22:165–72.

21. Hales NW, Krempl GA, Medina JE. Is there a role for fluorodeoxyglucose positron emission tomography/computed tomography in cytologically indeterminate thyroid nodules? Am J Otolaryngol. 2008;29:113–8.

22. Kim JM, Ryu JS, Kim TY, Kim WB, Kwon GY, Gong G, et al. ^{18}F-fluorodeoxyglucose positron emission tomography does not predict malignancy in thyroid nodules cytologically diagnosed as follicular neoplasm. J Clin Endocrinol Metab. 2007;92:1630–4.

23. Kresnik E, Gallowitsch HJ, Mikosch P, Stettner H, Igerc I, Gomez I, et al. Fluorine-18-fluorodeoxyglucose positron emission tomography in the preoperative assessment of thyroid nodules in an endemic goiter area. Surgery. 2003;133:294–9.

24. Smith RB, Robinson RA, Hoffman HT, Graham MM. Preoperative FDG-PET imaging to assess the malignant potential of follicular neoplasms of the thyroid. Otolaryngol Head Neck Surg. 2008;138:101–6.

25. Traugott AL, Dehdashti F, Trinkaus K, Cohen M, Fialkowski E, Quayle F, et al. Exclusion of malignancy in thyroid nodules with indeterminate fine-needle aspiration cytology after negative ^{18}F-fluorodeoxyglucose positron emission tomography: interim analysis. World J Surg. 2010;34:1247–53.

26. Sebastianes FM, Cerci JJ, Zanoni PH, Soares J Jr, Chibana LK, Tomimori EK, et al. Role of ^{18}F-fluorodeoxyglucose positron emission tomography in preoperative assessment of cytologically indeterminate thyroid nodules. J Clin Endocrinol Metab. 2007;92:4485–8.

27. Wang N, Zhai H, Lu Y. Is fluorine-18 fluorodeoxyglucose positron emission tomography useful for the thyroid nodules with indeterminate fine needle aspiration biopsy? A meta-analysis of the literature. J Otolaryngol Head Neck Surg. 2013;42:38.

28. Vriens D, de Wilt JH, van der Wilt GJ, Netea-Maier RT, Oyen WJ, de Geus-Oei LF. The role of [^{18}F]-2-fluoro-2-deoxy-D-glucose-positron emission tomography in thyroid nodules with indeterminate fine-needle aspiration biopsy: systematic review and meta-analysis of the literature. Cancer. 2011;117:4582–94.

Stage II Differentiated Thyroid Cancer: A Mixed Bag

KUMAR ALOK PATHAK, MD, FRCSC,[1,2]* THOMAS C. KLONISCH, MD, PhD,[2]
AND RICHARD W. NASON, MD, FRCSC[1]

[1]Head and Neck Surgical Oncology, Cancer Care Manitoba, Winnipeg, Manitoba, Canada
[2]Human Anatomy and Cell Science, University of Manitoba, Winnipeg, Manitoba, Canada

Background and Objectives: AJCC-TNM Stage II well-differentiated thyroid cancer (WDTC) comprises T2N0M0 tumors in patients ≥45 years of age or metastatic WDTC in patients younger than 45 years. The objectives of this study were to assess the oncological outcome of stage II WDTC and to compare the oncological outcome of metastatic WDTC in patient younger (stage II) and older (stage IVC) than 45 years.
Methods: This study involved review of clinical presentation and oncological outcome of population cohort of 2,128 consecutive WDTC, diagnosed during 1970–2010 that includes 215 Stage II WDTC and 61 metastatic WDTC. Cox proportional hazard model was used to assess independent impact of prognostic factors on disease-specific survival (DSS) and disease-free survival (DFS) as calculated by Kaplan–Meier method.
Results: Metastatic and non-metastatic stage II WDTC had a 15-year DSS of 41.7% and 96.7%, respectively ($P < 0.001$). Multivariable analysis showed a 52 times higher risk of death in metastatic stage II WDTC and the DSS of metastatic stage II WDTC was not statistically different from that of stage IVC WDTC.
Conclusion: Metastatic stage II WDTC is very different from non-metastatic stage II WDTC with oncological outcome similar to stage IVC WDTC.
J. Surg. Oncol. 2016;113:94–97.   © 2015 Wiley Periodicals, Inc.

INTRODUCTION

Well-differentiated thyroid carcinoma (WDTC) accounts for over 90% of all thyroid malignancies [1]. WDTC comprises papillary, follicular, and Hürthle cell variant of follicular carcinoma in descending order of incidence and carries excellent prognosis [2,3]. An age threshold of 45 years is currently used by the AJCC-TNM system for stage grouping of WDTC [4]. According to the TNM staging system, Stage II WDTC is defined as 2–4 cm tumors without any evidence of spread beyond thyroid gland (T2N0M0) in patients ≥45 years of age or WDTC with distant metastasis in patients younger than 45 years. Multitudes of risk stratification systems have considered distant metastasis as an important prognostic factor for predicting oncological outcome of WDTC [4–13].

The primary objective of this study was to analyze the oncological outcome of stage II WDTC in patients younger and older than 45 years and the secondary objective was to compare if the oncological outcome of metastatic WDTC is different in patients younger and older than 45 years.

PATIENTS AND METHODS

Our population-based Manitoba thyroid cancer cohort includes 2,128 consecutive WDTC diagnosed in 2,118 patients registered in Manitoba Cancer Registry in Canada, from January 1, 1970 to December 31, 2010. We reviewed 2,018 electronic and paper charts, including pathology and operative reports, 56 discharge summaries, and 44 autopsy records and identified 215 patients with Stage II WDTC and 61 patients with distant metastasis (M1). Details involving patient demographics, extent of disease at presentation, treatment, pathology, recurrences of cancer, and the final outcome status as of July 1, 2015 were recorded. Recurrences were defined as the presence of clinical and/or radiological/biochemical evidence of disease. As the TNM

staging system has evolved over time, all cases were restaged using the TNM criteria of American Joint Committee on Cancer (AJCC)/Union Internationale Contre le Cancer (UICC) staging for thyroid cancer (7th Edition, 2009) to ensure uniformity. As a part of our collaborative staging project, the pathology and treatment details of 683 (32.3%) cases were independently reviewed for accuracy.

IBM SPSS Statistics version 23.0 (IBM Corp., Armonk, NY) was used to manage and analyze data. After checking for normality assumption, the mean and standard deviation were used to express normally distributed data (such as the age) and the median with was used for non-normally distributed data (such as tumor size and the follow-up). Analysis of variance (ANOVA) was used to compare group means and the Pearson χ^2 test to compare categorical data with continuity correction as appropriate. Proportions were compared by using Z-test. Statistical significance was defined as $P < 0.05$, and 95% confidence intervals were used to express reliability of the estimates. The Kaplan–Meier product limit method was used to estimate the disease-free survival (DFS) and disease-specific survival (DSS) and log-rank test was used to compare survival between groups. Multivariable analyses were performed with Cox proportional hazard
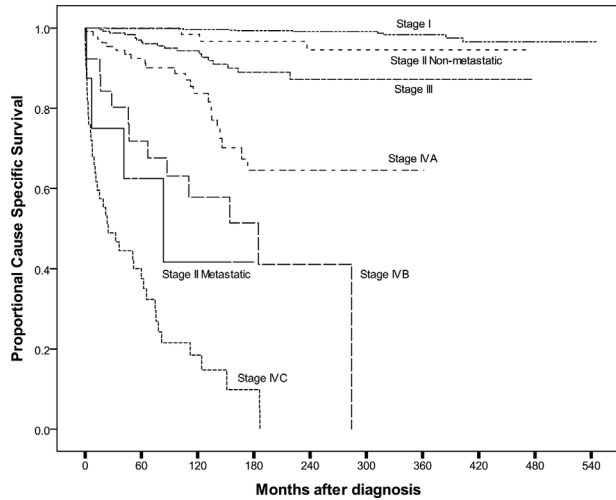
Fig. 1. Disease-specific survival of well-differentiated thyroid cancer in Manitoba thyroid cancer cohort.

TABLE I. Clinical Characteristics and Oncological Outcome of Non-Metastatic and Metastatic Stage II Well-Differentiated Thyroid Carcinoma (N = 215)

	T2N0M0 (patient age ≥45 years) (N = 207)	Any T, any N, M1 (patient age <45 years) (N = 8)	P-value
Mean age	58.9 ± 11.0 years	34.9 ± 7.7 years	<0.001
Gender (F:M)	4:1	1:3	0.001
Papillary thyroid carcinoma	69.6%	100%	NS
T2 tumor	100%	25%	<0.001
Lymph node involvement (N+)	0%	50.0%	<0.001
Distant metastasis (M1)	0%	100%	<0.001
Total thyroidectomy	50.5%	75.0%	NS
Radioactive iodine	38.2%	75.0%	0.027
Extra-thyroidal spread	0%	37.5%	<0.001
Complete resection	99%	75%	0.002
Recurrence or residual disease	5.8%	87.5%	<0.001
Dead of disease	2.4%	50%	<0.001
10-year DFS	93.3%	12.5%	<0.001
15-year DSS	96.7%	41.7%	<0.001

NS, Not significant

models to evaluate the independent impact of various prognostic factors on the DSS and DFS of our population-based cohort, after confirming the proportional hazard assumption.

RESULTS

Our population cohort of 2,118 consecutive WDTC patients showed DSS of stage II metastatic carcinoma to be very similar to stage IVB ($P = 0.530$, not significant [NS]) and IVC ($P = 0.127$, NS) (Fig. 1).

Stage II WDTC

The mean age of 215 stage II WDTC patients was 58.0 ± 11.8 years and 164 (76.3%) patients were females. Eight patients (3.7%) were younger than 45 years of age. The median tumor size was 30 mm (IQR = 25–35 mm) and 209 (97.2%) patients had T2 tumor; 2 (0.9%) had T1, 1 (0.5%) T3 tumor, and 3 (1.4%) had T4 tumor. Eight (3.7%) patients had metastatic WDTC and 5 (2.3%) were node positive. One hundred fifty-two (70.7%) patients had papillary carcinoma, followed by 40 (18.6%) follicular carcinoma, and 23 (10.7%) had Hürthle cell carcinoma. Total thyroidectomy was performed in 108 (50.2%) and 47 (21.9%) received adjuvant radioactive iodine treatment. During median follow-up of 134.3 months (IQR = 80.7–211.6 months), 19 (8.8%) patients had recurrent or persistent disease. At the time of last contact, 142 (66%) patients were alive without any evidence of disease and 3 (1.4%) with disease. Nine (4.2%) had died due to disease, 17 (7.9%) due to second primary, and 44 (20.4%) due to other causes. The demographics and clinical presentation of metastatic and non-metastatic stage II WDTC were significantly different apart from the proportion of patients with papillary thyroid cancer (Table I). Similar proportion of patients had total thyroidectomy in both groups. There was a significant difference ($P < 0.001$) in the DSS and DFS of metastatic and non-metastatic stage II WDTC (Table I).

Metastatic and non-metastatic stage II WDTC had a 15 year DSS of 41.7% and 96.7%, respectively. Cox proportional hazard model to assess the independent influence of various prognostic factors on oncological outcome of stage II WDTC showed a 52 times higher risk of death in metastatic stage II WDTC as compared to non-metastatic stage II WDTC and a 17 times higher risk of death was seen in males as compared to the females (Table II).

Metastatic WDTC

Manitoba thyroid cancer cohort contains 106 metastatic thyroid cancer that includes 61 metastatic WDTC (2.9% of all WDTC) with a mean age of 65.4 ± 16.1 years with 30 (49.2%) female patients. Forty-three (70.5%) patients had papillary carcinoma, 14 (23.0%) follicular carcinoma, and 4 (6.5%) had Hürthle cell carcinoma. Eleven (18.0%) patients had T1 tumor, 10 (16.4%) had T2, 19 (31.2%) T3 tumor, and 21 (34.4%) had T4 tumor. Fifty-three (86.9%) patients showed signs of clinical, radiological, or biochemical evidence of recurrent or persistent disease. At the time of last follow-up, three (4.9%) patients were alive without any evidence of disease and seven (11.5%) were alive with disease. In the meantime, 46 (75.4%) patients had died because of WDTC, and 5 (8.2%) due to other causes. The differences between the demographics and oncological outcomes of metastatic WDTC in patients younger (stage II) and older than 45 years (stage IVC) are summarized in Table III. There were significantly higher proportions of papillary carcinoma and female patients in <45 years age group. There was no difference in the DSS ($P = 0.127$) and DFS ($P = 0.591$) of the two groups (Table II). Multivariable analysis, by Cox proportional

TABLE II. Multivariable Analysis by Cox Proportional Hazard Model for Independent Influence of Prognostic Factors on Disease-Specific Survival of Stage II Well-Differentiated Thyroid Carcinoma (N = 215)

Prognostic factor	Hazard ratio (95%CI)
Distant metastasis (M stage)	52.28 (7.49–365.93), $P < 0.001$
Gender (male vs. female)	16.77 (2.81–99.94), $P = 0.002$
Completeness of resection (incomplete vs. complete)	$P = 0.057$ (NS)
Age at the time of diagnosis (per year)	$P = 0.147$ (NS)
Extent of thyroidectomy (hemi vs. total)	$P = 0.373$ (NS)
Adjuvant radioactive iodine (RAI vs. no RAI)	$P = 0.417$ (NS)
Lymph node involvement (N stage)	$P = 0.524$ (NS)
Histology (Hürthle cell vs. others)	$P = 0.795$ (NS)
Primary tumor (T stage)	$P = 0.859$ (NS)

NS, not significant.

TABLE III. Clinical Characteristics and Oncological Outcome of Metastatic Stage II Well-Differentiated Thyroid Carcinoma (n = 61)

	Stage II (any T, any N, M1) (N = 8)	Stage IVC (any T, any N, M1) (N = 53)	P-value
Age	34.9 ± 7.7 years	70.3 ± 11.1 years	<0.001
Gender (F:M)	1:3	1:1	<0.001
Papillary thyroid carcinoma	100%	57.4%	0.020
T1/T2 tumor	50%	31.1%	NS
T3/T4 tumor	50%	68.9%	NS
Lymph node involvement (N+)	50.0%	55.7%	NS
Total thyroidectomy	75.0%	84.2%	NS
Radioactive iodine	75.0%	68.4%	NS
Extra-thyroidal spread	37.5%	32.1%	NS
Complete resection	75%	66.7%	NS
Recurrence or residual disease	87.5%	93.0%	NS
Dead of disease	50%	78.9%	NS
10-year DFS	12.5%	4.7%	NS
15-year DSS	41.7%	9.9%	NS

NS, not significant.

hazard model, to assess the independent influence of various prognostic factors on DSS of metastatic WDTC showed no statistical difference between metastatic stages II and IVC WDTC (Table IV). Adjuvant radioactive iodine reduced the risk of death from metastatic WDTC by 80%. Males with metastatic WDTC were 6.3 times more likely to die of their disease as compared to their female counterpart. Incomplete resection and Hürthle cell histology were the other two independent determinants of survival in metastatic WDTC (Table IV).

DISCUSSION

Incidence of thyroid cancer has increased by almost fourfold over the last 4 decades in Manitoba, Canada [14]. Age has also been shown to be an important determinant of prognosis of WDTC [13–15]. The current version of AJCC-TNM staging system considers an age threshold of 45 years for stage grouping of WDTC [4]. However, the recent studies have shown that this might not be the best age cut off [15–17]. According to the TNM staging system, Stage II WDTC is defined as either T2N0M0 WDTC in patients ≥45 years of age or metastatic WDTC in patients younger than 45 years. Our study was designed to compare the demographic characteristics and the oncological

TABLE IV. Multivariable Analysis by Cox Proportional Hazard Model for Independent Influence of Prognostic Factors on Disease-Specific Survival of Metastatic Well-Differentiated Thyroid Carcinoma (N = 61)

Prognostic factor	Hazard ratio (95%CI)
TNM stage IV vs. TNM stage II	$P = 0.874$ (NS)
Gender (male vs. female)	6.33 (1.91–20.91), $P = 0.002$
Adjuvant radioactive iodine (RAI vs. no RAI)	0.190 (0.07–0.54), $P = 0.002$
Histology (Hürthle cell vs. others)	8.87 (1.08–72.55), $P = 0.042$
Completeness of resection (incomplete vs. complete)	3.43 (1.17–10.07), $P = 0.025$
Primary tumor (T stage)	$P = 0.187$ (NS)
Age at the time of diagnosis (per year)	$P = 0.354$ (NS)
Extent of thyroidectomy (Hemi vs. total)	$P = 0.553$ (NS)
Lymph node involvement (N stage)	$P = 0.831$ (NS)

NS, not significant.

outcomes of the two age groups of stage II WDTC patients. We also compared the oncological outcome of metastatic WDTC in patients younger and older than 45 years to see if there was any difference between these two groups.

As it is evident from Table I, the presentation of metastatic and non-metastatic stage II cancers was significantly different in terms of their clinical presentation and oncological outcome. Both DSS and DFS were significantly different between the two groups and a significantly higher proportion of patients with metastatic stage II WDTC died of their disease. This strongly suggests that the metastatic and non-metastatic stage II WDTC are very different entities grouped together. In an earlier study that compared TNM stages in patients in different age groups, younger patients had an 11-fold increase in mortality between stages I and II, whereas there was no difference for older patients [18]. It also showed a difference between the two age-based subgroups of stage II WDTC. The SEER database has inherent limitations in terms of coverage, coding reliability, patient migration to an area that is not covered by the SEER, and availability of limited information on the treatment details of the patients. A Swedish study had earlier failed to show any difference in the odds of death from WDTC between metastatic and non-metastatic WDTC [19]. In this article, on multivariable analysis, presence of distant metastasis was the single most important prognostic predictor of the oncological outcome of stage II WDTC and the presence of distant metastasis at diagnosis accorded a 52-fold increase in the hazard of death from WDTC (Table II).

Distant metastasis is considered an important prognostic factor determining the oncological outcome of WDTC in numerous prognostic scoring/staging systems. Metastatic WDTC have been variably staged as stages II [4], III [7], and IV [4,5,7,11] by different staging system. Similarly, different risk stratification system also have staged metastatic WDTC as high-risk [5,6,9] or intermediate risk [9,11] WDTC. Our comparison of clinical presentation and oncological outcome of metastatic WDTC in patients < or ≥45 years (Table III) does not show any significant difference between these two groups apart from increased proportion of female patients and papillary thyroid cancer in younger patients (stage II). There were statistically insignificant differences between the recurrence rates, risk of death from disease as well as DSS and DFS between stages II (M1) and IVC WDTC. Stage of presentation (stages II vs. IVC) had no influence on the DSS that was significantly lower for males, incomplete resection, and Hürthle cell histology. Adjuvant radioactive iodine significantly reduced the risk of death from WDTC.

Our cohort of WDTC was followed over a span of 4 decades with 42.5% had at least 15 years of follow-up. As a result, we have presented the DSS of our WDTC cohort at 15 years. We have presented 10-year DFS as all treatment failures in metastatic WDTC and 95% of those in stage II WDTC took place within 10 years. This long follow-up is both a strength and a limitation, as the staging has evolved over time. To ensure consistency, all cancers were uniformly restaged using the 2009 UICC/AJCC staging system. We controlled for the period of diagnosis and treatment in multi-variable analysis to eliminate any bias that might be introduced by this long follow-up. The major limitation of this study is the number of metastatic stage II WDTC (N = 8); however, the 55% difference in the DSS between metastatic and non-metastatic stage II WDTC renders post hoc power of 98.7% with α = 0.05. A large multi-institutional study with a larger number of metastatic stage II WDTC is suggested to confirm this significant finding.

To conclude, our study suggests that the oncological outcome of patients with metastatic stage II WDTC is very different from that of non-metastatic stage II WDTC. The outcome of metastatic disease in younger patient (stage II) is very similar to that in older patients with similar disease burden (stage IVC). We strongly advocate staging all metastatic WDTC as stage IV irrespective of the age of the patient.

ACKNOWLEDGMENTS

REFERENCES

1. Clark OH: Predictors of thyroid tumor aggressiveness. West J Med 1996;165:131–138.
2. Lang BH, Lo CY, Chan WF, et al.: Staging systems for papillary thyroid carcinoma: A review and comparison. Ann Surg 2007;245: 366–378.
3. Nixon IJ, Ganly I, Patel S, et al.: The impact of microscopic extra thyroid extension on outcome in patients with clinical T1 and T2 well-differentiated thyroid cancer. Surgery 2011;150:1242–1249.
4. Edge SB, Byrd DR, Compton CC, et al.: AJCC cancer staging handbook, 7th edition. New York, NY, USA: Springer-Verlag; 2010.pp. 87–96.
5. Beenken S, Roye D, Weiss H, et al.: Extent of surgery for intermediate-risk well-differentiated thyroid cancer. Am J Surg 2000;179:51–56.
6. Cady B, Rossi R: An expanded view of risk-group definition in differentiated thyroid carcinoma. Surgery 1988;104:947–953.
7. Sherman SI, Brierley JD, Sperling M, et al.: Prospective multicenter study of thyroid carcinoma treatment: Initial analysis of staging and outcome. Cancer 1998;83:1012–1021.
8. Hay ID, Grant CS, Taylor WF, et al.: Ipsilateral lobectomy versus bilateral lobar resection in papillary thyroid carcinoma: A retrospective analysis of surgical outcome using a novel prognostic scoring system. Surgery 1987;102:1088–1095.
9. Shaha AR, Loree TR, Shah JP: Intermediate-risk group for differentiated carcinoma of thyroid. Surgery 1994;116:1036–1041.
10. DeGroot LJ, Kaplan EL, McCormick M, et al.: Natural history, treatment, and course of papillary thyroid carcinoma. J Clin Endocrinol Metab 1990;71:414–424.
11. Mazzaferri EL, Jhiang SM: Long-term impact of initial surgical and medical therapy on papillary and follicular thyroid cancer. Am J Med 1994;97:418–428.
12. Lerch H, Schober O, Kuwert T, et al.: Survival of differentiated thyroid carcinoma studied in 500 patients. J Clin Oncol 1997; 15:2067–2075.
13. Pathak KA, Mazurat A, Lambert P, et al.: Prognostic nomograms to predict oncological outcome of thyroid cancers. J Clin Endocrinol Meta 2013;98:4768–4775.
14. Pathak KA, Leslie WD, Klonisch TC, et al.: The changing face of thyroid cancer in a population based cohort. Cancer Med 2013;2:537–544.
15. Mazurat A, Torroni A, Hendrickson-Rebizant J, et al.: The age factor in survival of a population cohort of well-differentiated thyroid cancer. Endocr Connect 2013;2:154–160.
16. Orosco RK, Hussain T, Brumund KT, et al.: Analysis of age and disease status as predictors of thyroid cancer-specific mortality using the surveillance, epidemiology, and end results database. Thyroid 2015;25:125–132.
17. Hendrickson-Rebizant J, Sigvaldason H, Nason RW, et al.: Identifying the most appropriate age threshold for TNM stage grouping of well-differentiated thyroid cancer. Eur J Surg Oncol 2015;41:1028–1032.
18. Tran Cao HS, Johnston LE, Chang DC, et al.: A critical analysis of the american joint committee on cancer (AJCC) staging system for differentiated thyroid carcinoma in young patients on the basis of the surveillance, epidemiology, and end results (SEER) registry. Surgery 2012;152:145–151.
19. Lundgren CI, Hall P, Dickman PW, et al.: Clinically significant prognostic factors for differentiated thyroid carcinoma: A population-based, nested case–control study. Cancer 2006; 106:524–531.

Prognostic Nomograms To Predict Oncological Outcome of Thyroid Cancers

K. Alok Pathak, Andrea Mazurat, Pascal Lambert, Thomas Klonisch, and Richard W. Nason

Cancer Care Manitoba (K.A.P., P.L., R.W.N.), Winnipeg, Manitoba R3E 0V9, Canada; and Department of Human Anatomy and Cell Science (K.A.P., A.M., T.K., R.W.N.), University of Manitoba, Winnipeg, Manitoba R3A 1R9, Canada

Context: Thyroid cancers represent a conglomerate of diverse histological types with equally variable prognosis. There is no reliable prognostic model to predict the risks of relapse and death for different types of thyroid cancers.

Objective: The purpose of this study was to build prognostic nomograms to predict individualized risks of relapse and death of thyroid cancer within 10 years of diagnosis based on patients' prognostic factors.

Design: Competing risk subhazard models were used to develop prognostic nomograms based on the information on individual patients in a population-based thyroid cancer cohort followed up for a median period of 126 months. Analyses were conducted using R version 2.13.2. The R packages cmprsk10, Design, and QHScrnomo were used for modeling, developing, and validating the nomograms for prediction of patients' individualized risks of relapse and death of thyroid cancer.

Setting: This study was performed at CancerCare Manitoba, the sole comprehensive cancer center for a population of 1.2 million.

Patients: Participants were a population-based cohort of 2306 consecutive thyroid cancers observed in 2296 patients in the province of Manitoba, Canada, during 1970 to 2010.

Main Outcome Measures: Outcomes were discrimination (concordance index) and calibration curves of nomograms.

Results: Our cohort of 570 men and 1726 women included 2155 (93.4%) differentiated thyroid cancers. On multivariable analysis, patient's age, sex, tumor histology, T, N, and M stages, and clinically or radiologically detectable posttreatment gross residual disease were independent determinants of risk of relapse and/or death. The individualized 10-year risks of relapse and death of thyroid cancer in the nomogram were predicted by the total of the weighted scores of these determinants. The concordance indices for prediction of thyroid cancer–related deaths and relapses were 0.92 and 0.76, respectively. The calibration curves were very close to the diagonals.

Conclusions: We have successfully developed prognostic nomograms for thyroid cancer with excellent discrimination (concordance indices) and calibration. (*J Clin Endocrinol Metab* **98: 4768–4775, 2013**)

Thyroid cancer is the fastest growing cancer in *Canadian Cancer Statistics 2012* with age-standardized incidence increasing at the rate of 6.8% per year in men (1998–2007) and 6.9% per year in women (2002–2007) (1). The 10-year relative survival ratio in 2004 to 2006 was 97% (95% confidence interval [CI], 96%–98%) (2). The

Abbreviations: CI, confidence interval; DSS, disease-specific survival; DTC, differentiated thyroid cancer; MTC, medullary thyroid cancer; RFS, relapse-free survival; SEER, Surveillance, Epidemiology, and End Results.

lifetime probability of developing thyroid cancer for a Canadian woman is 1 in 71 (1.4%) but only 1 in 1374 (0.1%) will actually die of it. Canadian men have a lower lifetime risk of developing thyroid cancer at 1 in 223 (0.4%) with the risk of death of thyroid cancer at 1 in 1937 (0.1%) (3). Survival of patients with thyroid cancer is significantly influenced by a variety of factors such as age, sex, histological type, stage of presentation, and treatment that have been incorporated into various staging/prognostic scoring systems for thyroid cancer (4–18) to predict oncological outcome. Most of these are applicable only to the differentiated thyroid cancers (DTCs) (6–18) and provide stratified group risks rather than individualized risks. A nomogram, on the other hand, can be applied across different histological types to generate the numerical probability of individual's clinical outcome, based on his or her risk assessment.

Nomograms provide visual explanation for predicted probabilities of an outcome as obtained by statistical predictive models that calculate the cumulative effect of weighted variables on the probability of that outcome. Nomograms have been used in prostate, lung, pancreas, breast, stomach, and renal cancers as well as for sarcomas to predict treatment outcomes (19–28). The only nomogram that has been developed to predict survival in thyroid cancer is based on the Surveillance, Epidemiology, and End Results (SEER) database (29) that has inherent limitations such as a lack of treatment and relapse details. For a nomogram to be universally acceptable, it should ideally be population-based or derived from multi-institutional data. Because most thyroid cancers have an indolent course and many failures take place years after diagnosis and treatment, a prolonged follow-up and a low attrition of cohort, such as ours, are critical for testing the validity of nomogram. This study was planned to build a prognostic nomogram to predict risks of relapse and death of thyroid cancer using data from the Manitoba thyroid cancer cohort.

Patient and Methods

Study cohort

This study involved a review of electronic and paper records of a population-based cohort of all 2306 consecutive thyroid cancers diagnosed in 2296 patients in Manitoba, Canada from January 1, 1970, to December 31, 2010 (Manitoba thyroid cancer cohort). Ethics approval for this study was obtained from the Research Ethics Board at the University of Manitoba. We reviewed individual electronic and paper records of diagnosis and treatment of individual patients of this cohort at CancerCare Manitoba, the tertiary cancer care center for the province of Manitoba with a catchment population of about 1.2 million and Manitoba Cancer Registry as a part of it. The primary sources of diagnostic information included 2148 pathology reports, 80 discharge summaries, 56 autopsy records, 18 operative reports, and death certificates. Patient demographics, extent of disease at initial presentation, treatment modalities used, pathology details, cancer recurrences during the follow-up, and the final oncological status as of January 1, 2013, were recorded. All patients who migrated out of the province (considered lost to follow-up) during the study period were censored at that point in time. Patients in whom cancer was initially diagnosed by autopsy or death certificate were excluded from the survival analyses.

Statistical methods

The data were managed and analyzed using SPSS for Windows version 20.0 (SPSS Inc). A value of $P < .05$ (two-sided) was considered to indicate statistical significance and 95% CIs were used to express reliability in the estimates. The patient characteristics, the extent of disease at presentation, and the tumor histology were recorded along with the treatment modalities, the patterns of failure, and the final oncological outcome. Relapse-free survival (RFS) and disease-specific survival (DSS) were estimated by the Kaplan-Meier product limit method. The effects of age at diagnosis, patient's sex, tumor size, extrathyroidal extension, lymph node metastasis, distant metastasis, the histological type, treatment modalities, and the presence of posttreatment gross residual disease on the 10-year probability of relapse and death by disease were evaluated by competing risk analysis (30) to assess the competing influence of other causes of mortality, such as death due to a second primary tumor or noncancer deaths.

Cumulative incidence function was used to describe the probability of relapse and death using a proportional hazards regression model to directly model the subdistribution of a competing risk (31). After exclusion of 60 thyroid cancers that were detected either at autopsy (56 patients) or by death certificate (4 patients) and 10 patients with familial medullary thyroid cancers, 2226 patients were included in the proportional hazards regression model for competing risk analysis for deaths due to thyroid cancer, Similarly, 1977 patients who had complete resection of their thyroid cancer without any posttreatment residual disease were included in the proportional hazards regression model for competing risks analysis of relapse of thyroid cancer. Period of di-

Table 1. Case Fatality Rate and DSS by Histological Types of Thyroid Cancers

Histological Type	Case Fatality Rate, %	10-y DSS (95% CI)	10-y RFS (95% CI)
Papillary (n = 1763)	3.6	96.8 (95.7–97.7)	87.7 (85.9–89.4)
Follicular (n = 268)	9.0	91.5 (87.0–94.5)	87.3 (82.4–91.0)
Hürthle cell (n = 85)	17.6	81.4 (69.7–89.0)	69.8 (57.9–79.0)
Medullary (n = 79)	26.6	77.6 (65.4–85.9)	27.3 (6.5–53.9)
Poorly differentiated (n = 39)	31.2	74.1 (28.9–93.0)	52.0 (38.5–63.9)
Anaplastic (n = 72)	83.3	7.3 (2.4–15.9)	1.4 (0.1–6.7)

Table 2.   Prognostic Factors Influencing Cumulative Incidence of Death From Thyroid Cancer in Proportional Hazards Regression for Subdistribution of Competing Risks (n = 2226)

Prognostic Factors	Subhazard Ratio	95% CI	P Value
Age (10-y increments)	1.67	1.47–1.91	.001
Sex (male vs female)	2.195	1.49–3.24	.001
Histology			
Histology(medullary vs papillary)	4.219	2.40–7.42	.001
Histology (Follicular vs papillary)	1.122	0.67–1.89	.664
Distant metastasis	8.462	4.86–14.75	.001
T stage			
T4 vs T1	3.439	1.73–6.83	.001
T3 vs T1	2.580	1.30–5.04	.007
T2 vs T1	1.519	0.74–3.13	.257
Posttreatment residual disease	2.412	1.40–4.15	.001
Regional lymph node involvement	2.212	0.97–5.03	.063
Extent of thyroidectomy (total vs hemi)	1.521	0.86–1.41	.151

agnosis was also included to produce estimates for the nomograms based on a more recent cohort. Analyses were conducted using R version 2.13.2 (www.r-project.org). The R packages cmprsk10, Design, and QHScrnomo were used for modeling and developing the nomograms. Restricted cubic splines were used for the continuous variable of age. The default setting for 4 knots was used for RFS, and the default setting for 3 knots was used for disease-specific survival. Twenty imputations were produced with the mice package for missing values among predictor variables.

Based on the weighted relative importance of individual prognostic factors on the 10-year risks of relapse and death of disease, prognostic nomograms were developed as described earlier (32). The models were internally cross-validated by calibration (calibration curve) and discrimination (concordance index) using QHScrnomo. Calibration curves and concordance indexes were produced using only 1 of the 20 complete datasets after multiple imputations.

Results

In total, 2306 thyroid cancers were observed in Manitoba in 2296 patients from 1970 to 2010 and followed up for 26 715.19 patient-years with a 2.1% loss to follow-up. Nine patients had a synchronous second primary tumor of a different histology along with papillary thyroid cancer (3 follicular, 3 Hürthle cell, 2 medullary, and 1 poorly differentiated), and 1 patient had a metachronous second papillary carcinoma in the contralateral thyroid lobe 25 years after initial management. The Manitoba thyroid cancer cohort included 570 (24.8%) men and 1726 (75.2%) women with a mean age of 49 ± 18 years. Papillary thyroid cancer was the most commonly observed histological type (Table 1). T1 tumors were seen in 978 (32.6%) patients, T2 tumors in 597 (26%) patients, T3 tumors in 468 (20.4%) patients, and T4 tumors in 246 (10.7%) patients. In 7 (0.3%) patients, a primary tumor was either not identified or could not be staged. At the time of diagnosis, 544 (23.7%) patients had lymph node involvement in the neck and 90 (3.9%) patients had evidence of distant metastasis. Multifocal thyroid cancers were observed in 742 (32.3%) patients and a gross extrathyroidal extension of tumor in 480 (20.9%) patients. Total thyroidectomy was performed in 55.1% of all pa-

Table 3.   Prognostic Factors Influencing Cumulative Incidence of Relapse of Thyroid Cancer in Proportional Hazards Regression for Subdistribution of Competing Risks (n = 1977)

Prognostic Factors	Subhazard Ratio	95% CI	P Value
Age[a]	0.952	0.92–0.98	.002
Age'[a]	1.118	0.99–1.25	.053
Age"[a]	0.788	0.55–1.13	.195
Sex (Male vs Female)	1.607	1.16–2.22	.004
Histology			
Medullary vs papillary	2.371	1.39–4.05	.002
Hürthle/poorly differentiated vs papillary	2.651	1.51–4.64	.001
Follicular vs papillary	0.768	0.43–1.37	.370
Distant metastasis	11.593	5.00–26.90	.001
Regional lymph node involvement	2.414	1.68–3.47	.001
T stage			
T4 vs T1	2.728	1.52–4.89	.001
T3 vs T1	2.372	1.62–3.47	.001
T2 vs T1	1.189	0.77–1.83	.432
Extent of thyroidectomy (hemi vs total)	0.803	0.56–1.12	.221

[a] Nonmonotonic relationship of age with relapse of thyroid cancer.

tients and 54.3% of patients with DTCs (73% of these received adjuvant radioactive radioiodine). All patients with unresectable macroscopic residual disease in the neck at the time of surgery after total thyroidectomy or those at a high risk of disease recurrence, such as those with T3/T4 tumors or regional and distant metastasis received radioactive iodine for differentiated thyroid cancer. Use of external beam radiation therapy was limited to unresectable macroscopic residual disease.

Oncological outcomes of treatment with curative intent were assessed in the 2065 patients who underwent primary surgical treatment after exclusion of those whose cancer was diagnosed only on autopsy or death reports (n = 60), those who died before surgery (n = 64), those who were not candidates for surgery (n = 35), those who refused treatment (n = 24), and those whose primary surgery or follow-up was performed in another province or country (n = 48). A further 78 (3.8%) patients had post-surgery macroscopic residual disease, and they were excluded from the model to predict the risk of relapse. During the median follow-up of 10.5 years (interquartile range, 4.8–18.8 years), another 200 (9.7%) patients had had clinical/radiological evidence of recurrent disease after at least 6 months following an initial successful treatment. The recurrences were in the residual thyroid lobe or thyroid bed in 23 (11.5%) patients, in the central compartment of the neck in 64 (32%) patients, in the lateral compartment of the neck in 44 (22%) patients, at a distant metastatic site in 54 (27%) patients, and at multiple sites in 15 (7.5%) patients. RFS at 10 years after radical treatment was 89.3% (95% CI, 87.7%–90.8%), and 90.5% of
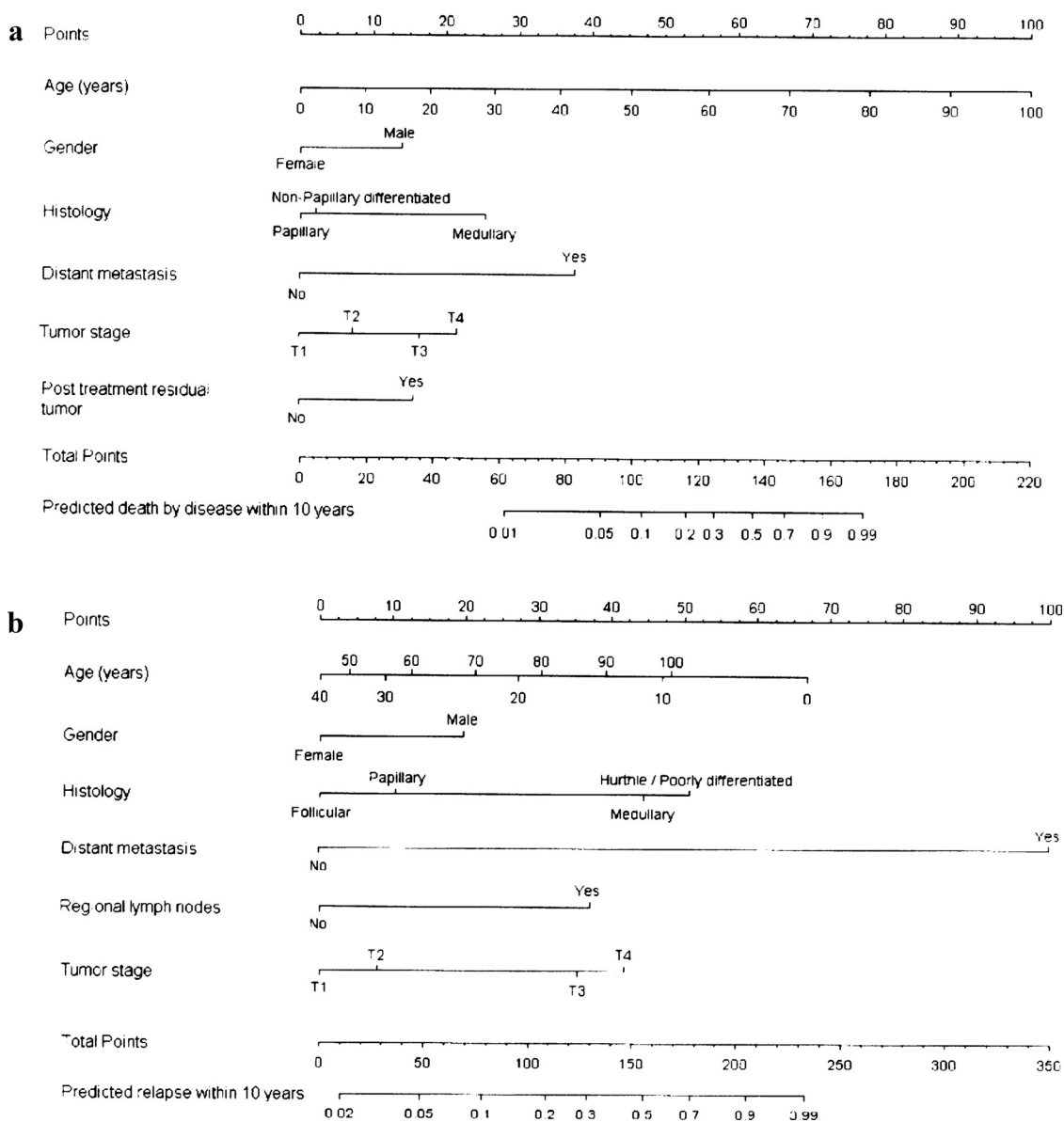

Figure 1. Thyroid cancer prognostic nomograms to predict risk of deaths (A) and relapses (B).

all recurrences were observed during this period (69.5% within the first 5 years).

The 10-year DSS of the Manitoba thyroid cancer cohort (N = 2296) was 91.8% (95% CI, 90.5%–92.9%) and 76% of all thyroid cancer–related deaths were observed within 10 years (54.9% within first 5 years). In all, 201 patients died of thyroid cancer (case fatality rate, 8.8%). Of the patients who died of thyroid cancer, 63 (31.3%) had papillary carcinoma, 60 (29.9%) had anaplastic cancer, 24 (11.9%) had follicular cancer 21 (10.4%) had medullary cancer, 15 (7.5%) had Hürthle cell cancer, 8 (4%) had poorly differentiated cancer, and 10 (5%) had an unspecified thyroid carcinoma. Because the case fatality rate of anaplastic thyroid cancer was extremely high and the 10-year DSS and RFS were very poor (Table 1), the multivariable analyses for computing risks of death and relapse were restricted to nonanaplastic thyroid cancers. In addition, because the behavior of familial medullary thyroid cancers (n = 10) is largely determined by their specific gene mutations, these patients were excluded from multivariable analysis. The patient's age at

diagnosis, sex, T stage, histological type, presence of distant metastasis, and posttreatment macroscopic residual disease were important determinants of the cumulative incidence of death due to thyroid cancer on multivariable analysis (Table 2). Lymph node positivity had a very significant impact on the cumulative incidence of relapses after complete resection of macroscopic disease (Table 3) but not on the incidence of deaths of thyroid cancer. The extent of thyroidectomy did not have any independent impact on the risk of dying of cancer, and adjuvant radioactive iodine showed collinearity with total thyroidectomy. Consequently, both of these were not included in the nomogram. Based on the subhazard ratio of the different independent prognostic factors, we constructed nomograms to predict the cumulative incidence of deaths due to thyroid cancer (Figure 1A) and posttreatment relapse of disease (Figure 1B). Our model had a high concordance index for predicting the risks of thyroid cancer–related death (0.92) and relapse (0.76), indicating an excellent discrimination capability. The marginal estimate was plotted vs model average predictive probability as calibration plots (Figure 2, A and B), and most of the predictions fell on the 45° diagonal line.

Discussion

Thyroid cancer is the most common malignant endocrine tumor and in 2012 about 5650 new cases were detected in Canada (1). It is a cancer of young women and accounts for 11% of all cancers in women younger than 40 years, second only to breast cancer. More than 90% of the thyroid cancers are either follicular or papillary carcinoma, often termed DTC and carry excellent prognosis. The age of the patient at the time of diagnosis has a significant impact on the oncological outcome of both DTC and medullary thyroid cancer (MTC) (4–11, 33). Surgery is the mainstay of treatment of nonanaplastic thyroid cancer and posttreatment gross residual disease is considered to be an important prognostic factor for both DTC and MTC (13, 34). The use of numerous age-based prognostic scoring systems for predicting the outcome of thyroid cancer signifies that none is universally acceptable. Moreover, most of these staging systems are valid only for DTC (6–18) and more specifically for papillary thyroid cancer (6, 10–13, 15, 17, 18). Prognostic scoring systems (4, 6, 9, 11, 13, 17) require lengthy calculations of prognostic scores that make individualized risk prediction quite arduous. Various risk stratification systems (5, 7, 8, 10, 12, 14–16, 18) are easier to use in clinics, but they provide stratified group risk estimates rather than individualized patient risk. The American Thyroid Association proposed a stag-
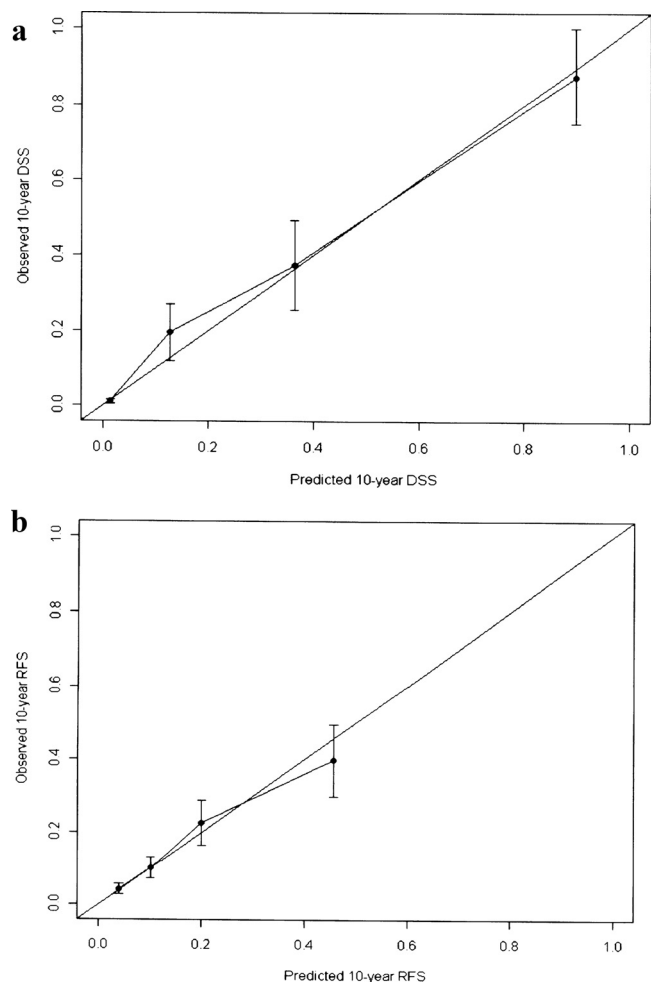

Figure 2. Calibration plots for predicting risks thyroid cancer related deaths (A) and relapses (B).

ing system (35) to predict the risk of recurrence in low-, intermediate-, and high-risk groups of DTCs, categorized on the basis of regional and distant metastases, completeness of resection, locoregional tumor invasion at initial surgery, aggressive histology, and ^{131}I uptake outside the thyroid bed on the whole-body radioactive iodine scan.

Nomograms combine multiple independent variables to predict an outcome using the prognostic weight of each variable in calculating the probability of such an outcome. Prognostic nomograms can be developed for a variety of clinical outcomes, such as survival (overall or disease-specific) and the probability of developing locoregional recurrence or metastasis. An ideal nomogram should be reliable, widely applicable, and also easy to use. Although thyroid cancers represent a conglomerate of different histological types with varying outcomes, the prognostic factors independently influencing the risks of relapse and death are similar for most nonanaplastic thyroid cancers as outlined in Tables 2 and 3. We explored the feasibility of outcome predictions at 5, 10, and 20 years in the nomograms. We opted for a 10-year time frame for outcome prediction because most of the nonanaplastic thyroid cancers are indolent and a 5-year period is very short to detect late recurrences and deaths of thyroid cancer. More than 30% of relapses and 45% of deaths of thyroid cancers were observed after 5 years, whereas more than 90% of thyroid cancer relapses and more than three quarters of deaths of thyroid cancers were observed within first 10 years. Although the outcome prediction at 20 years would have been ideal, it becomes less reliable because the median follow-up of the cohort is 10.5 years. We incorporated the clinically relevant prognostic factors independently influencing the incidences of relapse and deaths of thyroid cancers such as tumor stage (T), distant metastasis (M), age and sex of the patient, and tumor histology to construct an easy-to-use nomogram. Posttreatment gross residual disease was an important factor only for prediction of death of thyroid cancer. Understandably, the patients with residual tumor were excluded from the regression model to predict thyroid cancer relapse because the quantification of macroscopic residual disease is very subjective and variable. Lymph node metastasis predicted a higher risk of future disease relapse, but it did not alter the risk of dying of thyroid cancer.

Prognostic nomograms use the experience of a large group of patients to predict an individual's prognosis based on the individual's characteristics. The likelihood of a reliable prediction depends on the robustness of the model and its representativeness. A large population-based cohort with low attrition rates such as ours (only 2.1% loss to follow-up over 40 years) is probably the best possible model to study the oncological outcomes of thy-

roid cancer such as relapses and deaths. The Manitoban population (our cohort) is a mix of different ethnic groups from all over the world because of immigration over the years. It is likely that the nomogram applies to other populations, but this needs to be demonstrated. Our source of information was quite reliable because the individual medical records were reviewed for their accuracy and completeness. We included the period of diagnosis to produce estimates for the nomograms to minimize the impact of time-dependent changes in treatment practices, if any. Larger databases such as the SEER database are robust, but they have the inherent limitations in terms of coverage, coding reliability, patient migration to an area that is not covered by SEER, and availability of limited information on the treatment details for the patients. Yang et al (29) proposed nomograms based on SEER data to predict 5- and 10-year mortality related to thyroid cancer, other cancers, and other causes. However these nomograms do not take into consideration the presence of posttreatment residual disease, which is a known prognostic factor for both DTC and MTC (13, 34). We used T stage to quantify the extent of the primary tumor, incorporating both the size and the extrathyroidal extension, rather than classifying the extent as local, regional, and distant. Regional disease could signify either an extension into adjacent tissue or to the regional lymph node(s). In the latter case, the nodal disease figures twice in their nomogram, both in the extent of tumor as well as in the lymph node involvement. Sex of the patient is not included in their nomogram to predict the probability of death of thyroid cancer, even though its impact on cumulative incidence of thyroid cancer deaths in their study was very significant ($P < .001$). The other 2 nomograms published by Yang et al (29) deal with death of other cancers and noncancer deaths in which thyroid cancer does not have a major role. Our thyroid cancer population cohort offsets the limitations that are inherent to the nature of SEER database such as the lack of information on relapses that precludes the development of the nomogram to predict this important oncological outcome. Our nomogram predicting cumulative incidence of relapse of thyroid cancer shows a very interesting, nonmonotonic relationship between age of the patients and relapse (Figure 1B). There was a bimodal relationship (scales wraparound) between relapse and age of the patients even though this high relapse rate at a younger age does not lead to a higher number of deaths of thyroid cancer as it is evident from the 2 nomograms. Moreover, the lymph node involvement, an important determinant of risk of relapse, is more often observed in pediatric patients who tend to have more relapses (36).

Prognostic modeling has some limitations because the oncological outcome determined over a long period of

time could have been influenced by the changes in the treatment and follow-up recommendations. However, in our study cohort, more aggressive treatment by total thyroidectomy with adjuvant radioactive iodine has not resulted in any significant increase in the risk of relapse as long as there was no residual disease (Table 2). Consequently, the treatment modalities were not included in the nomogram. We had earlier reported an improvement in the survival of our thyroid cancer cohort over the last 4 decades independent of changes in the tumor size or treatment modalities (37). The prognostic factors that influenced the disease-specific survival have remained largely unaltered during the study period (37). Thus, the time period of this study is unlikely to have any independent influence on the nomograms. Some differences such as follicular vs papillary histology and T1 vs T2 tumor stage were not statistically significant but were incorporated in the nomogram because of the overall importance of the prognostic factor. The relapse prediction is valid only for those thyroid cancers that are treated with curative intent with no clinical or radiological evidence of residual disease as outlined in the model. We did not consider isolated hyperthyroglobulinemia or molecular markers such as *BRAF* (38) as independent prognostic factors because they were not a part of the standard clinical care in a large proportion of our cohort and their independent impact without discernible disease is contentious. We recognize that MTC represents a diverse group of cancers with specific gene mutations determining the prognosis of familial MTC. In our cohort, 10 (12.6%) patients had familial MTC and were excluded from the models to develop nomograms. Therefore, these nomograms are appropriate for use with sporadic MTC but not familial MTC.

Discrimination, the ability of a model to separate subject outcomes, can be measured with a concordance index between predicted probability and response, defined as the proportion of all evaluable ordered patient pairs for which predictions and outcomes are concordant (39, 40). Our nomograms had very good concordance indices of 0.92 (thyroid cancer deaths) and 0.76 (thyroid cancer relapses), where 0.5 is the worst (complete random prediction) and 1.0 is the best score (perfect prediction). Calibration is the other ability of the model to make unbiased estimates of outcome. On the calibration plot, most of the predictions fell on the 45° diagonal line, suggesting very high calibration.

To conclude, we were successful in developing unique nomograms to predict the likelihood of relapse and death from thyroid cancer in an individual patient with good calibration and discrimination capabilities. We have internally cross-validated these nomograms, and we look forward to their external validation as well as evolution into a web-based tool for popular use.

References

1. **Canadian Cancer Society Steering Committee on Cancer Statistics.** *Canadian Cancer Statistics 2012*. Toronto, ON, Canada: Canadian Cancer Society; 2012:7–60.
2. **Ellison LF, Wilkins K.** An update on cancer survival. *Health Rep*. 2010;21:55–60.
3. **Canadian Cancer Society Steering Committee on Cancer Statistics.** *Canadian Cancer Statistics 2011*. Toronto, ON, Canada: Canadian Cancer Society; 2011:25–60.
4. **Byar DP, Green SB, Dor P, et al.** A prognostic index for thyroid carcinoma. A study of the E.O.R.T.C. Thyroid Cancer Cooperative Group. *Eur J Cancer*. 1979;15:1033–1041.
5. **Sherman SI, Brierley JD, Sperling M, et al.** Prospective multicenter study of thyroid carcinoma treatment: initial analysis of staging and outcome. National Thyroid Cancer Treatment Cooperative Study Registry Group. *Cancer*. 1998;83:1012–1021.
6. **Hay ID, Grant CS, Taylor WF, McConahey WM.** Ipsilateral lobectomy versus bilateral lobar resection in papillary thyroid carcinoma: a retrospective analysis of surgical outcome using a novel prognostic scoring system. *Surgery*. 1987;102:1088–1095.
7. **Cady B, Rossi R.** An expanded view of risk-group definition in differentiated thyroid carcinoma. *Surgery*. 1988;104:947–953.
8. **Sobin L, Gospodarowicz M, Wittekind C.** *TNM Classification of Malignant Tumours*. 7th ed. New York, NY: John Wiley; 2009:58–62.
9. **Yildirim E.** A model for predicting outcomes in patients with differentiated thyroid cancer and model performance in comparison with other classification systems. *J Am Coll Surg*. 2005;200:378–392.
10. **Pasieka JL, Zedenius J, Auer G, et al.** Addition of nuclear DNA content to the AMES risk-group classification for papillary thyroid cancer. *Surgery*. 1992;112:1154–1159; discussion 1159–1160.
11. **Akslen LA.** Prognostic importance of histologic grading in papillary thyroid carcinoma. *Cancer*. 1993;72:2680–2685.
12. **DeGroot LJ, Kaplan EL, McCormick M, Straus FH.** Natural history, treatment, and course of papillary thyroid carcinoma. *J Clin Endocrinol Metab*. 1990;71:414–424.
13. **Hay ID, Bergstralh EJ, Goellner JR, Ebersold JR, Grant CS.** Predicting outcome in papillary thyroid carcinoma: development of a reliable prognostic scoring system in a cohort of 1779 patients sur-

gically treated at one institution during 1940 through 1989. *Surgery.* 1993;114:1050–1057; discussion 1057–1058.

14. **Mazzaferri EL, Jhiang SM.** Long-term impact of initial surgical and medical therapy on papillary and follicular thyroid cancer. *Am J Med.* 1994;97:418–428.

15. **Noguchi S, Murakami N, Kawamoto H.** Classification of papillary cancer of the thyroid based on prognosis. *World J Surg.* 1994;18:552–557.

16. **Shaha AR, Loree TR, Shah JP.** Intermediate-risk group for differentiated carcinoma of thyroid. *Surgery.* 1994;116:1036–1040; discussion 1040–1041.

17. **Sebastian SO, Gonzalez JM, Paricio PP, et al.** Papillary thyroid carcinoma: prognostic index for survival including the histological variety. *Arch Surg.* 2000;135:272–277.

18. **Sugitani I, Kasai N, Fujimoto Y, Yanagisawa A.** A novel classification system for patients with PTC: addition of the new variables of large (3 cm or greater) nodal metastases and reclassification during the follow-up period. *Surgery.* 2004;135:139–148.

19. **Kattan MW, Yu C, Salomon L, Vora K, Touijer K, Guillonneau B.** Development and validation of preoperative nomogram for disease recurrence within 5 years after laparoscopic radical prostatectomy for prostate cancer. *Urology.* 2011;77:396–401.

20. **Lachance JA, Choudhri AF, Sarti M, Modesitt SC, Jazaeri AA, Stukenborg GJ.** A nomogram for estimating the probability of ovarian cancer. *Gynecol Oncol.* 2011;121:2–7.

21. **Klar M, Jochmann A, Foeldi M, et al.** The MSKCC nomogram for prediction the likelihood of non-sentinel node involvement in a German breast cancer population. *Breast Cancer Res Treat.* 2008;112:523–531.

22. **Mariani L, Miceli R, Kattan MW, et al.** Validation and adaptation of a nomogram for predicting the survival of patients with extremity soft tissue sarcoma using a three-grade system. *Cancer.* 2005;103:402–408.

23. **Eilber FC, Brennan MF, Eilber FR, Dry SM, Singer S, Kattan MW.** Validation of the postoperative nomogram for 12-year sarcoma-specific mortality. *Cancer.* 2004;101:2270–2275.

24. **Peeters KC, Kattan MW, Hartgrink HH, et al.** Validation of a nomogram for predicting disease-specific survival after an R0 resection for gastric carcinoma. *Cancer.* 2005;103:702–707.

25. **Hoang T, Xu R, Schiller JH, Bonomi P, Johnson DH.** Clinical model to predict survival in chemonaive patients with advanced non-small-cell lung cancer treated with third-generation chemotherapy regimens based on eastern cooperative oncology group data. *J Clin Oncol.* 2005;23:175–183.

26. **Kattan MW, Karpeh MS, Mazumdar M, Brennan MF.** Postopera-tive nomogram for disease-specific survival after an R0 resection for gastric carcinoma. *J Clin Oncol.* 2003;21:3647–3650.

27. **Brennan MF, Kattan MW, Klimstra D, Conlon K.** Prognostic no-mogram for patients undergoing resection for adenocarcinoma of the pancreas. *Ann Surg.* 2004;240:293–298.

28. **Sorbellini M, Kattan MW, Snyder ME, et al.** A postoperative prog-nostic nomogram predicting recurrence for patients with conven-tional clear cell renal cell carcinoma. *J Urol.* 2005;173:48–51.

29. **Yang L, Shen W, Sakamoto N.** Population-based study evaluating and predicting the probability of death resulting from thyroid cancer and other causes among patients with thyroid cancer. *J Clin Oncol.* 2013;31:468–474.

30. **Gray RJ.** A class of *K*-sample tests for comparing the cumulative incidence of a competing risk. *Ann Stat.* 1988;16:1141–1154.

31. **Fine JP, Gray RJ.** A proportional hazards model for the subdistri-bution of a competing risk. *J Am Stat Assoc.* 1999;94:496–509.

32. **Iasonos A, Schrag D, Raj GV, Panageas KS.** How to build and in-terpret a nomogram for cancer prognosis. *J Clin Oncol.* 2008;26:1364–1370.

33. **Roman S, Lin R, Sosa JA.** Prognosis of medullary thyroid carcinoma: demographic, clinical, and pathologic predictors of survival in 1252 cases. *Cancer.* 2006;107:2134–2142.

34. **Brierley J, Tsang R, Simpson WJ, Gospodarowicz M, Sutcliffe S, Panzarella T.** Medullary thyroid cancer: analyses of survival and prognostic factors and the role of radiation therapy in local control. *Thyroid.* 1996;6:305–310.

35. **American Thyroid Association (ATA) Guidelines Taskforce on Thyroid Nodules and Differentiated Thyroid Cancer.** Revised American Thyroid Association management guidelines for patients with thyroid nodules and differentiated thyroid cancer. *Thyroid.* 2009;19:1167–1214.

36. **Gorlin JB, Sallan SE.** Thyroid cancer in childhood. *Endocrinol Metab Clin North Am.* 1990;19:649–662.

37. **Pathak KA, Leslie WD, Klonisch TC, Nason RW.** The changing face of thyroid cancer in a population based cohort. *Cancer Med.* doi: 10.1002/cam4.103.

38. **Wang TS, Sosa JA.** Thyroid gland: can a nomogram predict death in patients with thyroid cancer? *Nat Rev Endocrinol.* 2013;9:192–193.

39. **Harrell FE Jr, Lee KL, Mark DB.** Multivariable prognostic models: issues in developing models, evaluating assumptions and adequacy, and measuring and reducing errors. *Stat Med.* 1996;15:361–387.

40. **Wolbers M, Koller MT, Witteman JC, Steyerberg EW.** Prognostic models with competing risks: methods and application to coronary risk prediction. *Epidemiology.* 2009;20:555–561.

Cancer Medicine

ORIGINAL RESEARCH

The changing face of thyroid cancer in a population-based cohort

K. Alok Pathak[1,3], William D. Leslie[2], Thomas C. Klonisch[3] & Richard W. Nason[1]

[1]Head and Neck Surgical Oncology, Cancer Care Manitoba, Winnipeg, Canada
[2]Nuclear Medicine, Cancer Care Manitoba, Winnipeg, Canada
[3]Human Anatomy and Cell Science, University of Manitoba, Winnipeg, Canada

Abstract

In North America, the incidence of thyroid cancer is increasing by over 6% per year. We studied the trends and factors influencing thyroid cancer incidence, its clinical presentation, and treatment outcome during 1970–2010 in a population-based cohort of 2306 consecutive thyroid cancers in Canada, that was followed up for a median period of 10.5 years. Disease-specific survival (DSS) and disease-free survival were estimated by the Kaplan–Meier method and the independent influence of various prognostic factors was evaluated by Cox proportional hazard models. Cumulative incidence of deaths resulting from thyroid cancer was calculated by competing risk analysis. A P-value <0.05 was considered to indicate statistical significance. The age standardized incidence of thyroid cancer by direct method increased from 2.52/100,000 (1970) to 9.37/100,000 (2010). Age at diagnosis, gender distribution, tumor size, and initial tumor stage did not change significantly during this period. The proportion of papillary thyroid cancers increased significantly ($P < 0.001$) from 58% (1970–1980) to 85.9% (2000–2010) while that of anaplastic cancer fell from 5.7% to 2.1% ($P < 0.001$). Ten-year DSS improved from 85.4% to 95.6%, and was adversely influenced by anaplastic histology (hazard ratio [HR] = 8.7; $P < 0.001$), male gender (HR = 1.8; $P = 0.001$), TNM stage IV (HR = 8.4; $P = 0.001$), incomplete surgical resection (HR = 2.4; $P = 0.002$), and age at diagnosis (HR = 1.05 per year; $P < 0.001$). There was a 373% increase in the incidence of thyroid cancer in Manitoba with a marked improvement in the thyroid cancer-specific survival that was independent of changes in patient demographics, tumor stage, or treatment practices, and is largely attributed to the declining proportion of anaplastic thyroid cancers.

Introduction

Thyroid cancer is the most common malignant endocrine tumor and is the seventh most common cancer seen in Canadians with an estimated 5650 new thyroid cancers diagnosed in 2012 [1]. In Canada, the incidence of thyroid cancer is increasing more rapidly than any other cancer; by 6.8% per year in Canadian males (1998–2007) and by 6.9% per year in Canadian females (2002–2007) [1]. Similar trends have been reported globally [2–13]. By direct method, the age standardized incidence rate (ASIR) of thyroid cancer per 100,000 Canadians has increased from 1.1 in 1970–1972 to 6.1 in 2012 for males, and from

3.3 to 22.2 in females during the same period [1, 14]. The trends in the United States (US) mirror that of Canada with a threefold increase in the incidence of thyroid cancer from 4.85/100,000 in 1975 to 14.25/100,000 in 2009 and an annual percent increase (2000–2009) of 6.0% for the US males and 6.9% for the US females [15]. The age and delay adjusted incidence rate of thyroid cancer between 2006 and 2010 was 6.1/100,000 for the US males and 18.2/100,000 for the US females using joint point regression program. An estimated 56,460 new cases of thyroid cancers are likely to be seen in the US in 2012 and 1780 will die from it. The life time probability of developing a thyroid cancer for a Canadian female is 1 in

71 (1.4%) but only 1 in 1374 (0.1%) will actually die from it [16]. Canadian males have a lower life time risk of developing thyroid cancer at 1 in 223 (0.4%) with the risk of death from thyroid cancer at 1 in 1937 (0.1%).

Although the incidence of thyroid cancer has been rising, it had an excellent 5-year relative survival ratio of 98% in 2011 [16]. Thyroid cancers represent a conglomerate of different histological types that have diverse clinical behavior. Differentiated thyroid cancers (papillary and follicular) typically have an excellent survival, whereas poorly differentiated and anaplastic thyroid cancers have a very poor outcome. Although the time trends in the incidence of thyroid cancer in Canada have been reported earlier [14, 17], little has been recorded about the trends in outcome of thyroid cancer in a population cohort. The objective of this study was to assess the trends in the incidence, clinical presentation, treatment practices, and disease outcome of thyroid cancer in a population-based cohort spanning four decades from 1970 to 2010.

Patients and Methods

Study group

Manitoba thyroid cancer cohort is a historical cohort that includes all 2306 consecutive thyroid cancers observed in 2296 patients in the province of Manitoba, Canada, from 1 January 1970 to 31 December 2010, as registered in the Manitoba Cancer Registry. The Manitoba Cancer Registry is a member of the North American Association of Central Cancer Registries which administers a program that reviews member registries for their ability to produce complete, accurate, and timely data. CancerCare Manitoba is the sole comprehensive cancer care center in the province where all the cancer patients from the province are primarily referred and the Manitoba Cancer Registry is a part of CancerCare Manitoba. Ethics approval for this study was obtained from the Research Ethics Board at the University of Manitoba.

We reviewed individual electronic and paper records of diagnosis and treatment for this cohort of patient. The primary source of diagnostic information included 2148 pathology reports, 80 discharge summaries, 56 autopsy records, 18 operative reports, and 4 death certificates. ASIR was calculated by direct method (1). Age-specific incidence rates were initially calculated by using the age distributions of the newly diagnosed thyroid cancers cases in the province and that of the provincial population for each year obtained from the Manitoba Health's population registry, Manitoba Bureau of Statistics [18] and Statistics Canada [19]. Age-specific incidences were then applied to the 1991 standard Canadian population [1] to calculate the ASIR per 100,000 population.

Patient demographics, extent of disease at initial presentation; the treatment modalities employed; pathology details; cancer recurrences during follow-up and final outcome status as of 1 January 2013 were recorded. All patients who migrated out of province (considered lost to follow-up) or died during the study period, were censored at that point in time. All cases were restaged according to the American Joint Cancer Committee/Union Internationale Contre le Cancer (AJCC/UICC) staging for thyroid cancer (7th edition, 2009); the topography and the histology were recoded by WHO International Classification of Diseases for Oncology (3rd Edition) codes and the disease, signs, and symptoms by International Classification of Diseases (10th edition) codes to ensure uniformity. The pathology and treatment details of 683 (29.6%) were independently reviewed for accuracy as a part of a collaborative staging project.

Statistical analysis

Analysis of variance was used to compare group means, and categorical data were compared using the Pearson chi-square test with continuity correction, as appropriate. A P-value <0.05 was considered to indicate statistical significance and 95% confidence intervals were used to express reliability in the estimates. After checking for normality assumption the mean and standard deviation were used to express normally distributed data (such as age of the patients) and median with interquartile range were used for nonnormally distributed data (such as tumor size and follow-up). The data were managed and analyzed using SPSS for Windows version 20.0 (SPSS Inc., Chicago, IL). Disease-free survival (DFS) and disease-specific survival (DSS) were estimated by the Kaplan–Meier product limit method, and the effect of individual prognostic factors on survival was assessed by using the log rank test. Multivariate analyses were performed with Cox proportional hazard models to assess the independent effect of prognostic factors on DSS after testing for the proportional hazard assumption. The competing influence of other causes of mortality, such as death due to a second primary tumor or noncancer deaths, was analyzed by competing risk regression model using STATA version 12 (StataCorp. TX).

Results

Study cohort

In total, 2306 thyroid cancers were observed in Manitoba in 2296 patients from 1970 to 2010. Nine patients had a synchronous second primary tumor of a different histology along with papillary thyroid cancer (follicular-3,

hürthle cell-3, medullary-2, poorly differentiated-1), while one patient had a metachronous second papillary carcinoma in the contra-lateral thyroid lobe 25 years after initial management. According to 2011 census, the population of Manitoba was recorded at 1,208,268 that increased by an average of 0.56% per year from 1970 level of 988,245. The number of newly diagnosed thyroid cancers increased from 22 in 1970 to 122 in 2010, and the ASIR per 100,000 for thyroid cancer from 2.52 (95% confidence interval [CI] = 1.57–3.83) in 1970 to 9.37 (95% CI = 7.65–11.08) in 2010 (Fig. 1). The ASIR per 100,000 rose from 0.72 (95% CI = 1.57–3.83) in 1970 to 4.94 (95% CI = 3.35–7.03) in 2010 for males and the respective rates for females went up from 4.28 (95% CI = 2.56–6.71) to 13.75 (95% CI = 10.96–17.04). The ASIR per 100,000 for anaplastic thyroid cancers fell from 0.11 (95% CI = 0.05–0.19) during 1970–1980 to 0.05 (95% CI = 0.02–0.11) in 2001–2010 for both sexes and the respective rates for papillary thyroid cancer went up from 0.93 (95% CI = 0.75–1.15) to 6.64 (95% CI = 6.17–7.11).

The Manitoba thyroid cancer cohort included 570 (24.8%) males and 1726 (75.2%) females with a mean age (±standard deviation) of 49 ± 18 years. The mean age of patients at the time of diagnosis, median tumor size, and the tumor stage at presentation showed statistically nonsignificant change ($P > 0.05$, NS) over the past four decades (Table 1). Thyroid cancers ≤10 mm (microcarcinoma) represented 23.4% of all thyroid cancers and this proportion did not change significantly ($P = 0.87$) during the study period. Lymph node involvement was present in 23.7% cases and distant metastasis in 3.9% cases at the time of diagnosis. Multifocal disease was observed in 32.3% cases, gross extrathyroidal extension of tumor in 20.9% cases, and complete surgical excision of gross tumor was achieved in 96.1% cases. The distribution of T stage ($P = 0.50$), N stage ($P = 0.27$), and M stage ($P = 0.61$) as well as the proportion of patients with multifocal disease ($P = 0.26$), gross extrathyroidal extension of tumor ($P = 0.66$) or with complete excision of tumor ($P = 0.40$) remained unchanged during the study period.

Papillary thyroid cancer was the most common histological type, and the proportion of papillary thyroid cancers steadily increased from 58.0% (1970–1980) to 85.9% (2000–2010). Most of the thyroid cancers were classical papillary thyroid cancers (46.9%), followed by follicular (24.2%), encapsulated (2.3%), and microinvasive (1.6%) variants. Sclerosing, solid, tall cell, and columnar cell variants together accounted for only 1.9% of all thyroid cancers. During the same period, the proportion of all thyroid cancers that were diagnosed as follicular variants of papillary thyroid cancer increased from 12.4% to 32.9% (Table 1), whereas the proportion of follicular carcinoma fell from 26% to 5.1% ($P < 0.001$) and anaplastic carcinoma from 5.7% to 2.1% ($P < 0.001$). The proportion of medullary thyroid carcinoma has remained nearly unchanged. Total thyroidectomy was performed in 55.1% cases and 34.8% had adjuvant radioactive iodine (RAI). The percentage of the patients undergoing total thyroidectomy increased by two and a half times between 1970 and 1980 and 2001–2010 ($P < 0.001$) while those receiving adjuvant RAI increased by over five times ($P = 0.004$).

Oncological outcome of thyroid cancer

In all, 201 patients died from thyroid cancer (case fatality rate 8.8%). The case fatality rate for different histological types of thyroid cancer is summarized in Table 2. Of all deaths due to thyroid cancer, 63 (31.3%) had papillary carcinoma, 60 (29.9%) anaplastic, 24 (11.9%) follicular, 21 (10.4%) medullary, 15 (7.5%) hürthle cell, 8 (4%) poorly differentiated, and 10 (5%) had unspecified thyroid carcinoma. The 10-year DSS of Manitoba thyroid cancer cohort ($N = 2296$) was 91.8% (95% CI = 90.5–92.9%), which improved significantly from 85.4% (1970–1980) to 95.6% (2001–2010) (Table 1). Tumor histology had a very significant impact on the DSS and DFS survivals (Table 2). Papillary thyroid cancer had the best DSS rates (96.8% at 10 years and 94.6% at 20 years), whereas only 7.3% with anaplastic cancer survived for 10 years. The cumulative incidence function (CIF) by competing risk regression analysis (Fig. 2) shows an 8.1% reduction (from 12.6% to 4.5%) in death due to thyroid cancer at 10 years of follow-up.

Treatment outcomes were assessed in the 2065 patients who underwent primary surgical treatment with radical
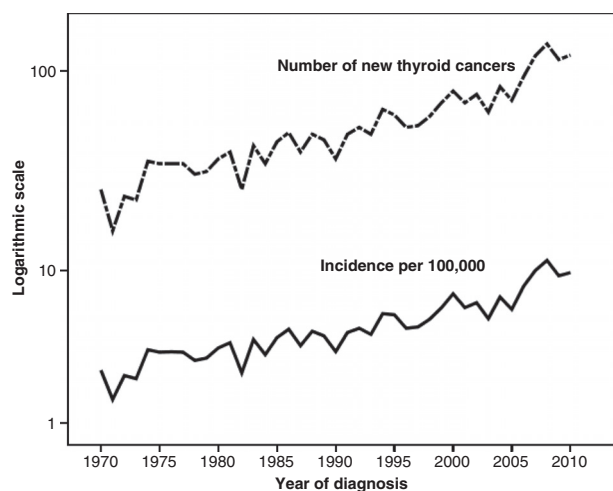

Figure 1. Trends in the age standardized incidence, the number of newly diagnosed thyroid cancers in Manitoba, Canada (1970–2010).

Table 1. Clinical characteristics of thyroid cancer by decade of presentation.

	1970–1980 (N = 331)	1981–1990 (N = 410)	1991–2000 (N = 594)	2001–2010 (N = 971)	P-value
Mean age in years	49.3 ± 18.4	47.5 ± 18.6	48.0 ± 18.7	49.1 ± 17.0	0.14 (NS)
Gender ratio (female:male)	2.5:1	2.8:1	3.6:1	3:1	0.45 (NS)
Median tumor size (interquartile range)	19.9 (15–22) mm	20 (20–25) mm	21 (20–24) mm	20 (19–22) mm	0.44 (NS)
Tumor size distribution					
≤1 cm	75 (22.6%)	117 (28.5%)	153 (25.8%)	242 (24.9%)	0.13 (NS)
1–2 cm	110 (33.2%)	93 (22.7%)	143 (24.1%)	247 (25.5%)	
2–4 cm	108 (32.6%)	152 (37.0%)	197 (33.1%)	310 (31.9%)	
>4 cm	38 (11.6%)	48 (11.8%)	101 (17.0%)	172 (17.7%)	
Stage I	207 (62.6%)	280 (68.4%)	380 (64.0%)	610 (62.8%)	0.22 (NS)
Stage II	23 (6.9%)	34 (8.3%)	62 (10.4%)	120 (12.4%)	
Stage III	32 (9.7%)	52 (12.6%)	62 (10.4%)	125 (12.9%)	
Stage IV	69 (20.8%)	44 (10.7%)	90 (15.2%)	116 (11.9%)	
Total thyroidectomy	94 (28.4%)	159 (38.9%)	293 (49.3%)	691 (71.2%)	<0.001
Adjuvant radioactive iodine	36 (10.9%)	79 (19.3%)	177 (29.8%)	603 (62.1%)	0.004
Histology					
Papillary (%)	192 (58.0%)	278 (67.8%)	459 (77.3%)	834 (85.9%)	<0.001
Follicular (%)	86 (26.0%)	70 (17.1%)	62 (10.4%)	50 (5.1%)	
Hürthle cell (%)	3 (0.9%)	24 (5.9%)	22 (3.7%)	36 (3.7%)	
Poorly differentiated (%)	9 (2.7%)	1 (0.2%)	3 (0.5%)	3 (0.3%)	
Medullary (%)	17 (5.1%)	24 (5.9%)	17 (2.9%)	21 (2.2%)	
Anaplastic (%)	19 (5.7%)	9 (2.2%)	24 (4.0%)	20 (2.1%)	
Unspecified (%)	5 (1.5%)	4 (1%)	7 (1.2%)	7 (0.7%)	
Median follow-up in months (95% CI)	419.4 (409.9–428.9)	304.9 (296.2–313.7)	188.4 (182.5–194.3)	68.5 (65.4–71.6)	<0.001
10 year DSS (N = 2296)	85.4 (82.9–90.0)%	92.2 (89.1–94.5)%	89.3 (86.5–91.6)%	95.6 (90.5–96.6)%	<0.001
Posttreatment 10 year DFS (N = 2065)	86.6 (81.1–90.6)%	88.9 (85.1–91.8)%	88.1 (84.7–90.6)%	91.9 (89.2–94.1)%	0.18 (NS)

Table 2. Case fatality rate and survival by histological types of thyroid cancers.

	Case fatality rate	10 year DSS (95% CI)	20 year DSS (95% CI)	10 year DFS (95% CI)	20 year DFS (95% CI)
Papillary	3.6%	96.8 (95.7–97.7)%	94.6 (92.9–95.9)%	87.7 (85.9–89.4)%	84.8 (82.5–86.9)%
Follicular	9.0%	91.5 (87.0–94.5)%	88.6 (83.1–92.4)%	87.3 (82.4–91.0)%	86.1 (80.8–90.0)%
Hürthle cell	17.6%	81.4 (69.7–89.0)%	75.6 (61.2–85.2)%	69.8 (57.9–79.0)%	69.8 (57.9–79.0)%
Poorly differentiated	31.2%	74.1 (28.9–93.0)%	74.1 (28.9–93.0)%	27.3 (6.5–53.9)%	27.3 (6.5–53.9)%
Medullary	26.9%	77.6 (65.4–85.9)%	62.6 (47.5–74.5)%	52.0 (38.5–63.9)%	43.1 (28.9–56.6)%
Anaplastic	83.3%	7.3 (2.4–15.9)%	7.3 (2.4–15.9)%	1.4 (0.1–6.7)%	1.4 (0.1–6.7)%
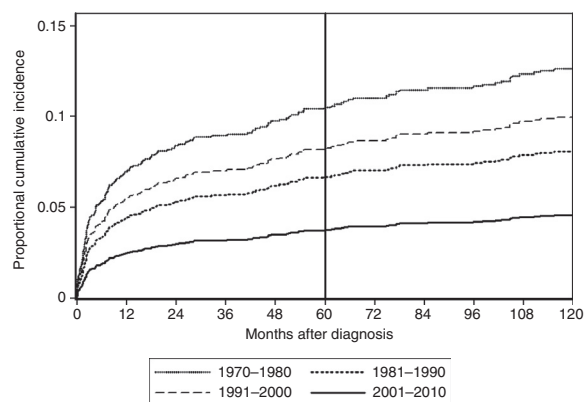
Figure 2. Cumulative incidence of death resulting from thyroid cancer over 10 years.

intent in Manitoba; after excluding cases that were diagnosed only on autopsy or death report ($n = 60$), those who died before surgery ($n = 64$), nonsurgical candidates ($n = 35$) or those who refused treatment ($n = 24$), and if primary surgery or follow-up performed in another province/country ($n = 48$). During median follow-up of 10.5 years (interquartile range = 4.8–18.8 years), 78 (3.8%) patients had posttreatment residual disease and another 200 (9.7%) patients had recurrence of disease at least 6 months after successful initial treatment. The recurrences were in the residual thyroid lobe or thyroid bed in 23 (11.5%) cases, in the central compartment of neck in 64 (32%), in the lateral compartment of neck in 44 (22%), at a distant metastatic site in 54 (27%), and at multiple sites in 15 (7.5%) cases. Ten-year DFS of the surgically treated patients was 89.3% (95%

Table 3. Multivariate analysis by Cox proportional hazard models for independent influence of prognostic factors on disease-specific survival.

Prognostic factor	Hazard ratio (95% confidence interval)
Age at the time of diagnosis (per year)	1.05 (1.03–1.06), $P < 0.001$
Gender (male vs. female)	1.79 (1.28–2.51), $P = 0.001$
Extent of thyroidectomy (hemi vs. total)	0.991 (0.60–1.64), $P = 0.971$ (NS)
Completeness of resection (incomplete vs. complete)	2.40 (1.37–4.19), $P = 0.002$
Adjuvant radioactive iodine (RAI vs. no RAI)	1.59 (0.91–2.79), $P = 0.101$ (NS)
AJCC TNM stage grouping	
Stage I	1.00 (reference)
Stage II	1.94 (0.78–4.84), $P = 0.155$ (NS)
Stage III	2.30 (1.00–5.29), $P = 0.05$
Stage IV	8.37 (3.99–17.54), $P < 0.001$
Histology	
Papillary	1.00 (reference)
Anaplastic	8.66 (5.18–14.49), $P < 0.001$
Medullary	2.62 (1.48–4.66), $P = 0.001$
Hürthle	2.23 (1.21–4.14), $P = 0.010$
Follicular	1.76 (1.01–3.09), $P = 0.047$
Decade of diagnosis	
1970–1980	1.00 (reference)
1981–1990	0.92 (0.56–1.53), $P = 0.753$ (NS)
1991–2000	1.40 (0.91–2.17), $P = 0.126$ (NS)
2001–2010	0.65 (0.40–1.08), $P = 0.096$ (NS)

CI = 87.7–90.8%) that has not changed significantly over the last four decades (Table 1).

On multivariate analysis by Cox proportional hazard model, DSS was adversely influenced independently by nonpapillary histology especially anaplastic (hazard ratio [HR] = 8.7; 95% CI = 5.2–14.5; $P < 0.001$), male gender (HR = 1.8; 95% CI = 1.3–2.5; $P = 0.001$), TNM stage III (HR = 2.30; 95% CI = 1.00–5.29, $P = 0.05$), and IV (HR = 8.37; 3.99–17.54, $P < 0.001$), incomplete surgical resection (HR = 2.4; 95% CI = 1.4–4.2, $P = 0.002$), and age at diagnosis (HR = 1.05 per year; 95% CI = 1.03–1.06; $P < 0.001$). Each of these factors, except the histology has remained unchanged during the study period (Table 1). The extent of thyroidectomy, use of adjuvant RAI, or the decade of diagnosis did not have any significant influence on DSS (Table 3). Competing risk subhazard model confirmed these observations of Cox regression analysis.

Discussion

A cohort is a population group, or subset thereof, that is followed over a period of time. The members of the cohort, based on defined criteria, share common experience which in this study was diagnosis of thyroid cancer in the province of Manitoba. By virtue of the residence in the same province our study cohort was expected to share similar risk of exposure and get similar standard of medical care in the publicly funded health care system of the province. The incidence trends of thyroid cancers in the US were reported by using the Surveillance, Epidemiology, and End Results (SEER) database, which is robust but it has its inherent limitations in terms of coverage, coding reliability, patient migration to an area that is not covered by SEER and limited information on the treatment details of the patients. These limitations make it difficult to interpret the time trend in treatment of thyroid cancer and its influence on thyroid cancer related survival. Due to the excellent treatment outcome of most thyroid cancers, randomized controlled trials to assess treatment response will require prohibitively large sample size and resources and therefore, they are not readily feasible [20]. A population-based cohort with low attrition rates such as ours (only 2.1% loss to follow-up over 40 years) is the probably the best possible model to study the time trends in thyroid cancer survival. As all members of the cohort received the same treatment, that was the standard of care for their era, and their medical records were individually reviewed for accuracy and completeness; our study cohort was a reliable and stable model to study the trends and factors influencing survival of patients with thyroid cancer.

Our study shows that the incidence of thyroid cancer in the province of Manitoba has increased by 373% from 1970 to 2010 that has resulted largely from an increase in the number of papillary thyroid cancers (Table 1). The proportion of cancers classified as follicular variant of papillary thyroid cancer has almost tripled from 12.4% to 32.9%; this has also contributed to the increase in the proportion of papillary thyroid cancer. At the same time, the proportion of follicular thyroid cancer has decreased from 26% to 5.1%, possibly due to a change in the criteria for diagnosing papillary carcinoma after 1988, whereby, all lesions with typical cytological features (ground-glass nuclei, nuclear grooves, and psammoma bodies) were classified as papillary carcinoma even if they did not show papillae [21]. Thus, many erstwhile follicular thyroid cancers are rechristened as follicular variant of papillary thyroid cancer. During the last four decades, the 10-year DSS has improved from 85.4% to 95.6%, whereas the 10 year DFS has remained stable (86.6–91.9%).

In 2012, thyroid cancers ($N = 5650$) were expected to account for 2.1% of all cancers ($N = 267,700$) in Canada [1]. The number of the newly diagnosed thyroid cancer in the province of Manitoba has increased by over threefold in the last four decades which is congruent with

reports from Canada and other countries [2–13]. However, this increase in our study cohort has not been restricted to the smaller thyroid cancers as has been thought of earlier [2, 4, 7, 17]. We observed an increase in the number of thyroid cancers of all sizes, which is a true increase in the incidence of thyroid cancer in Manitoba and it cannot be explained only by over diagnosis of subclinical disease. A single cause for this increase is not apparent and this may be multifactorial due to iodine deficiency [22], radiation exposure [23–25], long-standing goiters, and family history [26]. The shift in histological pattern of thyroid cancer has been reported from other regions also [27]. The decrease in proportion of anaplastic carcinoma could be a result of more aggressive treatment of goiters and differentiated thyroid cancers by thyroidectomies before they could undergo anaplastic transformation. The proportion of tumors >2 cm in our cohort is higher than that reported earlier [7, 16, 28], because of the strict criteria for fine needle biopsy of thyroid in Manitoba. Most of the microcarcinomas in our study were incidentally detected in thyroidectomy or autopsy specimens. Even before the introduction of the American Thyroid Association guidelines [29], which recommend threshold sizes of >1 cm (hypoechoic solid nodule), 1–1.5 cm (iso or hyperechoic solid nodule), 1.5–2 cm (mixed cystic–solid nodule with suspicious features), and ≥2.0 cm (mixed cystic–solid nodule without suspicious features) in a low-risk patient without cervical lymphadenopathy or microcalcification, radiologist and surgeons were very conservative in their approach. This is also reflected by a large proportion of patients (44.9%) having less than a total thyroidectomy.

During 1970–2010, the DSS for thyroid cancer has improved by 10.2%, cumulative incidence of death due to thyroid cancer fell by 8.1%, whereas the DFS for patients treated with radical intent has remained unchanged (Table 1). This improvement is not because of an increase in the proportion of early-stage disease or smaller tumors in recent years (Table 1). Although both total thyroidectomy and adjuvant RAI treatment have been used more often during the recent time (Table 1), they did not have any significant impact on DSS (Table 3). To maintain homogeneity of data across the study period, only clinically and radiologically detectable disease relapses were considered as recurrences. Isolated hyperthyroglobulinemia was not considered as an evidence of recurrence. More aggressive treatment of early stage disease has not resulted in a significantly better disease control, as reflected by a stable disease free survival during this period. Therefore, the aggressive use of adjuvant RAI should be judiciously balanced against the treatment-related morbidities and the risk of developing second primary cancer.

On multivariate analysis, DSS was negatively influenced by nonpapillary tumor histology, male gender, advanced tumor stage, incomplete surgical resection, and older age at diagnosis (Table 3). Patient demographics, completeness of surgery, and initial cancer stage have not changed significantly in our study cohort (Table 1), however, there has been a marked change in the relative proportion of various types of thyroid cancer diagnosed over this time period. The proportion of papillary thyroid cancer has increased from 58% (1970–1980) to 85.9% (2000–2010) and the proportion of anaplastic cancers fell from 5.7% (1970–1980) to 2.1% (2001–2010). As papillary thyroid cancer has the best survival rates (96.8% at 10 years) and anaplastic thyroid cancer has the worst (7.3% survival at 10 years), the opposite trends in the relative incidence of papillary and anaplastic thyroid cancers is most likely responsible for the improved outcome of thyroid cancer (Tables 1 and 2). After controlling for other independent prognostic factors influencing DSS of thyroid cancer in a multivariate model, there was no difference in the DSS of thyroid cancer observed over the last four decades (Table 3).

A time span of four decades is both strength as well as a limitation of our study as the diagnostic criteria, staging, and treatment recommendations have evolved over time. We tried to circumvent this challenge by uniformly restaging all cancers using the 2009 AJCC/UICC Cancer Staging System for thyroid cancer. Additionally, as a part of our collaborative staging project, the pathology and treatment details of 683 (29.6%) cases were independently reviewed for accuracy and topography, and histology were recoded by WHO International Classification of Diseases for Oncology (3rd edition) codes. In view of prolonged course of most thyroid cancers, it is possible that other causes of mortality, unrelated to thyroid cancer, could result in overestimation of thyroid cancer deaths by Kaplan–Meir method. Consequently, we used competing risk regression to obtain unbiased estimation of cumulative incidence of deaths resulting from thyroid cancer which showed a significant change over the study period. A competing risk is an event the occurrence of which either precludes or changes the probability of occurrence of another event of interest. In this study deaths to second primary cancer and noncancer deaths were treated as competing risks.

To conclude, we observed a true increase in the incidence of thyroid cancer in the province of Manitoba that cannot be attributed to over diagnosis of subclinical disease alone. A 10.2% improvement in DSS of thyroid cancer over the last four decades in our population cohort was independent of early diagnosis or more aggressive treatment. The major factor contributing to this improvement in survival is the increasing proportion of papillary

thyroid carcinoma diagnoses and a corresponding decrease in anaplastic thyroid carcinoma diagnoses, as outcomes for the former are usually excellent whereas outcomes for the latter are typically dismal.

Acknowledgments

Conflict of Interest

None declared.

References

1. Canadian Cancer Society's Steering Committee on Cancer Statistics. 2012. Pp. 7–60 *in* Canadian cancer statistics. 2012. Canadian Cancer Society, Toronto, ON.

2. Enewold, L., K. Zhu, E. Ron, A. J. Marrogi, A. Stojadinovic, G. E. Peoples, et al. 2009. Rising thyroid cancer incidence in the United States by demographic and tumor characteristics, 1980–2005. Cancer Epidemiol. Biomarkers Prev. 18:784–791.

3. Jung, K. W., S. Park, H. J. Kong, Y. J. Won, J. Y. Lee, H. G. Seo, et al. 2012. Cancer statistics in Korea: incidence, mortality, survival, and prevalence in 2009. Cancer Res. Treat. 44:11–24.

4. Grodski, S., T. Brown, S. Sidhu, A. Gill, B. Robinson, D. Learoyd, et al. 2008. Increasing incidence of thyroid cancer is due to increased pathologic detection. Surgery 144: 1038–1043.

5. Burgess, J. R., and P. Tucker. 2006. Incidence trends for papillary thyroid carcinoma and their correlation with thyroid surgery and thyroid fine-needle aspirate cytology. Thyroid 16:47–53.

6. Colonna, M., A. V. Guizard, C. Schvartz, M. Velten, N. Raverdy, F. Molinie, et al. 2007. A time trend analysis of papillary and follicular cancers as a function of tumor size: a study of data from six cancer registries in France (1983–2000). Eur. J. Cancer 43:891–900.

7. Davies, L., and H. G. Welch. 2006. Increasing incidence of thyroid cancer in the United States, 1973–2002. JAMA 295:2164–2167.

8. Yu, G. P., J. C. Li, D. Branovan, S. McCormick, and S. P. Schantz. 2010. Thyroid cancer incidence and survival in the national cancer institute surveillance, epidemiology, and end results race/ethnicity groups. Thyroid 20:465–473.

9. Leenhardt, L., P. Grosclaude, and L. Cherie-Challine. 2004. Increased incidence of thyroid carcinoma in France: a true epidemic or thyroid nodule management effects? Report from the French Thyroid Cancer Committee. Thyroid 14:1056–1060.

10. Lubina, A., O. Cohen, M. Barchana, I. Liphshiz, I. Vered, S. Sadetzki, et al. 2006. Time trends of incidence rates of thyroid cancer in Israel: what might explain the sharp increase. Thyroid 16:1033–1040.

11. Reynolds, R. M., J. Weir, D. L. Stockton, D. H. Brewster, T. C. Sandeep, and M. W. Strachan. 2005. Changing trends in incidence and mortality of thyroid cancer in Scotland. Clin. Endocrinol. (Oxf) 62:156–162.

12. Smailyte, G., E. Miseikyte-Kaubriene, and J. Kurtinaitis. 2006. Increasing thyroid cancer incidence in Lithuania in 1978–2003. BMC Cancer 6:284.

13. Fahey, T. J., T. S. Reeve, and L. Delbridge. 1995. Increasing incidence and changing presentation of thyroid cancer over a 30-year period. Br. J. Surg. 82:518–520.

14. Liu, S., R. Semenciw, A. M. Ugnat, and Y. Mao. 2001. Increasing thyroid cancer incidence in Canada, 1970-1996: time trends and age-period-cohort effects. Br. J. Cancer 85:1335–1339.

15. Howlader, N., A. M. Noone, M. Krapcho, N. Neyman, R. Aminou, W. Waldron, et al. (eds). SEER Cancer Statistics Review, 1975-2009 (Vintage 2009 Populations), National Cancer Institute, Bethesda, MD. Available at http://seer.cancer.gov/csr/1975_2009_pops09/, based on November 2011 SEER data submission, posted to the SEER web site (accesses April 2012).

16. Canadian Cancer Society's Steering Committee on Cancer Statistics. 2011. Pp. 25–60 *in* Canadian cancer statistics 2011. Canadian Cancer Society, Toronto, ON.

17. Kent, W. D. T., S. F. Hall, P. A. Isotalo, R. L. Houlden, R. L. George, and P. A. Groome. 2007. Increased incidence of differentiated thyroid carcinoma and detection of subclinical disease. CMAJ 177:1357–1361.

18. Manitoba Bureau of Statistics 2012. Pp. 1–7 *in* Latest population estimates. Winnipeg, MB.

19. Statistics Canada: Manitoba population trend. 2012. Available at http://www.statcan.gc.ca/tables-tableaux/sum-som/l01/cst01/demo62h-eng.htm (accessed 28 May 2012).

20. Carling, T., S. E. Carty, M. M. Ciarleglio, D. S. Cooper, G. M. Doherty, L. T. Kim, et al. 2012. American Thyroid Association Surgical Affairs Committee: American Thyroid Association design and feasibility of a prospective randomized controlled trial of prophylactic central lymph node dissection for papillary thyroid carcinoma. Thyroid 22:237–244.

21. Hedinger, C. 1988. Histological typing of thyroid tumours, 2nd ed. Springer-Verlag, Berlin Heidelberg.

22. Galanti, M. R., L. Hansson, R. Bergstrom, A. Wolk, A. Hjartåker, E. Lund, et al. 1997. Diet and the risk of

papillary and follicular thyroid carcinoma: a population-based case–control study in Sweden and Norway. Cancer Causes Control 8:205–214.

23. Sont, W. N., J. M. Zielinski, J. P. Ashmore, H. Jiang, D. Krewski, M. E. Fair, et al. 2001. First analysis of cancer incidence and occupational radiation exposure based on the national dose registry of Canada. Am. J. Epidemiol. 153:309–318.

24. Fincham, S. M., A. M. Ugnat, G. B. Hill, N. Kreiger, and Y. Mao. 2000. Is occupation a risk factor for thyroid cancer Canadian cancer registries epidemiology research group. J. Occup. Environ. Med. 42:318–324.

25. Fraker, D. L. 1995. Radiation exposure and other factors that predispose to human thyroid neoplasia. Surg. Clin. North Am. 75:365–375.

26. Haselkorn, T., L. Bernstein, S. Preston-Martin, W. Cozen, and W. J. Mack. 2000. Descriptive epidemiology of thyroid cancer in Los Angeles County, 1972–1995. Cancer Causes Control 11:163–170.

27. Han, J. M., W. B. Kim, T. Y. Kim, J. S. Ryu, G. Gong, S. J. Hong, et al. 2012. Time trend in tumor size and characteristics of anaplastic thyroid carcinoma. Clin. Endocrinol. (Oxf) 77:459–464.

28. Busco, S., P. Giorgi Rossi, I. Sperduti, P. Pezzotti, C. Buzzoni, and F. Pannozzo. 2013. Increased incidence of thyroid cancer in Latina, Italy: a possible role of detection of subclinical disease. Cancer Epidemiol. 37:262–269.

29. American Thyroid Association (ATA) Guidelines Taskforce on Thyroid Nodules and Differentiated Thyroid Cancer, D. S., Cooper, G. M., DohertyB. R. Haugen, R. T. Kloos, S. L. Lee, S. J. Mandel, E. L. Mazzaferri, B. McIver, F. Pacini, M. Schlumberger, S. I. Sherman, D. L. Steward, and R. M. Tuttle. 2009. Revised American Thyroid Association management guidelines for patients with thyroid nodules and differentiated thyroid cancer. Thyroid 19:1167–1214.

Identifying the most appropriate age threshold for TNM stage grouping of well-differentiated thyroid cancer

J. Hendrickson-Rebizant, H. Sigvaldason, R.W. Nason, K.A. Pathak*

Section of Surgical Oncology, CancerCare Manitoba, Department of Surgery, University of Manitoba, Winnipeg R3E 0V9, Canada

Abstract

Objective: Age is integrated in most risk stratification systems for well-differentiated thyroid cancer (WDTC). The most appropriate age threshold for stage grouping of WDTC is debatable. The objective of this study was to evaluate the best age threshold for stage grouping by comparing multivariable models designed to evaluate the independent impact of various prognostic factors, including age based stage grouping, on the disease specific survival (DSS) of our population-based cohort.

Methods: Data from population-based thyroid cancer cohort of 2125 consecutive WDTC, diagnosed during 1970–2010, with a median follow-up of 11.5 years, was used to calculate DSS using the Kaplan Meier method. Multivariable analysis with Cox proportional hazard model was used to assess independent impact of different prognostic factors on DSS. The Akaike information criterion (AIC), a measure of statistical model fit, was used to identify the most appropriate age threshold model. Delta AIC, Akaike weight, and evidence ratios were calculated to compare the relative strength of different models.

Results: The mean age of the patients was 47.3 years. DSS of the cohort was 95.6% and 92.8% at 10 and 20 years respectively. A threshold of 55 years, with the lowest AIC, was identified as the best model. Akaike weight indicated an 85% chance that this age threshold is the best among the compared models, and is 16.8 times more likely to be the best model as compared to a threshold of 45 years.

Conclusion: The age threshold of 55 years was found to be the best for TNM stage grouping.

© 2015 Elsevier Ltd. All rights reserved.

Keywords: Thyroid carcinoma; Risk stratification; Prognosis; Survival; Outcome; Staging

Introduction

Well-differentiated thyroid carcinoma (WDTC) arises from the thyroid follicular epithelial cells and accounts for over 90% of all thyroid malignancies.[1] This group is comprised of different histologic sub-types, including papillary, follicular, and Hürthle cell variant of follicular carcinoma in descending order of incidence and is associated with an excellent prognosis.[2,3]

Multitudes of risk stratification staging systems have been developed over the years for stratifying patients based on tumor and patient characteristics.[4–13] The age at diagnosis is universally considered to be a strong prognostic indicator, and has been consistently utilized in various scoring systems along with gender, the size and extension of the primary tumor, and the presence of distant metastases.[2,3,14–16] Recently published prognostic nomograms for thyroid cancer showed age to be an important determinant of risk of death from thyroid cancer.[17]

Although age has been consistently included as a risk factor in most of the risk stratification systems, there is a lack of consensus regarding the appropriate age threshold to be adopted for stage grouping. The selection of an appropriate age threshold is critically important, as an inaccurate value can lead to either over-treatment of low-risk patients, or under-treatment of high-risk ones. An age threshold of 45 years is currently used by the AJCC-TNM system for stage grouping of WDTC.[7] Those less than 45 years of age are considered low risk and staged I

* Corresponding author. 2048, CancerCare Manitoba, 675 McDermot Avenue, Winnipeg R3E 0V9, Canada. Tel.: +1 204 7878040 (office); fax: +1 204 7872768.

E-mail address: alok.pathak@cancercare.mb.ca (K.A. Pathak).

or II, depending on the presence or absence of distant metastases, regardless of tumor size (T) or nodal status (N). Our recent study to analyze the relationship between age at diagnosis and disease specific survival (DSS) of WDTC[18] concluded that the DSS was not independently influenced by age until the age of 55 years, and therefore 55 years was suggested as a more appropriate cut-off for risk stratification.

The primary objective of this study was to evaluate whether 55 years is the best age threshold for stage grouping by comparing multivariable models designed to evaluate the independent impact of various prognostic factors, including age based TNM stage grouping, on the DSS of our population based cohort. The secondary objective was to compare the appropriateness of this model to other competing models that were identical in all other prognostic parameters except the stage grouping based on different age thresholds.

Patients and methods

This study, approved by the Research Ethics Board of the University of Manitoba, utilized our population based cohort includes 2125 consecutive WDTC diagnosed in 2115 patients registered in Manitoba Cancer Registry in Canada, from January 1, 1970 to December 31, 2010. Electronic and paper charts, including pathology and operative reports, discharge summaries, and autopsy records, were reviewed. Details involving patient demographics, extent of disease at presentation, treatment, pathology, recurrences of cancer, and the final outcome status as of January 1, 2014 were recorded. Recurrences were defined as the presence of clinical and/or radiologic evidence of disease, and cytologic/pathologic confirmation was obtained for locoregional relapse whenever possible. Patients were censored if they left the province (lost to follow-up) or were deceased. As staging systems have evolved over time, all cases were restaged using the TNM criteria of American Joint Committee on Cancer (AJCC)/Union Internationale Contre le Cancer (UICC) staging for thyroid cancer (7th Edition, 2009) to ensure uniformity. All patients were then sequentially stage grouped into stages I to IV by AJCC/UICC[7] stage grouping criteria but using different age thresholds between 45 and 65 years (Table 1). In addition, the topography and histology were recoded using the

WHO International Classification of Diseases for Oncology (3rd edition) and the disease, signs and symptoms by International Classification of Diseases (10th Edition).

IBM SPSS Statistics version 22.0 (IBM Corp., Armonk, NY, USA) was utilized to manage and analyze data. ANOVA was used to compare group means and the Pearson χ^2 test to compare categorical data with continuity correction as appropriate. Statistical significance was defined as $p < 0.05$, and 95% confidence intervals were used to express reliability of the estimates. After checking for normality assumption, the mean and standard deviation were used to express normally distributed data (such as the age) and the median with interquartile range (IQR) was used for non-normally distributed data (such as tumor size and the follow-up). The Kaplan–Meier product limit method was used to estimate the disease free survival (DFS) and DSS. Multivariable analyses were performed with Cox proportional hazard models to evaluate the independent impact of various prognostic factors on the DSS of our population based cohort, after confirming the proportional hazard assumption. All these models were similar in all other prognostic parameters except the stage grouping that was based on different age thresholds.

Akaike information criterion (AIC) was used to select the most appropriate age based model for stage grouping of WDTC. AIC is defined as $AIC = -2LL + 2m$, where LL is the maximized log-likelihood and m is the number of parameters in the model (degrees of freedom).[19,20] Delta AIC was calculated to compare the models. It is defined as $Delta\ AIC = \Delta_i = AIC_i - minAIC$, where AIC_i is the AIC value for model i and min AIC is the AIC value of the best model identified by the lowest AIC.[21] Akaike weights were calculated to provide the relative strength of evidence for each model. Akaike weight $= w_i = \exp(-\Delta_i/2)/\sum_{r=1}^{R}\exp(-\Delta_{i/2})$, represents the ratio of delta AIC values for each model relative to the whole set of R candidate models.[21,22] Akaike weights (Δ_i) were adjusted to compare them on a scale of 1 (i.e $\sum w_i = 1$). Evidence ratios were calculated to compare the Akaike weights of the best model (w_j) with other competing models (w_i). This is calculated as evidence ratio $= w_j/w_i$.[21]

Results

Our population cohort of 2115 consecutive WDTC patients was comprised of 1621 (76.6%) females and 494 (23.4%) males, with a mean age of 47.3 ± 17.1 years. In all, 2125 WDTCs were identified in these patients, with a synchronous second primary thyroid cancer identified in nine patients and a metachronous papillary carcinoma of the contralateral lobe identified in one patient years after initial management. The overwhelming majority of 1762 (83.3%) patients were diagnosed with papillary carcinoma, followed by 268 (12.7%) follicular carcinoma, and 85 (4%) Hürthle cell carcinoma. The median tumour size was 20 mm (IQR = 10–34 mm) and 26.1% of all WDTC

Table 1
Stage distribution of patients with WDTC by different age thresholds.[a]

Age threshold (years)	Stage I	Stage II	Stage III	Stage IV
45	67.3%	10.5%	12.2%	10.0%
50	73.0%	8.0%	10.0%	9.0%
55	77.7%	6.4%	7.8%	8.1%
60	82.9%	5.0%	5.7%	6.5%
65	87.4%	3.8%	3.6%	5.1%

[a] AJCC-TNM staging system 7th edition.

were ≤10 mm (microcarcinoma). Gross extra-thyroidal extension of tumour was reported in 379 (17.9%) patients. At the time of diagnosis, regional lymph node metastases were observed in 472 (22.3%) of cases, and distant metastases in 54 (2.6%). The distribution of stage grouping of our WDTC cohort using different age thresholds is shown in Table 1.

As of January 1, 2014, 1622 (76.6%) patients were alive and disease free, 47 (2.2%) patients were living with disease, and 111(5.2%) were deceased as a result of thyroid cancer. 107 (5.0%) patients died of a second primary cancer, and 228 (10.8%) died of other causes. Thyroid cancers were incidentally identified during autopsy in 44 (2.1%) patients, and these were excluded from survival analysis as they had no treatment or follow-up. The three patients (0.1%) who had synchronous medullary or poorly differentiated carcinoma were also excluded as these malignancies were felt to be more aggressive than their papillary carcinoma. Other exclusions included 42 (2.0%) patients who died from unrelated causes prior to treatment, 15 (0.7%) patients considered unsuitable for surgery, 13 (0.6%) patients who refused thyroidectomy, and 11 (0.5%) patients who were followed for less than 36 months. Of the remaining 1987 patients, 1079 (54.3%) underwent total or near total thyroidectomy, and of these 788 (73%) received adjuvant RAI.

The median follow-up of these patients was 11.5 years (IQR = 6.2−19.9 years). During this time, post-treatment residual disease was identified in 112 (5.3%) patients, and disease recurrence in 154 (7.3%) patients (at least six months after successful initial treatment). 43 (2.0%) cases had recurrences in the residual thyroid lobe or thyroid bed, 66 (3.1%) in the central compartment, 45 (2.1%) in the lateral compartment, 66 (3.1%) at a distant site, and 15 (0.7%) at multiple sites. DFS was 87.2% (95% CI, 85.7−88.7%) at 10 years and 85.7% (95% CI 83.9−87.3%) at 20 years. DSS was 95.6% (95% CI, 94.6−96.5%) and 92.8% (95% CI, 91.2−94.1%) at 10 and 20 years respectively. Ten and 20 year DSS for different stages of WDTC grouped using various age thresholds is summarized in Table 2. All Cox proportional hazard models for independent influence of various prognostic factors using different age−threshold based stage grouping had 8 degrees of freedom. The multivariable model for the age threshold of 55 years is shown in Table 3.

Table 3
Cox proportional hazard model for prognostic factors for WDTC using the age threshold of 55 years for stage grouping.

Prognostic factor	Hazard ratio (95% CI)
Age at the time of diagnosis (per year)	1.04 (1.02−1.07), p = 0.001
Male versus female (reference)	1.40 (0.86−2.30), p = 0.179
Incomplete vs. complete resection (reference)	3.32 (1.87−5.92), p < 0.001
Stage II vs. Stage I (reference)	1.95 (0.62−6.15), p = 0.256(NS)
Stage III vs. Stage II (reference)	3.72 (1.69−8.18), p = 0.001
Stage IV vs. Stage III (reference)	8.08 (4.46−14.63), p < 0.001
Hürthle vs. Papillary (reference)	2.31 (1.23−4.34), p = 0.009
Follicular vs. Papillary (reference)	1.75 (0.82−3.74) 0.149 (NS)

AIC, Delta AIC, Akaike weights, and evidence ratios were calculated for different Cox proportional hazard models (Table 4). The model applying the age of 55 years for stage grouping showed the lowest AIC (792.0), as seen in Fig. 1. The Akaike weight for this model was the highest at 0.85, with the next closest being 0.10 for the age threshold of 50 years. An evidence ratio for the model based on 55 years age-threshold was 16.8 as compared to that based on 45 years age-threshold (Table 4).

Discussion

Age has been shown to be an important determinant of prognosis of WDTC, and various age cut offs between 40 and 60 years have been employed historically in various

Table 4
AIC, delta AIC, Akaike weight, and evidence ratio for various age thresholds.

Age threshold (years)	−2LL[a]	AIC[b]	Δ_i[c]	Akaike weight[d]	Evidence ratio[e]
45	782.0	797.6	5.6	0.05	16.8
50	780.3	796.3	4.4	0.10	8.8
55	776.0	792.0	0	0.85	1
60	791.1	807.1	15.2	4.3×10^{-4}	1968.4
65	808.3	824.3	32.4	7.9×10^{-8}	10745525.9

[a] −2 log likelihood.
[b] $AIC = -2LL + 2m$.[c] $\Delta_i = AIC_i - minAIC$.
[c] $\Delta_i = AIC_i - minAIC$.
[d] $w_i = \exp(-\Delta_{i/2})/\sum_{r=1}^{R}\exp(-\Delta_{i/2})$.
[e] Evidence ratio = w_j/w_i.

Table 2
Disease specific survival of WDTC using different age thresholds for stage grouping.

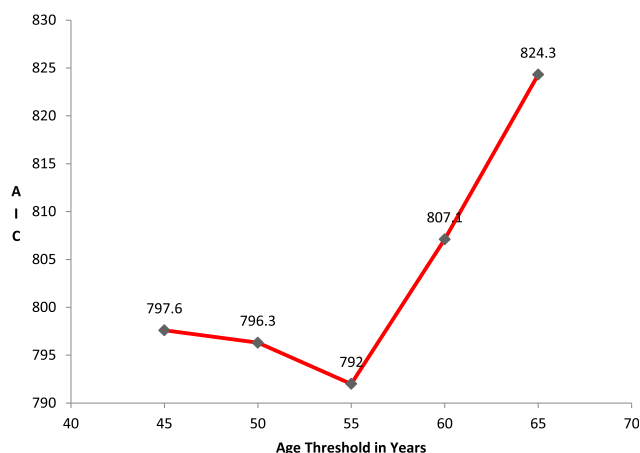| Age threshold (years)	Stage I		Stage II		Stage III		Stage IV	
	10yr	20yr	10yr	20yr	10yr	20yr	10yr	20yr
45	99.3%	98.7%	98.6%	94.9%	94.8%	86.9%	61.4%	41.5%
50	99.3%	98.5%	96.7%	91.7%	93.4%	84.3%	59.9%	38.6%
55	99.2%	98.4%	95.8%	89.7%	91.5%	79.3%	54.2%	32.6%
60	98.8%	97.3%	93.7%	87.9%	90.7%	79.7%	49.1%	26.7%
65	98.6%	96.8%	84.0%	72.4%	85.2%	77.9%	44.8%	24.6%

Figure 1. AIC values of different Cox proportional hazard models using different age thresholds. Age threshold of 55 years shows the lowest AIC value.

risk stratification systems.[4–13] More recent studies have used the Surveillance, Epidemiology, and End Results (SEER) database to assess the impact of age on survival in thyroid cancer.[16,23,24] Although these studies emphasize the importance of age as a prognostic factor in WDTC, there is a lack of unanimity on the right age threshold, if any, for predicting oncological outcome. Konturek at al showed increased relative risk of death from thyroid cancer only for age above 60 years.[25] A study by Mazurat et al showed that age didn't negatively influence the DSS till the age of 55, and therefore 55 years was suggested to be a more appropriate threshold for TNM stage grouping.[18] Larger databases such as the SEER database are robust, but they have the inherent limitations in terms of coverage, coding reliability, patient migration to an area that is not covered by SEER and availability of limited information on the treatment details of the patients.[17] In the present study we found 55 years to be the most appropriate age threshold in our population based thyroid cancer cohort by utilizing a statistical model fit measure, the Akaike information criterion (AIC) (Table 4 and Fig. 1).

AIC, developed in the early 1970s on solid statistical principles, based on information theory, provides an objective means for choosing between competing models.[19–22] It measures the relative quality of a statistical model for a given data set. In our study, the competing models were identical in all other prognostic parameters except the stage grouping that was derived for various age thresholds between 45 and 65 years. The lowest value of AIC indicates the preferred model, which in this case was for the age threshold of 55 years (AIC = 792.0).

The AIC value on its own can be misinterpreted, as there is no value of significance and it is only as good as the data used to generate it.[22] However, AIC values can be transformed to conditional probabilities, Akaike weights, which makes the results easier to interpret. First, Delta AIC (Δ_i) was calculated, which is a measure of each model relative

to the best model.[21] In general, a value of $\Delta_i < 2$ suggests substantial evidence for the model, values between 3 and 7 indicate the model has considerably less support, whereas $\Delta_i > 10$ indicates that the model is very unlikely. In our study, all the alternative models to using the age threshold of 55 years had Δ_i between 3 and 7 or >10 suggesting a low to extremely low likelihood of these alternative models being valid. Delta AIC (Δ_i) values were used to calculate Akaike weights (w_i) to indicate the probability of a particular model being the best among a set of candidate models. In our data set, the age threshold of 55 years has w_i of 0.85, which means that it has an 85% chance of being the best model. This far exceeds the weights of the other models (Table 4). Evidence ratio is a measure of the extent to which it is better than other models. In our study, the age threshold of 55 is 16.8 times more likely to be the best threshold than 45 years.

Currently, the widely adopted TNM-AJCC staging system uses an age threshold of 45 years for stage grouping, independent of other prognostic parameters. Those less than 45 years of age are staged as stage I or II, regardless of primary tumor extension (T) or nodal involvement (N). Concerns have been raised about under staging young patients with metastatic thyroid cancer.[16] By adopting an age cut-off of 55 years, as our study recommends, a greater proportion of patients would be stratified as low-risk, correlating with a more favorable DSS and thus potentially avoid over-treatment. Using the current age cut-off of 45 years, 67.3% of our population cohort had Stage I disease, with 99.2% 10-year DSS. In contrast, employing a threshold of 55 years results in 77.7% of patients being in Stage I, with a 99.2% 10-year DSS. As treatment choices have been guided by the risk stratification based on the currently practiced disease staging system, up to 10% of our cohort may have received overtreatment (more aggressive surgery with or without adjuvant radioactive iodine). Increasing the age threshold results in down staging, with a greater number of patients seen in stages I and II, and fewer patients in stages III and IV (Table 1). This also influences 10 and 20 year DSS (Table 2). The difference in 20-year DSS between stages I and II using 55 years age threshold was 8.7%, II and III was 10.4% and III and IV was 46.7%, which offers better stage discrimination than other age cut offs studied (Table 2). For the threshold age between 45 and 60 years, the 10 and 20 year DSS decreases with stage progression, as expected, however, employing a threshold of 65 years would result in incongruously better DSS for Stage III than stage II. This is because of the down staging of all metastatic WDTC from stage IV to stage II in patients younger than 65 years.

This cohort of WDTC was followed over a span of four decades. This proves to be both a strength and limitation, as the staging has evolved over time. To ensure consistency, all cancers were uniformly restaged using the 2009 UICC/AJCC staging system. As well, treatment recommendations have changed over this time frame with total

thyroidectomy and adjuvant RAI becoming more frequent over time. However, these were not shown to significantly influence DSS in our previous study.[24]

In conclusion, our study found the age of 55 years to be the most appropriate threshold for TNM stage grouping of WDTC. Larger multicenter studies would be beneficial to further evaluate the appropriateness of an age threshold of 55 years for stage grouping of WDTC.

Conflict of interest

None.

References

1. Clark OH. Predictors of thyroid tumor aggressiveness. *West J Med* 1996 Sep;**165**(3):131–8.
2. Lang BH, Lo CY, Chan WF, Lam KY, Wan KY. Staging systems for papillary thyroid carcinoma: a review and comparison. *Ann Surg* 2007 Mar;**245**(3):366–78.
3. Nixon IJ, Ganly I, Patel S, et al. The impact of microscopic extrathyroid extension on outcome in patients with clinical T1 and T2 well-differentiated thyroid cancer. *Surgery* 2011 Dec;**150**(6):1242–9.
4. Akslen LA. Prognostic importance of histologic grading in papillary thyroid carcinoma. *Cancer* 1993 Nov 1;**72**(9):2680–5.
5. Beenken S, Roye D, Weiss H, et al. Extent of surgery for intermediate-risk well-differentiated thyroid cancer. *Am J Surg* 2000 Jan;**179**(1):51–6.
6. Cady B, Rossi R. An expanded view of risk-group definition in differentiated thyroid carcinoma. *Surgery* 1988 Dec;**104**(6):947–53.
7. Edge SB, Byrd DR, Compton CC, Fritz AG, Greene FL, Trotti A, editors. *AJCC cancer staging handbook.* 7th ed. New York, NY, USA: Springer-Verlag; 2010;, p. 87–96.
8. Noguchi S, Murakami N, Kawamoto H. Classification of papillary cancer of the thyroid based on prognosis. *World J Surg* 1994 Jul-Aug;**18**(4):552–7. discussion 558.
9. Sherman SI, Brierley JD, Sperling M, et al. Prospective multicenter study of thyroiscarcinoma treatment: Initial analysis of staging and outcome. national thyroid cancer treatment cooperative study registry group. *Cancer* 1998 Sep 1;**83**(5):1012–21.
10. Sugitani I, Kasai N, Fujimoto Y, Yanagisawa A. A novel classification system for patients with PTC: addition of the new variables of large (3 cm or greater) nodal metastases and reclassification during the follow-up period. *Surgery* 2004 Feb;**135**(2):139–48.
11. Hay ID, Grant CS, Taylor WF, McConahey WM. Ipsilateral lobectomy versus bilateral lobar resection in papillary thyroid carcinoma: a retrospective analysis of surgical outcome using a novel prognostic scoring system. *Surgery* 1987 Dec;**102**(6):1088–95.
12. Shaha AR, Loree TR, Shah JP. Intermediate-risk group for differentiated carcinoma of thyroid. *Surgery* 1994 Dec;**116**(6):1036–40. discussion 1040–1.
13. Hay ID, Bergstralh EJ, Goellner JR, Ebersold JR, Grant CS. Predicting outcome in papillary thyroid carcinoma: development of a reliable prognostic scoring system in a cohort of 1779 patients surgically treated at one institution during 1940 through 1989. *Surgery* 1993 Dec;**114**(6):1050–7. discussion 1057–8.
14. Eustatia-Rutten CF, Corssmit EP, Biermasz NR, Pereira AM, Romijn JA, Smit JW. Survival and death causes in differentiated thyroid carcinoma. *J Clin Endocrinol Metab* 2006 Jan;**91**(1): 313–9.
15. Sherman SI. Thyroid carcinoma. *Lancet* 2003 Feb 8;**361**(9356):501–11.
16. Tran Cao HS, Johnston LE, Chang DC, Bouvet M. A critical analysis of the American Joint Committee on Cancer (AJCC) staging system for differentiated thyroid carcinoma in young patients on the basis of the surveillance, epidemiology, and end results (SEER) registry. *Surgery* 2012 Aug;**152**(2):145–51.
17. Pathak KA, Mazurat A, Lambert P, Klonisch T, Nason RW. Prognostic nomograms to predict oncological outcome of thyroid cancers. *J Clin Endocrinol Metab* 2013;**98**(12):4768–75.
18. Mazurat A, Torroni A, Hendrickson-Rebizant J, Benning H, Nason RW, Pathak KA. The age factor in survival of a population cohort of well-differentiated thyroid cancer. *Endocr Connect* 2013 Sep 23;**2**(3):154–60.
19. Everitt BS. *The Cambridge dictionary of statistics.* 3rd ed. Cambridge University Press; 2006;, p. 10.
20. Akaike H. Information theory and an extension of the maximum likelihood principle. In: *Selected papers of Hirotugu Akaike.* Springer; 1998;, p. 199–213.
21. Mazerolle MJ. *Appendix 1: making sense out of Akaike's information criterion (AIC): its use and interpretation in model selection and inference from ecological data. Mouvements et Reproduction des Amphibiens en Tourbières Perturbées* 2004;, p. 174–90.
22. Wagenmakers E, Farrell S. AIC model selection using Akaike weights. *Psychon Bull Rev* 2004;**11**(1):192–6.
23. Oyer SL, Smith VA, Lentsch EJ. Reevaluating the prognostic significance of age in differentiated thyroid cancer. *Otolaryngology–head neck Surg* 2012;**147**(2):221–6.
24. Orosco RK, Hussain T, Brumund KT, Oh DK, Chang DC, Bouvet M. Analysis of age and disease status as predictors of thyroid cancer-specific mortality using the Surveillance, Epidemiology, and end results database. *Thyroid* 2015;**25**(1):125–32.
25. Konturek A, Barczynski M, Nowak W, Richter P. Prognostic factors in differentiated thyroid cancer–a 20-year surgical outcome study. *Langeecks Arch Surg* 2012 Jun;**397**(5):809–15.

The age factor in survival of a population cohort of well-differentiated thyroid cancer

Andrea Mazurat, Andrea Torroni, Jane Hendrickson-Rebizant, Harbinder Benning, Richard W Nason and **K Alok Pathak**

Section of Surgical Oncology, Department of Surgery, CancerCare Manitoba, University of Manitoba, GF440 A, 820 Sherbrook Street, Winnipeg, Manitoba, Canada R3A 1R9

Correspondence should be addressed to K A Pathak
Email
alok.pathak@cancercare.mb.ca

Abstract

Well-differentiated thyroid carcinoma (WDTC) represents a group of thyroid cancers with excellent prognosis. Age, a well-recognized risk factor for WDTC, has been consistently included in various prognostic scoring systems. An age threshold of 45 years is currently used by the American Joint Cancer Committee-TNM staging system for the risk stratification of patients. This study analyzes the relationship between the patients' age at diagnosis and thyroid cancer-specific survival in a population-based thyroid cancer cohort of 2115 consecutive patients with WDTC, diagnosed during 1970–2010, and evaluates the appropriateness of the currently used age threshold. Oncological outcomes of patients in terms of disease-specific survival (DSS) and disease-free survival (DFS) were calculated by the Kaplan–Meier method, while multivariable analysis was done by the Cox proportional hazard model and proportional hazards regression for sub-distribution of competing risks to assess the independent influence of various prognostic factors. The mean age of the patients was 47.3 years, 76.6% were female and 83.3% had papillary carcinoma. The median follow-up of the cohort was 122.4 months. The DSS and DFS were 95.4 and 92.8% at 10 years and 90.1 and 87.6% at 20 years, respectively. Multivariable analyses confirmed patient's age to be an independent risk factor adversely affecting the DSS but not the DFS. Distant metastasis, incomplete surgical resection, T3/T4 stages, Hürthle cell histology, and male gender were other independent prognostic determinants. The DSS was not independently influenced by age until the age of 55 years. An age threshold of 55 years is better than that of 45 years for risk stratification.

Introduction

Well-differentiated thyroid carcinoma (WDTC) represents a group of thyroid cancers that are associated with increasing incidence and excellent posttreatment outcome (1). This group comprises different histological types, the most common being papillary carcinoma, followed by follicular carcinoma, and Hürthle cell variant of follicular carcinoma (2). Despite the high cure rates of WDTC, about 10% of the patients still die of this disease

and an even larger proportion will develop loco-regional recurrence (2, 3, 4). Identification of factors associated with aggressive behavior in WDTC has been extensively pursued over the past four decades, yielding a multitude of risk stratification systems, which aim to differentiate high-risk and low-risk patients on the basis of the tumor and patient characteristics. Several factors have been associated with aggressive behavior in WDTC, including the age at diagnosis, the gender of the patient, the size and extension of the primary tumor, and the presence of distant metastases (1, 2, 3, 4, 5).

The age at diagnosis, in particular, is considered to be a strong prognostic indicator of WDTC outcome and has been consistently included in the majority of risk stratification systems currently used in clinical practice (6, 7, 8, 9, 10, 11, 12, 13, 14, 15, 16). Interestingly, the widely adopted American Joint Cancer Committee (AJCC)-TNM staging system (10) includes age as a prognostic determinant exclusively for WDTC, classifying patients younger than 45 as low risk, independent of the presence of other risk factors such as primary tumor extension (T) or nodal involvement (N). Other risk stratification systems such as AMES (9), Noguchi *et al*. (11), GAMES (15), National Thyroid Cancer Treatment Cooperative Study (NTCTCS) (12), UAB and MDA (8), and CIH (13) follow the scheme of TNM adopting an age threshold ranging from 41 to 51 years, to stratify the patients in high- and low-risk groups. A different set of prognostic scoring systems, namely EORTC (7), AGES (14), MACIS (16), SAG (6), Murcia (17), and Ankara (18), on the other hand, considers age as a continuous variable that affects the total prognostic score in a multiplicative fashion without any stratification.

Several studies have shown that the relationship between the age at diagnosis and the disease-specific survival (DSS) of WDTC is inversely proportional and is better represented by an exponential function, suggesting that age should preferably be considered as a continuous prognostic variable, rather than a categorical parameter (5, 19). The rationale for including an age threshold in many risk stratification systems is the need for a standard, simple, and practical method to predict oncological outcome rather than generating complicated prognostic scores. However, the selection of an appropriate age threshold is critical to this process and an inaccurate value can lead to either overtreatment of low-risk patients, or under-treatment of high-risk ones. The objective of this study was to analyze the relationship between the age at diagnosis and the oncological outcome of WDTC.

Subjects and methods

This study was approved by the Research Ethics Board of the University of Manitoba. Our population-based historical cohort includes all 2125 consecutive well-differentiated thyroid cancers diagnosed in 2115 patients in the province of Manitoba, Canada, from January 1, 1970 to December 31, 2010. We reviewed the individual electronic and paper records of diagnosis and treatment for this cohort of patient registered in the Manitoba Cancer Registry at CancerCare Manitoba, the only comprehensive cancer center for a population of 1.2 million. The primary source of diagnostic information included 2007 pathology reports, 56 discharge summaries, 44 autopsy records, and eight operative reports. Patient demographics, the extent of their cancer at the initial presentation, the details of treatment modalities employed, pathology details, cancer recurrences during the follow-up, and the final outcome status as of January 1, 2013 were recorded. Clinically and radiologically detectable disease relapses were considered as recurrences and a cytology/biopsy confirmation was obtained for local/regional relapses whenever it was possible. For distant metastases, increased radioactive iodine (RAI) uptake with or without raised thyroglobulin was considered as evidence of recurrence. All patients who migrated out of the province (considered to be lost to follow-up) or died during the study period were censored at that point in time. Cause of death was obtained from autopsy records and death certificates, and individual patient records were reviewed to confirm exact cause of death and status of thyroid cancer at the time of death.

All cases were restaged according to the AJCC/Union Internationale Contre le Cancer (UICC) staging for thyroid cancer (7th Edition, 2009); the topography and the histology were re-coded by WHO International Classification of Diseases for Oncology (3rd Edition) codes and the disease, signs, and symptoms by International Classification of Diseases (10th Edition) codes to ensure uniformity. Additionally, as a part of our collaborative staging project, the pathology and treatment details of 683 (29.6%) cases were independently reviewed for accuracy.

Statistical analysis

The data were managed and analyzed using SPSS for Windows version 20.0 (SPSS, IBM Corp., Armonk, NY, USA). Group means were compared by ANOVA and categorical data using the Pearson χ^2 test with continuity correction, as appropriate. A P value <0.05 was considered

to indicate statistical significance and 95% CIs were used to express reliability in the estimates. After checking for normality assumption, the mean and s.d. were used to express normally distributed data (such as the age of the patients) and median with interquartile range (IQR) were used for non-normally distributed data (such as the tumor size and the follow-up). The disease-free survival (DFS) and the DSS were estimated by the Kaplan–Meier product limit method, and the effect of age and other prognostic factors on DSS was assessed using the log rank test for pairwise comparison. The competing influence of other causes of mortality, such as death due to a second primary tumor or non-cancer deaths, was analyzed by multivariable proportional hazards regression for sub-distribution of competing risks using STATA version 12 (StataCorp., College Station, TX, USA). Multivariable analyses were also performed with Cox proportional hazard models to assess the independent effect of different age cutoffs on DSS after confirming the proportional hazard assumption.

Results

The study cohort consisted of 1621 (76.6%) females and 494 (23.4%) males with a mean age of 47.3 ± 17.1 years. In all, 1762 (83.3%) patients had papillary carcinoma, 268 (12.7%) had follicular carcinoma, and 85 (4%) had Hürthle cell carcinoma. Nine patients had a synchronous second primary tumor of a different histology along with a papillary thyroid cancer (follicular-3, Hürthle cell-3, medullary-2, poorly differentiated-1), while one patient had a metachronous second papillary carcinoma in the contralateral thyroid lobe, 25 years after initial management. The median tumor size was 20 mm (IQR = 10–34 mm) and microcarcinoma (tumor size ≤10 mm) represented 26.1% of all WDTC. Multifocal thyroid cancers were observed in 600 (32.7%) cases and a gross extra-thyroidal extension of tumor in 379 (17.9%) cases. At the time of diagnosis, 472 (22.3%) patients had regional lymph node involvement and 54 (2.6%) had distant metastasis. On January 1, 2013, 1658 (78.5%) patients had no evidence of disease; 49 (2.3%) patients were alive with disease; 105 (5.0%) patients were dead because of thyroid cancer; 78 (3.7%) patients had died of a second primary tumor; and 225 (10.6%) patients died of other causes. Thyroid cancers, which were incidental autopsy findings in 44 (2.1%) patients, were excluded from survival analysis as they had no treatment or follow-up. Three (0.1%) patients who had a synchronous medullary or poorly differentiated carcinoma were excluded from further analysis as these synchronous

malignancies were thought to be more aggressive than their papillary thyroid cancer. Exclusions also included 42 (2.0%) patients, who died before their treatment due to unrelated causes; 15 (0.7%) patients, who were not considered as suitable surgical candidates; 13 patients (0.6%), who did not consent to thyroidectomy; and 11 (0.5%) patients, who were followed for <36 months. A total or near total thyroidectomy was performed in 1079 (54.3%) of the remaining 1987 patients, and of these patients, 788 (73%) had post-total thyroidectomy adjuvant RAI.

During the median follow-up of 124.6 months (IQR = 57.8–227.3 months), 78 (3.9%) patients had post-treatment residual disease and 185 (9.3%) had disease recurrence at least 6 months after a successful initial treatment. The recurrences were observed in the residual thyroid lobe or thyroid bed in 24 (1.2%) cases, in the central compartment of the neck in 59 (2.9%) cases, in the lateral compartment of the neck in 40 (2.0%) cases, at a distant site in 47 (2.4%) cases, and at multiple sites in 15 (0.8%) cases. Ten- and 20-year DFS were 90.1% (95% CI, 88.5–91.4%) and 87.6% (95% CI, 85.6–89.3%), respectively. On multivariable analysis by the Cox proportional hazard model, DFS was significantly influenced by distant metastasis (hazard ratio (HR) = 7.40; 95% CI, 4.54–12.07; $P<0.001$), incomplete surgical resection (HR = 6.18; 95% CI, 4.02–9.49, $P<0.001$), T stages – T4 (HR = 2.87; 95% CI, 1.80–4.58, $P<0.001$) and T3 (HR = 2.41; 95% CI, 1.72–3.37, $P<0.001$), Hürthle cell histology (HR = 2.34; 95% CI, 1.41–3.89; $P=0.001$), lymph node involvement (HR = 2.14; 95% CI, 1.57–2.91; $P<0.001$), and male gender (HR = 1.49; 95% CI, 1.11–2.00; $P=0.008$). The DFS was independent of the histology of follicular carcinoma ($P=0.712$, NS), extent of thyroidectomy ($P=0.136$, NS), and age of the patient at diagnosis ($P=0.846$, NS). Age had a non-monotonic relationship with the relapse of thyroid cancer.

The DSS was 95.4% (95% CI, 94.2–96.3%) at 10 years and 92.8% (95% CI, 91.2–94.2%) at 20 years. Twenty-year DSS was 99.0% (95% CI, 97.9–99.6%) for patients <45 years, 96.8% (95% CI, 93.1–98.5%) for patients in the age group of 45–54 years, 85.8% (95% CI, 78.7–90.7%) for patients in the age group of 55–64 years, and 74.0% (95% CI, 70.0–79.8%) for patients older than 65 years. Figure 1 shows no significant difference in the DSS in different age groups till the age of 55 years, when the first significant drop ($P=0.002$) was observed by log rank test for pairwise comparison. The case fatality rate of thyroid cancer also increased to 6.7% in the age group of 55–64 years from 2.2% in the age group of 45–54 years and thereafter it increased steadily with increasing age (Table 1).
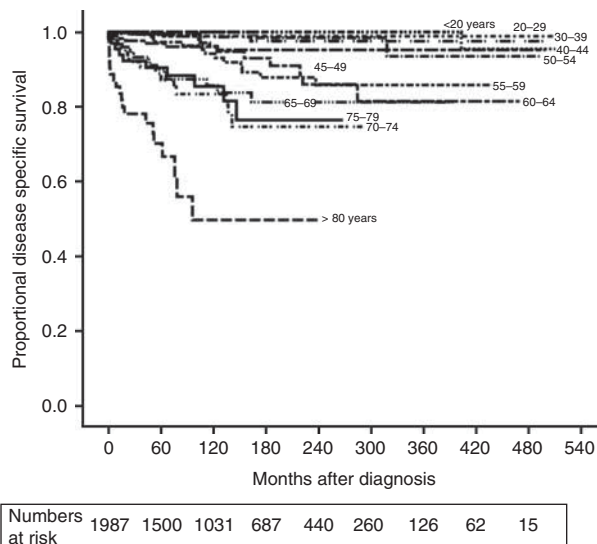
Figure 1
Disease-specific survival of well-differentiated thyroid cancer in different age groups.

Cumulative incidences of death due to thyroid cancer at 10 and 20 years by multivariable competing risk analysis were 0.3 and 0.9% (age group <45 years), 0.7 and 1.8% (age group 45–54 years), 1.4 and 3.3% (age group 55–64 years), and 3.0 and 6.7% (age group >65 years), respectively (Fig. 2). There was an insignificant difference in the risks of dying from thyroid cancer between the age groups <45 and 45–54 years but the risk was significantly higher in the age groups 55–64 and >65 years. The risk of death from thyroid cancer was significantly influenced independently by the presence of distant metastasis (sub-hazard ratio (SHR) = 12.65; 95% CI, 5.66–28.28; $P < 0.001$), patient's age, i.e., 55–64 years (SHR = 4.08;

95% CI, 1.52–10.92, $P = 0.005$) or >65 years (SHR = 5.72; 95% CI, 2.70–12.10, $P < 0.001$), incomplete surgical resection (SHR = 3.14; 95% CI, 1.52–6.47, $P = 0.002$), T3/T4 stages (SHR = 3.28; 95% CI, 1.74–6.17, $P < 0.001$), Hürthle cell histology (SHR = 4.67; 95% CI, 2.34–9.31; $P < 0.001$), and male gender (SHR = 2.08; 95% CI, 1.22–3.40; $P = 0.011$). Patient's age, i.e., 45–54 years ($P = 0.154$), histology of follicular carcinoma ($P = 0.204$, NS), regional node involvement ($P = 0.07$, NS), extent of thyroidectomy ($P = 0.136$, NS), and adjuvant RAI ($P = 0.597$) did not have any independent significant influence on the risk of death from thyroid cancer.

On multivariable analysis by the Cox proportional hazard model, the DSS was adversely influenced independently by age at diagnosis, distant metastasis, incomplete surgical resection, advanced T stage (T3/T4), Hürthle cell histology, and male gender (Table 2). The distribution of these prognostic factors in different age groups is summarized in Table 1. Lymph node involvement ($P = 0.07$), histology of follicular carcinoma ($P = 0.110$, NS), multifocality ($P = 0.956$), extent of thyroidectomy ($P = 0.136$), and adjuvant RAI ($P = 0.478$) did not have a significant impact on the DSS of WDTC. There was an insignificant difference between the DSS of patients younger than 45 years and those in the age group of 45–54 years ($P = 0.141$), but patients in the age group of 55–64 years had significantly higher risk of dying from thyroid cancer than those in the age group of 45–54 years (Table 2). On subset analysis of patients younger than 55 years and those 55 years and older, the advancing age was not an independent prognostic determinant of DSS in patients below 55 years (HR = 1.03; 95% CI, 0.98–1.12; $P = 0.103$); however, it had a significant impact on patients older than 55 years (HR = 1.03; 95% CI, 1.01–1.09; $P = 0.01$).

Table 1 Distribution of various prognostic factors and deaths from thyroid cancer in different age groups. HCTC, Hürthle cell thyroid carcinoma.

Age (years)	Males (%)	T3/T4 tumor (%)	HCTC (%)	Distant metastasis (%)	Incomplete resection (%)	Case fatality rate
00–19 ($n = 84$)	16.7	34.6	2.4	0	0	0 (0%)
20–29 ($n = 268$)	19.0	21.5	0	0.7	2.4	1 (0.4%)
30–39 ($n = 413$)	19.6	25.1	2.4	0.7	1.0	4 (1.0%)
40–44 ($n = 202$)	21.3	19.7	4.5	1.5	1.6	4 (2.0%)
45–49 ($n = 212$)	20.3	19.0	2.8	1.9	2.5	6 (2.8%)
50–54 ($n = 192$)	22.9	23.6	5.7	0	1.7	3 (1.6%)
55–59 ($n = 193$)	30.6	33.1	5.7	1.6	3.0	13 (6.7%)
60–64 ($n = 179$)	30.7	34.0	6.1	4.5	5.1	12 (6.7%)
65–69 ($n = 133$)	28.6	35.2	4.5	5.3	4.6	16 (12.0%)
70–74 ($n = 98$)	32.7	32.5	6.1	8.2	8.4	15 (15.3%)
75–79 ($n = 73$)	24.7	41.7	9.6	5.5	10.3	11 (15.1%)
80–89 ($n = 68$)	23.5	53.8	8.8	17.6	14.0	20 (29.4%)
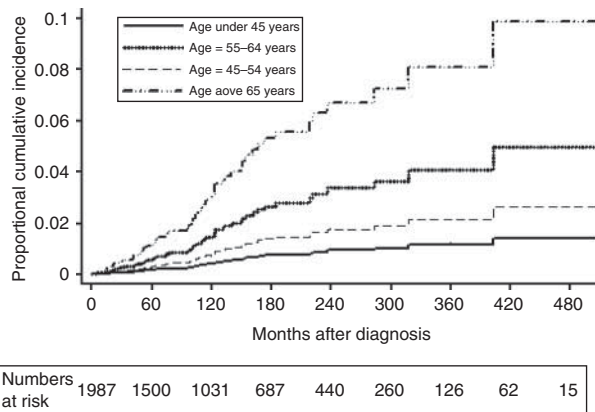
Figure 2

Cumulative incidence of death from thyroid cancer in different age groups by proportional sub-hazard model in competing risk analysis.

Discussion

According to Canadian Cancer Statistics 2013, thyroid cancer has an excellent 5-year relative survival ratio of 98% (20). The relatively low proportion of adverse events and the long-term follow-up required to assess the outcomes of WDTC make a randomized clinical trial impractical to study these cancers. A large population-based cohort, such as ours, that is followed over a prolonged time period with a very low attrition rates (only 2.1% lost to follow-up over 40 years) is the most practical model to study these cancers. A cohort is a population group, or subset thereof, that is followed over a period of time. The members of the cohort, based on defined criteria, share common experience, which in this study was diagnosis of thyroid cancer in the province of Manitoba. By virtue of residence in the same province, our study cohort was expected to share a similar risk of exposure and get a similar standard of medical care in the publicly funded health care system of the province. The stability of the population cohort and a long, meticulous follow-up make the observations of this study very reliable.

A time span of four decades is both a strength and a limitation of our study as the diagnostic criteria, staging, and treatment recommendations have evolved over time. We uniformly restaged all cancers using the 2009 AJCC/UICC Cancer staging system for thyroid cancer and histology was re-coded by WHO International Classification of Diseases for Oncology (3rd Edition) codes to ensure consistency. In view of the indolent course of WDTC, it is possible that other causes of mortality, unrelated to thyroid cancer, could result in overestimation of thyroid cancer deaths by the Kaplan–Meier method. Consequently, we used competing risk regression to obtain an unbiased estimation of cumulative incidence of deaths resulting from thyroid cancer. Deaths due to second primary cancer and non-cancer deaths were treated as competing risks. We realize that the treatment recommendations for WDTC have also changed over the last four decades with total thyroidectomy and adjuvant RAI becoming more popular in the later part of the study (21), but neither had any significant influence on the DSS (Table 2). To maintain homogeneity of data across the study period, only clinically and radiologically detectable disease relapses were considered as recurrences. Isolated hyper-thyroglobulin-aemia was not considered as evidence of recurrence.

Table 2 Multivariable analysis by Cox proportional hazard model for independent influence of different prognostic factors on disease-specific survival.

Prognostic factor	Hazard ratio (95% CI)	*P* value
Age at the time of diagnosis (years)		
<45	1.00 (reference)	
45–54	2.29 (0.76–6.89)	0.141 (NS)
55–64	5.62 (2.19–14.39)	<0.001
≥65	13.67 (5.78–35.38)	<0.001
Gender (male vs female)	2.13 (1.23–3.75)	0.007
T stage (early (T1–T2) vs advanced (T3–T4))	3.39 (1.79–6.43)	<0.001
Distant metastasis (M1 vs M0)	13.27 (6.47–27.21)	<0.001
Lymph node metastasis (N1 vs N0)	1.79 (0.96–3.33)	0.070 (NS)
Completeness of reaction (incomplete vs complete)	3.31 (1.70–6.43)	<0.001
Histology		
Papillary	1.00 (reference)	
Hürthle	4.40 (2.13–9.12)	0.001
Follicular	1.79 (0.88–3.68)	0.110 (NS)

Well-differentiated thyroid cancers, papillary, follicular, and Hürthle cell variants, account for over 90% of all thyroid malignancies (22, 23). Our analysis of all consecutive WDTC seen between 1970 and 2010 confirmed the excellent prognosis of WDTC with a DSS of 95.4% (95% CI, 94.2–96.3%) at 10 years. WDTC represents a group of unique cancers with the age of the patient at diagnosis being an important determinant of prognosis (Table 2). Although age has been consistently included as a risk factor in most of the risk stratification systems for WDTC, many of these (including the widely adopted TNM-AJCC) use age as a discrete categorical parameter for the ease of clinical staging. Nevertheless, there is a lack of consensus among the staging systems regarding the age threshold to be adopted. The AMES risk stratification system (9) recommends different age thresholds of 41 and 51 years for male and female patients, respectively, whereas Noguchi *et al*. (11), UAB and MDA (8), and CIH (13) risk stratification systems adopt an age threshold of 50 years. The TNM-AJCC staging system (10), along with the Memorial Sloan Kettering (15), and the NTCTCS (12) prognostic risk stratification systems use an age threshold of 45 years for WDTC patients independent of other prognostic parameters. Most of these recommendations are based on univariable analysis. In our study, the DSS for different age groups did not show a statistically significant decrease until the age of 55 years, when the first significant drop was observed (Fig. 1). This drop corresponds to an increase in the proportion of patients dying from thyroid cancer from 2.2 (45–54 years) to 6.7% (55–64 years) and an increase in the proportion of patients with T3/T4 tumors, Hürthle cell histology, incomplete resection, and distant metastasis (Table 1). We divided our study group into small age groups to find the most appropriate age threshold between 45 and 65 years. Even though the groups appear tiny, each group has close to 200 patients as the mean age of the cohort was 47.3 years. Once we arrived at the threshold of 55 years, we divided the cohort into bigger categories for multivariable comparison (Table 2 and Fig. 2). Multivariable analysis by the Cox proportional HR model and the competing risk analysis confirmed that the importance of age as an independent risk determinant becomes evident only after the age of 55 years (Fig. 2 and Table 2) and the subset analysis of patients above and below 55 years showed that the age was not an independent prognostic factor in patients below 55 years ($P=0.103$).

Age had a non-monotonic relationship with DFS and did not have an independent impact, which suggests that the recurrences in patients younger than 55 years are better salvaged. The currently practiced cutoff age of 45 years in TNM staging allocates patients between 45 and 55 years into a high-risk group and these patients may end up receiving unnecessary aggressive treatment even in the absence of other adverse prognostic factors such as distant metastasis, incomplete tumor resection, T3/T4 primary tumors, and Hürthle cell histology. However, it is interesting to see (Fig. 1) that the DSS of thyroid cancer continues to fall with a 3% reduction/year increase in age even beyond 55 years in the patients older than 55 years. A prognostic nomogram (24) incorporating the age and other prognostic factors may be a better tool to account for the variable influence of age in predicting the oncological outcome of thyroid cancer.

To conclude, our study confirms that patient age at the time of diagnosis is an independent risk factor with adverse impact on DSS of WDTC. The independent influence of age is not obvious till the age of 55 years. After the threshold age of 55 years, the DSS was found to fall in the older patients. An age threshold of 55 years is better than the threshold of 45 years currently used in the TNM staging.

References

1 Nixon IJ, Ganly I, Patel S, Palmer FL, Whitcher MM, Tuttle RM, Shaha AR & Shah JP. The impact of microscopic extra-thyroid extension on outcome in patients with clinical T1 and T2 well-differentiated thyroid cancer. *Surgery* 2011 **150** 1242–1249. (doi:10.1016/j.surg.2011.09.007)

2 Lang BH, Lo CY, Chan WF, Lam KY & Wan KY. Staging system for papillary carcinoma. A review and comparison. *Annals of Surgery* 2007 **245** 366–378. (doi:10.1097/01.sla.0000250445.92336.2a)

3 Eustatia-Rutten CF, Corssmit EP, Biermasz NR, Pereira AM, Romijn JA & Smit JW. Survival and death causes in differentiated thyroid carcinoma. *Journal of Clinical Endocrinology and Metabolism* 2006 **91** 313–319. (doi:10.1210/jc.2005-1322)

4 Sherman SI. Thyroid carcinoma. *Lancet* 2003 **361** 501–511. (doi:10.1016/S0140-6736(03)12488-9)

5 Tran Cao HS, Johnston LE, Chang DC & Bouvet M. A critical analysis of the American Joint Committee on Cancer (AJCC) staging system for differentiated thyroid carcinoma in young patients on the basis of the Surveillance, Epidemiology, and End Results (SEER) registry. *Surgery* 2012 **152** 145–151. (doi:10.1016/j.surg.2012.02.015)

6 Akslen LA. Prognostic importance of histologic grading in papillary thyroid carcinoma. *Cancer* 1993 **72** 2680–2685. (doi:10.1002/1097-0142(19931101)72:9<2680::AID-CNCR2820720926>3.0.CO;2-D)

7 Byar DP, Green SB, Dor P, Williams ED, Colon J, van Gilse HA, Mayer M, Sylvester RJ & van Glabbeke M. A prognostic index for thyroid carcinoma. A study of the E.O.R.T.C. Thyroid Cancer Cooperative Group. *European Journal of Cancer* 1979 **15** 1033–1041. (doi:10.1016/0014-2964(79)90291-3)

8 Beenken S, Roye D, Weiss H, Sellers M, Urist M, Diethelm A & Goepfert H. Extent of surgery for intermediate-risk well-differentiated thyroid cancer. *American Journal of Surgery* 2000 **179** 51–56. (doi:10.1016/S0002-9610(99)00254-8)

9 Cady B & Rossi R. An expanded view of risk-group definition in differentiated thyroid carcinoma. *Surgery* 1988 **104** 947–953.

10 Edge SB, Byrd DR, Compton CC, Fritz AG, Greene FL, Trotti A, eds 2010 *AJCC Cancer Staging Handbook*, 7th edn, pp 87–96. New York, NY, USA: Springer-Verlag.

11 Noguchi S, Murakami N & Kawamoto H. Classification of papillary cancer of the thyroid based on prognosis. *World Journal of Surgery* 1994 **18** 552–558. (doi:10.1007/BF00353763)

12 Sherman SI, Brierley JD, Sperling M, Ain KB, Bigos ST, Cooper DS, Haugen BR, Ho M, Klein I, Ladenson PW *et al*. Prospective multicenter study of thyroid carcinoma treatment: initial analysis of staging and outcome. *Cancer* 1998 **83** 1012–1021. (doi:10.1002/(SICI)1097-0142(19980901)83:5<1012::AID-CNCR28>3.0.CO;2-9)

13 Sugitani I, Kasai N, Fujimoto Y & Yanagisawa A. A novel classification system for patients with PTC: addition of the new variables of large (3 cm or greater) nodal metastases and reclassification during the follow-up period. *Surgery* 2004 **135** 139–148. (doi:10.1016/S0039-6060(03)00384-2)

14 Hay ID, Grant CS, Taylor WF & McConahey WM. Ipsilateral lobectomy versus bilateral lobar resection in papillary thyroid carcinoma: a retrospective analysis of surgical outcome using a novel prognostic scoring system. *Surgery* 1987 **102** 1088–1095.

15 Shaha AR, Loree TR & Shah JP. Intermediate-risk group for differentiated carcinoma of the thyroid. *Surgery* 1994 **116** 1036–1041.

16 Hay ID, Bergstralh EJ, Goellner JR, Ebersold JR & Grant CS. Predicting outcome in papillary thyroid carcinoma: development of a reliable prognostic scoring system in a cohort of 1779 patients surgically treated at one institution during 1940 through 1989. *Surgery* 1993 **114** 1050–1058.

17 Sebastian SO, Gonzalez JM, Paricio PP, Perez JS, Flores DP, Madrona AP, Romero PR & Tebar FJ. Papillary thyroid carcinoma: prognostic index for survival including the histological variety. *Archives of Surgery* 2000 **135** 272–277. (doi:10.1001/archsurg.135.3.272)

18 Yildirim E. A model for predicting outcomes in patients with differentiated thyroid cancer and model performance in comparison with other classification systems. *Journal of the American College of Surgeons* 2005 **200** 378–392. (doi:10.1016/j.jamcollsurg.2004.10.031)

19 Gilliland FD, Hunt WC, Morris DM & Key CR. Prognostic factors for thyroid carcinoma. A population-based study of 15,698 cases from the Surveillance, Epidemiology and End Results (SEER) program 1973–1991. *Cancer* 1997 **79** 564–573. (doi:10.1002/(SICI)1097-0142(19970201)79:3<564::AID-CNCR20>3.0.CO;2-0)

20 Canadian Cancer Society's Advisory Committee on Cancer Statistics 2013 Canadian Cancer Statistics 2013, pp 56–60. Toronto, ON, Canada: Canadian Cancer Society.

21 Pathak KA, Leslie WD, Klonisch TC & Nason RW. The changing face of thyroid cancer in a population based cohort. *Cancer Medicine* 2013 **2** 537–544. (doi:10.1002/cam4.103)

22 Clark OH. Predictors of thyroid tumor aggressiveness. *Western Journal of Medicine* 1996 **165** 131–138.

23 Ito Y, Ichihara K, Masuoka H, Fukushima M, Inoue H, Kihara M, Tomoda C, Higashiyama T, Takamura Y, Kobayashi K *et al*. Establishment of an intraoperative staging system (iStage) by improving UICC TNM classification system for papillary thyroid carcinoma. *World Journal of Surgery* 2010 **34** 2570–2580. (doi:10.1007/s00268-010-0710-2)

24 Pathak KA, Mazurat A, Lambert P, Klonisch TC & Nason RW. Prognostic nomograms to predict treatment outcomes of thyroid cancer. *Journal of Clinical Endocrinology and Metabolism* 2013 [in press].

An International Multi-Institutional Validation of Age 55 Years as a Cutoff for Risk Stratification in the AJCC/UICC Staging System for Well-Differentiated Thyroid Cancer

Iain J. Nixon[1], Laura Y. Wang[1], Jocelyn C. Migliacci[1], Antoine Eskander[2], Michael J. Campbell[3],
Ahmad Aniss[4], Lilah Morris[5], Fernanda Vaisman[6], Rossana Corbo[6], Denise Momesso[7], Mario Vaisman[7],
Andre Carvalho[8], Diana Learoyd[4], William D. Leslie[9], Richard W. Nason[9], Deborah Kuk[1],
Volkert Wreesmann[1], Luc Morris[1], Frank L. Palmer[1], Ian Ganly[1], Snehal G. Patel[1], Bhuvanesh Singh[1],
R. Michael Tuttle[1], Ashok R. Shaha[1], Mithat Gönen[1], K. Alok Pathak[9], Wen T. Shen[10], Mark Sywak[4],
Luis Kowalski[11], Jeremy Freeman[2], Nancy Perrier[5], and Jatin P. Shah[1]

Background: Age is a critical factor in outcome for patients with well-differentiated thyroid cancer. Currently, age 45 years is used as a cutoff in staging, although there is increasing evidence to suggest this may be too low. The aim of this study was to assess the potential for changing the cut point for the American Joint Committee on Cancer/Union for International Cancer Control (AJCC/UICC) staging system from 45 years to 55 years based on a combined international patient cohort supplied by individual institutions.

Methods: A total of 9484 patients were included from 10 institutions. Tumor (T), nodes (N), and metastasis (M) data and age were provided for each patient. The group was stratified by AJCC/UICC stage using age 45 years and age 55 years as cutoffs. The Kaplan–Meier method was used to calculate outcomes for disease-specific survival (DSS). Concordance probability estimates (CPE) were calculated to compare the degree of concordance for each model.

Results: Using age 45 years as a cutoff, 10-year DSS rates for stage I–IV were 99.7%, 97.3%, 96.6%, and 76.3%, respectively. Using age 55 years as a cutoff, 10-year DSS rates for stage I–IV were 99.5%, 94.7%, 94.1%, and 67.6%, respectively. The change resulted in 12% of patients being downstaged, and the downstaged group had a 10-year DSS of 97.6%. The change resulted in an increase in CPE from 0.90 to 0.92.

Conclusions: A change in the cutoff age in the current AJCC/UICC staging system from 45 years to 55 years would lead to a downstaging of 12% of patients, and would improve the statistical validity of the model. Such a change would be clinically relevant for thousands of patients worldwide by preventing overstaging of patients with low-risk disease while providing a more realistic estimate of prognosis for those who remain high risk.

Introduction

The incidence of well-differentiated thyroid cancer (WDTC) is rapidly rising (1–4). The biology of WDTC is highly dependent on age, with young patients out-performing older patients in terms of survival (5). As such, staging of WDTC is unique among adult malignancies in that the American Joint Committee on Cancer/Union for International Cancer Control (AJCC/UICC) includes age within the staging system for this disease (6). All patients <45 years

[1]Department of Surgery/Endocrinology, Memorial Sloan Kettering Cancer Center, New York, New York.
[2]Department of Otolaryngology, Mount Sinai Hospital, Toronto, Canada.
[3]Department of Surgery, University of California, Davis Medical Center, Sacramento, California.
[4]Department of Endocrine Surgery, Endocrine Surgical Unit, University of Sydney, Sydney, Australia.
[5]Department of Endocrine Surgery, MD Anderson, Houston, Texas.
[6]Department of Endocrinology, Endocrine Service, Instituto Nacional do Cancer, Rio de Janeiro, Brazil.
[7]Department of Endocrinology, Endocrinology Service, Faculdade de Medicina-Universidade Federal do Rio de Janeiro, Rio de Janeiro, Brazil.
[8]Department of Head and Neck Surgery, Barretos Cancer Hospital, Barretos, Brazil.
[9]Department of Surgery, Head and Neck Surgical Oncology and Nuclear Medicine, Cancer Care Manitoba and University of Manitoba, Winnipeg, Canada.
[10]Department of Endocrine Surgery, University of California, San Francisco, San Francisco, California.
[11]Department of Head and Neck Surgery, ACCamargo Cancer Center, São Paulo, Brazil.

old are considered stage I, unless there is evidence of distant metastases, which is considered stage II disease. However, patients ⌷⌷5 years are staged dependent on tumor characteristics, nodal involvement, and distant metastatic disease in a fashion similar to squamous-cell carcinoma of the head and neck.

Age 45 years was chosen as a cutoff based on historical patient cohorts that gave rise to many of the early staging systems (7). The median age of most cohorts is 45 years, making this a convenient cutoff for categorical variable analysis. Recent trends, however, suggest that the average age of patients presenting with disease is increasing (8), thus placing more patients at risk of being placed at a higher-stage group. In addition, there is mounting evidence that age cutoff of 45 years is too low, and that many older patients remain at low risk of disease-specific death (9⌷⌷).

A recent analysis of survival for patients treated at Memorial Sloan Kettering Cancer Center (MSKCC) between 1986 and 2005 concluded that a change from 45 to 55 years in the current AJCC/UICC model would lead to a significant increase in the number of patients being considered at a lower stage, while maintaining the excellent outcomes for those patients considered to have early-stage disease (12). The aim of this study was to validate the proposed change in age cutoff in a large international cohort of patients.

Methods

Approaches were made to a number of international groups with an interest in thyroid cancer outcomes analysis. All centers received approval from their Institutional Review Board or equivalent. Only patients treated at the respective

institutions were considered for inclusion. In order to ensure high-quality, reliable data, all groups were asked to provide clinician-collected data on tumor characteristics, nodal involvement, and distant metastatic disease (TNM), age at first treatment, disease-specific survival (DSS) status, and time to last follow-up.

A total of 10 institutions provided a total of eight data sets. The cohort included patients treated at MSKCC between 2005 and 2010. This MSKCC cohort was separate from the cohort used to develop the age 55 years model, who were treated between 1986 and 2005. Each institution was responsible for the accuracy of data provided. Following collation of the overall cohort at the coordinating center (MSKCC), any patients who could not be staged due to missing data were excluded. The remaining cohort was assigned an AJCC/UICC stage, and then re-staged using the AJCC/UICC model with age 55 years as a cutoff rather than age 45 years. Data from the Manitoba registry were also included. These data have previously been analyzed regarding the age cutoff for thyroid cancer staging, and for that reason, a subgroup analysis was also performed without these data (13,14).

In addition to analysis of the group as a whole, the outcomes of all patients who were effectively downstaged by the change were analyzed as a separate subgroup to confirm the effect on specific patient groups within the cohort.

The Kaplan⌷Meier method was used to express outcomes. A concordance probability estimate (CPE) was used to estimate the degree of concordance between stage and observed outcomes for each model (15). Ties from the calculation of CPE were excluded to prevent untoward consequences of a small number of prognostic categories.

Table 1. Data Relating to Each Contributing Data Set and Combined Cohort, Including Patient Number, Follow-Up, and Disease-Specific Survival

Institution	Total contribution	Inclusion dates	Median follow-up of censored patients (years)	Range follow-up of censored patients (years)	DSS⌷5 years	DSS⌷10 years
Combined	9484	1963⌷2012	5.3	0⌷4.0	98.3%	96.9%
Memorial Sloan Kettering Cancer Center	2173	2005⌷2010	3.3	0⌷5	99.10%	Not reached
University of Manitoba	1998	1970⌷2010	11.4	0⌷3.9	97.20%	95.70%
University of California, San Francisco	1851	1994⌷2004	4.6	0⌷5.4	98.20%	97.40%
University of Sydney Endocrine Surgical Unit	1129	1963⌷2012	3.0	0⌷4.0	98.20%	96.20%
Mount Sinai Hospital, Toronto	925	1963⌷2011	6.0	0⌷3.9	99.10%	97.50%
Endocrine Service, Instituto Nacional do Cancer/Universidade Federal do Rio de Janeiro	646	1986⌷2014	8.3	2.7⌷3	99.40%	97.30%
Barretos Cancer Hospital/ACCamargo Cancer Center	519	1980⌷2001	7.5	0⌷5.1	96.90%	96.10%
MD Anderson	243	2005⌷2012	3.8	0.5⌷3	100%	Not reached

DSS, disease-specific survival.

Table 2. Entire Cohort Stratified by Variables Required for AJCC/UICC Staging Model

Variable	N (%)
Age	
≤45 years	4546 (47.9)
≥45 years	4938 (52.1)
≤55 years	6648 (70.1)
≥55 years	2836 (29.9)
T Stage	
T1	4655 (49.1)
T2	1847 (19.5)
T3	2307 (24.3)
T4	510 (5.4)
T0/X	165 (1.7)
N Stage	
N0/Nx	6611 (69.7)
N1a	1424 (15)
N1b	1391 (14.7)
N1 NOS	58 (0.6)
M Stage	
M0/MX	9234 (97.4)
M1	250 (2.6)

AJCC/UICC, American Joint Committee on Cancer/Union for International Cancer Control.

Results

In total, 10 institutions provided data in eight separate data sets, which were combined for two units. In total, the combined data set described 9484 patients with a median follow-up of 5.3 years (range 0–44 years). The 10-year DSS for the entire cohort was 96.9%. A total of 224 patients died of disease. The details of the patients from each data set and the combined cohort, including patient number, follow-up, and DSS, are shown in Table 1.

The median age of the cohort was 45 years (range 4–96 years). Almost half of the patients (49.1%) had T1 tumors, and most (69.7%) were N0/NX. Nearly all patients had no metastatic disease, and so they were recorded as M0/MX (97.4%). Table 2 shows the breakdown of all elements required for AJCC/UICC staging.

Initially, patients were staged with the AJCC/UICC staging system using 45 years as the cutoff for age. A total of 6600 patients (69.6%) were reported as stage I, 741 patients (7.8%) as stage II, 1230 (13%) as stage III, and 913 (9.6%) as stage IV. The 10-year survival rates for stages I–IV were 99.7%, 97.3%, 96.6%, and 76.3%, respectively. Figure 1A shows the Kaplan–Meier plot for the AJCC/UICC staging with an age cutoff of 45 years.

The same cohort of patients was then staged with the AJCC/UICC staging system using 55 years as the cutoff for age. Similarly, stage I had the most patients with 7736 patients (81.5%). Stages II–IV made up less than a quarter of the total number of patients. Stage II had the fewest number of patients (441), stage III had 707 patients (7.5%), and stage IV had 600 patients (6.3%). The 10-year survival rates for stages I–IV were 99.5%, 94.7%, 94.1%, and 67.6%, respectively. Figure 1B shows the Kaplan–Meier curve for the AJCC/UICC staging with an age cutoff of 55 years.

The stage distributions of the entire cohort using age 45 years and age 55 years as a cutoff are shown in Table 3.

By changing the age cutoff in the AJCC/UICC staging system from 45 to 55 years, 1165 patients were downstaged (12.3%). A total of 329 patients (3.5%) went from stage II with the cutoff of 45 years to stage I with the cutoff of 55 years. A total of 523 patients (5.5%) were downstaged from stage III to stage I; 284 patients (3.0%) were downstaged from stage IV to stage I. Additionally, 29 patients (<1%) changed from stage IV to stage II. These data are shown in Table 4.

The DSS rate of those 1165 patients directly affected by the change in staging model was 97.6% at 10 years. When stratified by new stage, those patients downstaged to stage I (1136; 98%) have a 10-year DSS rate of 98.2%, whereas those downstaged to stage II (29, 2%) have a 10-year DSS rate of 75.5% (Fig. 2).

Detailed analysis of the effect of the proposed staging changes on each current stage group is shown in Figure 3A–C. Patients currently considered AJCC/UICC stage II (age ≥45 years T2N0M0, or young patients who are M1) continue to have excellent outcomes. As expected, those older patients with T2N0M0 disease who are considered as stage I with the proposed change have slightly superior outcomes to those who remain stage II (10-year DSS 99.1% vs. 95.9%; p = 0.027; Fig. 3A). Those patients currently considered to have stage III disease (≥45 years with T3N0M0 or T1-3N1aM0 disease) may either remain in stage III if ≥55 years or transition to stage I disease (those between 45 and 54 years). Those younger patients who are considered stage I with the proposed change have excellent outcomes compared with those who remain in stage III (10-year DSS 99.6% vs. 94.1%; p < 0.001; Fig. 3B). Patients currently considered stage IV are aged >45 years with advanced local (T4) regional (N1b), or distant (M1) disease. Those patients who are M0 (T4/N1b) and are aged between 45 and 54 years transition to stage I and have excellent outcomes (10-year DSS 94.8%). In contrast, those who transition to stage II disease (age 45–54 years M1) have poor outcomes compared with the current stage IV group (10-year DSS 75.5% vs. 67.6%; p = 0.7; Fig. 3C). Only 29 (0.3%) patients transition into stage II disease.

The CPE calculated for the AJCC model using age 45 years as a cutoff is 0.90 (standard error 0.02) compared with 0.92 (standard error 0.01) for the same model using age 55 years as a cutoff, suggesting an improvement.

Subgroup analysis with exclusion of the Manitoba data set was performed in an identical manner. Again, an improvement in CPE was seen when the cutoff was moved from 45 to 55 years (CPE 45-year cutoff 0.87 [SE = 0.03]; CPE 55-year cutoff 0.89 [SE = 0.03]).

Discussion

WDTC is being diagnosed with increased frequency worldwide. Few patients die of the disease, and therefore the vast majority of patients should not be considered to be at an advanced stage or high risk at the time of diagnosis.

Following the recognition in the 1960s and 1970s that histology was critical in predicting outcome for those patients with thyroid cancer, refinements in risk prediction were based on the experience of major centers across the world (16–19).

In 1976, Cady et al. published work that showed the association of age with outcome. They stratified their cohort as age <40 years, 40–50 years, and >50 years.
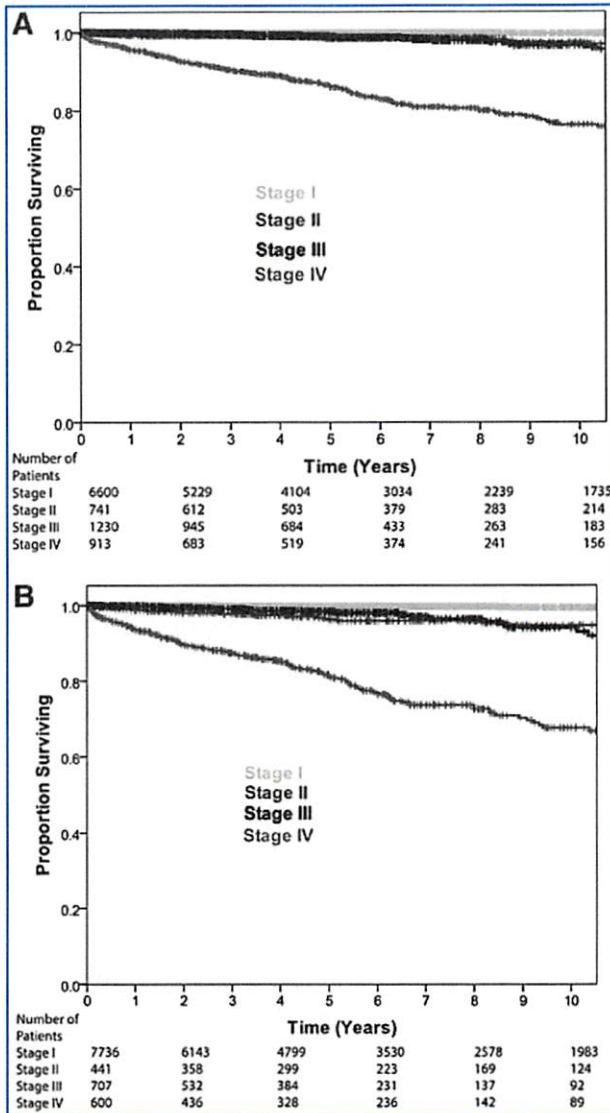
FIG. 1. Comparison of disease-specific survival by American Joint Committee on Cancer/Union for International Cancer Control (AJCC/UICC) staging system using an age cutoff of (A) 45 years and (B) 55 years.

Table 3. Entire Cohort Described by AJCC/UICC Staging Model Using Cutoffs Age of 45 Years and 55 Years

AJCC/UICC staging	N (%)	10-year DSS
Cutoff of 45 years		
I	6600 (69.6)	99.7%
II	741 (7.8)	97.3%
III	1230 (13.0)	96.6%
IV	913 (9.6)	76.3%
Cutoff of 55 years		
I	7736 (81.5)	99.5%
II	441 (4.6)	94.7%
III	707 (7.5)	94.1%
IV	600 (6.3)	67.6%

Table 4. Changes in AJCC/UICC Staging When Age 45 Years Is Substituted for Age 55 Years

	Age 55 I	Age 55 II	Age 55 III	Age 55 IV
AJCC/UICC 45 I	6600	0	0	0
AJCC/UICC 45 II	329	412	0	0
AJCC/UICC 45 III	523	0	707	0
AJCC/UICC 45 IV	284	29	0	600

In 1986, the Mayo Clinic reported outcomes for 859 patients with papillary thyroid cancer (PTC) treated between the 1940s and 1970s. Their results suggested that older age as well as extrathyroidal extension and distant metastases were predictors of disease-specific death. A number of groups, including Mazzaferri et al., reported similar findings (20,21).

The Mayo Clinic combined the risk factors of age, tumor grade, extent of disease, and size of primary lesion in to the AGES system for risk prediction, which was an early method of disease staging (17). Staging patients allowed low- and high-risk groups to be identified. This would later be refined to include completeness of surgical resection and reported as a MACIS score (22), which applied a greater weight to age from the cutoff of 40 years.

The experience of >800 patients managed at the Lahey Clinic over four decades was reported by Cady et al. in 1988 (18). They found similar results, introducing the AMES system, which included age, distant metastases, extrathyroidal extension, and size, again to stratify patients into high- and low-risk groups. This system used a different age cutoff dependent on sex (41 years for men and 51 years for women).

A similar group of risk factors was reported by Shah et al. from MSKCC (19), which gave rise to the GAMES system of stratification (including tumor grade on histology) (23). Age 45 years was chosen as the cutoff for this system. Sherman et al. reported the findings of the National Thyroid
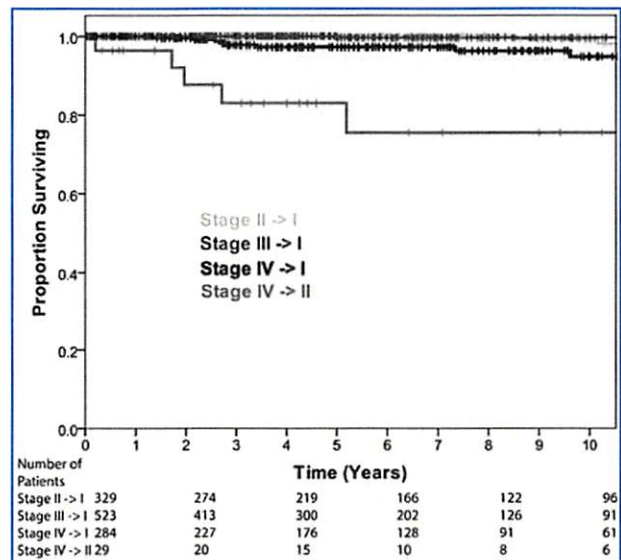

FIG. 2. Disease-specific survival of patients directly affected by the proposed change stratified by AJCC/UICC stage change.
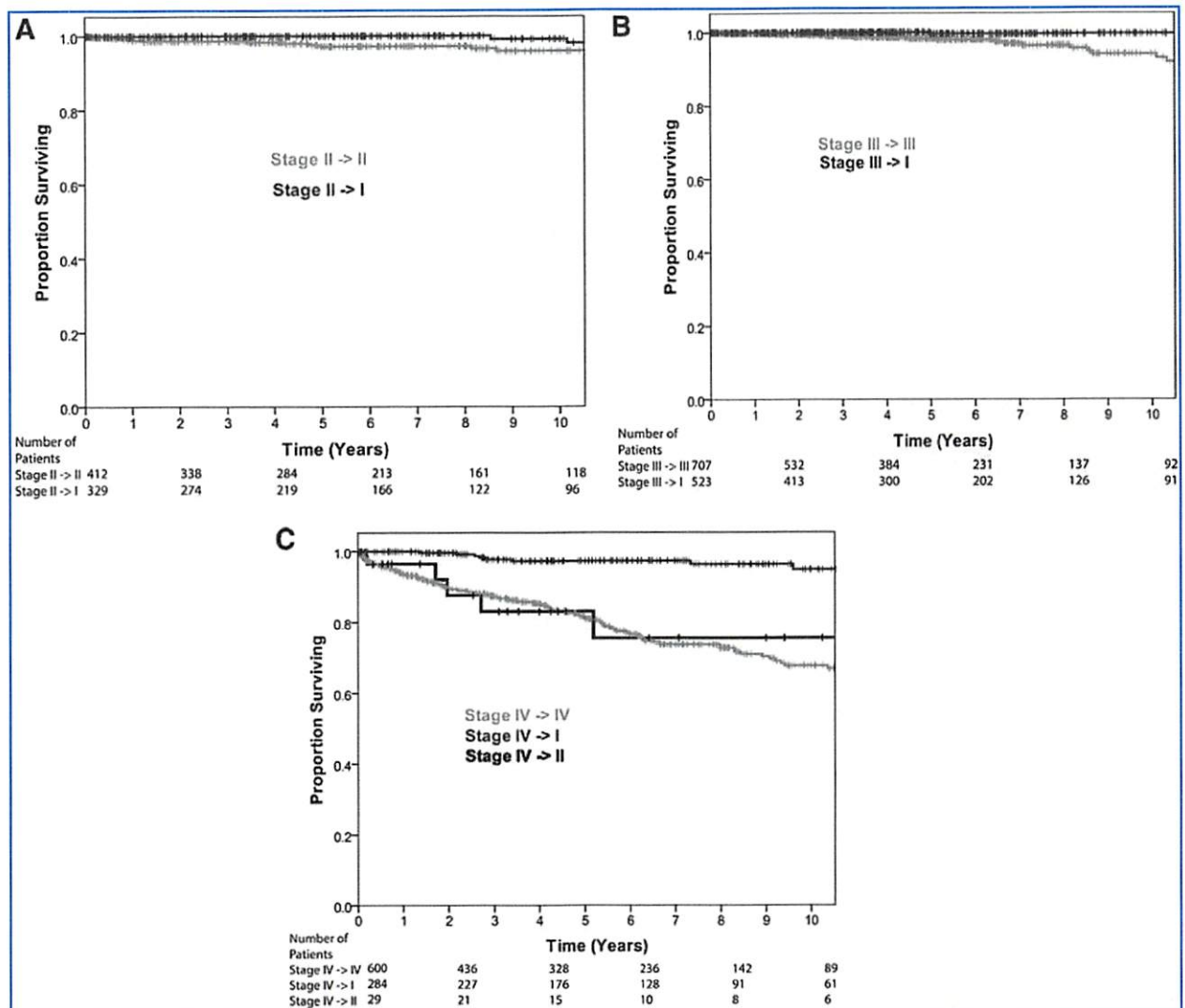
FIG. 3.   Detailed analysis of disease-specific survival by initial and re-stage groupings (A) initially stage II on AJCC/UICC, (B) initially stage III on AJCC/UICC, and (C) initially stage IV on AJCC/UICC.

Cancer Treatment Cooperative Study in 1998, again using age 45 years as a cutoff for PTC (24).

The AJCC published the second edition of its staging manual in 1977 (25), and first used an age cutoff of 45 years in 1983 (26). This has remained in use since that time, and has gained international acceptance (6). Age 45 years is used as a cutoff, with younger patients being limited to stage II disease in the presence of distant metastasis and stage I without. Patients who are ≥45 years are stage I or stage II with T1N0M0 or T2N0M0 disease, respectively. If older patients have pT3 primary disease or metastases to the central neck nodes, they are considered stage III. Those with pT4 primary disease, superior mediastinal, lateral neck, or distant metastases are considered stage IV.

Although younger patients outperform older patients in terms of survival, irrespective of the age cutoff selected, clinical experience led to the observation that many older patients remained at low risk of disease-specific death, despite the stage grouping assigned by the AJCC/UICC model.

This observation led to an analysis of the MSKCC institutional database in order to determine a statistically robust age cutoff using the current AJCC/UICC model. A process of recursive partitioning was used to determine that although no cutoff was perfect, age 55 years was more suitable than age 45 years (12). Such a change resulted in a wider spread of DSS between stage groups (stage I–IV for AJCC/UICC using 45 years 99.6–81% vs. 99.2–74%) while resulting in 12% of patients being downstaged. The vast majority of the downstaged patients (97%) were then considered as stage I disease, and the DSS rate of this specific group of patients was 98% at 10 years. This analysis suggested that using an age cutoff of 45 years leads to a significant number of patients who are at very low risk of death being inappropriately assigned an advanced disease stage. Not only does this approach lead to heightened patient anxiety, but it also encourages clinicians to recommend more aggressive primary therapy in a group of patients with little potential for gain. In addition, those patients who remain in stage groups III and IV have outcomes

more in keeping with the label of advanced disease (67.6% 10-year DSS in stage IV patients) (12).

International reports of the analysis of multiple institutional data sets have also suggested that age 45 years may not be the ideal cutoff for WDTC. Analysis of the National Thyroid Cancer Treatment Cooperative Study Group by Jonklaas et al. questioned whether a cutoff >45 years would improve current staging systems in a U.S. population (10). Study of a Japanese cohort of around 1000 patients by Ito et al. revealed that a change in survival was observed at 60 years (27).

Analysis of the Surveillance, Epidemiology, and End Results (SEER) database has also scrutinized the relationship between age and outcome. Oyer et al. demonstrated that prognosis remains unaffected by age until 35 years (28). Although Bischoff et al. found that survival deteriorated with age, no specific inflection point was seen at 45 years, and survival for all patients <65 years exceeded 90%, again raising the question of whether a cutoff of 45 years is appropriate (9). More recently, Kim et al. included >35,000 patients treated between 1988 and 2010, and found age 57 years to be the optimal age cutoff for determining DSS (29).

However, investigation into outcomes from WDTC is limited by the number of events. With such excellent overall outcomes, large cohorts and long follow-up are required. Although national registries such as SEER and the National Cancer Data Base provide such a resource, they lack critical detail, including that relating to lymph node characteristics, which may have a significant impact on the overall results (30). In contrast, single institutional data sets provide high-quality data, usually collected by clinicians and subjected to rigorous quality control. However, such resources are limited by patient numbers.

The aim of this study was to attempt to address the weaknesses of both approaches by combining a group of clinician-collected data sets into one multi-institutional cohort, which would provide large patient numbers and reliable clinical data.

The results show that a change in the age cutoff for the AJCC/UICC model would impact a large number of patients. The change leads to a widening of DSS outcomes at 10 years: 99.7–95.3% for age 45 years to 99.5–87.6% for 55 years. More importantly, however, 12% of patients are downstaged by the change, with 9% moving from "advanced" stage III or IV disease to stage I or II disease. It is critical to note that despite this downstaging, outcomes in the stage I and II disease categories remain excellent (99.5% and 94.7% 10-year DSS, respectively).

Patients who would be affected by this change are those between the ages of 45 and 54 years. A change in age cutoff would render all patients in this age category as stage I, unless they were M1 at presentation, which would result in assignment to stage II. The overwhelming majority of this group (98%) would be restaged to AJCC/UICC stage I. These patients have a 10-year DSS rate of 98.2%, suggesting that they are currently incorrectly assigned to a more advanced stage category. For almost all patients who are currently considered stage II–IV, the change in staging is appropriate, with 10-year DSS rates in re-staged patients of 95% (Fig. 3A).

Those patients who are between 45 and 54 years of age and have M1 disease would be restaged as stage II. The patients in this group have less favorable outcomes (10-year DSS 75.5%; Fig. 3C). This change has a number of detrimental effects on the overall staging system. The impact on stage II disease overall is to lower the DSS rate from 97.3% with age 45 years as a cutoff to 94.7% at 10 years with age 55 years as a cutoff. This results in the DSS of stage II being slightly lower than stage III (96.3% stage II vs. 98.3% stage III) due to the outcome of patients aged 45–54 years with distant metastases. In addition, these specific patients would be assigned to a stage group with significantly better outcomes than they would have if analyzed as a separate subgroup (96.3% vs. 83%). However, the number of patients who fall in this group is small (2% of those re-staged and 0.3% of the entire cohort in this study). In addition, those patients who present with distant metastases do not present a management dilemma, as all will be treated with total thyroidectomy, appropriate neck dissection, if indicated, and postoperative radioactive iodine (RAI).

The patients with limited disease represent the group in whom treatment remains most controversial. The need for aggressive treatment to primary and potential metastatic disease in terms of total thyroidectomy, elective central neck dissection, and postoperative RAI is unproven in the majority of these cases. Indeed, the approach to therapy will be tailored to the perceived nature of the disease on an individual basis. This highlights the importance of avoiding unnecessary overstaging of patients with biologically non-aggressive disease.

In particular, the presence of limited regional disease (particularly small-volume N1a disease) and moderately locally advanced (T3) disease, which can be managed surgically, currently upstages older patients to stage III, and very few will go on to die of their disease. The current results show that this group have excellent outcomes, irrespective of whether they are 45–54 years (99.6% 10-year DSS) or >55 years (94.1 10-year DSS), demonstrating the fact that such disease features do not seem to reflect aggressive disease, irrespective of age.

Assessment of the discriminatory power of the two staging models shows that both age cutoffs perform well. Using the current system, the CPE is 0.90. However, this rises to 0.92 when the cutoff of age 55 is applied. This suggests that such a change would be both clinically relevant and statistically robust.

This work is not without limitations. All groups collected data retrospectively, which limits the conclusions that can be drawn from any such study. In addition, diagnostic, treatment, and follow-up regimens vary between groups and have evolved over the decades described. Although this study includes a high number of patients with data from reliable sources, the follow-up time was limited. The vast majority of surgically treated recurrences occur within two years of initial therapy (31). However, it is likely that events will continue to occur beyond the five-year median reported here. It is also clear that no single age cutoff will be perfect. Analysis of outcomes for patients managed at MSKCC between 1986 and 2010 (including both the cohort of patients used to generate the initial model and patients used in this study) suggest that no specific cutoff is ideal (32). Indeed, it is likely that modular systems based upon continuous variables will outperform any such system. However, the AJCC/UICC model is simple to apply and internationally accepted. For this reason, it has been widely adopted, and the AJCC/UICC committee is

not likely to abandon the system in the next edition of the staging manual. Patients who transition into stage II have poor outcomes using this system (75.5% 10-year DSS). This has a limited impact on the overall performance of patients with stage II disease, and affects only 29 patients, which constitutes <0.5% of the overall cohort.

This work represents the largest multi-institutional clinician-collected cohort of patients treated for WDTC reported to date. Prospective studies of this size on this subject are not feasible, and cohorts described in national registries lack the accurate data required to draw robust conclusions in relation to disease-specific outcomes.

In conclusion, the present results suggest that the AJCC/ UICC should consider a change in the staging model for WDTC to incorporate an age cutoff of 55 years rather than 45 years. Such a change would improve the distribution of outcomes between stage I and IV disease and lead to a downstaging of 12% of patients. Almost 10% of low-risk patients would move out of the advanced disease stage category, which would maintain excellent outcomes in those with stage I–II disease while providing more accurate prognostic information for those considered to have stage IV disease. This improved recognition of disease biology would enable clinicians to counsel their patients more accurately and select appropriate therapy accordingly.

Acknowledgment

Author Disclosure Statement

The authors have nothing to disclose.

References

1. Cramer JD, Fu P, Harth KC, Margevicius S, Wilhelm SM 2010 Analysis of the rising incidence of thyroid cancer using the Surveillance, Epidemiology and End Results national cancer data registry. Surgery 148:1147–52; discussion 1152–43.
2. Davies L, Welch HG 2010 Thyroid cancer survival in the United States: observational data from 1973 to 2005. Arch Otolaryngol Head Neck Surg 136:440–44.
3. Enewold L, Zhu K, Ron E, Marrogi AJ, Stojadinovic A, Peoples GE, Devesa SS 2009 Rising thyroid cancer incidence in the United States by demographic and tumor characteristics, 1980–2005. Cancer Epidemiol Biomarkers Prev 18:784–91.
4. Chen AY, Jemal A, Ward EM 2009 Increasing incidence of differentiated thyroid cancer in the United States, 1988–2005. Cancer 115:3801–07.
5. Haymart MR 2009 Understanding the relationship between age and thyroid cancer. Oncologist 14:216–21.
6. Edge SB; American Joint Committee on Cancer 2010 AJCC Cancer Staging Manual. Seventh edition. Springer, New York.
7. Cady B, Sedgwick CE, Meissner WA, Wool MS, Salzman FA, Werber J 1979 Risk factor analysis in differentiated thyroid cancer. Cancer 43:810–20.
8. Hughes DT, Haymart MR, Miller BS, Gauger PG, Doherty GM 2011 The most commonly occurring papillary thyroid cancer in the United States is now a microcarcinoma in a patient older than 45 years. Thyroid 21:231–36.
9. Bischoff LA, Curry J, Ahmed I, Pribitkin E, Miller JL 2013 Is above age 45 appropriate for upstaging well-differentiated papillary thyroid cancer? Endocr Pract 19:995–97.
10. Jonklaas J, Nogueras-Gonzalez G, Munsell M, Litofsky D, Ain KB, Bigos ST, Brierley JD, Cooper DS, Haugen BR, Ladenson PW, Magner J, Robbins J, Ross DS, Skarulis MC, Steward DL, Maxon HR, Sherman SI, National Thyroid Cancer Treatment Cooperative Study G 2012 The impact of age and gender on papillary thyroid cancer survival. J Clin Endocrinol Metab 97:E878–87.
11. McLeod DS, Jonklaas J, Brierley JD, Ain KB, Cooper DS, Fein HG, Haugen BR, Ladenson PW, Magner J, Ross DS, Skarulis MC, Steward DL, Xing M, Litofsky DR, Maxon HR, Sherman SI 2015 Reassessing the NTCTCS staging systems for differentiated thyroid cancer, including age at diagnosis. Thyroid 25:1097–105.
12. Nixon IJ, Kuk D, Wreesmann V, Morris L, Palmer FL, Ganly I, Patel SG, Singh B, Tuttle RM, Shaha AR, Gonen M, Shah JP 2016 Defining a valid age cutoff in staging of well-differentiated thyroid cancer. Ann Surg Oncol 23:410–15.
13. Hendrickson-Rebizant J, Sigvaldason H, Nason RW, Pathak KA 2015 Identifying the most appropriate age threshold for TNM stage grouping of well-differentiated thyroid cancer. Eur J Surg Oncol 41:1028–32.
14. Mazurat A, Torroni A, Hendrickson-Rebizant J, Benning H, Nason RW, Pathak KA 2013 The age factor in survival of a population cohort of well-differentiated thyroid cancer. Endocr Connect 2:154–60.
15. Heller G, Mo Q 2015 Estimating the concordance probability in a survival analysis with a discrete number of risk groups. Lifetime Data Anal 2015 May 29. [Epub ahead of print].
16. Byar DP, Green SB, Dor P, Williams ED, Colon J, van Gilse HA, Mayer M, Sylvester RJ, van Glabbeke M 1979 A prognostic index for thyroid carcinoma. A study of the E.O.R.T.C. Thyroid Cancer Cooperative Group. Eur J Cancer 15:1033–41.
17. Hay ID, Grant CS, Taylor WF, McConahey WM 1987 Ipsilateral lobectomy versus bilateral lobar resection in papillary thyroid carcinoma: a retrospective analysis of surgical outcome using a novel prognostic scoring system. Surgery 102:1088–95.
18. Cady B, Rossi R 1988 An expanded view of risk-group definition in differentiated thyroid carcinoma. Surgery 104: 947–53.
19. Shah JP, Loree TR, Dharker D, Strong EW, Begg C, Vlamis V 1992 Prognostic factors in differentiated carcinoma of the thyroid gland. Am J Surg 164:658–61.
20. Mazzaferri EL, Young RL, Oertel JE, Kemmerer WT, Page CP 1977 Papillary thyroid carcinoma: the impact of therapy in 576 patients. Medicine (Baltimore) 56:171–96.
21. Mazzaferri EL, Young RL 1981 Papillary thyroid carcinoma: a 10 year follow-up report of the impact of therapy in 576 patients. Am J Med 70:511–18.
22. Hay ID, Bergstralh EJ, Goellner JR, Ebersold JR, Grant CS 1993 Predicting outcome in papillary thyroid carcinoma: development of a reliable prognostic scoring system in a cohort of 1779 patients surgically treated at one institution during 1940 through 1989. Surgery 114:1050–57; discussion 1057–58.
23. Shaha AR, Shah JP, Loree TR 1996 Risk group stratification and prognostic factors in papillary carcinoma of thyroid. Ann Surg Oncol 3:534–38.
24. Sherman SI, Brierley JD, Sperling M, Ain KB, Bigos ST, Cooper DS, Haugen BR, Ho M, Klein I, Ladenson PW,

Robbins J, Ross DS, Specker B, Taylor T, Maxon HR 3rd 1998 Prospective multicenter study of thyroid carcinoma treatment: initial analysis of staging and outcome. National Thyroid Cancer Treatment Cooperative Study Registry Group. Cancer 83:1012–1021.

25. American Joint Committee on Cancer Staging and End Results Reporting, American Cancer Society 1977 Manual for Staging of Cancer, 1977. American Joint Committee for Cancer Staging and End-Results Reporting, Chicago, IL.

26. American Joint Committee on Cancer 1983 Manual for Staging of Cancer. J.B. Lippincott, Philadelphia, PA.

27. Ito Y, Miyauchi A, Kihara M, Takamura Y, Kobayashi K, Miya A 2012 Relationship between prognosis of papillary thyroid carcinoma patient and age: a retrospective single-institution study. Endocr J 59:399–405.

28. Oyer SL, Smith VA, Lentsch EJ 2012 Reevaluating the prognostic significance of age in differentiated thyroid cancer. Otolaryngol Head Neck Surg 147:221–226.

29. Kim SJ, Myong JP, Suh H, Lee KE, Youn YK 2015 Optimal cutoff age for predicting mortality associated with differentiated thyroid cancer. PloS One 10:e0130848.

30. Mehra S, Tuttle RM, Milas M, Orloff L, Bergman D, Bernet V, Brett E, Cobin R, Doherty G, Judson BL, Klopper J, Lee S, Lupo M, Machac J, Mechanick JI, Randolph G, Ross DS, Smallridge R, Terris D, Tufano R, Alon E, Clain J, DosReis L, Scherl S, Urken ML 2015 Database and registry research in thyroid cancer: striving for a new and improved national thyroid cancer database. Thyroid 25:157–168.

31. Young S, Harari A, Smooke-Praw S, Ituarte PH, Yeh MW 2013 Effect of reoperation on outcomes in papillary thyroid cancer. Surgery 154:1354–1361; discussion 1361–1352.

32. Ganly I, Nixon IJ, Wang LY, Palmer FL, Migliacci JC, Aniss A, Sywak M, Eskander A, Freeman JL, Campbell MJ, Shen WT, Vaisman F, Momesso D, Corbo R, Vaisman M, Shaha ARM, Tuttle RMM, Shah JP, Patel SG 2015 Survival from differentiated thyroid cancer What has age got to do with it? Thyroid 25:1106–14.

Address correspondence to:
Jatin Shah, MD
Department of Surgery
Memorial Sloan Kettering Cancer Center
1275 York Avenue
New York, NY 10021

E-mail: shahj@mskcc.org

RAGE Mediates the Pro-Migratory Response of Extracellular S100A4 in Human Thyroid Cancer Cells

Manoj Reddy Medapati,[1] Mathias Dahlmann,[2] Saeid Ghavami,[1,3] Kumar Alok Pathak,[1,4] Lydia Lucman,[5] Thomas Klonisch,[1,4,6] Cuong Hoang-Vu,[7] Ulrike Stein,[2] and Sabine Hombach-Klonisch[1,8]

Background: Expression of the small calcium-binding protein S100A4 is associated with poor prognosis in patients with thyroid cancer (TC). The authors have previously shown that S100A4 is a target for relaxin and insulin-like peptide 3 signaling in TC cells and that S100A4 is secreted from human TC cells. Although the pro-migratory role of intracellular S100A4 in binding to non-muscle myosin is well known, this study investigated here whether extracellular S100A4 contributes to TC migration.

Methods: Human cell lines of follicular, papillary, and undifferentiated thyroid cancer, primary patient TC cells, and TC tissues were utilized to discover the presence of the receptor of advanced glycation end products (RAGE) in TC cells and TC tissues. Fluorescence imaging, protein pull-down assays, Western blot, siRNA protein silencing, small GTPase inhibitors, cell proliferation, and cell migration assays were used to investigate the interaction of extracellular S100A4 with RAGE in promoting a TC migratory response.

Results: It was demonstrated that RAGE served as receptor for extracellular S100A4 mediating cell migration in TC cells. The RAGE-mediated increase in cell migration was dependent on the intracellular RAGE signaling partner diaphanous-1 (Dia-1) and involved the activation of the small GTPases Cdc42 and RhoA. Although extracellular S100A4 consistently activated ERK signaling in TC cells, it was shown that ERK signaling was not mediated by RAGE and not essential for the migratory response in TC cells.

Conclusion: The data have identified the RAGE/Dia-1 signaling system as a mediator for the pro-migratory response of extracellular S100A4 in human TC. Thus, therapeutic targeting of the RAGE/Dia-1/small GTPases signaling may successfully reduce local invasion and metastasis in TC.

Introduction

THE ANNUAL INCIDENCE RATE FOR THYROID CANCER (TC) increased steadily from 1975 to 2010 in the United States (http://seer.cancer.gov/csr/1975_2010/). TC is the most common carcinoma of the endocrine glands, and more than 98% of all thyroid malignancies are categorized as papillary (PTC), follicular (FTC), anaplastic/undifferentiated (UTC), or medullary (MTC) thyroid carcinoma histological types. Despite the fact that most FTC and PTC can be cured by hemi-thyroidectomy, recurrences and treatment failures impose a poor prognosis. Increased local tumor size, capsular infiltration, vascular invasion, and the presence of distant metastasis are parameters predicting poor prognosis for pa-

tients with TC (1–3). The small calcium-binding protein S100A4 (metastasin) has been associated with enhanced tumor cell migration and increased metastasis in several human cancers (4–9). S100A4 gene expression has been described as a marker for poor prognosis in patients with TC (10). It serves as an early marker for metastasis in PTC, including papillary microcarcinomas, and correlates with invasiveness in FTC (11–13). The authors have previously shown that S100A4 production is significantly enhanced by relaxin/RXFP1 and insulin-like peptide 3 (INSL3)/RXFP2 signaling in human TC cells (14,15) and that S100A4 mediates the pro-migratory effects induced by these peptides in TC cells. It was observed that S100A4 is secreted by human TC cells endogenously expressing S100A4, and acts as a potent factor promoting

---

Departments of [1]Human Anatomy and Cell Science, [4]Surgery, [8]Obstetrics, Gynecology, and Reproductive Sciences, and [6]Medical Microbiology, University of Manitoba, Winnipeg, Canada.
[2]Experimental and Clinical Research Center, Charité Universitätsmedizin Berlin and Max-Delbrück-Center for Molecular Medicine, Berlin, Germany.
[3]Childrens Hospital Research Insitute of Manitoba, Winnipeg, Canada.
[5]Pathology, St. Boniface General Hospital, Winnipeg, Canada.
[7]Experimental Oncology Group, Department of Surgery, Martin-Luther-University Halle-Wittenberg, Halle, Germany.

angiogenesis in TC xenografts (14). Although S100A4 was shown to interact with intracellular targets such as liprin β1 and non-muscle myosin to mediate cytoskeletal changes promoting cell migration (16–19), the mechanisms elicited by secreted extracellular S100A4 on cancer cells are not well understood.

The receptor of advanced glycation end products (RAGE) is a pattern recognition receptor (20,21) and mediates the actions of several molecules of the danger-associated molecular pattern molecules (DAMPs) (22,23), such as HMGB1 in enhancing inflammatory and survival mechanisms in several human pathologies (23–25). RAGE is expressed in several human cancer entities (26–29), but its expression in TC is not known. S100A4 binds to RAGE in the dimeric and oligomeric form *in vitro* (30). Interaction of extracellular S100A4 with RAGE was recently demonstrated in chondrocytes of osteoarthritis patients (31), in endothelial cells (32), and in human colorectal cancer cells (33), and resulted in ERK1/2 phosphorylation. In a xenograft model of human prostate cancer, S100A4 acts via RAGE to promote tumor growth (34).

In this study, the expression of RAGE in human TC tissues and TC cells isolated from surgical tissue specimen was identified, and the interaction of recombinant human S100A4 (rhS100A4) with RAGE in TC cells with endogenous RAGE expression was demonstrated. It was shown that the motility promoting effect of S100A4 was dependent on RAGE. S100A4-RAGE signaling was mediated through its cytoplasmic interaction partner diaphanous-1 (Dia-1) and was dependent on the small GTPases Rac-1/Cdc42 and RhoA.

Materials and Methods

Cell culture

Human TC cell lines FTC133, FTC236, C643, TPC-1, and B-CPAP were cultured in Dulbecco's modified Eagle's medium/Nutrient F-12 Ham 1:1 (DME/F12, Hyclone; Thermo Scientific, Waltham, MA) with 10% fetal bovine serum (FBS; Invitrogen, Burlington, Canada) and passaged every three to four days to maintain a proliferative culture.

RAGE knockdown in TC cells through transient transfection

The human TC cell lines FTC 236 and C643 were seeded at a density of 1×10^5 cells/well and treated with small interference RNA (siRNA) for RAGE (#sc-36374) or scrambled siRNA (#sc-37007; both Santa Cruz Biotechnologies, Santa Cruz, CA) at a concentration of 80 nM using SilentFect (#170-3361; Bio-Rad, Mississauga, Canada).

Production of stable Dia-1 KO clones

FTC 236 and C643 cells were seeded at a density of 5×10^4 cells/well and treated with 15 μg/mL polybrene for 2 h followed by transduction of lentiviral Dia-1 shRNA particles or control shRNA, respectively (both Santa Cruz Biotechnologies; sc-35190-V, sc-108080). Stable clones were selected using puromycin at 4 μg/mL (#P9620; Sigma, St Louis, MO).

Primary human thyroid cell culture

Human thyroid primary cells were isolated from surgical tissues obtained from patients undergoing hemi-thyroidectomy at St. Boniface General Hospital with ethics approval from the University of Manitoba Human Ethics Board. TC cells were isolated using 500 μg/mL collagenase and 10 μg/mL DNAse (both Sigma) for tissue digestion, filtered through a 40 μm cell strainer (BD Bioscience, San Diego, CA) and subjected to red blood cell lysis. Primary cells from TC tissues were cultured in DME/F12 1:1 supplemented with 10% FBS and $1 \times$ penicillin/streptomycin (Gibco, Grand Island, NY).

Polymerase chain reaction

The cDNAs were generated using random primers. Transcripts were polymerase chain reaction (PCR) amplified from selected TC cell lines and primary TC cells. The PCR cycle consisted of an initial denaturation step at 95°C for 3 min, a denaturation step at 95°C for 1 min, annealing at specific temperature for 1 min, and a final elongation step at 72°C for 2 min. Glyceraldehyde-3-phosphate dehydrogenase (GAPDH) was used as a control to assess the quantity of cDNA used per PCR reaction. The specific oligonucleotide primer sequences for the detection of S100A4, RAGE, Toll-like receptor 4 (TLR4), and GAPDH and their respective melting temperatures are listed in Table 1.

Recombinant proteins, peptides, and inhibitors

Recombinant human S100A4 (rh S100A4; #GWB-P1718B) of *Escherichia coli* origin with N-terminal His-tag was purchased from GenWay Biotech (San Diego, CA). Advanced glycation end product–bovine serum albumin (AGE-BSA) was purchased from BioVision, Inc. (Milpitas, CA; #2221-10). The rhS100A4 and the AGE-BSA had been tested and were confirmed LPS-free. Inhibitors for Rac-1/Cdc42 (ML141; #217708) and Rho kinase (H-1152P, #555552) were both purchased from Calbiochem (Cambridge, MA). The MEK inhibitor U0126, the EGFR inhibitor AG1478, and EGF were purchased from Sigma.

RAGE pull-down assay

Dynabeads® (Antibody Coupling Kit 143.11D; Invitrogen) were coupled with rhS100A4 (4137S4; R&D Systems, Minneapolis, MN) or BSA, respectively, according to the manufacturers' protocol, and blocked with 2% BSA in phosphate-buffered saline (PBS). B-CPAP cells (3×10^7) were lysed in RIPA buffer supplemented with protease inhibitor cocktail (Roche, Mississauga, Canada). The lysate was split into three equal volumes. One volume of lysate was supplemented with 5 μg RAGE antibody (H-300; Santa Cruz Biotechnologies) before the beads were added. The lysates were incubated with 10 μg of coupled beads overnight at 4°C under constant rotation. The beads were washed three times with PBS and subjected to Western blotting and immunostaining of membranes with RAGE-specific antibody (A11; Santa Cruz Biotechnologies).

Western blotting

The preparation of protein lysates and polyacrylamide gels for Western blotting was performed as described previously (35). For the detection of RAGE, Dia-1 and S100A4, an anti-RAGE rabbit polyclonal antibody (1:1000) and an anti-Dia-1 mouse monoclonal antibody (1:1000; both Santa Cruz Biotechnologies), and an anti-S100A4 rabbit monoclonal antibody (1:1000; Cell Signaling Technology, Danvers, MA) were probed overnight at 4°C, respectively. Horseradish

TABLE 1. LIST OF OLIGONUCLEOTIDE PRIMER SEQUENCES WITH CORRESPONDING MELTING TEMPERATURES,
SIZE OF THE AMPLICONS, AND NUMBER OF PCR CYCLES USED FOR THE DETECTION OF THE TRANSCRIPT

Gene	Primer	Primer sequence (5′ to 3′)	Tm	Base pairs	No. of PCR cycles
S100A4	Forward Reverse	GAA GGC CCT GGA TGT GAT GGT G CAT TTC TTC CTG GGC TGC TTA TC	60	270	35
RAGE	Forward Reverse	TCC CCG TCC CAC CTT CTC CTG CTC CTC TTC CTC CTG GTT TTC TG	63	540	40
TLR4	Forward Reverse	CCT TCC TCT CCT GCG TGA GAC TTC ACA CCT GGA TAA ATC CAG	60	280	35
GAPDH	Forward Reverse	CAT CAC CAT CTT CCA GGA GCG TGA CCT TGC CCA CAG CCT TG	60	340	20

Tm, melting temperature; PCR, polymerase chain reaction; RAGE, receptor of advanced glycation end products; TLR4, Toll-like receptor 4; GAPDH, glyceraldehyde-3-phosphate dehydrogenase.

peroxidase (HRP) coupled goat anti-rabbit (Cell Signaling Technology) and goat anti-mouse (Sigma) secondary antibodies were used (both at 1:5000). For the detection of ERK1/2 signaling intermediates, antibodies for total ERK1/2 and phospho-ERK1/2 were purchased (Cell Signaling Technology), and blots were developed by autoradiography using ECL (Pierce, Nepean, Canada). Densitometry analysis of the X-ray films was done using the spot denso tool in Fluorchem software.

Immunofluorescence

TC cells were fixed with 3.7% formaldehyde, permeabilized with 0.01% Triton-X100 for 15 min, and blocked with 5% normal goat serum (NGS) for 1 h at room temperature (RT). Cells were incubated overnight at 4°C with the primary antibodies for RAGE (1:100), Dia-1 (1:100) (both Santa Cruz), and Pax-8 (1: 100; Biocare Medical, Inc., Concord, CA) and corresponding isotype control IgG immunoglobulins diluted in 5% NGS (Sigma). Slides were washed three times for 5 min and incubated with AlexaFluor conjugated goat anti rabbit (1:500; #A11012) and goat anti mouse (1: 1000; #A11005; both Invitrogen) secondary antibodies for 1 h at RT and washed three times for 5 min. 4′,6-diamidino-2-phenylindole (DAPI) was used for nuclear counterstain, and cells were covered in anti-fade mounting medium (Life Technologies, Burlington, Canada).

Immunohistochemistry

Human thyroid tissues of normal thyroid and TC were collected from surgical patient specimens at the Department of Surgery, University of Halle-Wittenberg, and formalin-fixed paraffin-embedded tissue sections (5 μm) were used for this study. This study was approved by the ethical committee of the Martin-Luther-University, Faculty of Medicine. The human TC tissue micro array (TMA) was obtained from US Biomax (Rockville, MD; TH208). It comprised of a total of 208 cores of 1 mm diameter and 60 cases with triplicate cores per case, including nine normal thyroid tissues. Dewaxing, antigen retrieval, and immunohistochemistry were performed as described previously (15). Sections were probed with the anti-RAGE rabbit primary antibody (1:100) or an isotype control antibody (Sigma) at equivalent protein concentrations overnight at 4°C. Following incubation with a biotin-conjugated goat anti-rabbit secondary antibody (1:500) and avidin-biotin complexes (Vectstain ABC kit, #PK-6105), specific staining was visualized using 3,3′-diaminobenzidine substrate (DAB).

Sections were imaged using a Zeiss M1 bright field microscope and a 20× objective.

Bromodeoxyuridine cell proliferation assay

Human TC cells were seeded at a density of 5×10^3 cells/well, serum starved for 24 h, and treated with rhS100A4 (100 nM, 250 nM, 500 nM). After 24 h of treatment, a calorimetric enzyme-linked immunosorbent assay (ELISA) was done using the Bromodeoxyuridine (BrdU) cell proliferation kit (Roche). The absorbance was measured at 450 nm using an ELISA reader (Perkin Elmer, Boston, MA).

Cell viability (WST-1) assay

Human TC cells were seeded at a density of 5×10^3 cells/well, serum starved, and treated with rhS100A4 (100 nM, 250 nM, 500 nM). After 24 h of treatment, WST-1 reagent was added to the cells and incubated at 37°C for 4 h. The formation of water-soluble formazan was measured at 450 nm.

Migration assay

Cells were cultured in 1% fetal calf serum medium and seeded onto a transwell filter membrane with 8 μm pore size (Costar, Corning, NY) at a density of 1×10^4 cells/well. TC cells were treated with rhS100A4 (100 nM, 250 nM, 500 nM) and AGE-BSA (10 μg/mL) for 24 h. For Rac-1/Cdc42 and RhoA inhibition experiments, cells were treated with the respective inhibitors at 10 μM for 24 h and then seeded on the filters along with the inhibitors. For MEK inhibition experiments, cells were treated with U0126 at 10 μM for 1 h prior to treatment with rhS100A4. After 24 h of migration, cells were washed, fixed with methanol, and stained with 0.1% toluidine blue dye (Sigma). Cells that had migrated to the underside of the filter were imaged and counted as described (15).

siRNA RAGE silencing

RAGE was silenced in transient transfections using SilentFect transfection reagent (BioRad) with RAGE siRNA and compared to non-silencing (scrambled) siRNA (both SantaCruz). At 48 h following siRNA treatment, cells were used for migration assays.

Cdc42 and RhoA pathway inhibition assays

Cells were serum starved and treated for 24 h with a Cdc42/Rac-1 inhibitor at 10 μM (ML141) and a Rho kinase

inhibitor at $10\,\mu M$ (H-1152P; both Calbiochem). Cells were lysed, and active GTPase proteins were pulled down using PAK-PBD (to bind GTP-Cdc42) and Rhotekin-RBD beads (to bind GTP-RhoA) using the RhoA/Rac1/Cdc42 Activation Assay Combo Biochem Kit (BK030; Cytoskeleton, Denver, CO). The immunoprecipitated active small GTPases were identified by Western blot using specific antibodies for Cdc42 and RhoA provided with the kit.

Statistical analysis

Statistical analyses were done using GraphPad Prism software. The differences between the groups were calculated using one way analysis of variance, and the confidence interval in each analyses was set at 95% so the comparisons having a p-value of <0.05 were considered significant.

Results

RAGE is expressed in human TC cells and tissues

The study demonstrated the expression of RAGE transcripts (Fig. 1A) and RAGE protein (Fig. 1B) utilizing human TC cell lines representing the three histological types of human TC: FTC (FTC133, FTC 236), PTC (TPC-1 and B-

CPAP), and UTC (C643). Expression of S100A4 was detected in FTC133 but was negligible in the other TC cell lines (Fig. 1B and C). S100A4-negative TC cells but positive for endogenous RAGE were used as the experimental model to investigate the role of extracellular S100A4 in TC. Primary TC cells isolated from surgical patient tissues (Supplementary Fig. S1A; Supplementary Data are available online at www.liebertpub.com/thy) were used in early passages (P1–P3) and expressed the thyroid cell transcription factor PAX8 as shown here with nuclear localization of PAX8 by immunofluorescence (Supplementary Fig. S1B). Primary human TC cells were tested from 18 patients, and RAGE transcripts were detected in 8 of 10 PTC and two of two FTC (Fig. 1D). RAGE transcripts were also present in four out of five primary cells isolated from follicular adenoma samples and in one goiter sample (Fig. 1D), indicating the presence of RAGE in both hyperplastic and neoplastic human TC. Immunofluorescence localization of RAGE protein was demonstrated in all human TC cell lines as shown here for FTC236 and TPC-1 (Fig. 2A). Following siRNA RAGE silencing, the detection of RAGE protein was negligible compared to the RAGE expression in untreated or scrambled siRNA treated cells (Fig. 2B) demonstrating the specificity of RAGE detection. RAGE protein was also demonstrated by immunofluorescence in

FIG. 1. Receptor of advanced glycation end products (RAGE) is expressed in established and primary thyroid cancer (TC) cells. RAGE transcripts (**A**) and RAGE protein (**B**) are expressed in the human TC cell lines FTC133 and FTC236 (both follicular thyroid cancer [FTC]), C643 (undifferentiated thyroid cancer [UTC]), and TPC1 and B-CPAP (both papillary thyroid cancer [PTC]). The expression of S100A4 transcripts in these cell lines is negligible (**C**) compared to S100A4 levels in FTC133 used as positive control. Eighteen primary thyroid cell isolates from patient tissues were tested, and RAGE transcripts were detected in 8 of 10 PTC and two of two FTC samples (**D**). Four out of five cases of primary cells isolated from follicular adenoma samples were positive for RAGE (**D**). Primary thyroid carcinoma cells and three out of five primary cells isolated from follicular adenoma were positive for S100A4 transcripts (**D**). Glyceraldehyde-3-phosphate dehydrogenase (GAPDH) was used to test for the amount and quality of the cDNA.
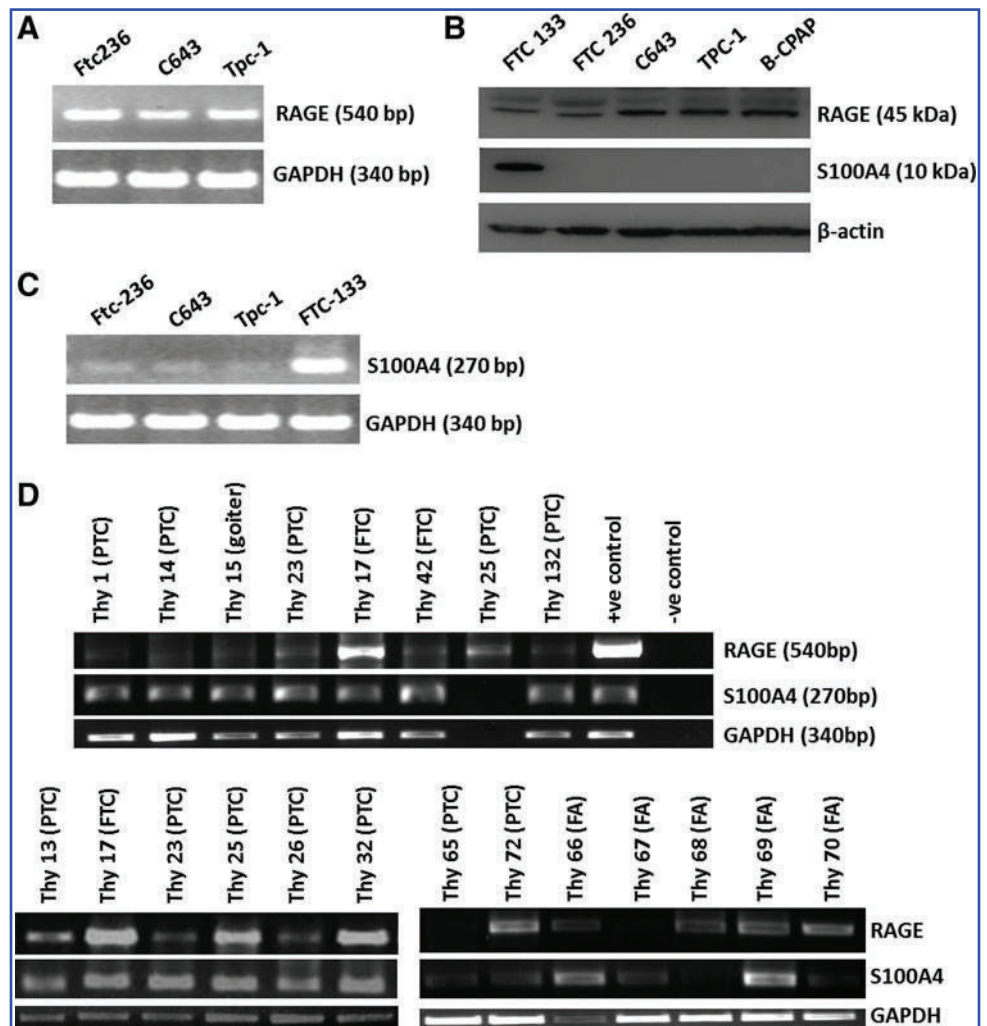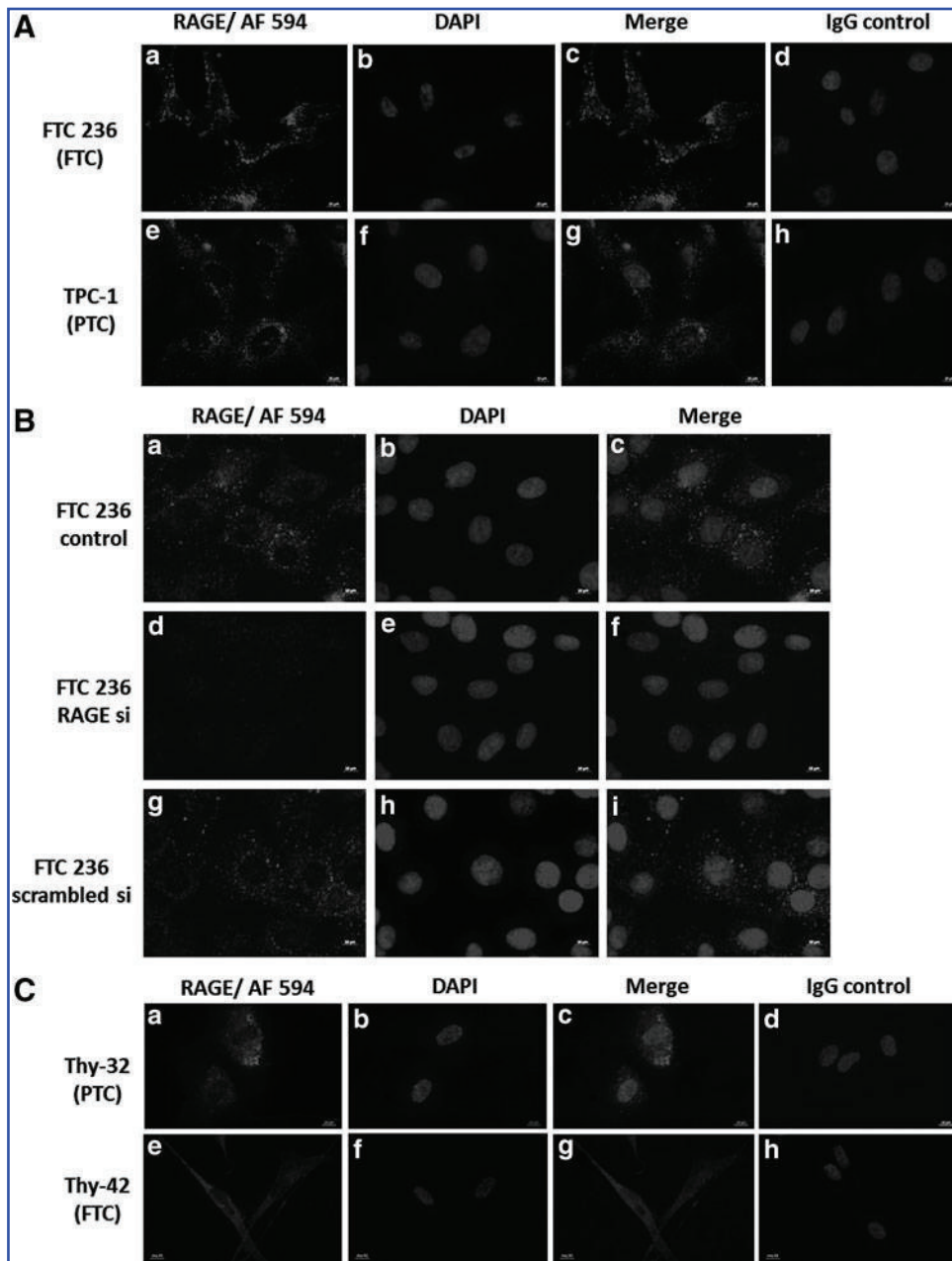
FIG. 2. RAGE protein detection by immunofluorescence in TC cells. RAGE protein was detected by immunofluorescence in all human thyroid carcinoma cell lines as shown here for FTC-236 (**A**: a and c) and TPC-1 (**A**: e and g) and in primary thyroid carcinoma cells (**C**: a, c, e, and g) positive for RAGE transcripts as shown here for Thy-32 (PTC) and Thy-42 (FTC) (**B**). Sections probed with a rabbit IgG control antibody substituting for RAGE antibody were negative for immunofluorescence staining (**A**: d and h; **C**: d and h). After treatment with RAGE siRNA, immunofluorescence was negative for RAGE, demonstrating successful RAGE silencing and specificity of the RAGE antibody (**B**: d and f). Cells probed with a scrambled non-silencing siRNA (**B**: g and i) showed positive immunostaining for RAGE similar to control cells (**B**: a and c).

primary TC cells (Fig. 2C). Human TC tissue sections revealed immunoreactive RAGE by immunohistochemistry in TC cells from FTC, PTC, and UTC tissue samples (Fig. 3A). Follicular thyroid epithelial cells in normal thyroid tissue controls were negative for RAGE (Fig. 3A). In addition, a human TC tissue microarray was used to detect RAGE protein expression in tissue cores of 60 cases with triplicate cores per case, including nine normal thyroid control tissues. It was found that 83% of PTC, 75% of FTC, and 70% of UTC tissues were positive for RAGE (Fig. 3B). Follicular thyroid epithelial cells of all normal thyroid tissue controls were negative for RAGE (Fig. 3B).
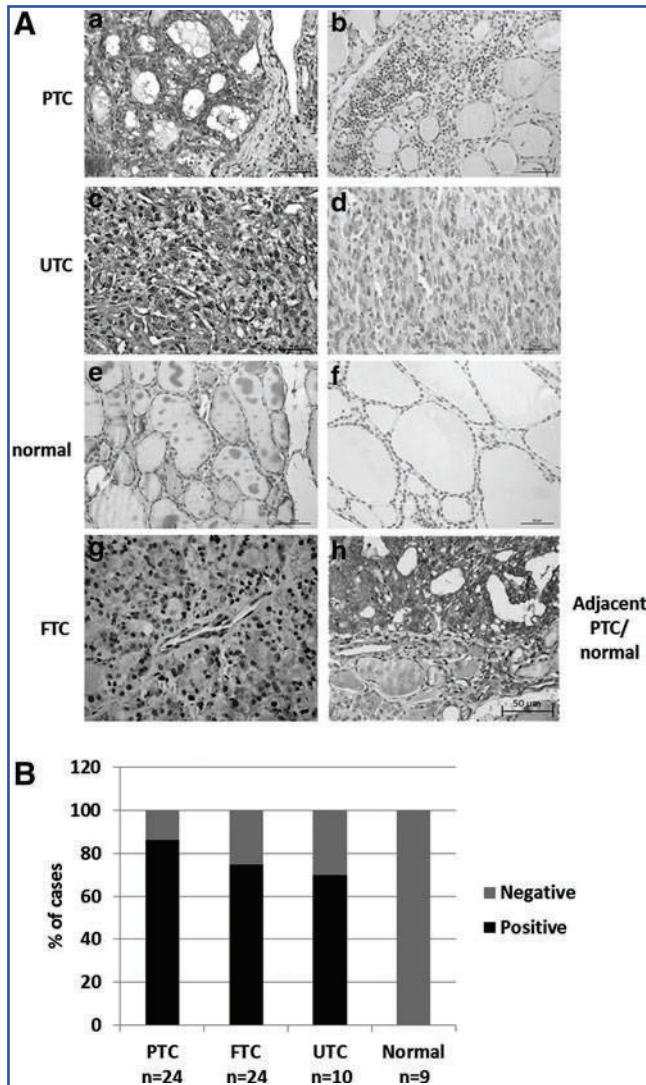
Extracellular S100A4 binds to RAGE to promote cancer cell migration

S100A4 has been described as a RAGE ligand in other human cell types (36). To determine whether exogenous S100A4 binds

to RAGE in TC cells, S100A4-coupled beads were utilized to pull down endogenous RAGE protein in human B-CPAP PTC cells. RhS100A4, but not BSA, was able to pull down RAGE protein, suggesting that S100A4 binds to RAGE (Fig. 4). RhS100A4 did not reduce cell viability (Fig. 5A) and failed to increase cell proliferation (Fig. 5B) in TC cells. However, rhS100A4 at 500 nM significantly increased cell migration (Fig. 5C) in TC cells, as demonstrated by two-chamber migration assays. The known physiological ligand of RAGE, advanced glycation end products (AGE), was used as a positive control and elicited a pro-migratory response in TC cells (Fig. 5D).

S100A4-induced TC cell migration is dependent on RAGE and Dia-1

RAGE expression in TC cells was silenced using RAGE siRNA and scrambled siRNA treatment was used as a control

FIG. 3. RAGE is expressed in neoplastic but not in normal thyroid tissues. Immunohistochemistry (IHC) was performed on sections from paraffin-embedded human thyroid tissues. Sections of human FTC, PTC, and UTC probed with the RAGE antibody showed positive staining in neoplastic thyroid cells, as shown here for PTC (**A**: a), UTC (**A**: c), and FTC (**A**: g). Specific staining was lacking when the primary antibody was substituted with an isotype control IgG (**A**: b, d, and f). Follicular thyroid epithelial cells of normal thyroid tissues were negative in RAGE IHC (**A**: e). The image in (**A**), part h, demonstrates positive immunostaining for RAGE in PTC tissue, whereas adjacent normal thyroid tissue was devoid of immunostaining. IHC for RAGE was also performed on a human TC tissue microarray comprising triplicates for 24 cases of PTC, 24 cases of FTC, 10 cases of UTC, and 9 cases of normal thyroid tissues. The IHC analysis revealed 83% of PTC, 75% of FTC, and 70% of UTC to be RAGE positive, whereas normal thyroid tissue controls were negative for RAGE staining (**B**).

to maintain endogenous RAGE expression (Fig. 6A). Upon specific RAGE knockdown, TC cells failed to respond to rhS100A4 or AGE with increased migration (Fig. 6B), whereas scrambled siRNA treated RAGE-positive TC control cells showed a significant pro-migratory response to both
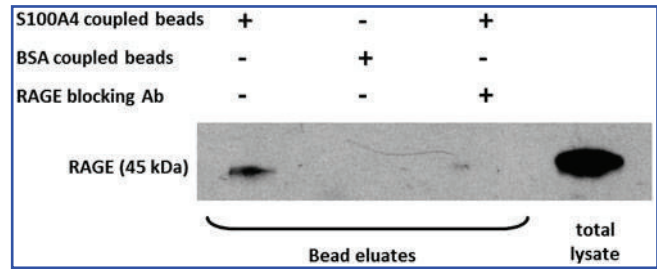

FIG. 4. Endogenous RAGE interacts with rhS100A4 in TC cells. Recombinant human (rh)S100A4 was covalently coupled to Dynabeads for immunoprecipitation. BSA-coupled beads were used as negative control. S100A4-coupled beads immunoprecipitated RAGE protein when incubated with total cell lysate of the human PTC cell line B-CPAP. When a RAGE-blocking antibody was added to the cell lysate, S100A4 failed to immunoprecipitate RAGE protein.

rhS100A4 and AGE (Fig. 6B). S100A4 has recently been shown to signal via TLR4 in mouse mammary carcinoma cells (37). This study sought to detect the presence of TLR4 in TC cells as a potential mediator for S100A4-induced migration. RAGE silencing did not affect the expression levels of TLR4. Thus, binding of S100A4 to TLR4 did not contribute to the S100A4-induced migratory response in TC (Fig. 6A). Dia-1 was identified as cytoplasmic interaction partner for RAGE, mediating increased cell migration toward modified human serum albumin in rat glioma cells (38). Dia-1 protein expression was detected by Western blot (Fig. 7A) and the presence of Dia-1 in the cytoplasm of TC cells was demonstrated by immunofluorescence (Fig. 7B). Stable Dia-1 knockdown clones of FTC236 and C643 cells were established using lentiviral shRNA silencing (Fig. 7C), and it was discovered that Dia-1 silencing completely abolished the pro-migratory response of rhS100A4 (Fig. 7D). Dia-1 silencing did not change the expression of RAGE protein in Dia-1 knockout clones (Fig. 7C), confirming that S100A4-induced and RAGE-mediated cell migration was dependent on the cytoplasmic RAGE interaction partner Dia-1 in TC cells.

S100A4/RAGE-mediated increased cell migration involves Cdc42 and RhoA kinase

This study investigated whether activation of the S100A4-RAGE/Dia-1 signaling pathway in TC cells included the small GTPases Cdc42 and RhoA as potential downstream RAGE/Dia-1 targets. S100A4 increased the active GTP-bound fractions of both RhoA and Cdc42 (Fig. 8A). The reduction of RAGE protein to approximately 50% of normal cellular levels coincided with a markedly diminished fraction of active GTP-RhoA but did not affect Cdc42 activation (Fig. 8B). To determine whether the S100A4-induced cell migration was dependent on the activation of small GTPases, the Rac-1/Cdc42 inhibitor ML141 and the Rho kinase inhibitor H-1152P were employed at non-toxic concentrations of $10\,\mu M$ each (Fig. 8C). Reduced levels of the GTP-bound RhoA and Cdc-42 indicated the successful inhibition of their GTPase activity (Fig. 8D). Inhibition of Cdc42 activation by ML141 almost completely abolished the ability of S100A4 to induce TC cell migration, whereas treatment with the Rho kinase inhibitor H-1152P caused an approximately 50%
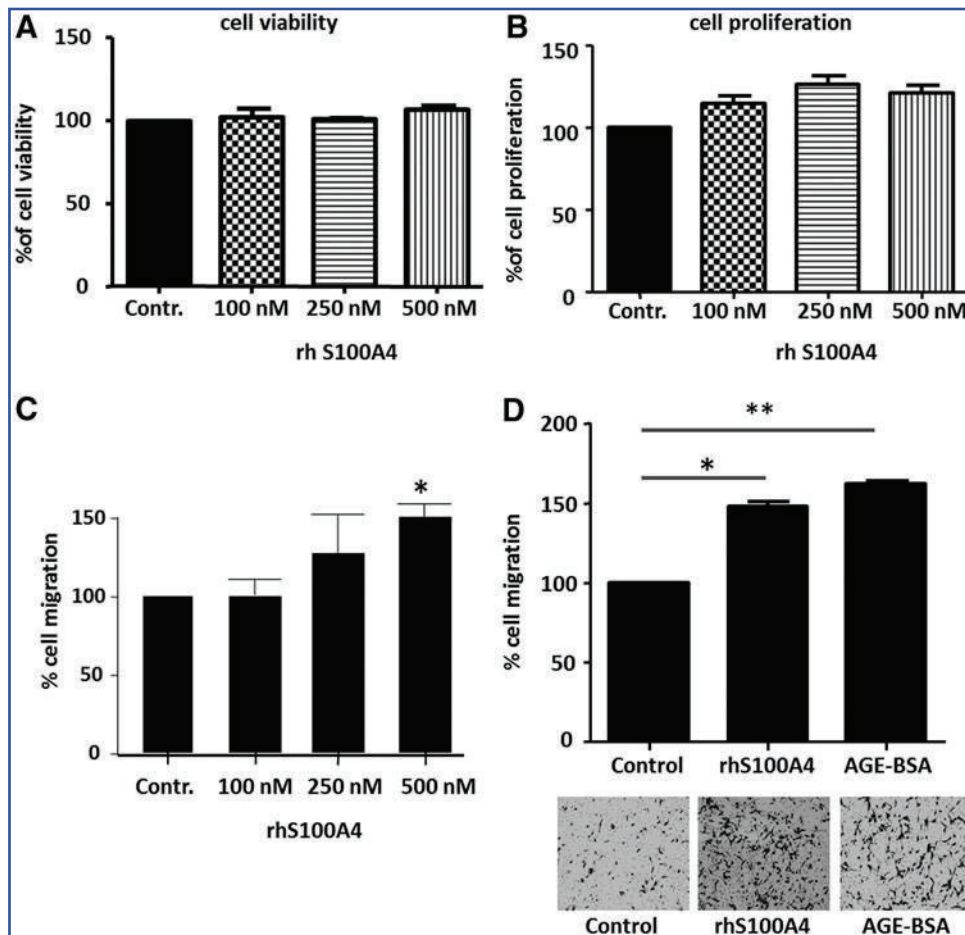
FIG. 5. Exogenous S100A4 is not mitogenic but increases cell migration. Extracellular rhS100A4 did not cause cytotoxic reactions in the concentrations used, as shown by WST-1 assays (**A**), and did not enhance cell proliferation in human thyroid carcinoma cells, as determined by bromodeoxyuridine (BrdU) incorporation assays (**B**) in FTC-236 ($p = 0.077$ for 100 nM; $p = 0.058$ for 250 nM; $p = 0.067$ for 500 nM S100A4). FTC236 cells were treated with increasing concentrations of rhS100A4 and subjected to filter-based migration assays for 24 h. A robust pro-migratory response was determined in response to 500 nM rhS100A4 (**C**), which was similar to the known RAGE-ligand AGE-BSA at 10 μg/mL (**D**). Results are shown for three independent experiments, and statistical analysis was determined using analysis of variance (ANOVA) with $p < 0.05$ considered significant (*$p < 0.05$; **$p < 0.005$).

reduction of TC migration (Fig. 8E). DMSO solvent had no effect on migration (Fig. 8E). Thus, the active forms of both Cdc42 and RhoA were identified as downstream mediators of the S100A4-RAGE/Dia-1 pathway leading to enhanced TC migration.

S100A4-induced p44/p42 MAPK signaling is independent of RAGE

Extracellular S100A4 induced a robust ERK1/2 phosphorylation in TC cells at concentrations of 250 nM of S100A4 (Fig. 9A), and the MEK inhibitor U0126 prevented this ERK1/2 phosphorylation (Fig. 9B). In cells treated with RAGE siRNA, rhS100A4 was still able to induce ERK1/2 phosphorylation (Fig. 9C), indicating a RAGE independent S100A4 signaling event. In Dia-1 knockdown cells, rhS100A4 mediated ERK1/2 phosphorylation was detectable but delayed compared to parental cells (Fig. 9D). Treatment with the MEK inhibitor U0126 at 10 μM failed to block the pro-migratory response in TC cells treated with exogenous rhS100A4, suggesting that ERK activation was not directly linked to cell migration in TC.

Discussion

This study reports the expression of RAGE in human TC tissues and in human primary and established TC cells. The study shows that the induction of cell motility in human thyroid carcinoma cells induced by extracellular S100A4 was RAGE-dependent and involved the cytoplasmic RAGE-interaction partner Dia-1 and the small GTPases of the RhoA/Cdc42/Rac-1 family. The data demonstrated that in TC cells, the small GTPases Cdc42 and RhoA, but not the MAP kinases ERK1/2, were activated by exogenous S100A4 downstream of RAGE/Dia-1 to increase cell motility.

The authors have previously shown that S100A4 is expressed and secreted in TC cells and increases TC cell motility (14,15), but the signaling pathway mediating this action in TC is not fully understood. Several S100 proteins were shown to bind to RAGE in their dimeric and oligomeric forms in a calcium-dependent manner (27,39,40). S100A4 was shown to bind to RAGE *in vitro* (30,33) and activate RAGE in human chondrocytes of patients with osteoarthritis (36). It was demonstrated in human colon cancer cells that RAGE mediates increased cell motility in the presence of S100A4 (33). On the other hand, RAGE-independent actions of extracellular S100A4 were reported in endothelial cells (41) and in hippocampal neurons (42). Intriguingly, it was found that TC cells and the majority of follicular thyroid cells isolated from thyroid adenoma expressed the pattern recognition receptor RAGE, whereas thyroid follicular epithelial cells derived from normal thyroid tissue lacked RAGE expression. Extracellular S100A4 had a potent auto-/paracrine effect on TC cells and enhanced cell motility via activation of RAGE.

To the best of the authors' knowledge, this is the first report on the expression of the cytoplasmic RAGE-interaction

FIG. 6. S100A4-induced cell migration in TC cells is RAGE-dependent. Reverse transcription polymerase chain reaction (RT-PCR) detection of RAGE and TLR4 transcripts is shown in FTC-236 cells following 48 h of RAGE knockdown using transient transfections with RAGE siRNA. Non-silencing "scrambled" siRNA served as a negative control (**A**). TLR4 transcripts were not affected by RAGE siRNA silencing (**A**). RAGE silencing abolished the motility-enhancing effect of rhS100A4 (500 nM) and AGE-BSA (10 μg/mL) in TC cells (**B**). Treatment with non-silencing siRNA did not diminish the pro-migratory effect of S100A4 (**B**). Three independent experiments were performed, and ANOVA was used to determine statistical significance (*$p < 0.05$) compared to the respective controls.
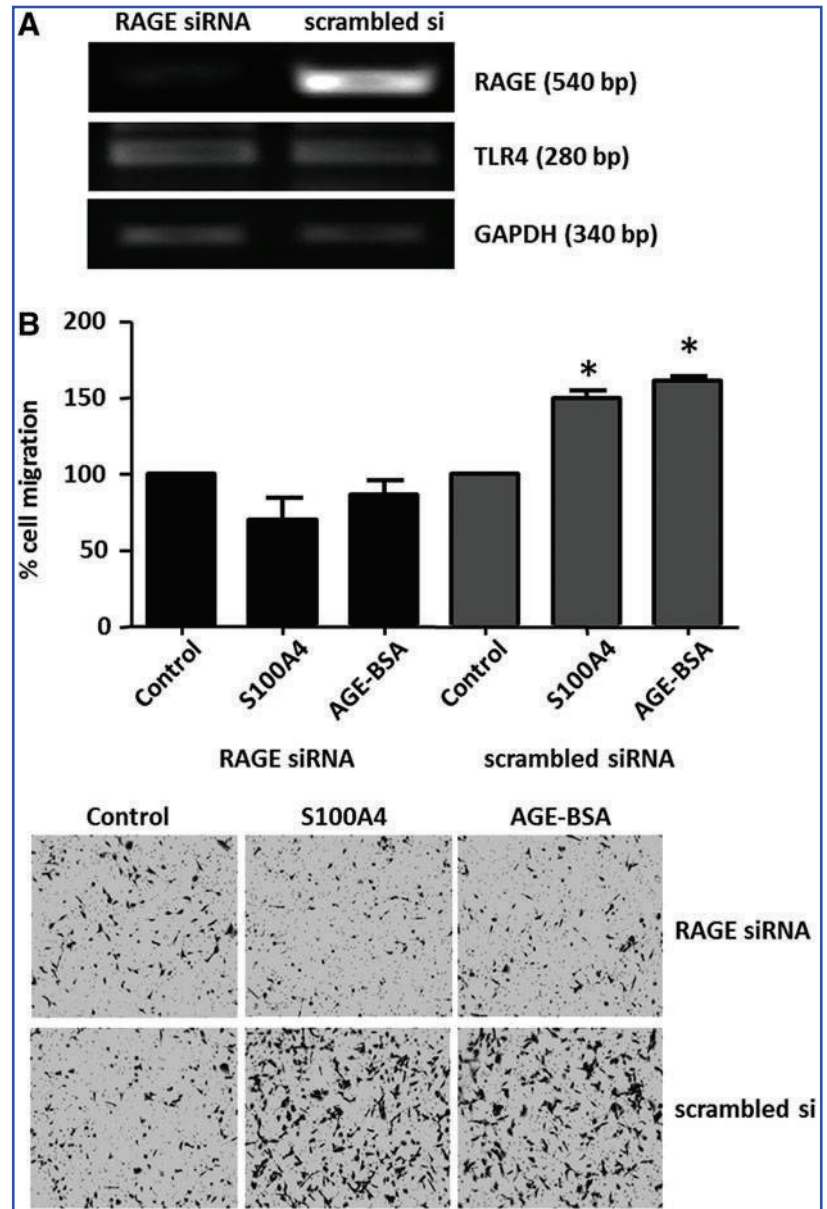
partner Dia-1 in TC cells. Dia-1 was essential for extracellular S100A4 to induce increased migration via RAGE in TC. Previously, glycosylated albumin species were used as RAGE ligands to induce RAGE-mediated cell migration in the C6 rat glioma cell line through the involvement of Dia-1 (38). In TC cells, the presence of S100A4 and activation of the S100A4-RAGE-Dia-1 signaling pathway coincided with an increase in cellular active GTP-bound protein fractions of Cdc42 and RhoA and increased TC migration. Blocking Cdc42 and the Rho kinase activation resulted in markedly reduced cell migration, and exogenous S100A4 was unable to rescue the reduced TC migration. Different from TC cells, RAGE-mediated rat glioma cell migration was independent of RhoA activity (38). The inhibitor H1152P was used, which acts on Rho-associated kinase (ROCK), a downstream mediator of RhoA, and can indirectly modulate the activity status of RhoA. H1152P was demonstrated *in vitro* to bind to and inhibit PKA at higher concentrations (43,44). PKA can

phosphorylate and increase the level of active GTP-RhoA at the leading edge of migrating cells (45). At the H1152P concentrations used here in TC cells, the reduction in GTP-bound RhoA likely resulted from PKA inhibition (Supplementary Fig. S2). This coincided with a 50% reduction of TC migration and could not be rescued by exogenous S100A4. Intriguingly, cellular RAGE levels had a profound impact on the level of GTP-bound RhoA in TC. Incomplete knockdown of RAGE in TC cells significantly reduced active GTP-bound RhoA but had little effect on GTP-Cdc42 levels in TC cells expressing S100A4. Thus, Cdc42 may be the major small GTPase targeted by the S100A4-RAGE-Dia-1 signaling pathway, whereas S100A4-mediated RhoA activation likely is indirect in TC cells.

S100A8/9 proteins have previously been shown to bind to and activate TLR4 (46). Recently, S100A4 was also shown to serve as a ligand for TLR4 in mammary adenocarcinoma cells and to activate pro-inflammatory pathways (37).
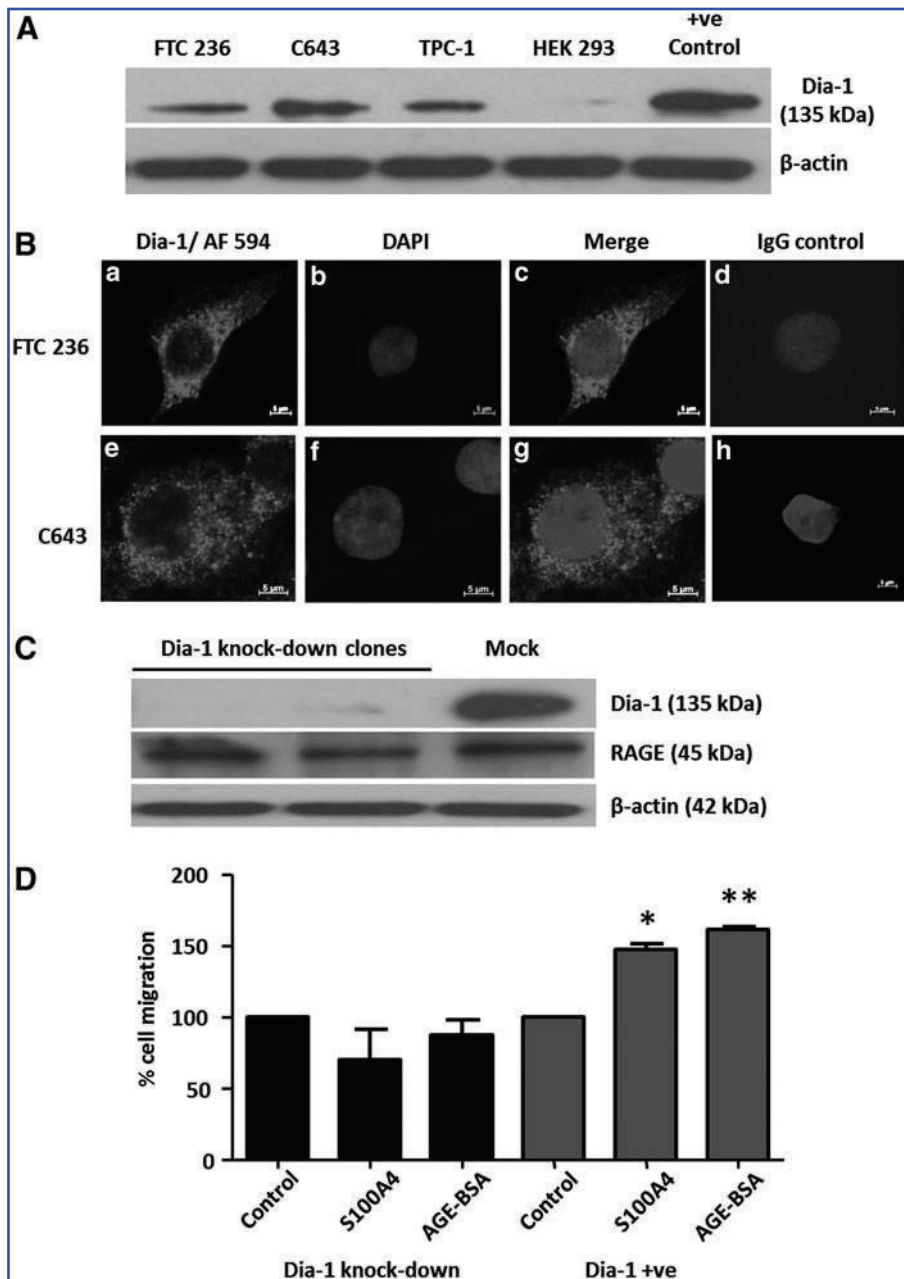
FIG. 7. Cell migration by S100A4/RAGE is mediated by Diaphanous-1 (Dia-1) in TC cells. Human TC cells expressed the 135 kDa Dia-1 protein, as shown by Western blot (**A**). HEK 293 and MCF-7 cells were used as negative and positive (+ve) control for Dia-1, respectively (**A**). Beta-actin served as loading control. Immunofluorescence detection of Dia-1 demonstrated cytoplasmic staining in thyroid carcinoma cells (**B**: a and e). When the primary antibody was substituted with an isotype control antibody, no staining was observed (**B**: d and h). DAPI was used as a nuclear counterstain (**B**: b and f). Dia-1 silencing was achieved in stable lentiviral Dia-1 shRNA knockdown clones of FTC-236 and the empty vector control clone (mock) (**C**). RAGE protein levels remained unaltered in Dia-1 KO cells (**C**). Two-chamber migration assays were performed on Dia-1-positive mock clones and Dia-1 knockdown transfectants (**D**). Results are shown for three independent experiments, and statistical analysis was determined using ANOVA, with $p < 0.05$ considered significant (*$p < 0.05$; **$p < 0.005$) compared to the respective controls.

Although TLR4 was expressed in TC cells, siRNA-mediated knockdown of RAGE did not affect the expression of TLR4 indicating that TLR4 likely plays no significant role in mediating the pro-migratory response of extracellular S100A4 in human TC cells.

The absence of RAGE in normal follicular thyroid cells and its presence in TC suggest that in their tumor microenvironment, TC cells can respond in an autocrine/paracrine manner to secreted S100A4. Cancer-associated fibroblasts in several cancer entities have been described to produce S100A4 (47,48), and several immune cells such as macrophages and activated lymphocytes were identified as a source for S100A4 in the vicinity of tumors (49). The authors have previously shown that S100A4 is secreted from TC cells *in vitro* (14,15), further emphasizing the role for S100A4 in paracrine intratumoral signaling. Similar to the previously described in-

duction of migration of endothelial cells (50) and in colorectal cancer cells (33) by S100A4, the migration-stimulating effect on TC cells was only seen at S100A4 concentrations ≥500 nM. The current model of RAGE–ligand interaction proposes the organization of RAGE as unstable preassembled receptor clusters, which requires stabilization through ligand binding to sustain RAGE signaling (25,40,51). RAGE clustering favors binding of multimeric S100 proteins (40,51), and this, in turn, enables stronger activation of RAGE (23). In agreement with previous work, the present data suggest that high intratumoral S100A4 concentrations activate RAGE and cause Cdc42/RhoA-mediated cytoskeletal rearrangements that facilitate enhanced TC cell migration.

Ligand-induced RAGE signaling was shown to activate the p44/42 MAPK pathway in several cell types (25,30,52–54), and a robust upregulation of the phosphorylated species

FIG. 8. S100A4/RAGE-induced cell migration required Cdc42 and RhoA. As shown by GTP pull-down assays, exogenous S100A4 increased the active GTP-bound fraction of RhoA and Cdc42 in C643 cells (**A**). Reduction of endogenous RAGE protein using siRNA markedly decreased the active fraction of RhoA, but not Cdc42 in S100A4 expressing C643 cells (**B**). S100A4-induced cell migration in TC cells was investigated by simultaneous incubation of a Cdc42/Rac-1 inhibitor and a Rho kinase inhibitor at concentrations of $10\,\mu$M each, which did not affect cell viability (**C**) but inhibited the activation of RhoA and Cdc42, respectively, as shown by the reduced amount of GTP-bound active fractions of RhoA and Cdc42 (**D**). Cell migration was markedly reduced under Cdc42/Rac-1 inhibition and was decreased to about 50% under Rho kinase inhibition. Exogenous S100A4 failed to induce a promigratory response in the presence of these inhibitors (**E**). DMSO solvent had no effect on migration (**E**). Results are shown for three independent experiments, and statistical analysis was determined using ANOVA, with $p < 0.05$ considered significant (**$p < 0.005$; ***$p < 0.0005$).
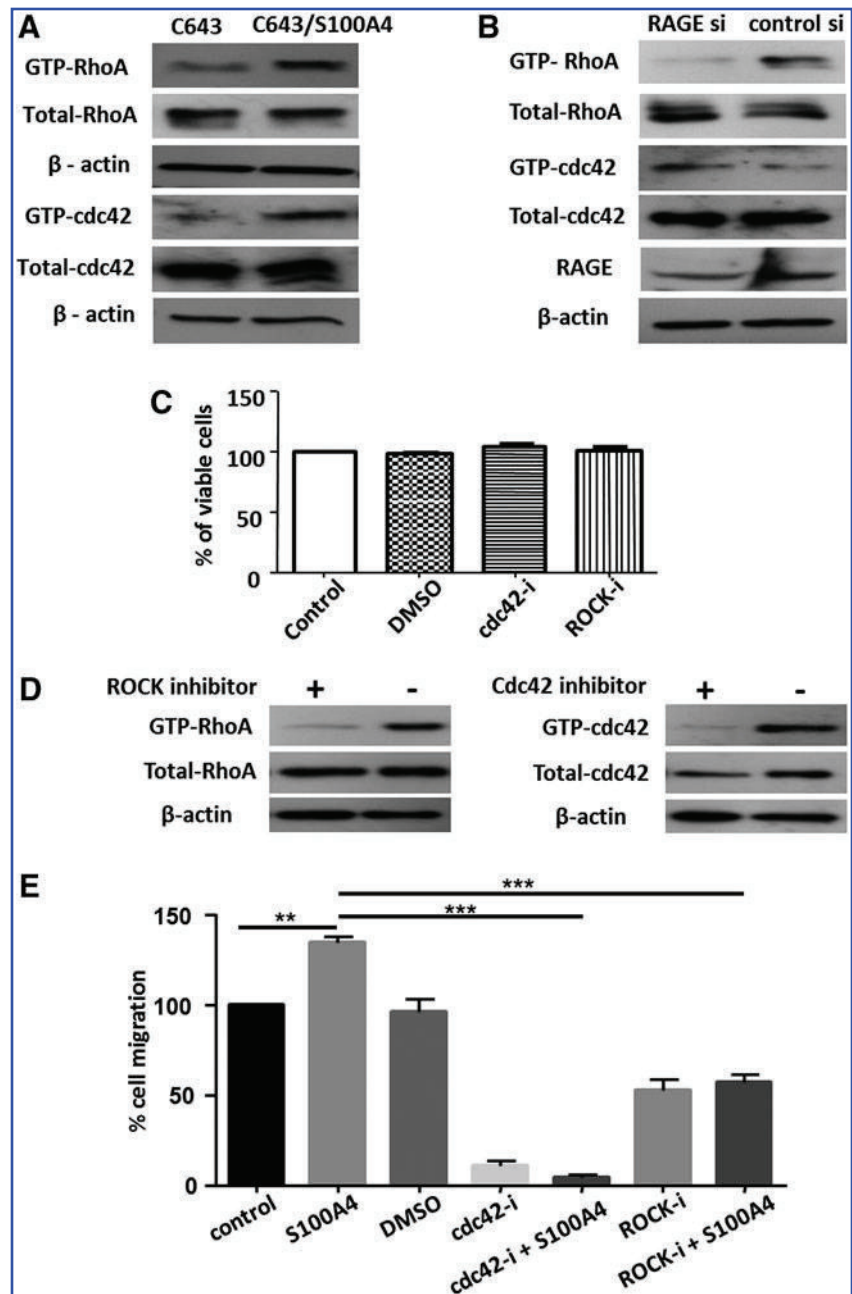
of MAP kinases ERK1/2 was also observed in TC cells exposed to S100A4. Was this ERK1/2 activation contributing to S100A4-mediated TC migration? S100A8/9 were shown to elicit ERK1/2 phosphorylation via RAGE in cancer cells (27,55), and S100A4-induced cell migration involved activation of ERK1/2 in vascular smooth muscle cells (56) and in human colon cancer cells (33). However, different experimental data are presented here, strongly suggesting that S100A4-induced ERK1/2 phosphorylation was not mediated through RAGE in human TC cells. Neither RAGE silencing nor Dia-1 knockdown was able to abolish ERK activation by rhS100A4. In addition, MAPK signaling in TC cells was robustly induced at concentrations of rhS100A4 well below those required to induce TC migration. Furthermore, exogenous S100A4 was still able to increase cell migration when

ERK1/2 phosphorylation was inhibited with the MEK inhibitor U0261. In light of previous research showing that extracellular S100A4 interacts with endogenous EGFR ligands such as amphiregulin, betacellulin, and EGF and induces ERK1/2 phosphorylation in murine embryonic fibroblasts (57), it is tempting to suggest that S100A4 may utilize more than one receptor in TC cells. By blocking EGFR phosphorylation, the activation of the p44/p42 MAPK pathway could be abolished (Supplementary Fig. S3). The authors are currently investigating the role of extracellular S100A4 in the activation of EGFR signaling in TC cells.

RAGE is considered a pattern-recognition receptor (58) recognizing several different ligands, among them HMGB1, which serves as mediator of inflammatory responses (23). The expression of RAGE in primary cells isolated from TC
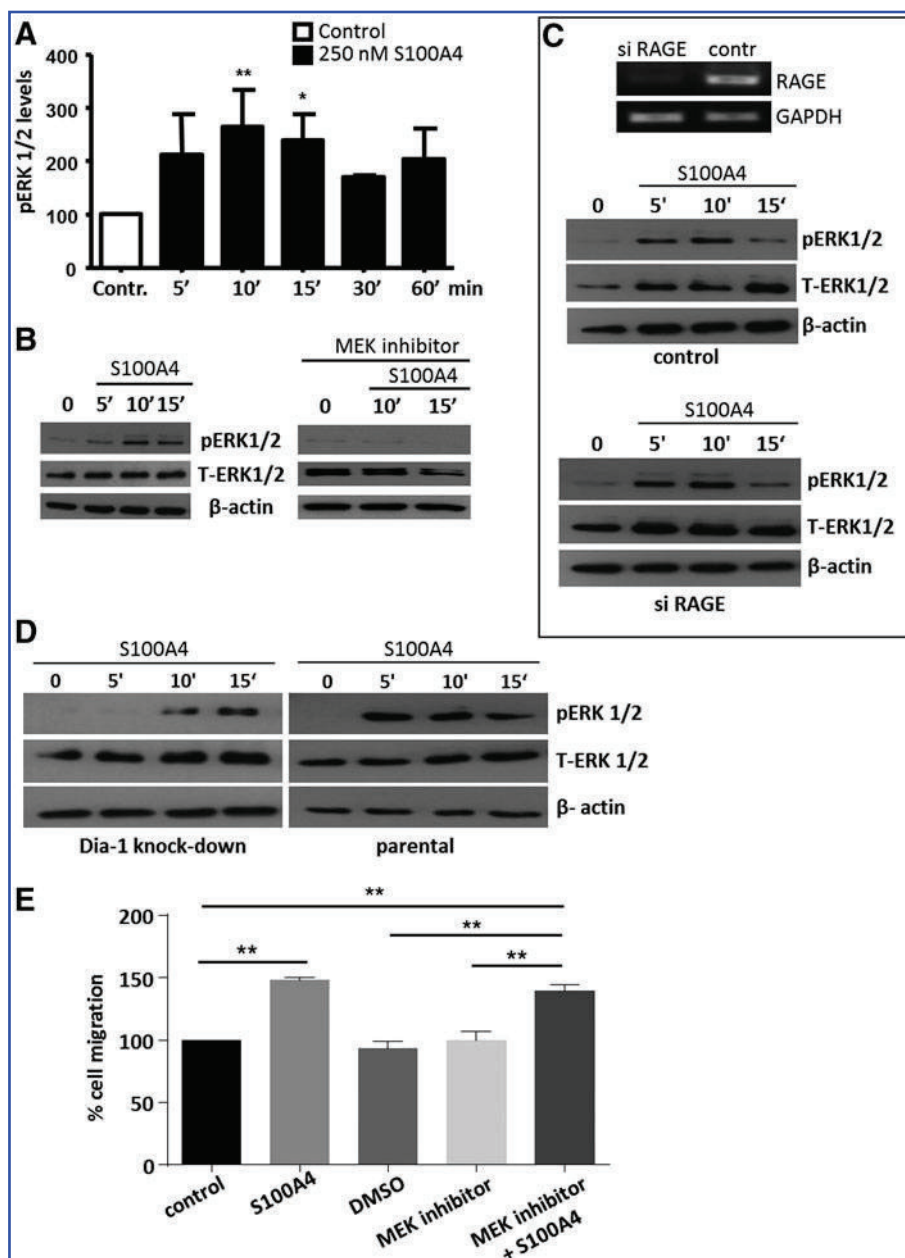
FIG. 9. S100A4-induced ERK1/2 activation is independent of RAGE. Recombinant human S100A4 at 250 nM resulted in the phosphorylation of the p44/p42 MAPK (ERK1/2) in FTC, PTC, and UTC cells, as shown here for C-643 (**A**). When treated with the MEK inhibitor U0126 at 10 μM, TC cells were unable to respond to extracellular S100A4 with phosphorylation of ERK1/2 (**B**). Following silencing of RAGE using transient siRNA transfections, the ability of rhS100A4 to induce ERK1/2 phosphorylation remained intact (**C**). Similarly, rhS100A4 was still able to activate the ERK1/2 pathway in Dia-1 knockdown transfectants, but cells showed a delayed response compared to parental Dia-1 positive cells (**D**). Treatment of TC cells expressing RAGE and Dia-1 with the MEK inhibitor U0126 at 10 μM was unable to prevent rhS100A4-induced TC cell migration (**E**). Results are shown for three independent experiments, and statistical analysis was determined using ANOVA, with $p < 0.05$ considered significant (*$p < 0.05$; **$p < 0.01$; ***$p < 0.001$).

and follicular adenoma specimens contributes to the understanding of inflammatory processes within the thyroid gland as a potential mechanism to promote cancer development and progression, especially for PTC (59), and supports a role for S100A4 during the early stages of PTC development (11).

In summary, secreted S100A4 targets RAGE, which is exclusively present on human TC derived from follicular epithelial cells. Within the tumor microenvironment, S100A4-induced RAGE/Dia-1/small GTPases signaling is likely an important promoter of TC migration. New therapeutic strategies targeting this signaling pathway may prevent TC invasion and metastasis.

Acknowledgments

Author Disclosure Statement

There are no competing interests to disclose for any of the authors of this manuscript.

References

1. Kim HJ, Sung JY, Oh YL, Kim JH, Son YI, Min YK, Kim SW, Chung JH 2014 Vascular invasion is associated with increased mortality in patients with minimally invasive follicular thyroid carcinoma but not widely invasive follicular thyroid carcinoma. Head Neck **36:**1695–1700.

2. Passler C, Scheuba C, Prager G, Kaczirek K, Kaserer K, Zettinig G, Niederle B 2004 Prognostic factors of papillary and follicular thyroid cancer: differences in an iodine-replete endemic goiter region. Endocr Relat Cancer **11:**131–139.

3. Phay JE, Ringel MD 2013 Metastatic mechanisms in follicular cell-derived thyroid cancer. Endocr Relat Cancer **20:**R307–319.

4. Chen M, Sinha M, Luxon BA, Bresnick AR, O'Connor KL 2009 Integrin alpha6beta4 controls the expression of genes associated with cell motility, invasion, and metastasis, including S100A4/metastasin. J Biol Chem **284:**1484–1494.

5. Jenkinson SR, Barraclough R, West CR, Rudland PS 2004 S100A4 regulates cell motility and invasion in an *in vitro* model for breast cancer metastasis. Br J Cancer **90:**253–262.

6. Sack U, Walther W, Scudiero D, Selby M, Aumann J, Lemos C, Fichtner I, Schlag PM, Shoemaker RH, Stein U 2011 S100A4-induced cell motility and metastasis is restricted by the Wnt/beta-catenin pathway inhibitor calcimycin in colon cancer cells. Mol Biol Cell **22:**3344–3354.

7. Stein U, Arlt F, Walther W, Smith J, Waldman T, Harris ED, Mertins SD, Heizmann CW, Allard D, Birchmeier W, Schlag PM, Shoemaker RH 2006 The metastasis-associated gene S100A4 is a novel target of beta-catenin/T-cell factor signaling in colon cancer. Gastroenterology **131:**1486–1500.

8. Tsukamoto N, Egawa S, Akada M, Abe K, Saiki Y, Kaneko N, Yokoyama S, Shima K, Yamamura A, Motoi F, Abe H, Hayashi H, Ishida K, Moriya T, Tabata T, Kondo E, Kanai N, Gu Z, Sunamura M, Unno M, Horii A 2013 The expression of S100A4 in human pancreatic cancer is associated with invasion. Pancreas **42:**1027–1033.

9. Zhang J, Zhang DL, Jiao XL, Dong Q 2013 S100A4 regulates migration and invasion in hepatocellular carcinoma HepG2 cells via NF-kappaB-dependent MMP-9 signal. Eur Rev Med Pharmacol Sci **17:**2372–2382.

10. Zou M, Famulski KS, Parhar RS, Baitei E, Al-Mohanna FA, Farid NR, Shi Y 2004 Microarray analysis of metastasis-associated gene expression profiling in a murine model of thyroid carcinoma pulmonary metastasis: identification of S100A4 (Mts1) gene overexpression as a poor prognostic marker for thyroid carcinoma. J Clin Endocrinol Metab **89:**6146–6154.

11. Ito Y, Yoshida H, Tomoda C, Uruno T, Miya A, Kobayashi K, Matsuzuka F, Kakudo K, Kuma K, Miyauchi A 2004 S100A4 expression is an early event of papillary carcinoma of the thyroid. Oncology **67:**397–402.

12. Min HS, Choe G, Kim SW, Park YJ, Park do J, Youn YK, Park SH, Cho BY, Park SY 2008 S100A4 expression is associated with lymph node metastasis in papillary microcarcinoma of the thyroid. Mod Pathol **21:**748–755.

13. Zou M, Al-Baradie RS, Al-Hindi H, Farid NR, Shi Y 2005 S100A4 (Mts1) gene overexpression is associated with invasion and metastasis of papillary thyroid carcinoma. Br J Cancer **93:**1277–1284.

14. Hombach-Klonisch S, Bialek J, Radestock Y, Truong A, Agoulnik AI, Fiebig B, Willing C, Weber E, Hoang-Vu C, Klonisch T 2010 INSL3 has tumor-promoting activity in thyroid cancer. Int J Cancer **127:**521–531.

15. Radestock Y, Willing C, Kehlen A, Hoang-Vu C, Hombach-Klonisch S 2010 Relaxin enhances S100A4 and promotes growth of human thyroid carcinoma cell xenografts. Mol Cancer Res **8:**494–506.

16. Ismail TM, Fernig DG, Rudland PS, Terry CJ, Wang G, Barraclough R 2008 The basic C-terminal amino acids of calcium-binding protein S100A4 promote metastasis. Carcinogenesis **29:**2259–2266.

17. Kriajevska M, Fischer-Larsen M, Moertz E, Vorm O, Tulchinsky E, Grigorian M, Ambartsumian N, Lukanidin E 2002 Liprin beta 1, a member of the family of LAR transmembrane tyrosine phosphatase-interacting proteins, is a new target for the metastasis-associated protein S100A4 (Mts1). J Biol Chem **277:**5229–5235.

18. Kriajevska MV, Cardenas MN, Grigorian MS, Ambartsumian NS, Georgiev GP, Lukanidin EM 1994 Non-muscle myosin heavy chain as a possible target for protein encoded by metastasis-related mts-1 gene. J Biol Chem **269:**19679–19682.

19. Zhang S, Wang G, Fernig DG, Rudland PS, Webb SE, Barraclough R, Barraclough R, Martin-Fernandez M 2005 Interaction of metastasis-inducing S100A4 protein *in vivo* by fluorescence lifetime imaging microscopy. Eur Biophys J **34:**19–27.

20. Sims GP, Rowe DC, Rietdijk ST, Herbst R, Coyle AJ 2010 HMGB1 and RAGE in inflammation and cancer. Ann Rev Immunol **28:**367–388.

21. Lotze MT, Zeh HJ, Rubartelli A, Sparvero LJ, Amoscato AA, Washburn NR, Devera ME, Liang X, Tör M, Billiar T 2007 The grateful dead: damage-associated molecular pattern molecules and reduction/oxidation regulate immunity. Immunol Rev **220:**60–81.

22. Halayko AJ, Ghavami S 2009 S100A8/A9: a mediator of severe asthma pathogenesis and morbidity? Can J Physiol Pharmacol **87:**743–755.

23. Sparvero LJ, Asafu-Adjei D, Kang R, Tang D, Amin N, Im J, Rutledge R, Lin B, Amoscato AA, Zeh HJ, Lotze MT 2009 RAGE (Receptor for Advanced Glycation Endproducts), RAGE ligands, and their role in cancer and inflammation. J Transl Med **7:**17.

24. Bierhaus A, Nawroth PP 2009 Multiple levels of regulation determine the role of the receptor for AGE (RAGE) as common soil in inflammation, immune responses and diabetes mellitus and its complications. Diabetologia **52:**2251–2263.

25. Fritz G 2011 RAGE: a single receptor fits multiple ligands. Trends Biochem Sci **36:**625–632.

26. Ghavami S, Chitayat S, Hashemi M, Eshraghi M, Chazin WJ, Halayko AJ, Kerkhoff C 2009 S100A8/A9: a Janus-faced molecule in cancer therapy and tumorgenesis. Eur J Pharmacol **625:**73–83.

27. Ghavami S, Rashedi I, Dattilo BM, Eshraghi M, Chazin WJ, Hashemi M, Wesselborg S, Kerkhoff C, Los M 2008 S100A8/A9 at low concentration promotes tumor cell growth via RAGE ligation and MAP kinase-dependent pathway. J Leukoc Biol **83:**1484–1492.

28. Hsieh HL, Schafer BW, Sasaki N, Heizmann CW 2003 Expression analysis of S100 proteins and RAGE in human tumors using tissue microarrays. Biochem Biophys Res Commun **307:**375–381.

29. Logsdon CD, Fuentes MK, Huang EH, Arumugam T 2007 RAGE and RAGE ligands in cancer. Curr Mol Med **7:**777–789.

30. Leclerc E, Fritz G, Vetter SW, Heizmann CW 2009 Binding of S100 proteins to RAGE: an update. Biochim Biophys Acta **1793:**993–1007.

31. Yammani RR, Long D, Loeser RF 2009 Interleukin-7 stimulates secretion of S100A4 by activating the JAK/

STAT signaling pathway in human articular chondrocytes. Arthritis Rheum **60:**792–800.

32. Hernández JL, Padilla L, Dakhel S, Coll T, Hervas R, Adan J, Masa M, Mitjans F, Martinez JM, Coma S, Rodríguez L, Noé V, Ciudad CJ, Blasco F, Messeguer R 2013 Therapeutic targeting of tumor growth and angiogenesis with a novel anti-S100A4 monoclonal antibody. PloS One **8:**e72480.

33. Dahlmann M, Okhrimenko A, Marcinkowski P, Osterland M, Herrmann P, Smith J, Heizmann CW, Schlag PM, Stein U 2014 RAGE mediates S100A4-induced cell motility via MAPK/ERK and hypoxia signaling and is a prognostic biomarker for human colorectal cancer metastasis. Oncotarget **5:**3220–3233.

34. Siddique HR, Adhami VM, Parray A, Johnson JJ, Siddiqui IA, Shekhani MT, Murtaza I, Ambartsumian N, Konety BR, Mukhtar H, Saleem M 2013 The S100A4 oncoprotein promotes prostate tumorigenesis in a transgenic mouse model: regulating NFκB through the RAGE receptor. Genes Cancer **4:**224–234.

35. Glogowska A, Kunanuvat U, Stetefeld J, Patel TR, Thanasupawat T, Krcek J, Weber E, Wong GW, Del Bigio MR, Hoang-Vu C, Hombach-Klonisch S, Klonisch T 2013 C1q-tumor necrosis factor-related protein 8 (CTRP8) is a novel interaction partner of relaxin receptor RXFP1 in human brain cancer cells. J Pathol **231:**466–479.

36. Yammani RR, Carlson CS, Bresnick AR, Loeser RF 2006 Increase in production of matrix metalloproteinase 13 by human articular chondrocytes due to stimulation with S100A4: role of the receptor for advanced glycation end products. Arthritis Rheum **54:**2901–2911.

37. Hansen MT, Forst B, Cremers N, Quagliata L, Ambartsumian N, Grum-Schwensen B, Klingelhöfer J, Abdul-Al A, Herrmann P, Osterland M, Stein U, Nielsen GH, Scherer PE, Lukanidin E, Sleeman JP, Grigorian M 2015 A link between inflammation and metastasis: serum amyloid A1 and A3 induce metastasis, and are targets of metastasis-inducing S100A4. Oncogene **34:**424–435.

38. Hudson BI, Kalea AZ, Del Mar Arriero M, Harja E, Boulanger E, D'Agati V, Schmidt AM 2008 Interaction of the RAGE cytoplasmic domain with diaphanous-1 is required for ligand-stimulated cellular migration through activation of Rac1 and Cdc42. J Biol Chem **283:**34457–34468.

39. Leclerc E, Fritz G, Weibel M, Heizmann CW, Galichet A 2007 S100B and S100A6 differentially modulate cell survival by interacting with distinct RAGE (receptor for advanced glycation end products) immunoglobulin domains. J Biol Chem **282:**31317–31331.

40. Ostendorp T, Leclerc E, Galichet A, Koch M, Demling N, Weigle B, Heizmann CW, Kroneck PMH, Günter F 2007 Structural and functional insights into RAGE activation by multimeric S100B. EMBO J **26:**3868–3878.

41. Semov A, Moreno MJ, Onichtchenko A, Abulrob A, Ball M, Ekiel I, Pietrzynski G, Stanimirovic D, Alakhov V 2005 Metastasis-associated protein S100A4 induces angiogenesis through interaction with Annexin II and accelerated plasmin formation. J Biol Chem **280:**20833–20841.

42. Kiryushko D, Novitskaya V, Soroka V, Klingelhöfer J, Lukanidin E, Berezin V, Bock E 2006 Molecular mechanisms of Ca(2+) signaling in neurons induced by the S100A4 protein. Mol Cell Biol **26:**3625–3638.

43. Breitenlechner C, Gassel M, Hidaka H, Kinzel V, Huber R, Engh RA, Bossemeyer D 2003 Protein kinase A in complex with Rho-kinase inhibitors Y-27632, Fasudil, and H-1152P: structural basis of selectivity. Structure **11:**1595–1607.

44. Ikenoya M, Hidaka H, Hosoya T, Suzuki M, Yamamoto N, Sasaki Y 2002 Inhibition of rho-kinase-induced myristoylated alanine-rich C kinase substrate (MARCKS) phosphorylation in human neuronal cells by H-1152, a novel and specific Rho-kinase inhibitor. J Neurochem **81:**9–16.

45. Tkachenko E, Sabouri-Ghomi M, Pertz O, Kim C, Gutierrez E, Machacek M, Groisman A, Danuser G, Ginsberg MH 2011 Protein kinase A governs a RhoA-RhoGDI protrusion-retraction pacemaker in migrating cells. Nature Cell Biol **13:**660–667.

46. Vogl T, Tenbrock K, Ludwig S, Leukert N, Ehrhardt C, van Zoelen MA, Nacken W, Foell D, van der Poll T, Sorg C, Roth J 2007 Mrp8 and Mrp14 are endogenous activators of Toll-like receptor 4, promoting lethal, endotoxin-induced shock. Nat Med **13:**1042–1049.

47. Bochet L, Lehuede C, Dauvillier S, Wang YY, Dirat B, Laurent V, Dray C, Guiet R, Maridonneau-Parini I, Le Gonidec S, Couderc B, Escourrou G, Valet P, Muller C 2013 Adipocyte-derived fibroblasts promote tumor progression and contribute to the desmoplastic reaction in breast cancer. Cancer Res **73:**5657–5668.

48. Rasanen K, Sriswasdi S, Valiga A, Tang HY, Zhang G, Perego M, Somasundaram R, Li L, Speicher K, Klein-Szanto AJ, Basu D, Rustgi AK, Speicher DW, Herlyn M 2013 Comparative secretome analysis of epithelial and mesenchymal subpopulations of head and neck squamous cell carcinoma identifies S100A4 as a potential therapeutic target. Mol Cell Proteomics **12:**3778–3792.

49. Cabezón T, Celis JE, Skibshøj I, Klingelhöfer J, Grigorian M, Gromov P, Rank F, Myklebust JH, Maelandsmo GM, Lukanidin E, Ambartsumian N 2007 Expression of S100A4 by a variety of cell types present in the tumor microenvironment of human breast cancer. Int J Cancer **121:**1433–1444.

50. Ambartsumian N, Klingelhöfer J, Grigorian M, Christensen C, Kriajevska M, Tulchinsky E, Georgiev G, Berezin V, Bock E, Rygaard J, Cao R, Cao Y, Lukanidin E 2001 The metastasis-associated Mts1(S100A4) protein could act as an angiogenic factor. Oncogene **20:**4685–4695.

51. Koch M, Chitayat S, Dattilo BM, Schiefner A, Diez J, Chazin WJ, Fritz G 2010 Structural basis for ligand recognition and activation of RAGE. Structure **18:**1342–1352.

52. Huttunen HJ, Rauvala H 2004 Amphoterin as an extracellular regulator of cell motility: from discovery to disease. J Intern Med **255:**351–366.

53. Jin Q, Chen H, Luo A, Ding F, Liu Z 2011 S100A14 stimulates cell proliferation and induces cell apoptosis at different concentrations via receptor for advanced glycation end products (RAGE). PloS One **6:**e19375.

54. Li JH, Wang W, Huang XR, Oldfield M, Schmidt AM, Cooper ME, Lan HY 2004 Advanced glycation end products induce tubular epithelial-myofibroblast transition through the RAGE-ERK1/2 MAP kinase signaling pathway. Am J Pathol **164:**1389–1397.

55. Reeb AN, Li W, Sewell W, Marlow LA, Tun HW, Smallridge RC, Copland JA, Spradling K, Chernock R, Lin RY 2015 S100A8 is a novel therapeutic target for anaplastic thyroid carcinoma. J Clin Endocrinol Metab **100:**E232–E242.

56. Spiekerkoetter E, Guignabert C, de Jesus Perez V, Alastalo TP, Powers JM, Wang L, Lawrie A, Ambartsumian N, Schmidt AM, Berryman M, Ashley RH, Rabinovitch M

2009 S100A4 and bone morphogenetic protein-2 code-pendently induce vascular smooth muscle cell migration via phospho-extracellular signal-regulated kinase and chloride intracellular channel 4. Circ Res **105:**639–647, 13 p following 47.

57. Klingelhöfer J, Moller HD, Sumer EU, Berg CH, Poulsen M, Kiryushko D, Soroka V, Ambartsumian N, Grigorian M, Lukanidin EM 2009 Epidermal growth factor receptor ligands as new extracellular targets for the metastasis-promoting S100A4 protein. FEBS J **276:**5936–5948.

58. Schmidt AM, Yan SD, Yan SF, Stern DM 2001 The multiligand receptor RAGE as a progression factor amplifying immune and inflammatory responses. J Clin Invest **108:**949–955.

59. Bozec A, Lassalle S, Hofman V, Ilie M, Santini J, Hofman P 2010 The thyroid gland: a crossroad in inflammation-induced carcinoma? An ongoing debate with new therapeutic potential. Curr Med Chem **17:**3449–3461.

Address correspondence to:
Sabine Hombach-Klonisch, MD, PhD
Department of Human Anatomy and Cell Science
College of Medicine, Faculty of Health Sciences
University of Manitoba
130–745 Bannatyne Avenue
Winnipeg R3E 0J9
Canada

E-mail: Sabine.Hombach-Klonisch@umanitoba.ca

Mechanisms of therapeutic resistance in cancer (stem) cells with emphasis on thyroid cancer cells

Sabine Hombach-Klonisch[1,2], **Suchitra Natarajan**[1], **Thatchawan Thanasupawat**[1], **Manoj Medapati**[1], **Alok Pathak**[1,3], **Saeid Ghavami**[1,4] and **Thomas Klonisch**[1,3,4,5] *

[1] Department of Human Anatomy and Cell Science, University of Manitoba, Winnipeg, MB, Canada
[2] Department of Obstetrics, Gynecology and Reproductive Sciences, University of Manitoba, Winnipeg, MB, Canada
[3] Department of Surgery, University of Manitoba, Winnipeg, MB, Canada
[4] Manitoba Institute of Child Health, University of Manitoba, Winnipeg, MB, Canada
[5] Department of Medical Microbiology and Infectious Diseases, University of Manitoba, Winnipeg, MB, Canada

The two main reasons for death of cancer patients, tumor recurrence and metastasis, are multi-stage cellular processes that involve increased cell plasticity and coincide with elevated resistance to anti-cancer treatments. Epithelial-to-mesenchymal transition (EMT) is a key contributor to metastasis in many cancer types, including thyroid cancer and is known to confer stem cell-like properties onto cancer cells. This review provides an overview of molecular mechanisms and factors known to contribute to cancer cell plasticity and capable of enhancing cancer cell resistance to radio- and chemotherapy. We elucidate the role of DNA repair mechanisms in contributing to therapeutic resistance, with a special emphasis on thyroid cancer. Next, we explore the emerging roles of autophagy and damage-associated molecular pattern responses in EMT and chemoresistance in tumor cells. Finally, we demonstrate how cancer cells, including thyroid cancer cells, can highjack the oncofetal nucleoprotein high-mobility group A2 to gain increased transformative cell plasticity, prevent apoptosis, and enhance metastasis of chemoresistant tumor cells.

Keywords: thyroid cancer, therapeutic resistance, stem cells, HMGA2, DAMP, autophagy, ER stress, DNA repair

INTRODUCTION

Tissue invasion, metastasis, as well as radio- and chemotherapeutic resistance to anti-cancer treatments are common and main causes of death in cancer patients. Tumor cells mount complex and still poorly understood molecular defense mechanisms to counteract and evade oxygen deprivation, nutritional restrictions, as well as radio- and chemotherapeutic treatment regimens aimed at destabilizing their genomes and important cellular processes. In thyroid cancer, as in other tumors, such defense strategies include the reactivation in cancer cells of early developmental programs normally active exclusively in stem cells, the stimulation of cancer stem-like cells resident within the tumor tissue, and the recruitment of bone marrow-derived progenitors into the tumor (1–3). Metastasis and therapeutic resistance in cancer (stem) cells involve the epithelial-to-mesenchymal transition (EMT)-mediated enhancement in cellular plasticity, which includes coordinated dynamic biochemical and nuclear changes (4). The purpose of the present review is to provide an overview of the role of DNA repair mechanisms contributing to radio- and chemotherapeutic resistance in cancer with an emphasis on thyroid cancer and highlight the emerging roles of autophagy and damage-associated molecular pattern (DAMP) responses in EMT and chemoresistance in tumor cells. Finally, we use the stem cell factor and nucleoprotein high-mobility group A2 (HMGA2) as an example to demonstrate how factors intended to protect stem cells are wielded by cancer (stem) cells to gain increased transformative cell plasticity, which enhances metastasis, chemotherapeutic resistance, and cell survival. Wherever possible, we have included information on these cellular processes and associated factors as they relate to thyroid cancer cells.

THYROID CANCER: HIGH INCIDENCE AND NEW WAYS TO PREDICT RISK OF DEATH

Thyroid cancer is the most common malignant endocrine tumor and the seventh most common cancer seen in Canadians accounting for 11% of all cancers in women <40 years. In Canada, the incidence of thyroid cancer is increasing more rapidly than any other cancer; by 6.8% per year in Canadian males (1998–2007) and by 6.9% per year in Canadian females (2002–2007) (5). A 373% increase in the incidence of thyroid cancer was reported in a population-based cohort in Canada (6). The trends in the United States (US) mirror that of Canada, with an increase in the incidence of thyroid cancer from 4.85/100,000 in 1975 to 14.25/100,000 in 2009 and an annual percent increase (2000–2009) of 6.0% for the US males and 6.9% for the US females (7). The life time probability of developing a thyroid cancer for a Canadian female is 1 in 71 (1.4%) but only 1 in 1,374 (0.1%) will actually die from it. Canadian males have a lower lifetime risk of developing thyroid cancer at 1 in 223 (0.4%) with the risk of death from thyroid cancer at 1 in 1,937 (0.1%) (8). Although the incidence of thyroid cancer has been rising, this tumor has an excellent 5-year relative survival ratio of 98% in 2011 (8). Thyroid cancer represents a conglomerate of different histological types with diverse clinical behavior. Over 90% of all thyroid cancers are either follicular or papillary carcinoma, termed differentiated thyroid cancer (DTC),

and carry excellent prognosis. By contrast, poorly differentiated and anaplastic thyroid cancers (ATC) have a very poor outcome. Surgery and/or radioactive iodine exposure is the mainstay of treatment for DTC. ATC are usually diagnosed at an advanced stage when surgery is not feasible and radiation and chemotherapy are the only option. Thyroid cancer stem cell populations have been described for both DTC and ATC (2, 9–11). The histology and age of the patient at diagnosis are two principal determinants of thyroid cancer-specific survival. The improvement in the thyroid cancer-specific survival over the last four decades is largely attributed to the declining proportion of ATC (12). An age threshold of 45 years at the time of diagnosis of DTC used by the TNM classification system of the American Joint Committee on Cancer and International Union against Cancer (TNM-AJCC/IUCC) for stratification into low- and high-risk thyroid cancers has been questioned and an alternative age cut off of 55 years was suggested (13). To predict an individual's risk of death from thyroid cancer within 10 years of diagnosis, we recently developed a prognostic nomogram which accounts for the patient's age and gender, TNM stage and histology, and the presence of post-treatment macroscopic residual disease as important independent determinants of thyroid cancer-specific survival (12).

MECHANISMS OF THERAPY RESISTANCE IN THYROID CANCER

DNA REPAIR MECHANISMS

Mechanisms involved in single-stranded [base excision repair (BER), nucleotide excision repair (NER), mismatch repair (MMR)] and double-stranded [homologous recombination (HR), non-homologous end-joining (NHEJ)] DNA repair significantly affect the ability of thyroid cancer (stem) cells to counteract and survive radio- and chemotherapy. Here, we focus on factors and their polymorphic genotypes that are involved in specific DNA repair pathways and have been shown to affect the incidence of thyroid cancer.

The multistep BER pathway is the main mechanism responsible for the replacement of individual DNA bases that have been altered by alkylation, oxidation, and deamination [for review see Ref. (14)]. The damaged base is recognized by specific DNA glycosylases like OGG1, which recognizes and excises 8-oxoguanine to generate an apurinic/apyrimidinic (AP) abasic site. Loss of heterozygosity (LOH) of the glycosylase OGG1 is strongly associated with papillary thyroid cancer (PTC) (15). The apurinic/apyrimidinic endonuclease 1 (APE1) recognizes the AP site and cleaves the phosphodiester bond at the 5′ end to yield a 3′-OH nucleotide and 5′-deoxyribose phosphate (dRp) terminus. The 5′-dRp site is cytotoxic and conversion into an inert 3′-OH requires lyase activity provided by BER-associated APE1, DNA polymerase β (PolB), and stem cell nucleoprotein members high-mobility group A1 and A2 (HMGA1/2) (16). Presence of HMGA1 and/or HMGA2 confers enhanced BER capacity and chemoresistance against alkylating agents onto thyroid cancer cells (16, 17). The scaffolding protein X-ray repair cross-complementing group 1 (XRCC1) facilitates the assembly of the PolB–DNA ligase III–PARP complex and the formation of phosphodiester bonds to complete the BER repair of AP sites (18). Investigations into the possible association of XRCC1 Arg399Gln, Arg280His,

and Arg194Trp polymorphisms with thyroid cancer revealed that hetero- and homozygous XRCC1 Arg399Gln polymorphism coincided with a decreased risk of DTC in the Caucasian population and mixed population (19–22). The XRCC1 Arg280His polymorphism enhanced susceptibility of DTC in Caucasians but protect against DTC in Asians (21, 23), whereas a homozygous XRCC1 Arg194Trp polymorphic genotype may increase the risk of PTC and lymphatic metastasis (19, 20, 24, 25).

The ERCC2 DNA helicase is a member of the NER pathway and contributes to the repair of distorted DNA regions due to bulky DNA adducts and UV light-induced DNA damage [for review see Ref. (26)]. The ERCC2 G23591A gene polymorphism results in an Asp312Asn mutation in a conserved region and the A35931C polymorphism causes a Lys751Gln substitution. Both polymorphisms are in linkage equilibrium and those patients homozygous for both rare variant alleles show an increased risk for PTC but not follicular thyroid cancer (FTC) (27).

The MMR pathway eliminates mismatched bases and incorrect insertions/deletions as a result of faulty DNA replication. The heterodimer of MutS complex (MSH2 pairing with MSH6 and MSH3, respectively) locks onto the base mismatch and recruits heterodimeric endonuclease MutL, composed of PMS2 and MLH1, and the exonuclease 1 (EXO1) to remove the mismatched base. The abasic gap is filled and ligated by DNA polymerase δ/ε and DNA ligase, respectively (28). Higher expression of MLH1, MSH2, and PMS1 were observed in malignant thyroid tumors than in benign lesions (29). BRAF V600E mutations, RET/PTC rearrangements, and transitions (IDH1 and NRAS) are associated with low expression of MLH1 in thyroid cancer patients (30).

Genotoxic ionizing radiation and DNA-damaging agents can cause double-strand breaks (DSBs). This triggers DNA DSB repair in the form of either HR or NHEJ (31). HR uses a sister chromatid template and thus functions in late G2–S cell cycle phase. HR is a highly accurate and error-free repair process [for review see Ref. (28, 31, 32)]. Radiation-induced thyroid tumors are the direct result of radiation-related DSBs and chromosomal rearrangements (33–35). In the Saudi Arabian population, the RAD52 Gln221Glu polymorphic genotype and RAD52 2259C > T genotype, and variants thereof carrying a T allele, were reported to have a significantly higher risk of developing thyroid cancer (36). Two other studies identified the combinations of RAD52 2259C > T, XRCC2 R188H and XRCC3 T241M polymorphisms (37) and RAD51 Exon1/59G > T, XRCC3 Thr241Met variant alleles to have predictive value for the polygenic risk of thyroid cancer (19).

Non-homologous end-joining is a DSB repair that does not require homologous DNA as a template and, thus, functions throughout the cell cycle [for review see Ref. (38–40)]. The Ku70/80 protein complex recognizes DSBs and participates in the recruitment of DNA-dependent protein kinases. The human pituitary tumor transforming gene (PTTG) is highly expressed in human thyroid carcinoma and binds to and inhibits Ku70 protein. Suppression of PTTG gene expression coincides with an up-regulation of DNA repair proteins in thyroid cancer suggesting a role for PTTG in therapeutic resistance (41–45). XRCC7 is another NHEJ factor and XRCC7 Ile3434Thr polymorphism has recently been associated with increased incidence of DTC (46).

ENDOPLASMIC RETICULUM STRESS, AUTOPHAGY, AND EPITHELIAL-TO-MESENCHYMAL TRANSITION

ENDOPLASMIC RETICULUM STRESS AND EPITHELIAL MESENCHYMAL TRANSITION

Unfolded protein response (UPR) pathways are activated to offset the adverse effects of protein accumulation in the endoplasmic reticulum (ER), following the induction of ER stress [reviewed in Ref. (47)]. Activating transcription factor 6 (ATF6), inositol-requiring protein-1 (IRE1), and PKR-like ER kinase (PERK) constitute the three arms of the UPR which control specific regulatory mechanisms to ease protein translation, regulate metabolism rate and redox events, augment expression of protein-folding chaperones, and increase the production of protein degradation enzymes (48, 49). The first step of UPR activation includes GRP78 chaperone dissociation from ER membrane-spanning UPR receptor proteins, PERK, IRE1, and ATF6 (UPR arms), to facilitate protein refolding [reviewed in Ref. (49)]. Several metabolic and environmental cues can trigger ER stress induction and initiate UPR pathways. Cancer-related impairment in UPR response might affect the ability of cells to maintain homeostasis during ER stress (50). Rapidly growing tumors are highly dependent on nutrients and oxygen delivered by the tumor vasculature. Activated ER stress stimulates an adaptive UPR process and helps cancer (stem) cells to survive. The X-box binding protein-1 (XBP-1) has an important involvement in UPR-induced cell survival and is induced via the IRE1 pathway of UPR (47, 51). XBP-1 is often over-expressed in cancer cells and, importantly, increases drug resistance by interfering with cell cycle regulation and by down-regulating tumor apoptotic responses to anti-cancer drugs. This makes XBP-1 an attractive cellular factor for dedifferentiation and EMT in breast cancer cells that negatively regulates the organization of polarized epithelial cells in estrogen-dependent and -independent breast tumors (52). Intriguingly, ER stress inducers (thapsigargin and tunicamycin) were shown to increase XBP-1 splicing in PC-Cl3 thyroid cells, impeding the thyroglobulin folding process and inducing accumulation of this glycoprotein in the ER. In the absence of apoptosis, differentiation of PC-Cl3 cells was inhibited. ER stress inducers also down-regulated thyroid-specific genes encoding thyroglobulin, thyroperoxidase, thyroid transcription factors TTF-1, TTF-2, and Pax-8 in these thyrocytes (53). This coincides with the establishment of a mesenchymal, stem-like phenotype consistent with EMT and included the down-regulation of E-cadherin transcripts, the up-regulation of mRNAs encoding vimentin, α-smooth muscle actin, the formation of actin stress fibers, and the loss of trans-epithelial resistance. All of these EMT events in thyroid cancer cells were stimulated with thapsigargin and tunicamycin (53). ER stressors likely facilitate EMT in different ways. In human kidney proximal tubular cells, this was shown to involve the induction of GRP78, GRP94, and phospho-eIF2α with subsequent EMT phenomenon (54). Thapsigargin and tunicamycin can also deregulate the intracellular Ca^{2+} metabolism, up-regulate the pleckstrin member T cell death-associated gene 51 (TDAG51), which sensitizes human kidney proximal tubular cells to mesenchymal transformation via Wnt signaling and primes these cells for TGF-β1-induced EMT response (54).

AUTOPHAGY AND EMT

Autophagy is considered a lysosomal degradation pathway responsible for the digestion of intracellular materials and the recycling of damaged cellular organelles (55, 56). Up to now, three types of autophagy have been described; these including macro-autophagy, micro-autophagy, and chaperone-mediated autophagy (CMA). They differ in their physiological functions and the pathways involved in their degradation mechanisms. Macro-autophagy includes a process of engulfing cellular waste in autophagosomes, which subsequently fuse with lysosomes and form autophagolysosomes, whereas micro-autophagy involves the direct uptake of cytoplasm by lysosomal membranes. CMA is considered the most selective form of autophagy and has so far only been described in mammalian cells. CMA involves a chaperone-guided process of internalization of soluble proteins by lysosomes [reviewed in Ref. (55, 57, 58)].

Physiologic basal autophagy plays an essential role in cellular homeostasis. It enables the cells to break down long-lived proteins and tightly regulates organelle turnover. Recycling of ER and mitochondria prevents ER stress and the accumulation of reactive oxygen and nitrogen species. During metabolic stress conditions, autophagy is initiated to sustain cellular energy in form of adenosine triphosphate (ATP) required for survival (59). Selective autophagy assists cells to rid themselves of damaged organelles, toxic protein aggregates (59), and invading microorganisms [reviewed in Ref. (60, 61)]. Autophagy is induced by an initial membrane nucleation that requires the ULK1 complex, and a class III phosphoinositide 3-kinase (PI3K) complex, which includes Bcl2 proteins member beclin 1 (62, 63). The isolation membrane selects its cargo and elongates until its edges fuse to form a double-membrane structure known as the autophagosome. Two ubiquitin-like conjugation systems, Atg5–Atg12 and microtubule-associated protein-1 light chain 3-phosphatidylethanolamine (LC3-II), are essential for the elongation of the isolation membrane to occur (51, 64–66). The autophagosome matures by fusing with endosomes and lysosomes to finally form the autophagolysosome where cargo degradation occurs (32, 67, 68).

Autophagy plays an essential function in tumor progression, metastasis, and the inhibition of cancer cell death (69, 70). While EMT promotes several mechanisms facilitating tumor invasiveness and increased cancer cell survival under stress conditions (71, 72), the association between EMT and autophagy in cancer invasiveness is less clear. Autophagy is involved in the regulation of epithelial plasticity (70). EMT is a form of enhanced epithelial plasticity and known to increase therapeutic resistance of cancer cells to cytotoxic agents and/or radiation. A strong link has recently been demonstrated between EMT, autophagy, stem-like characteristics, and resistance of cancer cells to cytotoxic T cell-induced killing, and targeting autophagy may help avoid immune resistance in breast cancer (73). Whether cancer (stem) cells opt for an aggressive phenotype, choose to enter an inactive state supported by autophagy, or endure cell death depends on the activation of different intracellular pathways and specific changes in gene expression profiles upon external stimuli (74). The hedgehog signaling pathway is one example of a

cellular signaling system balancing invasion versus autophagy. Active hedgehog signaling promotes an aggressive phenotype (75), while its inhibition activates autophagy (76). Another example is the activation of 5′ adenosine monophosphate-activated protein kinase (AMPK) which reduces tumor cell invasion (77) and induces autophagy in response to genotoxic stress (78) and nutrient starvation (79). In hepatocarcinoma cells, the induction of autophagy represses the expression of epithelial markers but promotes the expression of mesenchymal markers and the activation of the TGF-β/Smad3-dependent signaling pathway (80). Importantly, data from numerous cell systems, including thyroid cancer, identify autophagy as an important new player in EMT plasticity, therapeutic resistance, and metastasis. Clearly, the role of autophagy and ER stress/UPR responses in thyroid (cancer) stemness is a newly emerging and exiting field with potentially important innovation in the treatment of thyroid cancer.

DAMAGE-ASSOCIATED PATTERN RECOGNITION IN CANCER STEM CELLS

Damage-associated molecular patterns are a group of endogenous molecules acting as danger signals to initiate cellular repair and survival mechanisms (81, 82). Endogenous soluble molecules released during cell damage, necrosis, and cell stress are referred to as alarmins (82, 83). DAMP signaling induces an early immune response involving the innate and adaptive immune system, thus, initiating a "sterile inflammatory" reaction (83). In contrast, pathogen-associated molecular patterns (PAMPs) are exogenous danger signals derived from pathogens which activate diverse cellular receptors of the innate immune system to initiate host defense mechanisms (83). DAMPs may be exposed at the cell surface, e.g., calreticulin (CRT) and heat shock protein 90 (HSP90), or are secreted from cells, e.g., ATP, S100A8/A9 proteins, and high-mobility group box 1 protein (HMGB1). Secreted by tumor cells, these factors promote tumor growth and chemoresistance (81, 84–86); for a comprehensive list of DAMPs and their receptors, see Ref. (85).

Damage-associated molecular patterns act through membrane-anchored pattern recognition receptors (PRR) which recognize a structural pattern rather than a specific ligand. Examples for PRR are the NOD-like receptors (NLRs), toll-like receptors (TLRs), and the receptor for advanced glycation end products (RAGEs) (21, 87, 88). Several PRR, in particular TLRs and RAGE, are expressed in cancer cells and share distinct DAMP ligands such as HMGB1 and S100 proteins (89). In leukocytes or dendritic cells, PRR signaling results in the release of cytokines (innate immunity) or the initiation of adaptive immune responses. Interestingly, several PRR such as the TLRs recognize both PAMP and DAMP ligands (83). Also, DAMPs can interact with PAMPs to activate several PRR (90), suggesting the utilization of common cellular pathways when sensing exogenous and endogenous dangers.

All TLRs comprise a leucine-rich repeat extracellular domain responsible for ligand binding and a transmembrane domain and an intracellular toll/IL-1 receptor (TIR) domain for signal transduction. Ligand-binding results in the homo- or hetero-dimerization of TLRs as a requirement for intracellular signaling

(87). Engaging with the intracellular TIR domains of dimerized TLRs are five cytoplasmic adaptor molecules which activate intracellular signaling, including NF-κB and MAPK pathways. These intracellular TLR signaling adaptors are myeloid differentiation factor 88 (MyD88), MyD88 adapter-like protein (MAL), TIR domain-containing adaptor protein inducing interferon-beta (TRIF), TRIF-related adaptor molecule (TRAM), and sterile α- and armadillo-motif-containing protein (SARM) [reviewed in Ref. (82, 91)]. MyD88 is used by all TLRs and was shown to have a particular role in tumorigenesis (92).

Receptor for advanced glycation end product belongs to the immunoglobulin-like family of transmembrane receptors (88, 93) and is expressed in several human cancers (94). The three extracellular domains of RAGE, the V-, C1-, and C2-domain, function in ligand binding (93). The single transmembrane domain connects to the short cytoplasmic tail of RAGE which interacts with the cytoplasmic adaptor molecule diaphanous-1 (Dia-1) (95) and with toll-interleukin 1 receptor domain-containing adaptor protein (TIRAP) and MyD88; the latter two are also adapters for TLR 2 and 4 (96). Depending on the ligand and cell context, activated RAGE can signal through multiple signaling pathways, including extracellular ERK1/2, p38 MAP kinase, Cdc42/Rac-1, c-Jun-NH2-terminal kinase/stress-activated protein kinase (JNK/SAPK). This finally results in the activation of NF-κB and the induction of pro-inflammatory and pro-migratory responses (97). RAGE ligands include HMGB1, S100/calgranulin proteins, advanced glycation end products (AGEs), and amyloid β proteins (98). RAGE signaling can be modified by soluble RAGE species. Endogenously produced soluble RAGE splice variant (esRAGE), unable to insert into the membrane, is secreted from cells and acts as a decoy for RAGE ligands (88). Cleavage of the extracellular domains by a disintegrin and metalloproteinase 10 (ADAM10) releases soluble RAGE which can also act as scavenger for ligands (99). Unfortunately, soluble RAGE species are not reliable clinical predictors of outcome in cancer or inflammatory diseases (88). Ligand binding to RAGE induces RAGE expression in a positive feedback loop and promotes clustering of RAGE at the cell surface leading to sustained RAGE signaling by multimeric ligands (97, 100, 101). In the thyroid gland, RAGE is not expressed in normal follicular epithelial cells, but its expression is up-regulated in thyroid epithelial cells of follicular adenoma and thyroid carcinoma (102) suggesting that hyperactive and neoplastic thyroid cells respond to DAMPs.

Utilizing HMGB1 as an example, we demonstrate how DAMP–PRR signaling can influence tumorigenesis and stem cell functions. HMGB1 is a non-histone DNA-binding protein of the high-mobility group protein family and is composed of two DNA-binding HMG-box motives and an acidic C-terminus. Originally described as an exclusively nuclear protein involved in the modulation of gene transcription and chromosomal stability, HMGB1 is now known to have a cytoplasmic role in regulating autophagy, cell survival, and EMT (103). HMGB1 is passively released from dead or injured cells and actively secreted from immune cells and cancer cells in response to cellular stress signals (83, 103). HMGB1 secretion is modulated by various post-translational modifications and by secondary messengers such as cytosolic calcium, nitric oxide,

and reactive oxygen species (ROS) (103). Extracellular HMGB1 binds to several receptors, including TLR2, TLR4, and RAGE (89), to promote cell migration, proliferation, and differentiation. Secreted HMGB1 functions in the repair of tissue damage and chronic inflammation and leads to increased tumor growth and metastasis, promotes angiogenesis, regulates vascular remodeling, and enhances stem cell renewal (88, 89, 104). The influence of HMGB1 on stem/progenitor cells is mediated via RAGE and TLRs and results in enhanced stem cell functions (104–106).

HMGB1–RAGE–NF-κB signaling promotes neuronal stem cell proliferation/differentiation (107) and enhances xenograft metastasis via EMT and the activation of MAPK pathways (108). Astrocyte-derived HMGB1 enhances stem cell recruitment in the brain during stroke recovery (109, 110). HMGB1–TLR2 signaling via signal transducer and activator of transcription factor 3 (STAT3) and Smad3 activation enhances breast cancer stem cell self-renewal and increases breast cancer metastasis (104). HMGB1 aids in the recruitment of endothelial precursor cells (EPC) using RAGE (111) and TLR2/TLR4 in c-kit-positive EPC (112), thus, contributing to tissue repair and tumor growth. In PTC, the HMGB1–RAGE interaction increases the expression of the microRNAs miR221 and miR222 and promotes PTC cell growth and motility by inhibiting the cell cycle regulator p27kip1 (113).

The role of TLR in cancer is not fully understood. TLR receptor activation by PAMPs and distinct endogenous (DAMPs) signals has been associated with either tumor promoting or anti-tumor activities in human cancers (114, 115). Very little information exists on the function of DAMP–PRR interactions in the thyroid gland and in thyroid cancer (stem) cells. Normal human and rat thyroid cells express TLR 2 and TR4. Activation of TLR in the rat thyroid cell line FRTL-5 induces NF-κB activation and secretion of the pro-inflammatory cytokines interferon-beta (IFN-β), indicating that the thyroid gland is capable of responding to DAMPs and PAMPs with the initiation of "sterile inflammatory responses" to promote proliferation and angiogenesis in the thyroid (116). In FTC, TLR4 was localized to inflammatory tissue regions surrounding the tumor and TLR4 expression was associated with metastasis in FTC patients (117). TLR10 polymorphism has been associated with increased tumor size in patients with PTC (118). In mouse breast progenitor cells, PAMP ligands of TLR4 enhance cell proliferation and mammosphere growth (119), whereas similar activity in intestinal stem cells induces a p53-dependent apoptosis (120). Also, flagellin–TLR5 signaling in human breast cancer cells reduces cell proliferation and anchorage-independent growth in human breast cancer xenografts (121). TLR4 activation was shown to suppress TGF-beta signaling and promote chemoresistance in tumor-initiating cells of virus-induced hepatocellular carcinoma (21). Cancer stem cells may respond to DAMPs differently from normal stem cells and the nature of the ligand affects the cellular responses to PRR activation.

In summary, cross talk between different PRR, the activation of several PRR by the same DAMP, and the response of one PRR to more than one DAMP altogether suggest that cellular responses to DAMPs are: (i) (stem) cell-type and tissue-specific, (ii) influenced by the nature of the cellular stresses, and (iii) affected by the spatial and temporal distribution and concentration of DAMPs. It is intriguing to speculate that the complex DAMP–PRR system with

its functional roles in cell plasticity, autophagy, and cellular stress control represents an important and as yet under-valued novel topic in stem cell research and a potentially lucrative therapeutic target to manipulate cancer stem cell functions.

HIGH-MOBILITY GROUP A2: A LINK BETWEEN STEMNESS, EMT, AND CHEMORESISTANCE

The low molecular weight HMGA2, formerly named HMGI-C, is a member of the HMGA family of non-histone nuclear protein, which also includes HMGA1 and its splice forms. Structural analysis of HMGA2 revealed three DNA-binding domains, called AT-hook motifs, which facilitate binding to AT-rich regions of the minor groove of B-form DNA (122, 123). Blockage of HMGA2 can prevent the transformation of rat thyroid cells by murine retroviruses (124). HMGA2 is a marker of stem cells, absent in most adult tissues, and re-expressed in many cancer (stem) cells (125–129). HMGA2 binds to the AT-rich G-bands in the chromosomes and to centromeres and telomeres of metaphase preparations (130). Chromosomal rearrangements of both HMGA1 and HMGA2 proteins have been correlated with neoplastic transformation. HMGA2 overexpression, dysregulation, or truncation has been linked to benign and malignant tumors. This includes benign mesenchymal tumors (131), uterine leiomyomata (127, 132), pituitary adenoma (132), human prolactinoma (133), pancreatic cancer (134, 135), retinoblastoma (136), embryonic rhabdomyosarcoma (80), chondrosarcoma (137), lung cancer (138), and hepatocellular carcinoma (104). In thyroid cancer, elevated levels of HMGA2 are considered a molecular marker to distinguish benign and malignant thyroid neoplasms (139, 140).

PROTECTIVE ROLES OF HMGA2

Multifunctional HMGA1 and 2 are localized in the nucleus and regulate transcriptional genes activity, DNA replication, and DNA repair (141). HMGA2 is a new member of the BER protein complex and interacts with human AP endonuclease 1 (APE1) to promote chemoresistance in cancer cells, including human undifferentiated thyroid cancer cells (16). HMGA1 and 2 serve as substrate for the phosphatidylinositol 3-kinase-related kinase (PIKK) family member ataxia telangiectasia mutated (ATM) and downstream checkpoint kinase 2 (CHK2) which are important for DNA damage signaling. Upon exposure to genotoxicants, increased HMGA1/2 expression correlates with increased ATM expression levels and enhanced cellular DNA damage response (142, 143). HMGA2 also interacts with ataxia telangiectasia and Rad3-related kinase (ATR) and HMGA2-mediated activation of the ATR–checkpoint kinase 1 (CHK1) signaling pathway with resulting G2/M arrest increases chemoresistance against BER-inducing genotoxic alkylating agents in human thyroid and other cancer cells (17). Recently, we showed that HMGA2 plays an important novel role in protecting the integrity and functionality of arrested replication forks in cancer cells. HMGA2 preferentially binds with higher affinity to DNA Y- (replication fork) and X- (Holliday junctions) structures typically observed at replication forks (45). Binding of HMGA2 to these DNA conformations protected stalled replication forks from endonuclease digestion and conferred a survival advantage onto HMGA2^{+} cancer cells,

including thyroid cancer cells, when exposed to chemotherapeutics such as hydroxyurea used in the treatment of cancer patients (45).

HMGA2 IN STEMNESS AND EMT

Cancer initiating cells (CIC) evade cell death and attenuate the cytotoxic effects of radio- and chemotherapy by modulating DNA damage repair mechanisms to promote therapeutic resistance and tumor recurrence (80, 144). The Lin28–HMGA2–let-7 axis plays a significant role in promoting EMT, tissue invasion/metastasis, and therapeutic resistance in cancer cells (21). Ectopically expressed of the microRNA binding protein, Lin28 down-regulates the miR let-7 which attenuates the inhibitory let-7-mediated association with the $3'$ untranslated region of HMGA2 mRNA, resulting in the up-regulation of HMGA2 protein (145). Presence of HMGA2 in retinoblastoma and pancreatic cancer cells was shown to enhance cell proliferation and increase stemness (135, 136). HMGA2 also has a key role in maintaining high self-renewing capacity in hematopoietic stem cells and this involves the inhibition of the micro RNA let-7 by Lin28 (146). Let-7 suppresses both H-Ras and HMGA2 and this causes reduced proliferation and differentiation of breast CIC (44). In addition to the phenotypic and/or cell surface markers like CD133, CD34, CD90, SOX2, OCT4, and NANOG, functional markers such as the aldehyde dehydrogenase (ALDH) activity also determine the stemness in a cancer subpopulation. The inhibition of ALDH activity reduces stemness and sensitizes CIC to cytotoxic insult (80). Cellular levels of HMGA2 directly correlate with ALDH activity in breast cancer and contribute to tumor migration and resistance toward DNA-damaging agents (21). HMGA2 is found at the invasive front of the tumor to promote tissue invasion and tumor recurrence following therapy (147). HMGA2-induced EMT is promoted by TGF-β signaling (147) and the pro-inflammatory cytokine oncostatin M (OSM) (148) which signal via the STAT3 (148), the Ras/MAPK signaling pathway (135), and Twist and Snail, the two key regulators of EMT and major contributors to metastasis and tumor recurrence (104, 149). Suppression of Lin28 or HMGA2 increases let-7 and this reverses EMT and affects the level of therapeutic resistance. HMGA2$^+$ cancer cells were shown to exhibit resistance against 4 of 11 anti-cancer drugs tested (128).

In conclusion, cancer (stem) cells capable of utilizing HMG proteins to enhance DNA repair mechanisms in response to DNA-damaging drugs are likely contributing to therapeutic resistance to anti-cancer treatments in metastatic or recurrent cancers. Modulation of the EMT, ER stress, and autophagy regulation in cancer (stem) cells serves as important survival strategy in avoiding apoptosis under nutritional or oxygen deprivation. Similarly, DAMP signaling via several PRR may serve as another tumor survival response by controlling cell proliferation, inflammatory, and autophagy responses in cancer (stem) cells.

REFERENCES

1. Thomas D, Friedman S, Lin RY. Thyroid stem cells: lessons from normal development and thyroid cancer. *Endocr Relat Cancer* (2008) 15:51–8. doi:10.1677/ERC-07-0210
2. Klonisch T, Hoang-Vu C, Hombach-Klonisch S. Thyroid stem cells and cancer. *Thyroid* (2009) 19:1303–15. doi:10.1089/thy.2009.1604
3. Derwahl M. Linking stem cells to thyroid cancer. *J Clin Endocrinol Metab* (2011) 96:610–3. doi:10.1210/jc.2010-2826
4. Ahmed N, Abubaker K, Findlay J, Quinn M. Epithelial mesenchymal transition and cancer stem cell-like phenotypes facilitate chemoresistance in recurrent ovarian cancer. *Curr Cancer Drug Targets* (2010) 10:268–78. doi:10.2174/156800910791190175
5. Statistics CCSSSCOC. In: Society CC, editor. *Canadian Cancer Statistics 2012.* (2012).
6. Pathak KA, Leslie WD, Klonisch TC, Nason RW. The changing face of thyroid cancer in a population-based cohort. *Cancer Med* (2013) 2:537–44. doi:10.1002/cam4.103
7. Howlader N, Noone AM, Krapcho M, Neyman N, Aminou R, Waldron W, et al. *SEER Cancer Statistics Review, 1975–2009 (Vintage 2009 Populations).* Bethesda, MD: National Cancer Institute (2012).
8. Mazurat A, Torroni A, Hendrickson-Rebizant J, Benning H, Nason RW, Pathak KA. The age factor in survival of a population cohort of well-differentiated thyroid cancer. *Endocr Connect* (2013) 2:154–60. doi:10.1530/EC-13-0056
9. Lin RY. Thyroid cancer stem cells. *Nat Rev Endocrinol* (2011) 7:609–16. doi:10.1038/nrendo.2011.127
10. Ahn SH, Henderson YC, Williams MD, Lai SY, Clayman GL. Detection of thyroid cancer stem cells in papillary thyroid carcinoma. *J Clin Endocrinol Metab* (2013) 99(2):536–44. doi:10.1210/jc.2013-2558
11. Yun JY, Kim YA, Choe JY, Min H, Lee KS, Jung Y, et al. Expression of cancer stem cell markers is more frequent in anaplastic thyroid carcinoma compared to papillary thyroid carcinoma and is related to adverse clinical outcome. *J Clin Pathol* (2014) 67:125–33. doi:10.1136/jclinpath-2013-201711
12. Pathak KA, Mazurat A, Lambert P, Klonisch T, Nason RW. Prognostic nomograms to predict oncological outcome of thyroid cancers. *J Clin Endocrinol Metab* (2013) 98:4768–75. doi:10.1210/jc.2013-2318
13. Statistics CCSSSCOC. In: Society CC, editor. *Canadian Cancer Statistics 2011.* (2011).
14. Dianov GL. Base excision repair targets for cancer therapy. *Am J Cancer Res* (2011) 1:845–51.
15. Royer MC, Zhang H, Fan CY, Kokoska MS. Genetic alterations in papillary thyroid carcinoma and Hashimoto thyroiditis: an analysis of hOGG1 loss of heterozygosity. *Arch Otolaryngol Head Neck Surg* (2010) 136:240–2. doi:10.1001/archoto.2010.20
16. Summer H, Li O, Bao Q, Zhan L, Peter S, Sathiyanathan P, et al. HMGA2 exhibits dRP/AP site cleavage activity and protects cancer cells from DNA-damage-induced cytotoxicity during chemotherapy. *Nucleic Acids Res* (2009) 37:4371–84. doi:10.1093/nar/gkp375
17. Natarajan S, Hombach-Klonisch S, Dröge P, Klonisch T. HMGA2 inhibits apoptosis through interaction with ATR-CHK1 signaling complex in human cancer cells. *Neoplasia* (2013) 15:263–80. doi:10.1593/neo.121988
18. Horton JK, Watson M, Stefanick DF, Shaughnessy DT, Taylor JA, Wilson SH. XRCC1 and DNA polymerase beta in cellular protection against cytotoxic DNA single-strand breaks. *Cell Res* (2008) 18:48–63. doi:10.1038/cr.2008.7
19. Bastos HN, Antao MR, Silva SN, Azevedo AP, Manita I, Teixeira V, et al. Association of polymorphisms in genes of the homologous recombination DNA repair pathway and thyroid cancer risk. *Thyroid* (2009) 19:1067–75. doi:10.1089/thy.2009.0099
20. Fard-Esfahani P, Fard-Esfahani A, Fayaz S, Ghanbarzadeh B, Saidi P, Mohabati R, et al. Association of Arg194Trp, Arg280His and Arg399Gln polymorphisms in X-ray repair cross-complementing group 1 gene and risk of differentiated thyroid carcinoma in Iran. *Iran Biomed J* (2011) 15:73–8.
21. Bao Y, Jiang L, Zhou JY, Zou JJ, Zheng JY, Chen XF, et al. XRCC1 gene polymorphisms and the risk of differentiated thyroid carcinoma (DTC): a meta-analysis of case-control studies. *PLoS One* (2013) 8:e64851. doi:10.1371/journal.pone.0064851
22. Hu Z, Hu X, Long J, Su L, Wei B. XRCC1 polymorphisms and differentiated thyroid carcinoma risk: a meta-analysis. *Gene* (2013) 528:67–73. doi:10.1016/j.gene.2013.07.005
23. Garcia-Quispes WA, Perez-Machado G, Akdi A, Pastor S, Galofre P, Biarnes F, et al. Association studies of OGG1, XRCC1, XRCC2 and XRCC3 polymorphisms with differentiated thyroid cancer. *Mutat Res* (2011) 70(9–710):67–72. doi:10.1016/j.mrfmmm.2011.03.003
24. Chiang FY, Wu CW, Hsiao PJ, Kuo WR, Lee KW, Lin JC, et al. Association between polymorphisms in DNA base excision repair genes XRCC1, APE1,

and ADPRT and differentiated thyroid carcinoma. *Clin Cancer Res* (2008) **14**:5919–24. doi:10.1158/1078-0432.CCR-08-0906

25. Ryu RA, Tae K, Min HJ, Jeong JH, Cho SH, Lee SH, et al. XRCC1 polymorphisms and risk of papillary thyroid carcinoma in a Korean sample. *J Korean Med Sci* (2011) **26**:991–5. doi:10.3346/jkms.2011.26.8.991

26. Scharer OD. Nucleotide excision repair in eukaryotes. *Cold Spring Harb Perspect Biol* (2013) **5**:a012609. doi:10.1101/cshperspect.a012609

27. Silva SN, Gil OM, Oliveira VC, Cabral MN, Azevedo AP, Faber A, et al. Association of polymorphisms in ERCC2 gene with non-familial thyroid cancer risk. *Cancer Epidemiol Biomarkers Prev* (2005) **14**:2407–12. doi:10.1158/1055-9965.EPI-05-0230

28. Iyama T, Wilson DM III. DNA repair mechanisms in dividing and non-dividing cells. *DNA Repair* (2013) **12**:620–36. doi:10.1016/j.dnarep.2013.04.015

29. Ruschenburg I, Vollheim B, Stachura J, Cordon-Cardo C, Korabiowska M. Analysis of DNA mismatch repair gene expression and mutations in thyroid tumours. *Anticancer Res* (2006) **26**:2107–12.

30. Santos JC, Bastos AU, Cerutti JM, Ribeiro ML. Correlation of MLH1 and MGMT expression and promoter methylation with genomic instability in patients with thyroid carcinoma. *BMC Cancer* (2013) **13**:79. doi:10.1186/1471-2407-13-79

31. O'Driscoll M, Jeggo PA. The role of double-strand break repair – insights from human genetics. *Nat Rev Genet* (2006) **7**:45–54. doi:10.1038/nrg1746

32. Klionsky DJ, Abdalla FC, Abeliovich H, Abraham RT, Acevedo-Arozena A, Adeli K, et al. Guidelines for the use and interpretation of assays for monitoring autophagy. *Autophagy* (2012) **8**:445–544. doi:10.4161/auto.19496

33. Nikiforov YE, Koshoffer A, Nikiforova M, Stringer J, Fagin JA. Chromosomal breakpoint positions suggest a direct role for radiation in inducing illegitimate recombination between the ELE1 and RET genes in radiation-induced thyroid carcinomas. *Oncogene* (1999) **18**:6330–4. doi:10.1038/sj.onc.1203019

34. Ciampi R, Knauf JA, Rabes HM, Fagin JA, Nikiforov YE. BRAF kinase activation via chromosomal rearrangement in radiation-induced and sporadic thyroid cancer. *Cell Cycle* (2005) **4**:547–8. doi:10.4161/cc.4.4.1631

35. Leeman-Neill RJ, Brenner AV, Little MP, Bogdanova TI, Hatch M, Zurnadzy LY, et al. RET/PTC and PAX8/PPARgamma chromosomal rearrangements in post-Chernobyl thyroid cancer and their association with iodine-131 radiation dose and other characteristics. *Cancer* (2013) **119**:1792–9. doi:10.1002/cncr.27893

36. Siraj AK, Al-Rasheed M, Ibrahim M, Siddiqui K, Al-Dayel F, Al-Sanea O, et al. RAD52 polymorphisms contribute to the development of papillary thyroid cancer susceptibility in Middle Eastern population. *J Endocrinol Invest* (2008) **31**:893–9.

37. Fayaz S, Karimmirza M, Tanhaei S, Fathi M, Torbati PM, Fard-Esfahani P. Increased risk of differentiated thyroid carcinoma with combined effects of homologous recombination repair gene polymorphisms in an Iranian population. *Asian Pac J Cancer Prev* (2013) **14**:6727–31. doi:10.7314/APJCP.2013.14.11.6727

38. Povirk LF. Biochemical mechanisms of chromosomal translocations resulting from DNA double-strand breaks. *DNA Repair (Amst)* (2006) **5**:1199–212. doi:10.1016/j.dnarep.2006.05.016

39. Gospodinov A, Herceg Z. Chromatin structure in double strand break repair. *DNA Repair (Amst)* (2013) **12**:800–810. doi:10.1016/j.dnarep.2013.07.006

40. Kakarougkas A, Jeggo PA. DNA DSB repair pathway choice: an orchestrated handover mechanism. *Br J Radiol* (2014). doi:10.1259/bjr.20130685

41. Romero F, Multon MC, Ramos-Morales F, Dominguez A, Bernal JA, Pintor-Toro JA, et al. Human securin, hPTTG, is associated with Ku heterodimer, the regulatory subunit of the DNA-dependent protein kinase. *Nucleic Acids Res* (2001) **29**:1300–7. doi:10.1093/nar/29.6.1300

42. Kim D, Pemberton H, Stratford AL, Buelaert K, Watkinson JC, Lopes V, et al. Pituitary tumour transforming gene (PTTG) induces genetic instability in thyroid cells. *Oncogene* (2005) **24**:4861–6. doi:10.1038/sj.onc.1208659

43. Saez C, Martinez-Brocca MA, Castilla C, Soto A, Navarro E, Tortolero M, et al. Prognostic significance of human pituitary tumor-transforming gene immunohistochemical expression in differentiated thyroid cancer. *J Clin Endocrinol Metab* (2006) **91**:1404–9. doi:10.1210/jc.2005-2532

44. Chesnokova V, Zonis S, Rubinek T, Yu R, Ben-Shlomo A, Kovacs K, et al. Senescence mediates pituitary hypoplasia and restrains pituitary tumor growth. *Cancer Res* (2007) **67**:10564–72. doi:10.1158/0008-5472.CAN-07-0974

45. Yu H, Lim HH, Tjokro NO, Sathiyanathan P, Natarajan S, Chew TW, et al. Chaperoning HMGA2 protein protects stalled replication forks in stem and cancer cells. *Cell Rep* (2014) **6**(4):684–97. doi:10.1016/j.celrep.2014.01.014

46. Rahimi M, Fayaz S, Fard-Esfahani A, Modarressi MH, Akrami SM, Fard-Esfahani P. The role of Ile3434Thr XRCC7 gene polymorphism in differentiated thyroid cancer risk in an Iranian population. *Iran Biomed J* (2012) **16**:218–22.

47. Sovolyova N, Healy S, Samali A, Logue SE. Stressed to death – mechanisms of ER stress-induced cell death. *Biol Chem* (2014) **395**:1–13. doi:10.1515/hsz-2013-0174

48. Tanjore H, Cheng DS, Degryse AL, Zoz DF, Abdolrasulnia R, Lawson WE, et al. Alveolar epithelial cells undergo epithelial-to-mesenchymal transition in response to endoplasmic reticulum stress. *J Biol Chem* (2011) **286**:30972–80. doi:10.1074/jbc.M110.181164

49. Deegan S, Saveljeva S, Gorman AM, Samali A. Stress-induced self-cannibalism: on the regulation of autophagy by endoplasmic reticulum stress. *Cell Mol Life Sci* (2013) **70**:2425–41. doi:10.1007/s00018-012-1173-4

50. Vandewynckel YP, Laukens D, Geerts A, Bogaerts E, Paridaens A, Verhelst X, et al. The paradox of the unfolded protein response in cancer. *Anticancer Res* (2013) **33**:4683–94.

51. Ghavami S, Yeganeh B, Stelmack GL, Kashani HH, Sharma P, Cunnington R, et al. Apoptosis, autophagy and ER stress in mevalonate cascade inhibition-induced cell death of human atrial fibroblasts. *Cell Death Dis* (2012) **3**:e330. doi:10.1038/cddis.2012.61

52. Shajahan AN, Riggins RB, Clarke R. The role of X-box binding protein-1 in tumorigenicity. *Drug News Perspect* (2009) **22**:241–6. doi:10.1358/dnp.2009.22.5.1378631

53. Ulianich L, Garbi C, Treglia AS, Punzi D, Miele C, Raciti GA, et al. ER stress is associated with dedifferentiation and an epithelial-to-mesenchymal transition-like phenotype in PC Cl3 thyroid cells. *J Cell Sci* (2008) **121**:477–86. doi:10.1242/jcs.017202

54. Carlisle RE, Heffernan A, Brimble E, Liu L, Jerome D, Collins CA, et al. TDAG51 mediates epithelial-to-mesenchymal transition in human proximal tubular epithelium. *Am J Physiol Renal Physiol* (2012) **303**:F467–81. doi:10.1152/ajprenal.00481.2011

55. Klionsky DJ, Saltiel AR. Autophagy works out. *Cell Metab* (2012) **15**:273–4. doi:10.1016/j.cmet.2012.02.008

56. Gong C, Bauvy C, Tonelli G, Yue W, Delomenie C, Nicolas V, et al. Beclin 1 and autophagy are required for the tumorigenicity of breast cancer stem-like/progenitor cells. *Oncogene* (2013) **32**:2261–72. doi:10.1038/onc.2012.252

57. Arias E, Cuervo AM. Chaperone-mediated autophagy in protein quality control. *Curr Opin Cell Biol* (2011) **23**:184–9. doi:10.1016/j.ceb.2010.10.009

58. Ghavami S, Shojaei S, Yeganeh B, Ande SR, Jangamreddy JR, Mehrpour M, et al. Autophagy and apoptosis dysfunction in neurodegenerative disorders. *Prog Neurobiol* (2014) **112**:24–49. doi:10.1016/j.pneurobio.2013.10.004

59. Mehrpour M, Codogno P. Drug enhanced autophagy to fight mutant protein overload. *J Hepatol* (2011) **54**:1066–8. doi:10.1016/j.jhep.2010.11.032

60. Mathew R, White E. Why sick cells produce tumors: the protective role of autophagy. *Autophagy* (2007) **3**:502–5.

61. Yeganeh B, Rezaei Moghadam A, Tran AT, Rahim MN, Ande SR, Hashemi M, et al. Asthma and influenza virus infection: focusing on cell death and stress pathways in influenza virus replication. *Iran J Allergy Asthma Immunol* (2013) **12**:1–17. doi:012.01/ijaai.117

62. Levine B, Klionsky DJ. Development by self-digestion: molecular mechanisms and biological functions of autophagy. *Dev Cell* (2004) **6**:463–77. doi:10.1016/S1534-5807(04)00099-1

63. Ravikumar B, Sarkar S, Davies JE, Futter M, Garcia-Arencibia M, Green-Thompson ZW, et al. Regulation of mammalian autophagy in physiology and pathophysiology. *Physiol Rev* (2010) **90**:1383–435. doi:10.1152/physrev.00030.2009

64. Mizushima N. Autophagy in protein and organelle turnover. *Cold Spring Harb Symp Quant Biol* (2011) **76**:397–402. doi:10.1101/sqb.2011.76.011023

65. Weidberg H, Elazar Z. TBK1 mediates crosstalk between the innate immune response and autophagy. *Sci Signal* (2011) **4**:e39. doi:10.1126/scisignal.2002355

66. Ghavami S, Cunnington RH, Yeganeh B, Davies JJ, Rattan SG, Bathe K, et al. Autophagy regulates trans fatty acid-mediated apoptosis in primary cardiac myofibroblasts. *Biochim Biophys Acta* (2012) **1823**:2274–86. doi:10.1016/j.bbamcr.2012.09.008

67. Debnath J, Baehrecke EH, Kroemer G. Does autophagy contribute to cell death? *Autophagy* (2005) **1**:66–74. doi:10.4161/auto.1.2.1738

68. Yorimitsu T, Klionsky DJ. Autophagy: molecular machinery for self-eating. *Cell Death Differ* (2005) **12**(Suppl 2):1542–52. doi:10.1038/sj.cdd.4401765

69. Lavieu G, Scarlatti F, Sala G, Levade T, Ghidoni R, Botti J, et al. Is autophagy the key mechanism by which the sphingolipid rheostat controls the cell fate decision? *Autophagy* (2007) **3**:45–7.

70. Akalay I, Janji B, Hasmim M, Noman MZ, Andre F, De Cremoux P, et al. Epithelial-to-mesenchymal transition and autophagy induction in breast carcinoma promote escape from T-cell-mediated lysis. *Cancer Res* (2013) **73**:2418–27. doi:10.1158/0008-5472.CAN-12-2432

71. Yang J, Weinberg RA. Epithelial-mesenchymal transition: at the crossroads of development and tumor metastasis. *Dev Cell* (2008) **14**:818–29. doi:10.1016/j.devcel.2008.05.009

72. Yang J, Wu LJ, Tashino S, Onodera S, Ikejima T. Reactive oxygen species and nitric oxide regulate mitochondria-dependent apoptosis and autophagy in evodiamine-treated human cervix carcinoma HeLa cells. *Free Radic Res* (2008) **42**:492–504. doi:10.1080/10715760802112791

73. Akalay I, Janji B, Hasmim M, Noman MZ, Thiery JP, Mami-Chouaib F, et al. EMT impairs breast carcinoma cell susceptibility to CTL-mediated lysis through autophagy induction. *Autophagy* (2013) **9**:1104–6. doi:10.4161/auto.24728

74. Marcucci F, Bellone M, Caserta CA, Corti A. Pushing tumor cells towards a malignant phenotype: stimuli from the microenvironment, intercellular communications and alternative roads. *Int J Cancer* (2013). doi:10.1002/ijc.28572

75. Takebe N, Harris PJ, Warren RQ, Ivy SP. Targeting cancer stem cells by inhibiting Wnt, Notch, and Hedgehog pathways. *Nat Rev Clin Oncol* (2011) **8**:97–106. doi:10.1038/nrclinonc.2010.196

76. Jimenez-Sanchez M, Menzies FM, Chang YY, Simecek N, Neufeld TP, Rubinsztein DC. The Hedgehog signalling pathway regulates autophagy. *Nat Commun* (2012) **3**:1200. doi:10.1038/ncomms2212

77. Fitzgerald JP, Nayak B, Shanmugasundaram K, Friedrichs W, Sudarshan S, Eid AA, et al. Nox4 mediates renal cell carcinoma cell invasion through hypoxia-induced interleukin 6- and 8- production. *PLoS One* (2012) **7**:e30712. doi:10.1371/journal.pone.0030712

78. Liu Y, Li H, Feng J, Cui X, Huang W, Li Y, et al. Lin28 induces epithelial-to-mesenchymal transition and stemness via downregulation of Let-7a in breast cancer cells. *PLoS One* (2013) **8**:e83083. doi:10.1371/journal.pone.0083083

79. Diresta GR, Nathan SS, Manoso MW, Casas-Ganem J, Wyatt C, Kubo T, et al. Cell proliferation of cultured human cancer cells are affected by the elevated tumor pressures that exist in vivo. *Ann Biomed Eng* (2005) **33**:1270–80. doi:10.1007/s10439-005-5732-9

80. Abdullah L, Chow E-H. Mechanisms of chemoresistance in cancer stem cells. *Clin Transl Med* (2013) **2**:1–9. doi:10.1186/2001-1326-2-3

81. Lotze MT, Zeh HJ, Rubartelli A, Sparvero LJ, Amoscato AA, Washburn NR, et al. The grateful dead: damage-associated molecular pattern molecules and reduction/oxidation regulate immunity. *Immunol Rev* (2007) **220**:60–81. doi:10.1111/j.1600-065X.2007.00579.x

82. Suresh R, Mosser DM. Pattern recognition receptors in innate immunity, host defense, and immunopathology. *Adv Physiol Educ* (2013) **37**:284–91. doi:10.1152/advan.00058.2013

83. Srikrishna G, Freeze HH. Endogenous damage-associated molecular pattern molecules at the crossroads of inflammation and cancer. *Neoplasia* (2009) **11**:615–28.

84. Huang J, Ni J, Liu K, Yu Y, Xie M, Kang R, et al. HMGB1 promotes drug resistance in osteosarcoma. *Cancer Res* (2012) **72**:230–8. doi:10.1158/0008-5472.CAN-11-2001

85. Krysko DV, Garg AD, Kaczmarek A, Krysko O, Agostinis P, Vandenabeele P. Immunogenic cell death and DAMPs in cancer therapy. *Nat Rev Cancer* (2012) **12**:860–75. doi:10.1038/nrc3380

86. Krysko O, Love Aaes T, Bachert C, Vandenabeele P, Krysko DV. Many faces of DAMPs in cancer therapy. *Cell Death Dis* (2013) **4**:e631. doi:10.1038/cddis.2013.156

87. Takeda K, Akira S. Toll-like receptors in innate immunity. *Int Immunol* (2005) **17**:1–14. doi:10.1093/intimm/dxh186

88. Bierhaus A, Nawroth PP. Multiple levels of regulation determine the role of the receptor for AGE (RAGE) as common soil in inflammation, immune responses

89. and diabetes mellitus and its complications. *Diabetologia* (2009) **52**:2251–63. doi:10.1007/s00125-009-1458-9

90. van Beijnum JR, Buurman WA, Griffioen AW. Convergence and amplification of toll-like receptor (TLR) and receptor for advanced glycation end products (RAGE) signaling pathways via high mobility group B1 (HMGB1). *Angiogenesis* (2008) **11**:91–9. doi:10.1007/s10456-008-9093-5

90. Escamilla-Tilch M, Filio-Rodriguez G, Garcia-Rocha R, Mancilla-Herrera I, Mitchison NA, Ruiz-Pacheco JA, et al. The interplay between pathogen-associated and danger-associated molecular patterns: an inflammatory code in cancer? *Immunol Cell Biol* (2013) **91**:601–10. doi:10.1038/icb.2013.58

91. Kenny EF, O'Neill LA. Signalling adaptors used by toll-like receptors: an update. *Cytokine* (2008) **43**:342–9. doi:10.1016/j.cyto.2008.07.010

92. Kfoury A, Virard F, Renno T, Coste I. Dual function of MyD88 in inflammation and oncogenesis: implications for therapeutic intervention. *Curr Opin Oncol* (2014) **26**:86–91. doi:10.1097/CCO.0000000000000037

93. Leclerc E, Fritz G, Vetter SW, Heizmann CW. Binding of S100 proteins to RAGE: an update. *Biochim Biophys Acta* (2009) **1793**:993–1007. doi:10.1016/j.bbamcr.2008.11.016

94. Logsdon CD, Fuentes MK, Huang EH, Arumugam T. RAGE and RAGE ligands in cancer. *Curr Mol Med* (2007) **7**:777–89. doi:10.2174/156652407783220697

95. Hudson BI, Kalea AZ, Del Mar Arriero M, Harja E, Boulanger E, D'Agati V, et al. Interaction of the RAGE cytoplasmic domain with diaphanous-1 is required for ligand-stimulated cellular migration through activation of Rac1 and Cdc42. *J Biol Chem* (2008) **283**:34457–68. doi:10.1074/jbc.M801465200

96. Sakaguchi M, Murata H, Yamamoto K, Ono T, Sakaguchi Y, Motoyama A, et al. TIRAP, an adaptor protein for TLR2/4, transduces a signal from RAGE phosphorylated upon ligand binding. *PLoS One* (2011) **6**:e23132. doi:10.1371/journal.pone.0023132

97. Fritz G. RAGE: a single receptor fits multiple ligands. *Trends Biochem Sci* (2011) **36**:625–32. doi:10.1016/j.tibs.2011.08.008

98. Sparvero LJ, Asafu-Adjei D, Kang R, Tang D, Amin N, Im J, et al. RAGE (receptor for advanced glycation end products), RAGE ligands, and their role in cancer and inflammation. *J Transl Med* (2009) **7**:17. doi:10.1186/1479-5876-7-17

99. Metz VV, Kojro E, Rat D, Postina R. Induction of RAGE shedding by activation of G protein-coupled receptors. *PLoS One* (2012) **7**:e41823. doi:10.1371/journal.pone.0041823

100. Ostendorp T, Leclerc E, Galichet A, Koch M, Demling N, Weigle B, et al. Structural and functional insights into RAGE activation by multimeric S100B. *EMBO J* (2007) **26**:3868–78. doi:10.1038/sj.emboj.7601805

101. Koch M, Chitayat S, Dattilo BM, Schiefner A, Diez J, Chazin WJ, et al. Structural basis for ligand recognition and activation of RAGE. *Structure* (2010) **18**:1342–52. doi:10.1016/j.str.2010.05.017

102. Medapati M, Dahlmann M, Stein U, Ghavami S, Hombach-Klonisch S. S100A4 signaling in thyroid cancer. *Experimental Biology Meeting*. Boston: EB2013 (2013). 4052 p.

103. Kang R, Zhang Q, Zeh HJ III, Lotze MT, Tang D. HMGB1 in cancer: good, bad, or both? *Clin Cancer Res* (2013) **19**:4046–57. doi:10.1158/1078-0432.CCR-13-0495

104. Conti L, Lanzardo S, Arigoni M, Antonazzo R, Radaelli E, Cantarella D, et al. The noninflammatory role of high mobility group box 1/toll-like receptor 2 axis in the self-renewal of mammary cancer stem cells. *FASEB J* (2013) **27**:4731–44. doi:10.1096/fj.13-230201

105. Riuzzi F, Sorci G, Donato R. The amphoterin (HMGB1)/receptor for advanced glycation end products (RAGE) pair modulates myoblast proliferation, apoptosis, adhesiveness, migration, and invasiveness. Functional inactivation of RAGE in L6 myoblasts results in tumor formation in vivo. *J Biol Chem* (2006) **281**:8242–53. doi:10.1074/jbc.M509436200

106. Sorci G, Riuzzi F, Giambanco I, Donato R. RAGE in tissue homeostasis, repair and regeneration. *Biochim Biophys Acta* (2013) **1833**:101–9. doi:10.1016/j.bbamcr.2012.10.021

107. Meneghini V, Francese MT, Carraro L, Grilli M. A novel role for the receptor for advanced glycation end-products in neural progenitor cells derived from adult subventricular zone. *Mol Cell Neurosci* (2010) **45**:139–50. doi:10.1016/j.mcn.2010.06.005

108. Taguchi A, Blood DC, Del Toro G, Canet A, Lee DC, Qu W, et al. Blockade of RAGE-amphoterin signalling suppresses tumour growth and metastases. *Nature* (2000) **405**:354–60. doi:10.1038/35012626

109. Hayakawa K, Pham LD, Katusic ZS, Arai K, Lo EH. Astrocytic high-mobility group box 1 promotes endothelial progenitor cell-mediated neurovascular remodeling during stroke recovery. *Proc Natl Acad Sci U S A* (2012) **109**:7505–10. doi:10.1073/pnas.1121146109

110. Hayakawa K, Pham LD, Arai K, Lo EH. High-mobility group box 1: an amplifier of stem and progenitor cell activity after stroke. *Acta Neurochir Suppl* (2013) **118**:31–8. doi:10.1007/978-3-7091-1434-6_5

111. Chavakis E, Hain A, Vinci M, Carmona G, Bianchi ME, Vajkoczy P, et al. High-mobility group box 1 activates integrin-dependent homing of endothelial progenitor cells. *Circ Res* (2007) **100**:204–12. doi:10.1161/01.RES.0000257774.55970.f4

112. Furlani D, Donndorf P, Westien I, Ugurlucan M, Pittermann E, Wang W, et al. HMGB-1 induces c-kit+ cell microvascular rolling and adhesion via both toll-like receptor-2 and toll-like receptor-4 of endothelial cells. *J Cell Mol Med* (2012) **16**:1094–105. doi:10.1111/j.1582-4934.2011.01381.x

113. Mardente S, Mari E, Consorti F, Di Gioia C, Negri R, Etna M, et al. HMGB1 induces the overexpression of miR-222 and miR-221 and increases growth and motility in papillary thyroid cancer cells. *Oncol Rep* (2012) **28**:2285–9. doi:10.3892/or.2012.2058

114. Huang B, Zhao J, Li H, He KL, Chen Y, Chen SH, et al. Toll-like receptors on tumor cells facilitate evasion of immune surveillance. *Cancer Res* (2005) **65**:5009–14. doi:10.1158/0008-5472.CAN-05-0784

115. Kelly MG, Alvero AB, Chen R, Silasi DA, Abrahams VM, Chan S, et al. TLR-4 signaling promotes tumor growth and paclitaxel chemoresistance in ovarian cancer. *Cancer Res* (2006) **66**:3859–68. doi:10.1158/0008-5472.CAN-05-3948

116. Kawashima A, Yamazaki K, Hara T, Akama T, Yoshihara A, Sue M, et al. Demonstration of innate immune responses in the thyroid gland: potential to sense danger and a possible trigger for autoimmune reactions. *Thyroid* (2013) **23**:477–87. doi:10.1089/thy.2011.0480

117. Hagstrom J, Heikkila A, Siironen P, Louhimo J, Heiskanen I, Maenpaa H, et al. TLR-4 expression and decrease in chronic inflammation: indicators of aggressive follicular thyroid carcinoma. *J Clin Pathol* (2012) **65**:333–8. doi:10.1136/jclinpath-2011-200402

118. Kim SK, Park HJ, Hong IK, Chung JH, Eun YG. A missense polymorphism (rs11466653, Met326Thr) of toll-like receptor 10 (TLR10) is associated with tumor size of papillary thyroid carcinoma in the Korean population. *Endocrine* (2013) **43**:161–9. doi:10.1007/s12020-012-9783-z

119. Lee SH, Hong B, Sharabi A, Huang XF, Chen SY. Embryonic stem cells and mammary luminal progenitors directly sense and respond to microbial products. *Stem Cells* (2009) **27**:1604–15. doi:10.1002/stem.75

120. Neal MD, Sodhi CP, Jia H, Dyer M, Egan CE, Yazji I, et al. Toll-like receptor 4 is expressed on intestinal stem cells and regulates their proliferation and apoptosis via the p53 up-regulated modulator of apoptosis. *J Biol Chem* (2012) **287**:37296–308. doi:10.1074/jbc.M112.375881

121. Cai Z, Sanchez A, Shi Z, Zhang T, Liu M, Zhang D. Activation of toll-like receptor 5 on breast cancer cells by flagellin suppresses cell proliferation and tumor growth. *Cancer Res* (2011) **71**:2466–75. doi:10.1158/0008-5472.CAN-10-1993

122. Reeves R, Nissen MS. The AT-DNA-binding domain of mammalian high mobility group I chromosomal proteins. A novel peptide motif for recognizing DNA structure. *J Biol Chem* (1990) **265**:8573–82.

123. Banks GC, Mohr B, Reeves R. The HMG-I(Y) AT-hook peptide motif confers DNA-binding specificity to a structured chimeric protein. *J Biol Chem* (1999) **274**:16536–44. doi:10.1074/jbc.274.23.16536

124. Berlingieri MT, Pierantoni GM, Giancotti V, Santoro M, Fusco A. Thyroid cell transformation requires the expression of the HMGA1 proteins. *Oncogene* (2002) **21**:2971–80. doi:10.1038/sj.onc.1205368

125. Chiappetta G, Avantaggiato V, Visconti R, Fedele M, Battista S, Trapasso F, et al. High level expression of the HMGI (Y) gene during embryonic development. *Oncogene* (1996) **13**:2439.

126. Rogalla P, Drechsler K, Frey G, Hennig Y, Helmke B, Bonk U, et al. HMGI-C expression patterns in human tissues. Implications for the genesis of frequent mesenchymal tumors. *Am J Pathol* (1996) **149**:775.

127. Gattas GJ, Quade BJ, Nowak RA, Morton CC. HMGIC expression in human adult and fetal tissues and in uterine leiomyomata. *Genes Chromosomes Cancer* (1999) **25**:316–22. doi:10.1002/(SICI)1098-2264(199908)25:4<316::AID-GCC2>3.0.CO;2-0

128. Györffy B, Surowiak P, Kiesslich O, Denkert C, Schäfer R, Dietel M, et al. Gene expression profiling of 30 cancer cell lines predicts resistance towards 11 anticancer drugs at clinically achieved concentrations. *Int J Cancer* (2006) **118**:1699–712. doi:10.1002/ijc.21570

129. Ben-Porath I, Thomson MW, Carey VJ, Ge R, Bell GW, Regev A, et al. An embryonic stem cell-like gene expression signature in poorly differentiated aggressive human tumors. *Nat Genet* (2008) **40**:499–507. doi:10.1038/ng.127

130. Disney JE, Johnson KR, Magnuson NS, Sylvester SR, Reeves R. High-mobility group protein HMG-I localizes to G/Q- and C-bands of human and mouse chromosomes. *J Cell Biol* (1989) **109**:1975–82. doi:10.1083/jcb.109.5.1975

131. Schoenmakers EF, Wanschura S, Mols R, Bullerdiek J, van den Berghe H, Van de Ven WJ. Recurrent rearrangements in the high mobility group protein gene, HMGI-C, in benign mesenchymal tumours. *Nat Genet* (1995) **10**:436–44. doi:10.1038/ng0895-436

132. Fedele M, Battista S, Kenyon L, Baldassarre G, Fidanza V, Klein-Szanto AJ, et al. Overexpression of the HMGA2 gene in transgenic mice leads to the onset of pituitary adenomas. *Oncogene* (2002) **21**:3190–8. doi:10.1038/sj.onc.1205428

133. Finelli P, Pierantoni GM, Giardino D, Losa M, Rodeschini O, Fedele M, et al. The high mobility group A2 gene is amplified and overexpressed in human prolactinomas. *Cancer Res* (2002) **62**:2398–405.

134. Hristov AC, Cope L, Di Cello F, Reyes MD, Singh M, Hillion JA, et al. HMGA1 correlates with advanced tumor grade and decreased survival in pancreatic ductal adenocarcinoma. *Mod Pathol* (2009) **23**:98–104. doi:10.1038/modpathol.2009.139

135. Watanabe S, Ueda Y, Akaboshi S-I, Hino Y, Sekita Y, Nakao M. HMGA2 maintains oncogenic RAS-induced epithelial-mesenchymal transition in human pancreatic cancer cells. *Am J Pathol* (2009) **174**:854–68. doi:10.2353/ajpath.2009.080523

136. Chau KY, Manfioletti G, Cheung-Chau KW, Fusco A, Dhomen N, Sowden JC, et al. Derepression of HMGA2 gene expression in retinoblastoma is associated with cell proliferation. *Mol Med* (2003) **9**:154–65. doi:10.2119/2003-00020.Ono

137. Dahlen A, Mertens F, Rydholm A, Brosjo O, Wejde J, Mandahl N, et al. Fusion, disruption, and expression of HMGA2 in bone and soft tissue chondromas. *Mod Pathol* (0000) **16**:1132–40. doi:10.1097/01.MP.0000092954.42656.94

138. Di Cello F, Hillion J, Hristov A, Wood LJ, Mukherjee M, Schuldenfrei A, et al. HMGA2 participates in transformation in human lung cancer. *Mol Cancer Res* (2008) **6**:743–50. doi:10.1158/1541-7786.MCR-07-0095

139. Belge G, Meyer A, Klemke M, Burchardt K, Stern C, Wosniok W, et al. Upregulation of HMGA2 in thyroid carcinomas: a novel molecular marker to distinguish between benign and malignant follicular neoplasias. *Genes Chromosomes Cancer* (2008) **47**:56–63. doi:10.1002/gcc.20505

140. Lappinga PJ, Kip NS, Jin L, Lloyd RV, Henry MR, Zhang J, et al. HMGA2 gene expression analysis performed on cytologic smears to distinguish benign from malignant thyroid nodules. *Cancer Cytopathol* (2010) **118**:287–97. doi:10.1002/cncy.20095

141. Cleynen I, Van de Ven WJ. The HMGA proteins: a myriad of functions (review). *Int J Oncol* (2008) **32**:289.

142. Pentimalli F, Palmieri D, Pacelli R, Garbi C, Cesari R, Martin E, et al. HMGA1 protein is a novel target of the ATM kinase. *Eur J Cancer* (2008) **44**:2668–79. doi:10.1016/j.ejca.2008.07.033

143. Palmieri D, Valentino T, D'Angelo D, De Martino I, Postiglione I, Pacelli R, et al. HMGA proteins promote ATM expression and enhance cancer cell resistance to genotoxic agents. *Oncogene* (2011) **30**:3024–35. doi:10.1038/onc.2011.21

144. Lundholm L, Hååg P, Zong D, Juntti T, Mörk B, Lewensohn R, et al. Resistance to DNA-damaging treatment in non-small cell lung cancer tumor-initiating cells involves reduced DNA-PK/ATM activation and diminished cell cycle arrest. *Cell Death Dis* (2013) **4**:e478. doi:10.1038/cddis.2012.211

145. Lee YS, Dutta A. The tumor suppressor microRNA let-7 represses the HMGA2 oncogene. *Genes Dev* (2007) **21**:1025–30. doi:10.1101/gad.1540407

146. Copley MR, Babovic S, Benz C, Knapp DJ, Beer PA, Kent DG, et al. The Lin28b-let-7-Hmga2 axis determines the higher self-renewal potential of fetal haematopoietic stem cells. *Nat Cell Biol* (2013) **15**:916–25. doi:10.1038/ncb2783

147. Morishita A, Zaidi MR, Mitoro A, Sankarasharma D, Szabolcs M, Okada Y, et al. HMGA2 is a driver of tumor metastasis. *Cancer Res* (2013) **73**(14):4289–99. doi:10.1158/0008-5472.CAN-12-3848

148. Guo L, Chen C, Shi M, Wang F, Chen X, Diao D, et al. Stat3-coordinated Lin-28-let-7-HMGA2 and miR-200-ZEB1 circuits initiate and maintain oncostatin M-driven epithelial-mesenchymal transition. *Oncogene* (2013) **32**:5272–82. doi:10.1038/onc.2012.573

149. Thuault S, Valcourt U, Petersen M, Manfioletti G, Heldin C-H, Moustakas A. Transforming growth factor-β employs HMGA2 to elicit epithelial-mesenchymal transition. *J Cell Biol* (2006) **174**:175–83. doi:10.1083/jcb.200512110

Conflict of Interest Statement: The authors declare that the research was conducted in the absence of any commercial or financial relationships that could be construed as a potential conflict of interest.